U.S. DEPARTMENT OF COMMERCE
NOAA/ERL Wave Propagation Laboratory
July 1986

PROJECT CONDORS

Convective Diffusion Observed by Remote Sensors

PROJECT CONDORS

Convective Diffusion Observed by Remote Sensors

J. C. Kaimal, W. L. Eberhard, W. R. Moninger
J. E. Gaynor, S. W. Troxel and T. Uttal

G. A. Briggs

G. E. Start

Report Number Seven
July 1986

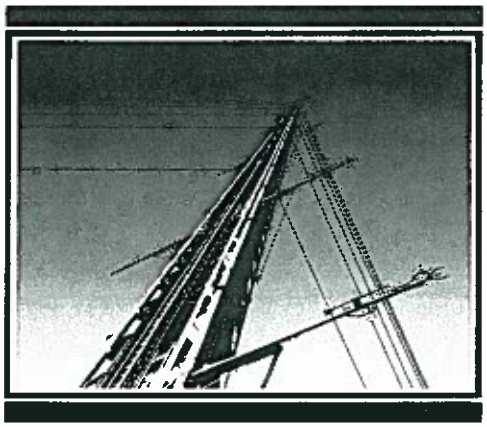

NOAA
Boulder Atmospheric Observatory

U.S. Department of Commerce
National Oceanic and Atmospheric Administration
Environmental Research Laboratories

A NOAA publication available from NOAA/ERL, Boulder, CO 80303.

PROJECT CONDORS -

CONVECTIVE DIFFUSION OBSERVED BY REMOTE SENSORS

by

J. C. Kaimal, W. L. Eberhard, W. R. Moninger
J. E. Gaynor, S. W. Troxel and T. Uttal
NOAA/ERL Wave Propagation Laboratory
Boulder, Colorado 80303

G. A. Briggs*
EPA/Atmospheric Sciences Research Laboratory
Research Triangle Park, North Carolina 27711

G. E. Start
NOAA/ERL/Air Resources Laboratory
Idaho Falls, Idaho 83401

This study was conducted for
U.S. Environmental Protection Agency
under Interagency Agreement No. AD13F2A251

Wave Propagation Laboratory
Environmental Research Laboratories
U.S. Department of Commerce
Boulder, Colorado 80303

* On assignment from the National Oceanic and Atmospheric Administration.

NOTICE

Acquisition of information provided in this document was funded in part by the United States Environmental Protection Agency under Interagency Agreement No. AD13F2A251. It has been subject to the Agency's peer and administrative review, and it has been approved for publication as an EPA document. This study was conducted jointly by the NOAA/Environmental Research Laboratory and the Environmental Protection Agency.

OTHER BAO REPORTS

1. BAO Report 1: PROJECT PHOENIX - The September 1978 Field Experiment, W. H. Hooke (Editor), December 1979, 281 pp.

2. BAO Report 2: The Boulder Low-Level Intercomparison Experiment - Preprint of WMO Report, J. C. Kaimal, H. W. Baynton, and J. E. Gaynor (Editors), June 1980, 189 pp.

3. BAO Report 3: Turbulence Statistics for Design of Wind Turbine Generators - Preprint of Report to DOE, J. C. Kaimal, J. E. Gaynor and D. E. Wolfe, December 1980, 102 pp.

4. BAO Report 4: Studies of Nocturnal Stable Layers, J. C. Kaimal (Editor), January 1983, 129 pp.

5. BAO Report 5: An Evaluation of Wind Measurements by Four Doppler Sodars, J. C. Kaimal, J. E. Gaynor, P. L. Finkelstein, M. E. Graves and T. J. Lockhart, July 1984, 110 pp.

6. BAO Report 6: A Field Comparison of In Situ Meteorological Sensors, J. C. Kaimal, J. E. Gaynor, P. L. Finkelstein, M. E. Graves and T. J. Lockhart, December 1984, 96 pp.

CONTENTS

ABSTRACT

This report presents results from two diffusion experiments conducted at the Boulder Atmospheric Observatory (BAO) in 1982 and 1983. The objective was to compare diffusion in the atmospheric convective boundary layer with that observed in laboratory tank experiments and numerical computer models. In both experiments at the BAO, two different tracers, oil fog and aluminized chaff, were released simultaneously and tracked by lidar and radar, respectively, for periods up to two hours. In 1982, both tracers were released from the same surface or elevated point; in 1983, the two were also released from separate levels, the oil fog from near the surface, the chaff from an elevated point on the tower. The 1983 experiment included tracer gas releases with in situ samplers measuring surface concentrations downwind of the tower. The BAO tower provided data on the mean and turbulent state of the atmosphere, while mixing depths were monitored by balloon soundings, sodar, lidar and radar. A detailed description of the experiment and the measurements obtained from the different sensors are provided. The strengths and limitations of the experiment are discussed in the context of a case study of one of the periods analyzed.

FIGURES

TABLES

ACKNOWLEDGMENTS

We acknowledge with gratitude the valuable contributions made by Daniel Wolfe, Norbert Szczepczynski, Robert Kropfli, Terrance McNice and Susan Carlson of the Wave Propagation Laboratory to the field experiment and to the analysis of the data. We also thank Markuu Riikonen of Kuopio University, Finland, and Li Zong-Kai of Nanjing University, Peoples Republic of China, for their assistance during the field experiment. The patience and technical competence of Mildred Birchfield and Alison Aragon in producing this report is gratefully acknowledged. This project was supported in part by the U.S. Environmental Protection Agency under Interagency Agreement No. AD13F2A251.

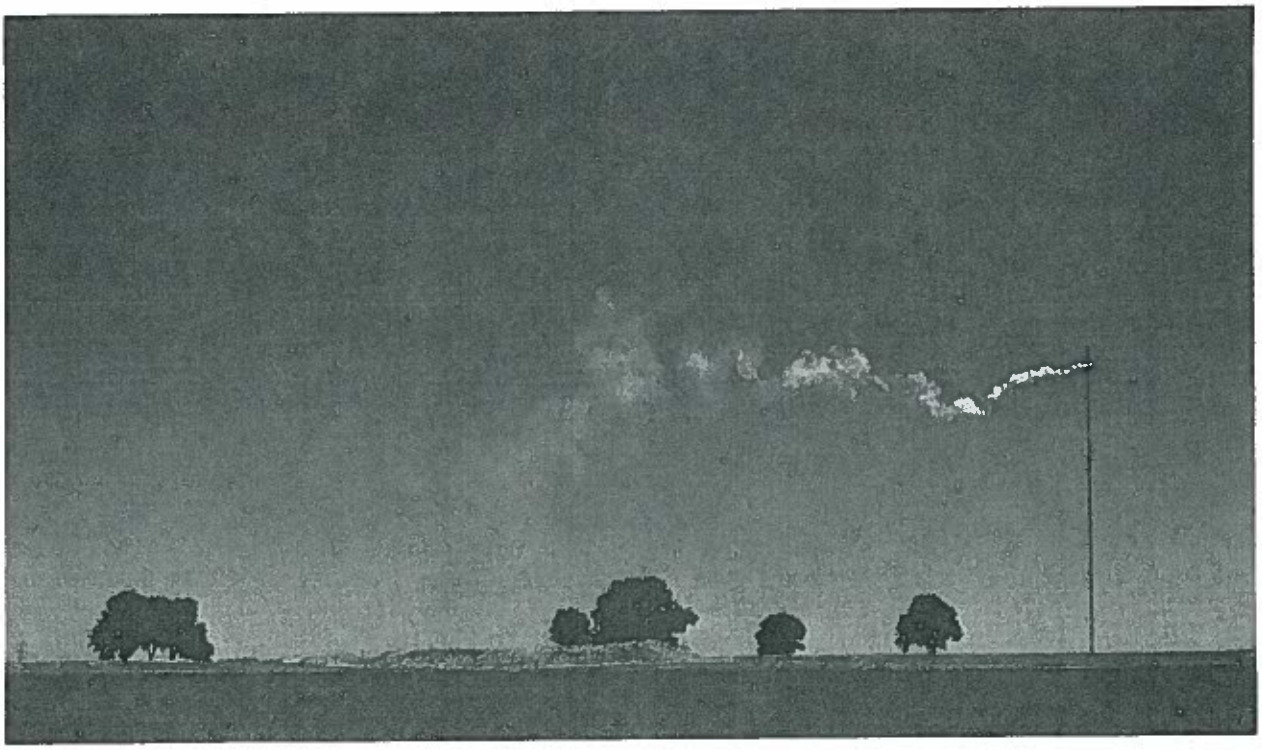

Fig. 1.1. Oil fog plume released from the 280 m level on the BAO tower during CONDORS 83. Aluminized chaff was also released simultaneously from a chaff cutter at the same level on the tower and tracked by radar.

1. BACKGROUND AND INTRODUCTION

J. C. Kaimal

Diffusion experiments were conducted at the Boulder Atmospheric Observatory (BAO) to study diffusion in the convective boundary layer with both remote and in situ sensors measuring downwind tracer concentrations from both ground and elevated sources. The experiments were carried out jointly by the National Oceanic and Atmospheric Administration (NOAA) and the Environmental Protection Agency (EPA) under an interagency agreement. The participating laboratories were the Wave Propagation Laboratory (WPL) and the Air Resources Laboratory (Idaho Falls) of NOAA, and the Meteorology Division of EPA. The 1982 experiment was primarily a test of the adequacy and limitations of the two remote sensing techniques being considered, while the 1983 experiment (Fig. 1.1) provided the type of data needed to compare diffusion in the atmosphere with that observed in laboratory and numerical studies. The two remote sensing techniques considered were:

1) Oil fog monitored by WPL's lidar operating at 0.53 μm.

2) Aluminized 'chaff' monitored by WPL's 3-cm Doppler radar.

The two techniques have the advantage of being different enough to be free of interference from each other, an essential requirement for observing diffusion from simultaneous ground and elevated releases. The 1982 experiment was designed to uncover systematic biases and other differences that might exist between the two techniques. Both tracers were released simultaneously at ground level or at typical stack heights while being tracked from optimum

directions by the lidar and the radar. In the 1983 experiment the two sources were separated most of the time, to contrast diffusion patterns from simultaneous ground and elevated releases. The decision to release the chaff only from the elevated location in 1983 was based on the 1982 findings. The 1983 experiment included a set of tracer gas releases (SF_6 and Freon 13B1) with in situ samplers measuring surface concentrations downwind of the tower.

Supporting observations used in the experiment included measurements of the mean and turbulent properties of the flow from the eight instrumented levels on the 300 m BAO tower. Mixing depths were monitored with balloon soundings, sodar, lidar and radar.

The experiments proceeded as planned. Two-hour releases were made near midday during four days in 1982 and eight days in 1983 when meteorological conditions were optimum. The 1982 experiment extended over a period of ten days in September; the 1983 experiment encompassed four weeks from mid-August to mid-September. This report describes the experiments and their main findings. Data summaries for 17 periods selected for analysis are included to serve as a reference set for future studies. The experiments will be referred to as CONDORS 82 and CONDORS 83, using the acronym derived from the title "Convective Diffusion Observed by Remote Sensors."

2. DEFINITION OF GOALS AND OBSERVING STRATEGIES

G. A. Briggs and J. C. Kaimal

2.1 Primary Goals

The primary goal of these experiments was to verify in the Earth's convective boundary layer diffusion phenomena observed in both laboratory and numerical modeling experiments (Willis and Deardorff 1976a, 1976b, 1978, 1980; Lamb, 1978 and 1979). In these experiments, for a source of passive tracer near the surface, the maximum concentration was observed to lift off the ground after a time of travel equal to about half the time it takes fluid in a thermal to rise to the top of the mixed layer. Thereafter the concentration at the surface reduced rapidly, as most of the material lofted into the upper half of the mixed layer; at larger distances the material became more or less uniformly mixed through the depth of the mixed layer. In contrast to this, the maximum concentration of passive material from elevated sources was observed to descend until it reached the surface; thereafter it behaved in a manner similar to material released near the surface at the point of initial ground contact. These phenomena have considerable impact on surface concentrations from either source type, and call into question some assumptions routinely made in mathematical models of diffusion, namely, Gaussian distribution of concentration in the vertical and constant elevation of the concentration maximum. For elevated sources, the maximum crosswind integrated surface concentrations observed in the above laboratory and numerical experiments was up to 80% more than those predicted using the assumptions just mentioned.

Because both laboratory (convective tank) and numerical experiments have been done with source heights of about one-fourth and one-half of the mixed layer depth, it was thought desirable to be able to adjust the height of an elevated source in the field to approximate one of these heights, in order to make comparison of field, laboratory, and numerical experimental results more straightforward, with no interpolations necessary. It was also thought desirable to detect and define simultaneously a plume from an elevated release and a plume from a near-surface release, since the above-mentioned experiments indicate dramatically different behaviors of these plumes near their sources. Confirmation of these observations in "real world" field experiments would greatly increase confidence in the laboratory and numerical convective diffusion modeling techniques.

2.2 Secondary Goals

First priority was given to field measurements of plume geometry, but the next most immediate goal was to measure or estimate (based on plume geometry) x/Q, the ratio of concentration to source strength. This is the quantity of most concern to air pollution modelers, and is most desirable for quantitative comparisons of results from field, laboratory, and numerical techniques. A related goal was to test the versatility and accuracy of two remote sensing plume tracing techniques used simultaneously--specifically, lidar and radar. These tools can provide plume concentration measurements in three dimensions much more easily than with direct sampling, especially when a plume diffuses through one or several kilometers of height. Another goal was to obtain a large variety of convective boundary layer measurements, especially turbulence

measurements, in the atmosphere concurrent with diffusion measurements. These would help determine the importance of factors that cannot be resolved by convective tank experiments or present numerical models.

2.3 The Site

The Boulder Atmospheric Observatory was chosen as the site for this experiment primarily because of the facilities--the 300 m, well instrumented meteorological tower and a unique array of remote sensing devices--but there are some meteorological advantages as well. The dry climate, especially in autumn, favors good convective boundary layer development on most days. Since late 1979, instrumentation on the tower has operated most of the time, and 20 min averages of the measurements have been archived. These records show that at 1300 MST in September, the favored conditions of sunny skies, wind speeds of 2 to 6 m/s, and wind direction from a particular sector occur nearly half the time (22 of the 45 days with data available) (Gaynor, 1982). The frequented sector is easterly, with directions ranging from 50° to 105°, suggesting that these winds may be thermally-driven upslope winds toward the Front Range of the Rocky Mountains. The frequency of occurrence of these conditions was about the same for all three data years in September, but in October and November the frequency averaged about one-fourth of the data days, and ranged from 12% to 45% in individual years. In December the number of suitable days declined to less than 10% in two of the three years, so winter months are unsatisfactory. The bar graph in Fig. 2.1 shows the wind direction frequency of sunny days with $\bar{u}$ between 2 and 6 m/s measured in September of 1979, 1980, and 1981 (45 days of measurements). Mixing depth climatology is not known, but during Project PHOENIX at the BAO during September 1978, mixing

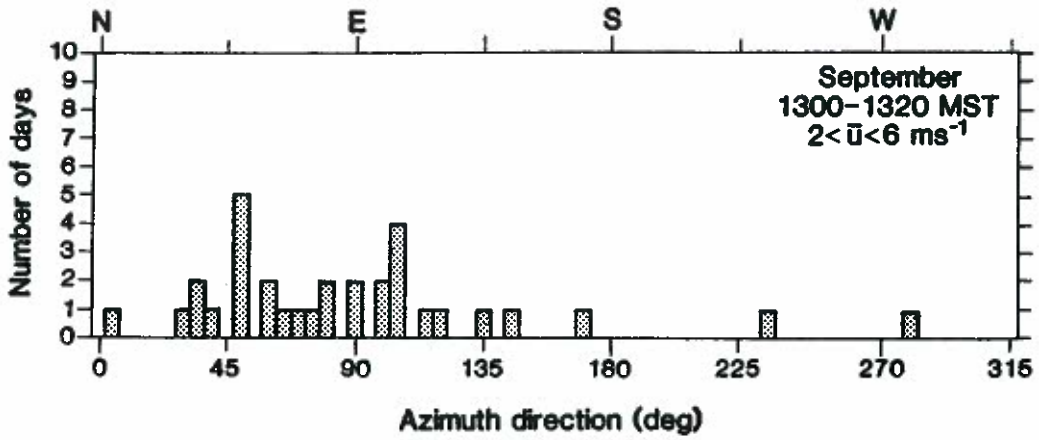

Figure 2.1. Number of sunny days with $2 < \bar{u} < 6$ m s^{-1} between 1300 and 1320 MST in September of 1979, 1980, 1981 per 5° segment of wind direction.

depths at 1300 MST ranged from 700 to 1000 m. Again, this is a very favorable range for this experiment.

The high frequency of easterly winds during convective conditions was advantageous for optimum siting of the remote sensing devices, which could not be moved during the experiments. However, the prevailing winds above the mixing layer, being nearly geostrophic, were westerly. Thus, the momentum of air within the mixing layer and the momentum of air entrained from above were frequently in opposition, which is uncommon in boundary layers distant from mountain slopes or shorelines. This opposition sometimes produced undesirable effects, particularly during periods of rapid mixing depth growth. One effect was unusually large wind direction shear in the upper part of the mixing layer, which tends to increase lateral plume dispersion; there were even a few occasions when a "renegade" elevated fragment of chaff plume was observed moving in nearly the opposite direction of the main plume. Another probable effect was an increased variability in mixing layer winds caused by shifts

in the balance of opposing forces; this variability increased uncertainties in operations, such as judging when to begin a release, and may have shortened the length of acceptable averaging periods with reasonably steady winds.

The terrain of the BAO site is neither "ideal" nor complex. It is gently rolling relief, with a 1 to 2% downward slope toward the north from the tower (see Fig. 2.2). Within 6 km, terrain elevations range from a hill 40 m higher

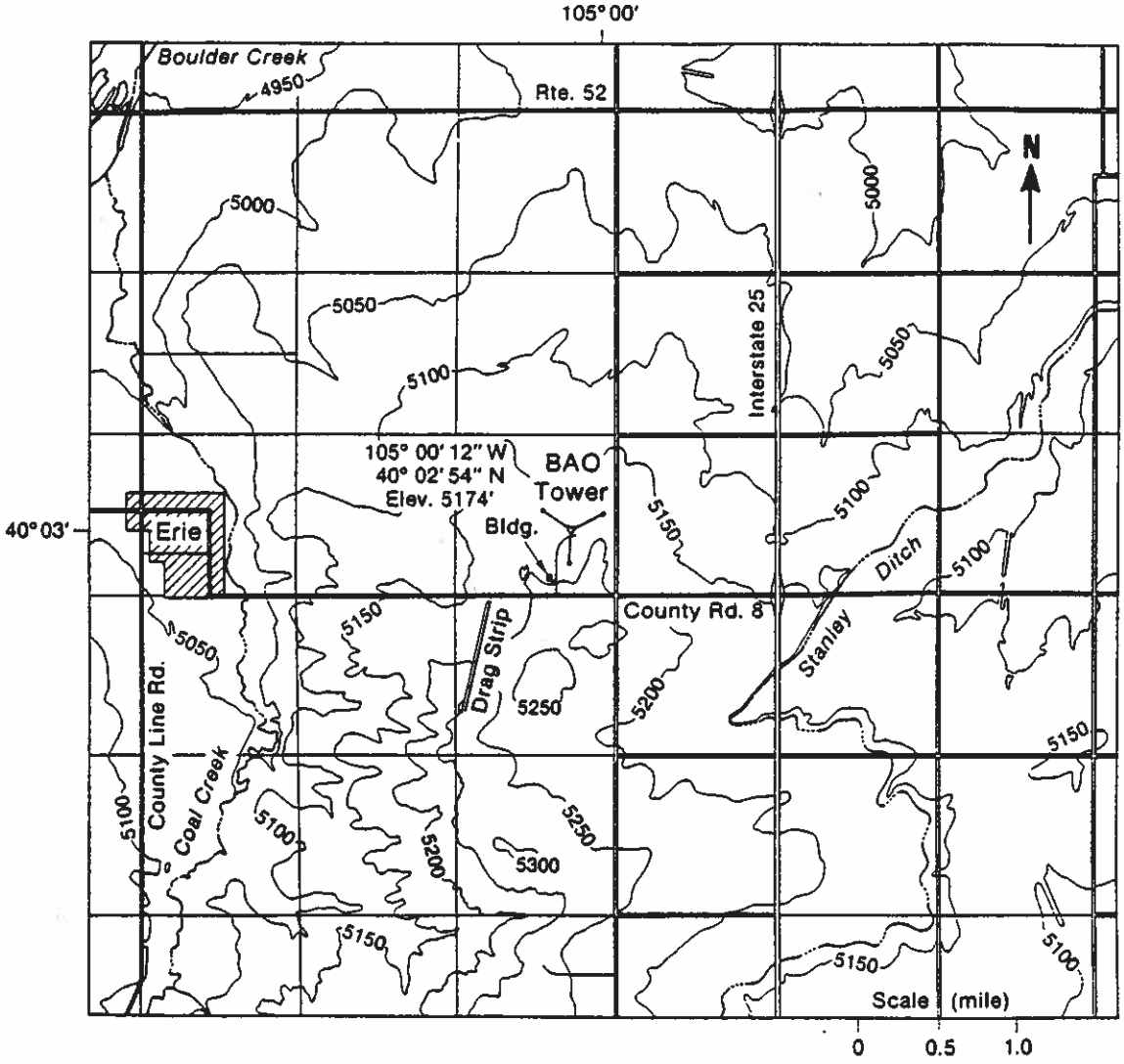

Figure 2.2. USGS topographical map showing height contours in feet and location of the BAO tower.

than the tower base, located 3.3 km S to SSW, to a creek valley about 70 m lower, 6 km to the NW and oriented approximately SW-NE. Such terrain variations were not expected to appreciably channel the flow or affect large scale turbulent eddies in daytime convective conditions, with mixing depths during the experiments ranging from 500 m to 1600 m. (The terrain drop to the west of the tower is about 45 m at 3.5 km in a north-running stream valley; this was the plume direction considered for the experiment.)

The surface cover is primarily long grasses, spotted with widely scattered trees and building clusters. The surface roughness length is very dependent on the wind direction, ranging from about 3 to 30 cm. The latter value is for southerly winds, from the direction of the hill. For long grass cover on flat terrain, the expected value would be more like 3 cm.

2.4 Wave Propagation Laboratory Facilities

The facilities of the Boulder Atmospheric Observatory as of 1978 are broadly reviewed in the Project PHOENIX report (Hooke, 1979), and are detailed in the many references found in this report. Only those features of most interest to the present experiment will be covered here, in brief.

The centerpiece, so to speak, is the 300 m tower (Kaimal and Gaynor, 1983). This served as a primary source of meteorological information, as well as a very convenient release point for the tracers. As a platform for elevated releases, the carriage was especially suitable because its height could be adjusted just prior to an experiment, according to the depth of the mixed layer predicted for the center time of the run.

The meteorological instrumentation on the tower included three-component sonic anemometers, quartz thermometers for mean temperature, platinum wire thermometers for temperature fluctuations, and dew point hydrometers, all at eight levels, 10 m to 300 m. This array of sophisticated instrumentation was more than adequate for the experiment, at least to heights up to 300 m. Quantities of special interest were mean wind speeds at all plume levels, mean wind direction, wind direction shear, and lateral and vertical velocity variances; these were all available from the sonic anemometers. In addition, the heat flux, in the form of $\overline{w'T'}$ measured near the surface, was essential for scaling the results for comparison with laboratory, numerical, and future field experiments. (There are a few past field experiments that can be compared also, e.g., Prairie Grass; however, these were very limited in that both sources and samplers were located near the surface, and quantities like $\overline{w'T'}$ were not measured directly with any accuracy.) The above quantities were routinely measured on the tower and listed as averages over 20 min time segments. Such averaging was useful for defining periods of relative steady state, particularly for wind speed and direction. For data analysis, the raw data were reprocessed to provide averages over selected time periods.

In addition to the tower, the Wave Propagation Laboratory has a unique array of remote sensors, since part of its mission is to develop and test these. Two of these instruments were particularly appropriate to an experiment of this nature.

For monitoring vertical cross sections of plume aerosol concentration, lidar is a proven and unsurpassed tool. The 10 Hz pulse firing rate of the frequency-doubled neodynium: yag laser permits a detailed plume scan (in range

and elevation) in about 15 seconds. Suitable plume sources for good lidar returns such as silica, soot, or oil fog droplets release large numbers of light scattering particles in the 1 μm diameter range. For CONDORS, WPL deployed oil fog generators, which dispensed a moderately viscous oil with a slow evaporation rates in the form of a mist.

To contrast the behavior of elevated and ground source plumes, we wished to simultaneously release two different tracers that could be detected separately. This could not be accomplished by using aerosol releases and lidar alone. So, a second remote sensor was used: a 3.2 cm (X-band) radar capable of very sensitive tracking of chaff composed of 1.6 cm long aluminized mylar filaments. The quantity of chaff dispersed has a small lidar cross section compared to the aerosol, so the effect on the lidar returns was negligible. WPL's Doppler radar is capable of detecting concentrations as low as five filaments in a 10^6 m^3 volume of air. Also, the interpretation of radar returns was not distorted by background aerosols, since they are much too small to be detected. Since attenuation is not a problem, the radar was able to look lengthwise down the plume axis. Being a Doppler radar, it also measured the axial mean and turbulent velocities of the chaff.

A drawback of the radar-chaff system is the fall velocity of the thinnest available filaments, which is about 0.3 m/s, the fall rate of a large piece of house dust. This velocity is a significant fraction of the vertical turbulent velocities in a convective atmosphere, about 1 m/s. However, a preliminary observation of chaff released from 300 m on the BAO tower (Moninger and Kropfli, 1982) showed evidence of plume behavior similar to what Willis and Deardorff (1978) observed from elevated sources in their laboratory tank.

The plume appeared to initially descend, with maximum concentrations appearing near the surface from 1 to 2 km downwind, then gradually rose to about 300 m at 4 km and beyond. Close-in behavior was not observable in that experiment because the radar returns within 1 km of the source exceeded the dynamic range of the radar receiver. This problem was minimized in CONDORS by the use of receivers with larger dynamic range. The chaff concentration maximum failed to reach the upper half of the 900 m mixing depth, contrary to laboratory plume behavior at the larger diffusion times; this was probably a consequence of the chaff's fall velocity. The primary purpose of CONDORS 82 was to establish just how much this effect distorts the plume relative to a passive plume. This was accomplished with collocated releases of oil fog and chaff mapped with the lidar and the radar.

2.5 In Situ Tracer Measurements

In addition to the above measurements, we wanted in situ measurements of the concentration of a standard tracer to compare with values inferred from the lidar and radar scans. These remote sensors are well suited for determining three-dimensional plume geometry, the primary objective of this experiment. However, the main motivation behind the need to determine plume geometries is to be able to predict ground concentrations with less uncertainty than is inherent in present modeling methods. Remote sensing systems are not yet developed to the point of giving reliable direct determinations of X/Q, (concentration divided by source strength) because of problems with accurate determination of Q, dropout of chaff, evaporation of oil fog droplets, etc. With these problems, it is extremely difficult to calibrate

lidar and radar returns in terms of χ. However, these instruments adequately define the plume geometry in terms of relative concentration at a given distance. Thus, with good measurements of mean wind speed as a function of height, we can infer the χ/Q field for any conservative tracer by assuming uniform relative depletion of mass. That is, assume that $\chi \propto \chi'$ at any given downwind distance, where χ' is a linearized radar or lidar return, corrected for background, attenuation, and $1/r^2$ response. Then, multiply the conservative-tracer flux relationship

$$\iint \chi \, \bar{u} \, dydz = Q$$

by the constant χ'/χ. Thus we infer that

$$\chi/Q = \chi'/\iint \chi' \, \bar{u} \, dydz.$$

The validity of this string of assumptions can be checked by some direct sampling of a tracer known to be reasonably conservative, such as SF_6. While the budget of this program did not permit an extensive sampling network, one arc of samplers at a distance expected to be frequented by high surface concentrations was provided as a valuable check on χ/Q values inferred using remote sensors. NOAA's Air Resources Laboratory in Idaho Falls conducted the release, sampling and analysis of the in situ gas tracer concentrations measurements made during CONDORS 83.

2.6 Experimental Design Parameters

As explained in Sec. 2.1, it was desirable for purposes of comparison to make releases from both the surface and from near one-fourth or one-half of the mixing depth z_i. With a maximum platform height of 300 m at the BAO, this limited desirable experimental runs with elevated releases to $z_i < 1200$ m,

which generally excluded the possibility of a springtime or summertime experiment on the Colorado high plains. In the fall, especially in late fall, there are days when $z_i < 600$ m, low enough to permit running an elevated source at either $z_i/4$ or $z_i/2$. In an ideal experiment, z_i would be nearly constant during a run, as in the laboratory and numerical experiments. In the real atmosphere, at best only a "quasi-steady" state can be found. We attempted to start the runs during periods of slow relative growth, in order to minimize $\Delta z_i/z_i$ during the runs. Normally, the growth rate of z_i is nearly constant in the early morning hours, then gradually diminishes through midday and afternoon hours. However, inspection of the observations of z_i versus time of day from project PHOENIX, carried out at the BAO site in September 1978, shows that on three of the six days there was an acceleration, or even a jump, in z_i growth shortly after solar noon (Kaimal et al., 1980). In these three cases, the morning rawinsonde soundings revealed layers of nearly neutral temperature stratification extending to heights exceeding 2000 m overlying more stable air near the ground. When z_i reached the near-neutral layer, its growth accelerated sharply. It was considered best to run before accelerated growth of z_i occurred on such days, or else to not run at all. For CONDORS 83 the behavior of z_i with time was predicted to some extent on the basis of morning temperature soundings, using the model developed by Wilczak and Phillips (1984).

Another important parameter for this study is the convective scale velocity,

$$w_* \equiv (z_i \, H_*)^{1/3} , \tag{2.1}$$

where

$$H_* = (g/T) \, \overline{w'T'} \tag{2.2}$$

at the surface, preferably an area average. This velocity has been shown to be the chief determinant of horizontal and vertical turbulent velocities in

strongly convective mixing layers (Kaimal et al., 1976). H_* is proportional to the surface heat flux, which itself is approximately proportional to solar insolation, so this quantity maximizes near solar noon on clear days. During such days, H_* is constant, for practical purposes, between 1000 and 1400 solar time. Incidentally, the BAO site stands only 1/300 of a degree west of 105°W longitude, so standard time at the site (Mountain Standard Time) is within one second of solar time. During this midday period, if the relative growth of z_i is slow, the relative growth rate of w_* is even slower, since it depends only on $z_i^{1/3}$. Generally, w_* maximizes in the early afternoon, when the growth of z_i counterbalances the diminution of H_*. Under ideal conditions, the best hours for this experiment were expected to be between 1200 and 1400 MST. Conditions could be degraded by a near-neutral temperature stratification above z_i, a sudden increase in cloudiness, and, of course, more dramatic meteorological event, such as a front or a nearby thunderstorm.

Another important factor to consider was the mean wind speed, $\overline{u}$. If $\overline{u}$ is too large, wind shear plays too dominant a role in the organization of convective elements, and mechanical production of turbulent energy competes with convective production. This experiment focussed on highly convective conditions, which occur only during low wind speeds. However, if $\overline{u}$ is too small, longitudinal diffusion becomes another influencing factor. In addition, when $\overline{u}$ is of the order of w_*, lateral turbulent velocities also are of the order of $\overline{u}$, and the plume goes through very wide swings, which could cause some observational problems for the lidar. According to Deardorff and Willis (1975), longitudinal diffusion has little effect when $\overline{u}$ exceeds 1.5 w_*. This criterion would also exclude excessively wide plumes, since the lateral velocity standard deviation in a convective boundary layer is about 0.6 w_*.

At midday on sunny days in the fall, we can expect H_* to range between 40 and 70 cm^2/s^3. For z_i ranging between 500 m and 1200 m, we can then expect w_* values ranging between about 1.3 to 1.9 m/s, the higher values occurring chiefly with higher z_i. Therefore, the minimum desirable wind speed is 2 to 3 m/s, at upper tower levels. A slightly smaller $\bar{u}$ would not be seriously detrimental, but a $\bar{u}$ of only 1 m/s would present both observational and interpretational difficulties.

The maximum acceptable wind speed is determined by the ratio $-z_i/L$, where

$$L = -u_*^3/kH_* \tag{2.3}$$

is the Obukhov length, and

$$u_* = (-\overline{u'w'})^{1/2} \tag{2.4}$$

(measured at the surface) is the friction velocity. At the very minimum, $|z_i/L|$ must exceed the order of 10 to avoid organized convective rolls and to get into a more horizontally isotropic regime. Isotropic convection with little influence from wind shear is likely for $|z_i/L|$ exceeding about 50 (Deardorff, 1972). To translate these ratios into $\bar{u}$ values, a wind profile analysis is needed. In an unpublished analysis of the Minnesota 1973 experimental data, Briggs (1977) suggested a very simple wind profile law that fit the data at least as well as the more well known profile laws:

$$k\bar{u}/u_* = \ln z/z_o', \tag{2.5}$$

where

$$z_o' = z_o(1 - 4z/L)^{0.6} . \tag{2.6}$$

This holds up to about $z = 0.2\ z_i$ ($-z/L$ values as large as 30), above which there is negligible wind shear. Table 1 is based on this profile law applied to $z = 0.2\ z_i$, and assumes that $k = 0.4$ and the roughness length $z_o = 3$ cm.

Table 2.1 Typical mean wind speeds for different values of z_i/L

z_i(m)	H_* (cm^2/s^3)	$z_i = -10\ L$	$z_i = -50\ L$
1000	70	$\bar{u}$ = 12.2 m/s	6.3 m/s
500	50	$\bar{u}$ = 7.9 m/s	4.0 m/s

The criterion $|z_i/L| > 10$ was easily satisfied by the prevailing wind speeds at the BAO (see Sec. 2.3), but $|z_i/L| > 50$ requires $\bar{u}$ values half as large. The ideal range of wind speeds at tower top level is roughly 3 to 6 m/s for the larger acceptable z_i values, and 2 to 4 m/s for z_i values in the 500 m range.

Two considerations affected optimum siting of the lidar and radar units. One was the most favorable wind direction sector, which was discussed in Sec. 2.3. The other was the distances of greatest interest downwind of the source, especially for improvement of diffusion modeling. Very close to the source, the distribution of the time-averaged elevated plume is determined by the distance, x, times the wind angle distribution; this is just the "waved garden hose" effect, and does not require special study (the plume concentration isopleths here can be inferred from the sonic anemometer wind statistics measured on the tower). The ground source plume initially behaves similarly in its lateral spread, and its vertical spread is a function of x, z_0, and L; this, too, has already received much study (Briggs, 1982). The distances of most interest are those where the ground source plume departs radically from a Gaussian vertical distribution, with its maximum value leaving the ground, while the elevated source plume comes down to the ground. An idea of these distances can be obtained from Fig. 2.3, which is based on the laboratory tank

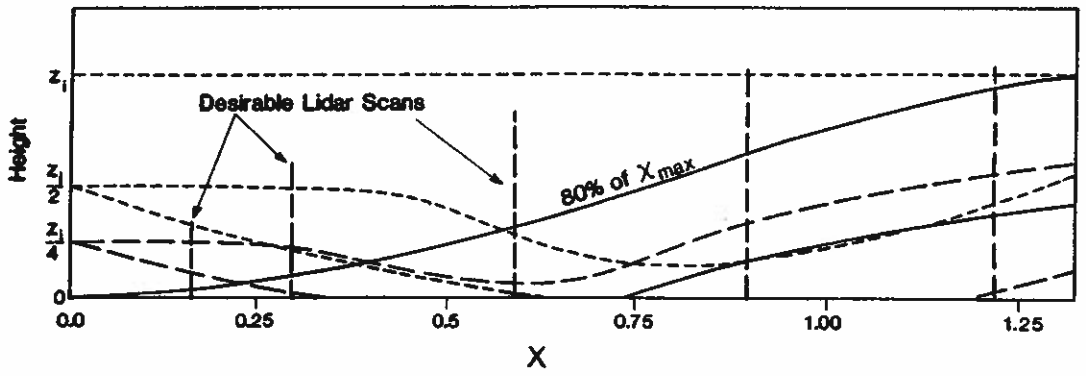

Figure 2.3. Plume transport according to Willis and Deardorff (1976a, 1978, 1981) for different release heights. Desired lidar scans are shown superimposed.

experiments (Willis and Deardorff, 1976a and 1978). In this representation the time of travel, $t = x/\bar{u}$, or time after release in the tank, is nondimensionalized by the characteristic time for turbulent motions to traverse the mixing layer depth, z_i/w_*. Thus the nondimensional distance is

$$X = (x/z_i)(w_*/\bar{u}) \ . \tag{2.7}$$

In terms of X, the ground source plume begins a rapid growth stage at about 0.3, and its height of maximum concentration begins to leave the ground at 0.6. By the distance 1.2, the maximum concentration reaches the upper half of the mixing layer, and the ground concentration is reduced to less than half the maximum; by the distance 3, concentrations vary less than ±10% in the vertical, having become well mixed through the depth of the mixing layer. For the elevated sources at $z/z_i \approx 1/4$ and $1/2$, high concentrations begin reaching the ground at X = 0.3 and 0.5, and remain at the surface until about 0.8 and 1.0, near which point the plumes begin to re-elevate. For the source at $z/z_i \approx 1/4$, the concentration again becomes very well mixed by X = 3, but there is still

about ±15% variation at this distance for the source at $z/z_i \simeq 1/2$. One result from the laboratory experiments that is quite surprising, and begs further confirmation, is that at $X \sim 1$ the ground concentration produced by an elevated source can be up to three times <u>larger</u> than that produced by a ground source of the same strength.

For the purposes of CONDORS, the most critical range of distance was between $X = 0.3$ and 1.2. Since estimates of the parameters before each run were imprecise, and since the plumes in the atmosphere may behave differently from the laboratory plumes, we extended this range at least a factor of 2 each way, from $X = 0.15$ to 2.4 (for $z/z_i = 0.5$ chosen as a source height, $X = 0.25$ would be an acceptable minimum distance). To translate these distances into dimensional distance, use $x = X(z_i\overline{u}/w_*)$. For the upper end of the acceptable z_i range, $z_i \simeq 1000$ m, $w_* \simeq 1.9$ m/s, and acceptable $\overline{u}$ ranges from 3 to 6 m/s, so $(z_i\overline{u}/w_*)$ ranges from about 1.5 to 3.2 km. For the lower end of the expected z_i range, $z_i \simeq 500$ m, $w_* \simeq 1.4$ m/s, and acceptable $\overline{u}$ ranges from 2 to 4 m/s, so $(z_i\overline{u}/w_*)$ ranges from about 0.7 to 1.5 km. Accepting some truncation of the desired distances in the extreme cases, it appeared that the radar and lidar units should be sited so that good observations could be obtained in the range $x \simeq 0.2$ km to 6 km. However, in a given run, a smaller geometric range was sufficient. In practice, an x less than 6 km was needed to adequately distinguish the diffused oil fog from the haze in the mixed layer. The height chosen for release, the mid-run estimated value of $(z_i\overline{u}/w_*)$ and the maximum x for adequate detection determined the azimuth angles chosen for lidar cross sections.

2.7 Remote Sensor and Sampler Siting

With the foregoing distance ranges in mind, as well as the expected most prevalent wind directions (50° to 105°), it was possible to consider some possible siting choices for the lidar and radar units. These are shown on the topographic map (Fig. 2.4) of the BAO site and surroundings. As a somewhat arbitrary starting point, for the lidar site it was desired that the angle between the site, the tower, and the plume axis be larger than 45° when the wind

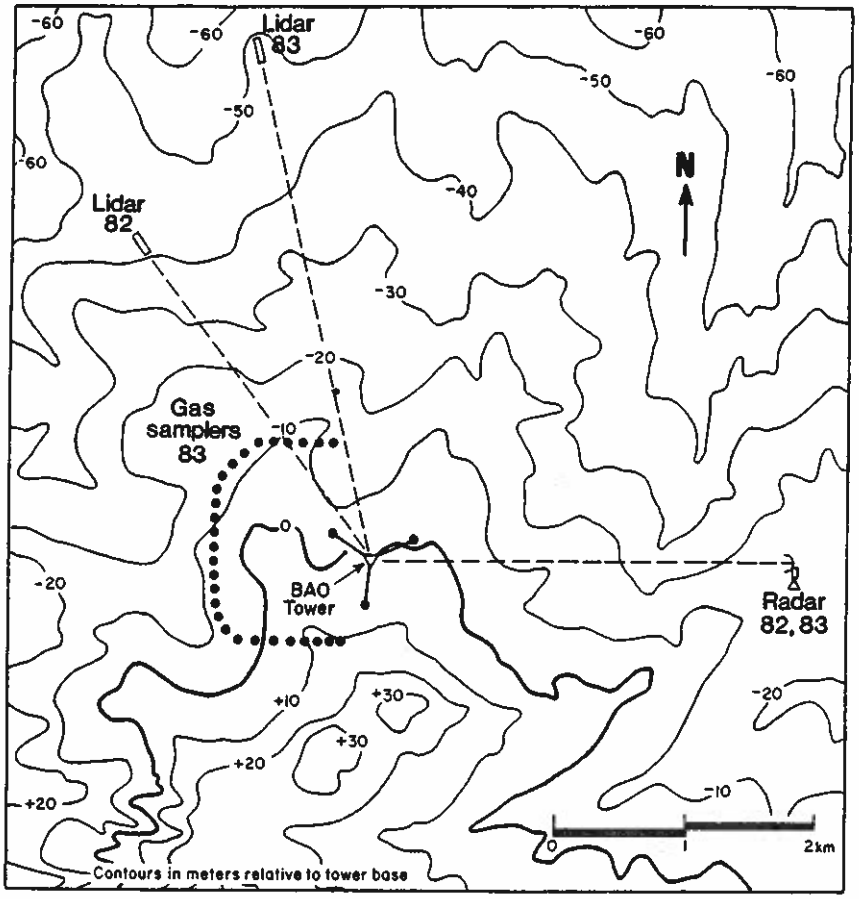

Figure 2.4. Contour map of the BAO site and vicinity showing location of lidar, radar and surface samplers for the CONDORS experiments. Contours are indicated in meters referenced to tower base.

was from the above sector. There is wide variability in the largest axial distance of interest (X = 3 may range from 2 to 10 km) so another criterion was that the angle between the tower, 6 km downwind, and the lidar site be greater than 30° when the wind was from the above sector. This generally assured a lidar shot angle greater than 45° across the plume axis within distance ranges of most interest (X < 1.2). Of course, a 90° angle is ideal, but some compromise was necessary. The net result of the above criteria was that the lidar should be located about 3-4 km to the NNW or S of the tower (see Fig. 2.4). The site chosen for CONDORS 82 was 3.0 km at 324.8° azimuth from the tower. For CONDORS 83 a location 4.05 km away at 345.9° azimuth was chosen for better lateral perspective of the plumes. Both locations are indicated in Fig. 2.4.

Attenuation of the beam by the tracer material is not a problem for the radar, so its siting with respect to the plume axis was chosen to minimize the solid angle scanned. A position upwind of the plume source was best in this respect. Near the source, the minimum acceptable plume resolution is about one-third of the elevated plume source height, which could be as low as 150 m. To resolve 50 m with a 0.8° beam, the radar had to be less than 3.6 km from the tower. Because the plume grows much wider and deeper after a few kilometers travel, much coarser resolution is acceptable farther away, and is not a limitation. When the radar is located approximately 3.5 km upwind of the tower, and if the maximum range of interest is 6 km downwind, the range to the target varies by approximately a factor of 3, and the $1/r^2$ signal decrease due to range varies by a factor of 9. Moreover, plume concentrations may vary by a factor of 1000, with highest concentrations near the source. The net

effect, a factor of 10^4 in signal strength between near and far ranges, is well within the 10^6 dynamic range of the radar electronics. Thus, the site finally chosen for both CONDORS 82 and CONDORS 83 was 3.5 km east (90.4° azimuth) of the tower (see Fig. 2.4).

With easterly winds, there is only one road west of the tower that provided good access to a line of samplers. It is a north-south road about 1.2 km west of the tower, an appropriate distance for plume interception. With elevated source heights ranging from about 150 m to 300 m, and $\bar{u}/w_*$ ranging from about 1.5 to 3, the high concentrations from the elevated plume were expected to reach the ground by this distance nearly all the time. The smallest σ_y value expected at x = 1.2 km within the acceptable ranges of $w_*/\bar{u}$ and z_i without shift in wind direction was about 150 m. The lateral distribution of the plume as it crossed this road could be adequately defined with samplers set about 100 m apart, or at about every 5° of bearing from the tower in the range 205° to 305° (21 samplers along a 3.4 km line).

An example of a typical pattern for lidar scans and radar sweeps of the plume is shown in Fig. 2.5. For purpose of concrete illustration, we assumed that $z_i\bar{u}/w_* = 1.5$ km and $z_i = 800$ m. The radar sweeps are not at a constant elevation along the plume centerline because they are made at a constant elevation angle, and the distance to the plume varies. The azimuth angles of the lidar scans were chosen with closer spacing at small distances, to get more detail in the descending and ground-hugging phase of the elevated source plume. Since it was always desirable to make a scan crossing the plume axis at the same distance as the arc of surface samplers, one lidar azimuth was dictated by only the plume (wind) direction.

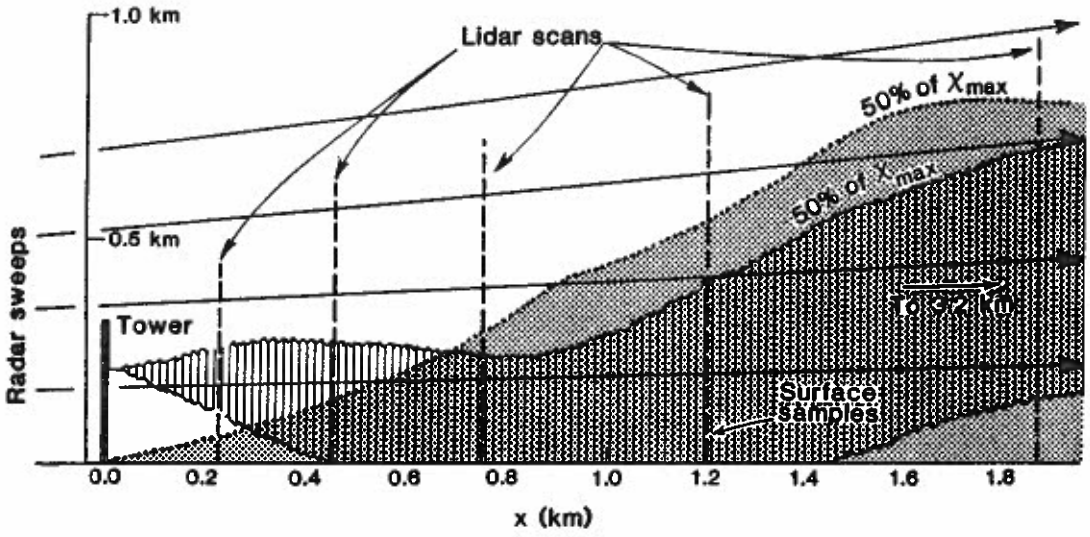

Figure 2.5. Typical patterns for lidar scans and radar sweeps for the CONDORS experiments shown in relation to expected plume behavior. Surface gas sampler location indicated at 1.2 km distance from tower base.

3. LIDAR SENSING OF OIL FOG

W. L. Eberhard and S. W. Troxel

3.1 The Lidar Technique

The lidar measures the position of the oil fog plume and the concentrations of particles in it by performing a repeating series of vertical cross-sectional scans at discrete distances from the source. The concentration of the particles is inferred by measuring the fraction of transmitted light they scatter back to the receiving telescope. Collis and Russell (1976) provided a comprehensive, easily understood description and bibliography of lidar theory and operation. Signal processing must account for the effect of ambient haze, optical geometry, and system calibration on the raw signal. These adjustments to the signal yield the volumetric backscatter coefficient β_p, which is a characteristic of the composition and size distribution of the oil fog droplets as well as the mass loading. The spatial distribution of β_p provides valuable information on the location and shape of the plume. In CONDORS, sufficient data were also available to obtain an empirical calibration between β_p and mass concentration, which allowed us to estimate the absolute concentrations of tracer oil from the lidar data.

The equation of radiative transfer, or the "lidar equation", that describes the raw lidar signal is

$$P(R) = \frac{K_L}{R^2} [\beta_p(R) + \beta_a] \exp\{-2 \int_0^R [\sigma_p(R) + \sigma_a] dR\} , \qquad (3.1)$$

where R is range along the lidar line of sight, and K_L is the calibration factor that includes pulse energy, telescope aperture, optics efficiency, detec-

tor responsivity, and electronic amplification. β_p is the backscatter coefficient of the plume material, and β_a is the backscatter coefficient of the ambient molecules and haze particles. The exponential describes attenuation of the probing radiation on its round-trip path to R due to scattering and a much smaller amount of absorption. The extinction coefficient σ_p applies to the plume particles, and σ_a applies to the ambient haze, including both molecules and non-plume particles. While β_a and σ_a may be weak functions of R, averaged values were used for solving Eq. (3.1). Data processing consists of solving Eq. (3.1) for each lidar pulse to obtain β_p and then combining the many pulses in each scan into a format convenient to the atmospheric scientist.

WPL's lidar has participated in several plume experiments using oil fog as a tracer. These include EPA's Complex Terrain Model Development project (Eberhard, 1983; Venkatram, Strimaitis, and Eberhard, 1983) and DOE's 1980 ASCOT experiment (Gudiksen et al., 1984). Other lidar researchers have also used oil fog as a tracer, e.g., Uthe, Johnson, and Till (1979).

The configuration of the WPL lidar (Fig. 3.1) for CONDORS included a frequency-doubled Nd:YAG laser transmitter, Newtonian receiver telescope, and photomultiplier detector. The detector output was digitized and recorded on magnetic tape by the computer data-acquisition system for later processing. The energy in each pulse was measured and also recorded along with other essential information, such as pointing angle and time. The scan was controlled by computer but included the option for the operators to modify the scan without interrupting the data acquisition. Real-time displays allowed the operators to monitor the equipment for proper performance and report plume

Figure 3.1. Lidar system. The telescope with laser and detector mounted astride scanned in elevation angle at several azimuth directions downwind of the source. The observer disabled the laser whenever an airplane approached the laser beam. When not operating, the scan assembly retracts into the semitrailer, which also contains workbenches and storage space. The operator's console and computer data acquisition system are contained in the vehicle on the right.

position and height of the haze layer to other participants. Additional lidar specifications are listed in Table 3.1. The dynamic range of the linear detection system was optimized according to the peak plume concentration in each scan by adjusting calibrated filters in the receiving optics with controls at the operator's console.

Table 3.1 Lidar operating configuration for CONDORS

Wavelength	532 μm
Pulse energy	0.1 J
Pulse rate	10 s^{-1}
Beam divergence (full angle)	0.5 mr
Spatial resolution (FWHM)	7 m
Receiver aperture diameter	70 cm
Interference filter passband	1.0 nm
Detector quantum efficiency	0.13
Minimum sampling increments:	
Range	3.00 m
Azimuth	0.1°
Elevation	0.01°
Signal digitizer	linear, 256 levels

The most important and frequent quality assurance procedure was the calibration of the system sensitivity during equipment setup and at least once each week during the field phase. In this procedure, the light scattered from a standard, diffuse target is measured at a variety of system gain settings. The calibration tests were examined separately and together in order to discover any malfunctions or changes in the lidar's sensitivity. The absolute accuracy of the calibration for system sensitivity was judged to be within 30%. However, the conversion from β_p to mass concentration depended on the oil fog size distribution, which was not measured. Therefore, an empirical conversion factor was obtained by the method described in Sec. 3.5. During the 1983 experiment, a special check of the lidar's accuracy in range and

pointing angle was completed. Range and direction to several landmarks agreed within measurement accuracy with a commercial surveyor's report. The pointing direction to several celestial bodies also fell within expected limits. We are therefore confident that the lidar operated properly during CONDORS.

3.2 Oil Fog Tracer

The tracer for the lidar was a continuously released plume containing a large number of oil droplets with mode diameter of a few micrometers. The generator sprayed the oil into a jet of air that had been heated during flow through the fogger's kerosene furnace to a temperature well above the evaporating point of the oil. The combination of the mechanical breakup of the oil drops and the heat caused most of the oil to evaporate. When the jet cooled by mixing with the exterior air, the oil vapor condensed into small droplets.

During 1982 we used a commercially built fogger, Curtis Dyna-Products Corporation model 1200, designed for insecticide dispersal. The fogger is shown mounted on the BAO tower's instrument carriage in Fig. 3.2. The oil was a pale paraffin type ("Corvus 13", Texaco) that was expected to suffer insignificant evaporation after generation. The steady decline with downwind distance of the integrated signal in the cross section convinced us that evaporation still exceeded acceptable limits. We also found that the 35 g/s oil release rate did not provide sufficient plume signal above the ambient haze as far downwind as desired.

During 1983 two model 1200's were operated side by side for surface releases (Fig. 3.3). A considerably heavier (i.e., higher viscosity and lower

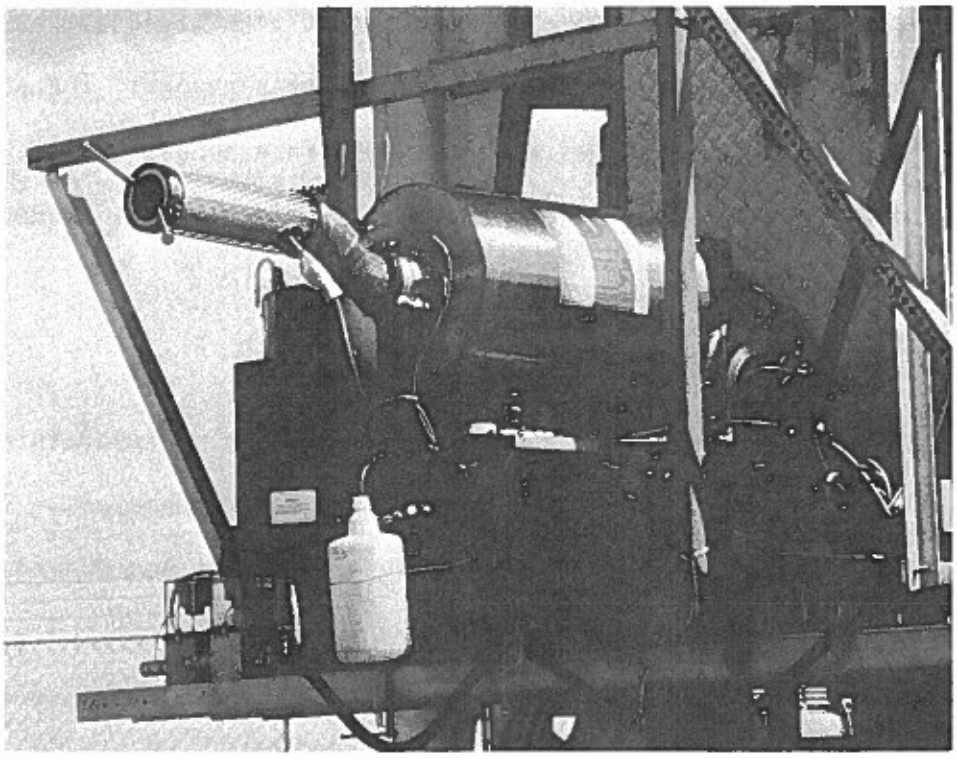

Figure 3.2. Oil fogger and chaff cutter on BAO carriage.

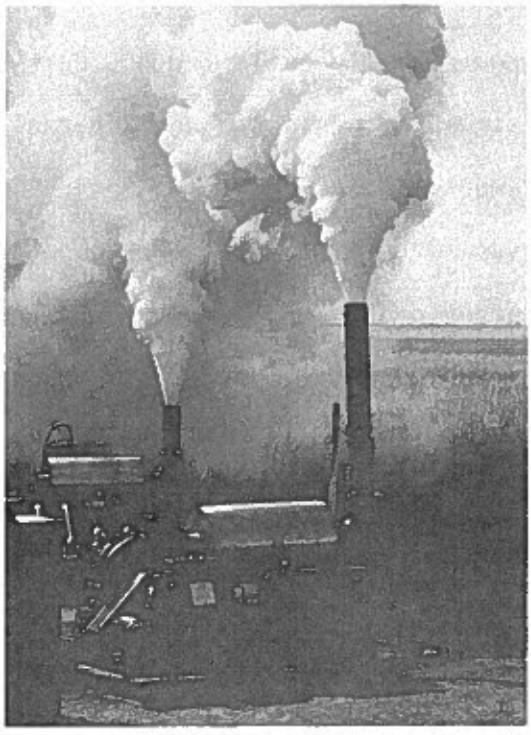

Figure 3.3. Oil foggers operating at high release rates during CONDORS 83.

vapor pressure) oil designed for use in hydraulic systems ("Rando", Texaco) was successful in producing a more conservative tracer. In order to spray sufficiently small drops into the air jet, we modified the oil fog generators to preheat the oil. Release rates from the combined pair of generators were as high as 72 g/s. Limited size and weight capacity of the tower carriage permitted operation of only one of the fogger units during elevated releases. Table 3.2 lists the periods of oil fog release and lidar plume scanning, including three periods that were cut short due to unfavorable wind shifts.

Table 3.2 Summary of oil fogger and lidar operation

Date	Release Ht.	Release Begin	Release End	Scan Begin	Scan End
9/10/82	Surface	1133	1252	1135	
		1254	1318		1321
9/16/82	235m	1247	1445	1250	1449
9/18/82	167m	1333	1505	1349	1511
9/20/82	Surface	1130	1316	1140	
		1318	1353		1355
9/21/82	Surface	1207	1238	1209	1236
9/22/82	Surface	1116	1125	1119	1130
8/26/83	Surface	1230	1350	1237	1349
8/27/83	Surface	1220	1430	1225	1433
8/28/83	Surface	1120	1330	1125	1335
8/31/83	Surface	1045	1255	1051	1259
9/ 6/83	285m	1040	1250	1044	1255
9/ 7/83	265m	1200	1410	1205	1414
9/12/83	Surface	1305	1510	1309	1514
9/13/83	Surface	1120		1124	1225
			1430	1237	1433
9/15/83	Surface	1025	1250	1027	1257

3.3 Lidar Scan Modes

In order to observe the dispersion of the oil fog plume, the lidar performed a series of vertical scans. Each pulse in a scan provided a profile of plume concentration along the lidar's line of sight. A cross section of the plume was obtained by recording the signal from a series of pulses while the elevation angle decreased from above the plume to very near the surface. A repeating sequence of scans at typically five discrete azimuth directions (Fig. 3.4) produced a description of the three-dimensional evolution of the plume.

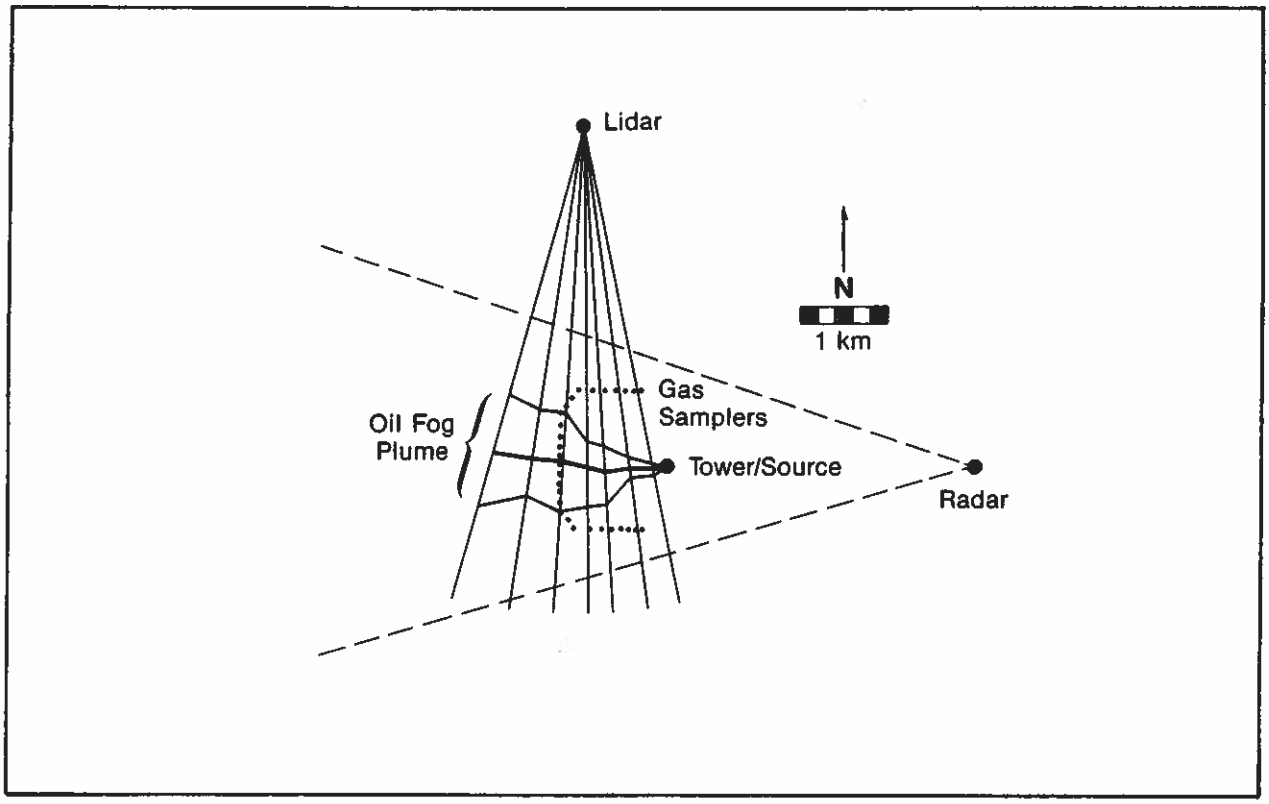

Figure 3.4. Experiment layout and lidar scan planes during Period 9. The centerline and edges (10% of cross section peak) of the vertically integrated oil fog plume averaged over the period are shown. The dashed lines delineate the azimuth limits of the radar scan.

After setting up the lidar, the lidar crew prepared a list of azimuth directions where the scan would avoid trees and other tall obstructions. From this list the azimuth directions for the day were selected just prior to tracer release. Scans were kept above the local horizon because the laser radiation was not eyesafe at typical ranges to the plume. A crew member acted as spotter and disabled the laser when an aircraft occasionally approached. The lidar operators adjusted the upper elevation angle to include the top of the plume as the mixing layer height increased or wind direction changed. They also adjusted the scan rate to intercept the plume with typically 100 pulses during each scan.

The vertical scan planes were usually not exactly in a cross section perpendicular to the plume direction. Instead, each scan was a slant section turned at some horizontal angle α from the plane normal to the plume direction. When α was less than about 30°, the slant section provided an excellent representation of the plume's cross section by projection onto the normal plane. Sometimes the angle was considerably larger; care must be taken in interpreting those data.

3.4 Solution to Lidar Equation

The first stage of data processing involved solution of the lidar equation (3.1) for each pulse to isolate the profile of β_p along the line of flight of the pulse. This stage is divided into five parts.

1. The system sensitivity factor K_L, determined during the calibration runs, was applied to each pulse. This result was then multiplied by the square of the range.

2. The signal profile in each pulse was corrected for the attenuation caused by the ambient haze. In order to determine σ_a, a representative sample of typically 20 pulses scattered over the analysis period was selected. The value of σ_a was calculated for each of these pulses over a range interval where no plume was evident. The average of these was used during processing on all pulses in the period. Although the attenuation coefficient did vary somewhat, our experience has shown that the average value provides more consistent and dependable results in the well-mixed layer than if we attempted to adjust σ_a within or between pulses.

3. A staff member edited each scan with interactive computer graphics (Fig. 3.5) in order to define the region where the plume was located. An area between the lidar and plume was also defined where the signal level from ambient haze was accurately measured.

4. Each pulse was corrected for extinction caused by the oil fog. Unlike the extinction by the haze, which was relatively uniform, the extinction by the plume varied with its density. We therefore found a representative value of extinction to backscatter ratio for each analysis period. A representative sample of pulses was chosen, and the transmission loss caused by the oil fog in each pulse was determined from the decrease in signal from the haze at ranges beyond the plume compared to ranges between the plume and the lidar. The extinction to backscatter ratio was calculated for the plume traversed by each of these pulses, and the results then averaged. During processing, this average ratio was multiplied by the measured plume backscatter to correct for extinction due to the oil fog (using (3.1), working from small to large R).

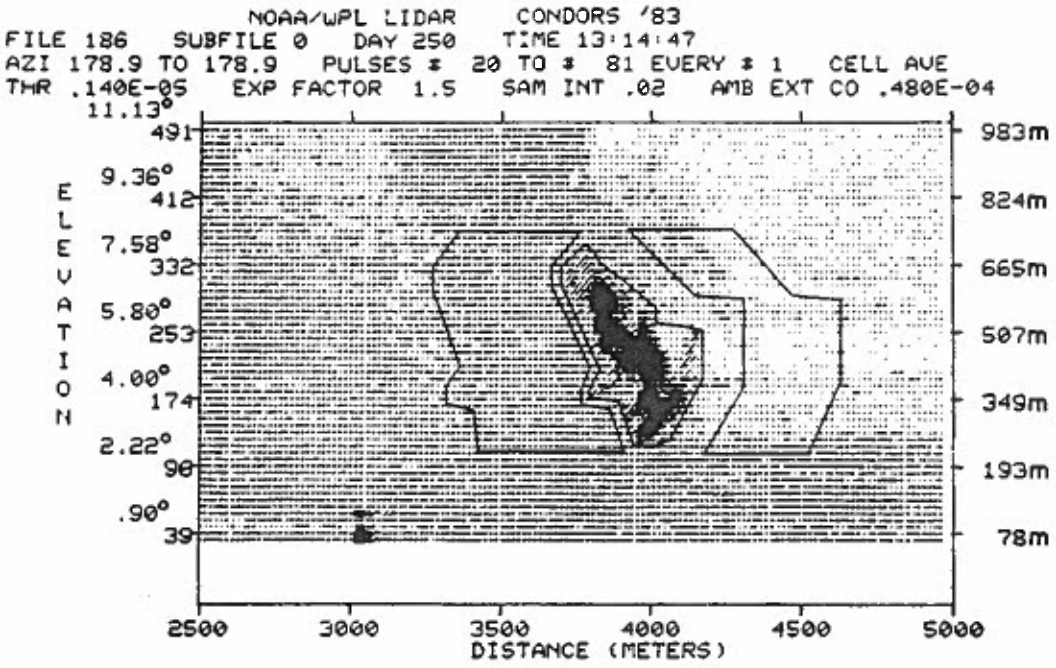

Figure 3.5. Display of lidar scan for editing. The profile of signal magnitude for each pulse after correction for calibration, range, and attenuation by ambient haze is displayed in a crude gray scale. The abscissa is distance n from the lidar, and elevation angles are marked on the ordinate. The height above the lidar of the probing pulse at the near and far distance limits of the display are also given along the vertical axes. Scan identifiers and processor selections of display settings are above the graph. The signal from the oil fog is surrounded by the plume box drawn by the processor in the center. The box to the left defines a region of plume-free haze signal. The box to the right is used only in determining signal to noise ratio. High voltage transmission lines caused the strong signal near the bottom at 3000 m distance.

5. At the same time, the average value of haze density β_a for each pulse (determined between the boundaries of the ambient region defined in step 3) was subtracted from the attenuation-corrected profile of the pulse, leaving the oil fog profile β_p. At all data points outside the plume box, β_p was set equal to zero.

Figure 3.6 shows an example of a pulse before and after steps 2 through 5 were completed except points outside the plume box are not yet zeroed. In

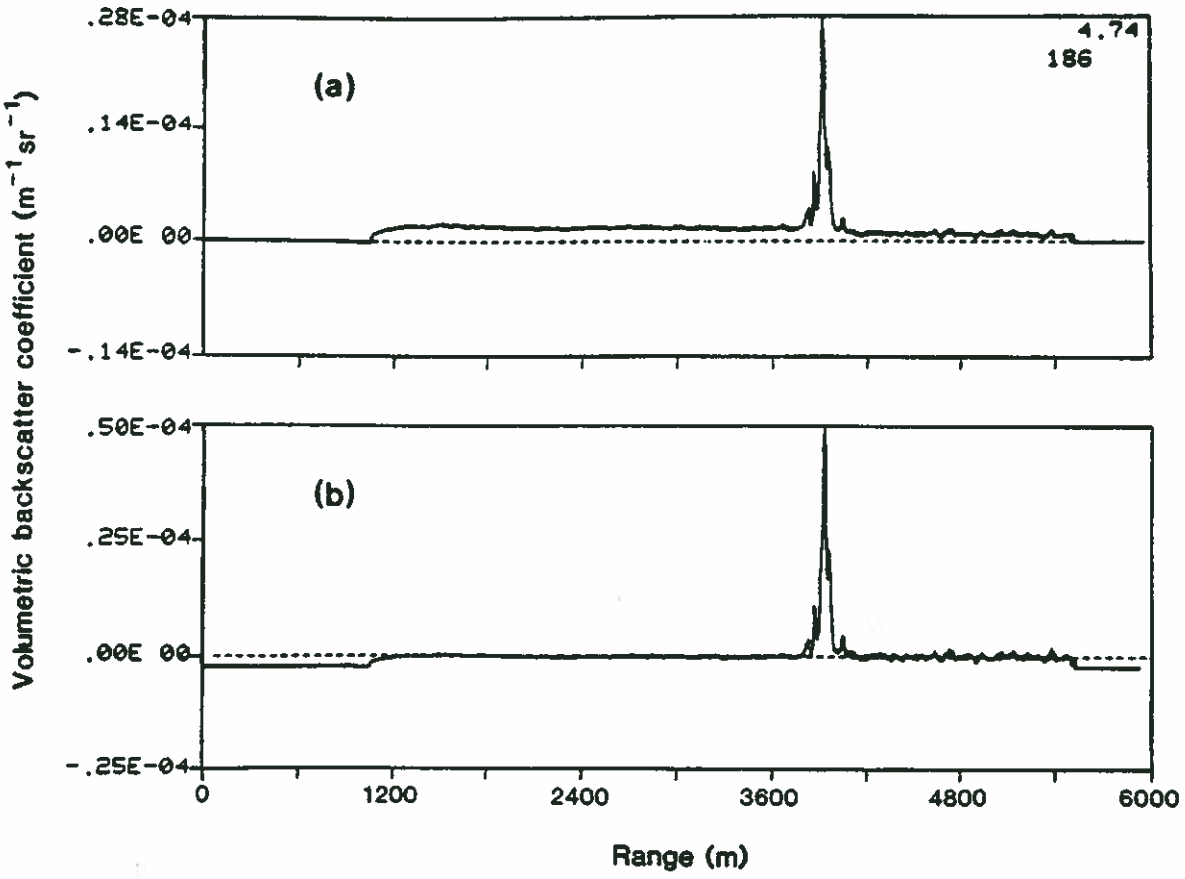

Figure 3.6. Lidar single pulse (a) before and (b) after corrections for attenuation and ambient signal. The bottom frame shows the corrected data, with the dashed line at zero β_p. The measured signal before 1000 m is zero because the detector was disabled to prevent strong saturation by the raw signal, which decreases with the square of the range. The digitizer recorded the signal to 5600 m, after which zeros were entered to fill a conveniently formatted data array. The numbers in the upper right corner are the elevation angle of the pulse and lidar file (i.e., scan) number.

this example the adjustments by σ_a, σ_p, and β_a all had a significant effect and achieved very satisfactory results.

The accuracy requirement for each step depended on the distance from the source. Near the source where the plume was dense and $\beta_p >> \beta_a$, error in β_a was easily tolerated. Since the range to the plume near the source varied

little with changes in wind direction, accuracy in σ_a was not crucial either. The σ_p correction is relatively important near the source. In convective conditions, however, we have found that the shape of the time-averaged plume depends more on the meander than on proper choice of σ_p. Far downwind, where diffusion had made the oil fog signal weak compared to the haze signal, accuracy in the choice of σ_a and β_a was much more critical. Here, attenuation by the oil fog was a minor factor.

The greatest deficiencies in the oil fog data were near the surface and at the top of the mixed layer. Because of eye safety constraints and blockage by intervening terrain, we could not measure plume concentrations in the first few tens of meters above the surface. When strong vertical gradients in average plume concentrations were not present, an extrapolation of concentrations from the bottom of the scan to the surface was reasonable. At the top of the mixed layer, changes in haze concentration made it difficult to properly separate β_p from β_a. Usually the haze signal decreased in the transition from mixed layer to cleaner air above. Near the end of the measurement run on a few days, however, hygroscopic growth of aerosols led to an increase in β_a and even small clouds at the top of thermals. Averaged scans that contained strong hygroscopically enhanced haze signals have been edited from the data reported here. Although the accuracy of the oil fog profile at the top of the mixed layer is questionable, the overall vertical profiles were not seriously affected by haze.

The scan was difficult to edit properly when the plume enveloped the high voltage lines, that ran along an east-west line very near the northern straight leg of the gas sampler arc. The processor had to either include the

signal scattered by the wires in the plume box along with all of the plume signal in the pulse, or else exclude part of the oil fog signal with the wires. In the latter case, the part of the plume that was only on one side of the wires or the other could be enclosed in the plume box. When the plume near the wires was dense, the wire signal was usually included; when the plume was diffuse, the wires and the smaller fraction of the plume were excluded. This was a problem only for the low elevation angles, or a maximum of about 70 m above the lidar at azimuths pointed near the BAO tower. The affected plume area was small, so the plume integrals were not significantly affected. The near-surface averaging layers were raised, when necessary, to exclude power line contamination.

3.5 Preparation of Data

The second stage of processing included several steps to prepare the data on β_p, or inferred oil fog concentrations, for interpretation and comparison with theory and models. This stage consisted of converting to a more convenient coordinate system, averaging scans, and then calculating profiles and plume descriptors.

The lidar operated in a spherical coordinate system (range, azimuth angle, and elevation angle) with the lidar at the origin. We elected to first convert data through a bi-directional interpolation scheme to a two-dimensional Cartesian system in the vertical plane of each scan, with the lidar at the origin. As a practical matter, the vertical and horizontal grid spacings were automatically set for each scan to encompass the plume area that was defined during the editing phase of the processing (Fig. 3.4). The Cartesian array

typically had 65 grid points in the vertical and 100 in the horizontal. Results were recorded on digital magnetic tape and plotted on graphs.

The various scans at the same azimuth for an analysis period were averaged together with a grid spacing of 50 m, or sometimes smaller near the source. Interpolation was performed when grid points of the individual scans did not exactly coincide with those of the chosen averaging array. Tapes and graphs of the average two-dimensional arrays were made in a manner similar to the individual scans.

Figure 3.7 shows a routine example of an average array graph and its associated profiles and plume descriptors. The vertical profile was obtained by integrating the average array horizontally, and the horizontal profile by integrating vertically through the plume. The zero, first, and second moments of each profile were calculated. The zero moment gives the total optical signal from the oil fog in the scan. The first moments give the coordinates of the plume's centroid. The second moments are a measure of the vertical and horizontal size of the plume. The moments are tabulated under the graph in Fig. 3.7. The position of the plume's centroid is given in three coordinate systems: distance (η), height, and azimuth θ_L from the lidar; distance, height, and azimuth from the source location; and distance, height, and azimuth from the origin of the "user coordinates", which was the base of the tower. The second moment of the vertical profile ("sigma vertical" in Fig. 3.7) is the vertical dispersion coefficient. The projection angle α shows how close the scan azimuth was to the perpendicular to the plume direction. Multiplication of "sigma horizontal" in Fig. 3.7 by cosine(α) gives the horizontal dispersion coefficient.

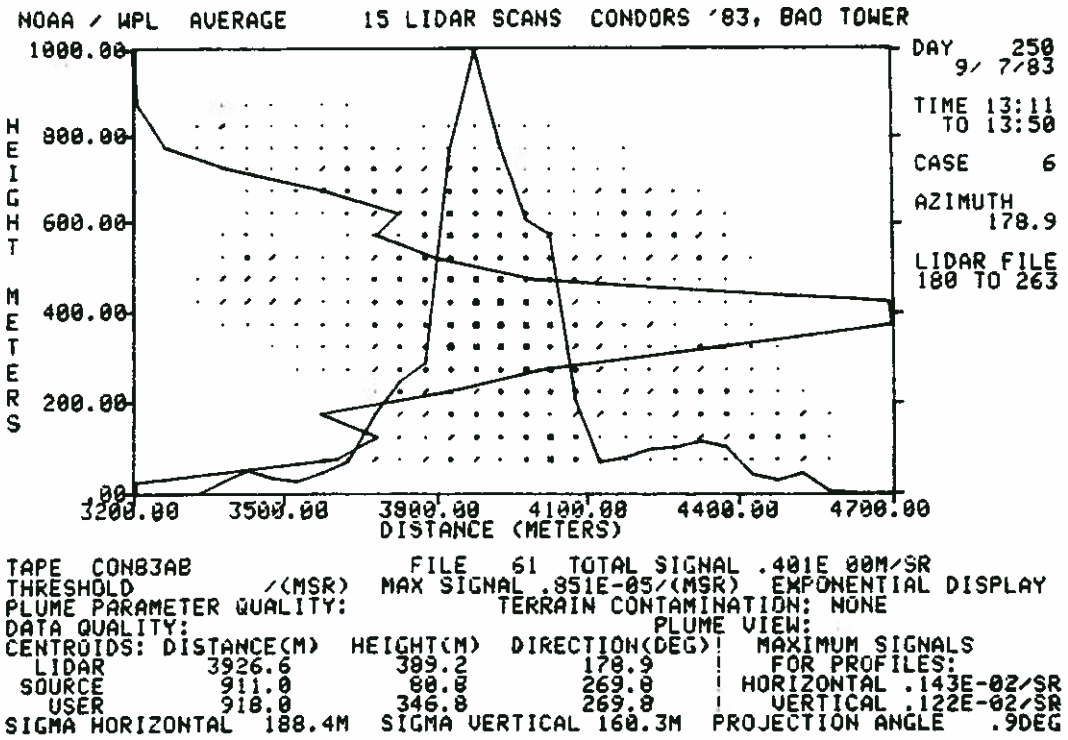

Figure 3.7. Average oil fog concentrations at one azimuth for an analysis period. Coordinates are relative to the lidar, with description of incorporated data (including 178.9 degree azimuth) listed at the upper right. The larger/darker pixel symbols indicate greater concentration. The sharp peak of the horizontal profile appears at the top center of the graph with zero at the bottom axis; the value at the peak is listed near the lower right. The vertical profile is plotted with zero at the left axis and two nearly identical values at the peak on the right. The text explains the centroids, sigmas, and projection angle.

An empirical calibration of β_p with oil fog mass was obtained by assuming mass was conserved and defining

$$K_0 = \left[\int_0^\infty \int_0^\infty \beta_p dz d\eta\right] U \cos\alpha/Q \ , \qquad (3.2)$$

where Q is the oil release rate. The value of K_0 versus downwind distance of the centroid is plotted for several periods in Fig. 3.8. If the optical properties of the oil fog were independent of travel time and fogger settings, the plots should be approximately straight and overlap. The decline with

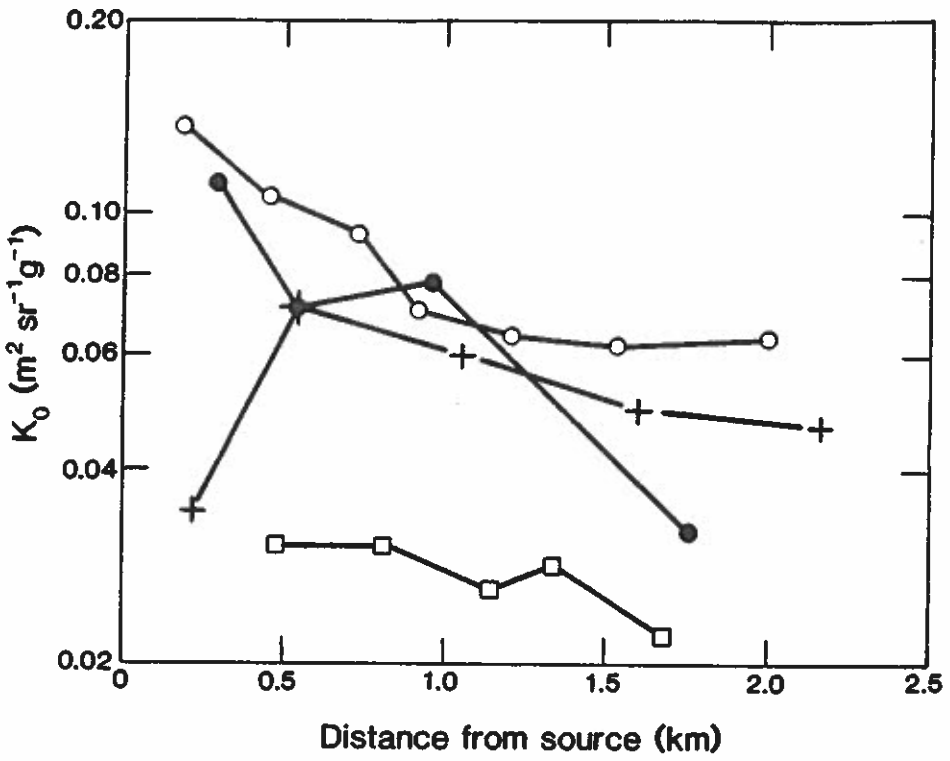

Figure 3.8. Example of empirical lidar calibration factors for oil fog mass concentration. (+) Period 2-83 with surface release of high viscosity oil at high rate. (o) Period 9-83 with elevated release of high viscosity oil at moderate rate. (□) Period 7-83 with elevated release of high viscosity oil at low rate. (●) Period 1-82 with elevated release of moderate viscosity oil at high rate.

downwind distance we attribute mainly to evaporation of the oil droplets. The decline was less severe in 1983 when we used the heavier oil with lower vapor pressure. Deposition loss is believed small in comparison. Some of the decline is probably caused by loss of diffuse parts of the plume in the haze. The initial increase in K_0 near the surface release is the result of missing a significant portion of the plume below the lower scan limit. The vertical displacements of the curves are caused by differences in the evaporation rate, by changes in the release conditions that alter the size distribution, and by errors in the lidar calibration and in measurement of oil release rate.

3.6 Equations in Lidar Processing

Listed here are the mathematical definitions of the data reported in Chapter 8 and in Appendix A. The equations appear in the discrete form applicable to the digital storage format. The beginning point is the rectangular array of $\beta_p(\eta_i, z_j)$, which are the average volumetric backscatter coefficients of oil fog at one azimuth. CONDORS averaging periods ranged from 29 to 60 min and typically contained 11 individual scans at each lidar azimuth.

The total backscatter in the array is

$$\beta_{p,\eta z} = \sum_i \sum_j \beta_p(\eta_i, z_j)\Delta\eta\Delta z \ , \tag{3.3}$$

where $\Delta\eta$ and Δz are the grid spacings in the horizontal and vertical directions, respectively. The horizontal and vertical profiles in Table A.1 are normalized to total 1000 when the standard grid spacing of 50 m is used. The normalized horizontal and vertical profiles are

$$\chi_z^n(\eta_i) = 1000 \frac{50 \text{ m}}{\beta_{p,\eta z}} \sum_j \beta_p(\eta_i, z_j)\Delta z \ . \tag{3.4}$$

$$\chi_\eta^n(z_j) = 1000 \frac{50 \text{ m}}{\beta_{p,\eta z}} \sum_i \beta_p(\eta_i, z_j)\Delta\eta \ . \tag{3.5}$$

Note that profiles presented with a spacing finer than 50 m will total to a larger amount, e.g., 2000 for 25 m spacing. This was done so the listed normalized concentrations would be the same for identical profile concentration irrespective of the grid spacing.

The height of the centroid above the surface (i.e., the base of the tower) is

$$\bar{z} = \sum_j z_j \chi_\eta^n(z_j) / \sum_j \chi_\eta^n(z_j) \ . \tag{3.6}$$

The height of the centroid above the release, or $\bar{z}_s$, is obtained by subtracting the release height from $\bar{z}$. The distance between the lidar and the centroid is

$$\bar{\eta} = \sum_i \eta_i \ \chi_z^n(\eta_i) / \sum_i \chi_z^n(\eta_i) \ . \tag{3.7}$$

A coordinate transformation on the point defined by $\bar{\eta}$ and the lidar azimuth θ_L produced the distance $\bar{\rho}_s$ and direction $\bar{\theta}_s$ of the centroid from the source. For surface releases, which were sited 141 m WNW (288°) of the tower, the position of the centroid in the horizontal plane from the tower are also reported as $\bar{\rho}$ and $\bar{\theta}$. The centroid coordinates are reported in Tables 8.1 to 8.16.

The second moments of the profiles are also reported in the same tables. The vertical dispersion coefficient σ_z is defined by

$$\sigma_z^{\,2} = \sum_j (z_j - \bar{z})^2 \ \chi_\eta^n(z_j) / \sum_j \chi_\eta^n(z_j) \ . \tag{3.8}$$

The horizontal dispersion coefficient σ_y was estimated by calculating σ_η according to

$$\sigma_\eta^{\,2} = \sum_i (\eta_i - \bar{\eta})^2 \ \chi_z^n(\eta_i) / \sum_i \chi_z^n(\eta_i) \tag{3.9}$$

and projecting onto the plane normal to the plume direction according to

$$\sigma_y = \sigma_\eta \cos\alpha \ , \tag{3.10}$$

where

$$\alpha = |\bar{\theta}_s - (\theta_L + 90°)| \ . \tag{3.11}$$

The empirical calibration factor K_0 was calculated according to (3.2) and listed in Tables 8.1 to 8.16.

The height where the maximum in the vertical profile occurred was obtained from the version of the profile with the finest vertical spacing; a profile

with coarser resolution will show the maximum at a slightly different height, or possibly a substantially different height in multi-peaked profiles. All parameters in Tables 8.1 to 8.16 are for the data resulting from routine processing, except z of $(X_\eta)_{max}$, which also incorporated the following adjustment to the lowest useable data point.

When a scan covered most of a layer in the vertical profile, but missed the far lower corner, a correction to X_η^n was estimated and listed in Table A.2. The correction considered the fraction of the layer not scanned and also the slight diagonal slope of the bottom pulse in each scan. Scans in each average were first selected that showed significant oil fog within the layer. The average of the lowest elevation angles in these scans was calculated, yielding $\bar{\varepsilon}_\ell$. The addition to the value of $X_\eta^n(z_j)$ was

$$\Delta X_\eta^n(z_j) = X_\eta^n(z_j) \left[\frac{\Delta z}{z_j + \Delta z/2 - \eta_c \tan \bar{\varepsilon}_\ell} - 1\right] + X_\eta^n(z_j - \Delta z) , \quad (3.12)$$

where η_c is the distance from the lidar to the center of mass of the horizontal profile near the surface (the last term in (3.12) was nonzero only when some pulses grazed the near upper corner of the layer below). In a few cases $\Delta X_\eta^n(z_j)$ was slightly negative; in such cases, no correction was applied. When the scans all terminated in the upper part of a layer, no attempt was made to adjust the vertical profile. Of course, if the adjusted data point is used, the total X_η^n in the profile is no longer 1000.

The near-surface profiles in Appendix A provide our best estimate of surface concentrations of oil fog by assuming that a negligible gradient existed from the surface to the lowest layer fully scanned by the lidar, typically

encompassing 25 to 75 m above the surface. The profiles in Table A.3 are expressed in terms of dilution factors using the empirical mass-backscatter calibration K_0 for the same averaged scans. Thus, in continuous form,

$$\chi(n)/Q = \frac{1}{K_0 Q(z_u - z_b)} \int_{z_b}^{z_u} \beta_p(n,z)dz \ , \qquad (3.13)$$

where z_b and z_u are the bottom and upper limits of the horizontal strip near the surface that was encompassed by all of the scans. The actual integration was accomplished with the scan-averaging computer program with only one grid point in the vertical with $z_j = (z_u + z_b)/2$ and $\Delta z = z_u - z_b$.

4. RADAR SENSING OF ALUMINIZED CHAFF

W. R. Moninger and T. Uttal

4.1 The Radar Technique

Doppler radars traditionally have been used to study clouds and precipitation. In the last few years, however, such radars have proven to be equally useful in the study of the clear planetary boundary layer using a combination of natural targets and artificial chaff. This technique has been utilized in the study of the transport and dispersion characteristics of a plume of microwave-reflecting chaff from a continuous point source (Moninger and Kropfli, 1982). The NOAA X-band radar and the data processing techniques that were deployed in the CONDORS experiment are described in this chapter.

The X-band Doppler radar (see Fig. 4.1) operates at a wavelength of 3.22 cm, with a peak transmitted power of 20 kW, a pulse duration of 1.0 s and a beamwidth of 0.8°. The radar acquires data in pulse volumes, beams, sweeps and volume scans. The pulse volume is determined by the duration of the transmitted pulse and by the angular width of the antenna. With the antenna stationary, a pulse has a volume 90 m in depth and 0.8° (0.014 radians) in diameter. The pulse volume, V, is:

$$V = \pi \, (0.007 \, R)^2 \, (90 \text{ m}) \, , \qquad (4.1)$$

where R is the range referenced to the radar. If the antenna is moving through an azimuth angle θ_r (radians), the pulse volume is also a function of the antenna motion that smears the pulse volume through space. The distance x that the volume moves during a pulse is:

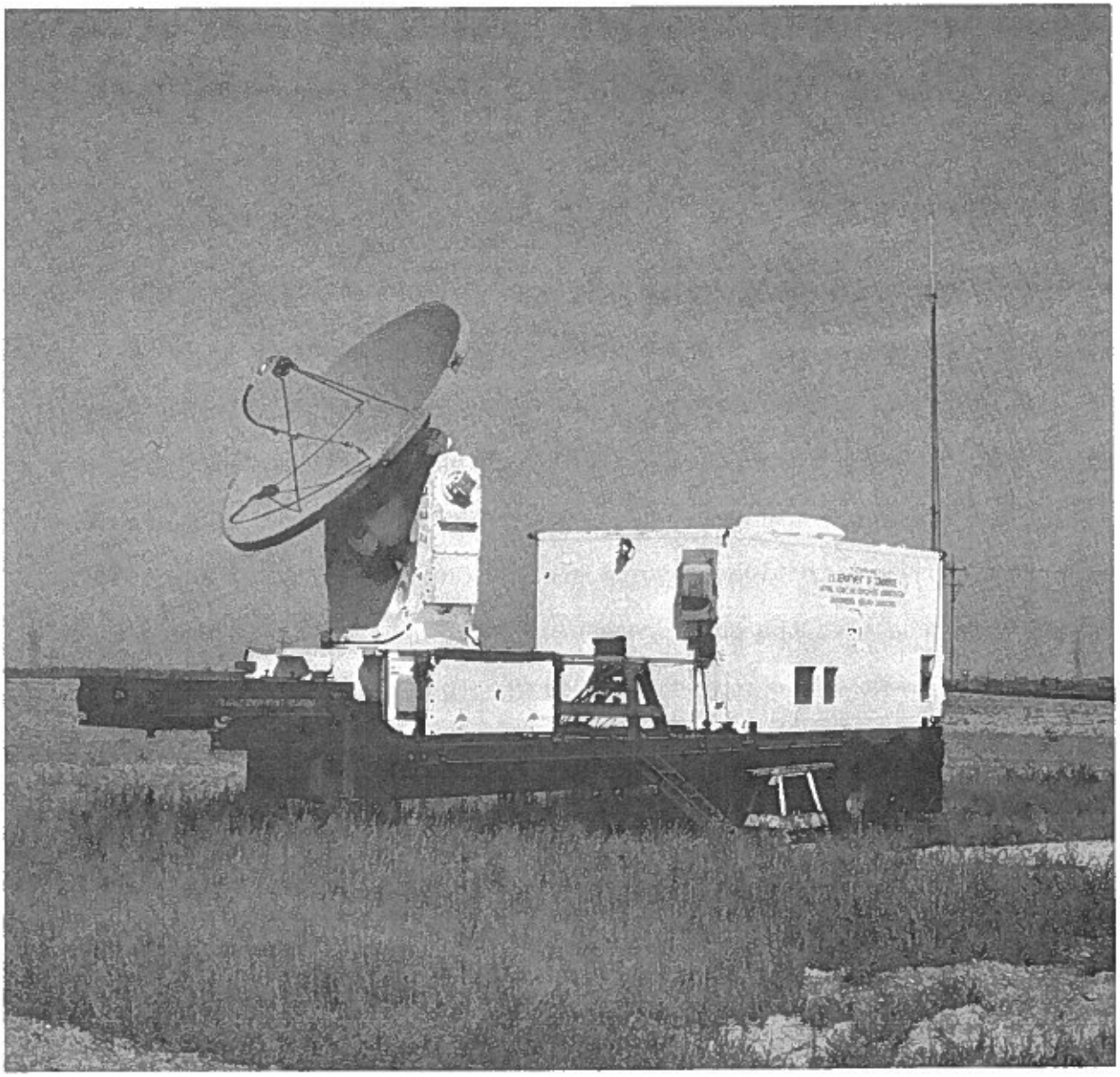

Figure 4.1. Wave Propagation Laboratory's X-band Doppler radar on location for the CONDORS experiments.

$$x = \frac{d\theta_r}{dt} R \times (\text{dwell}) \ . \qquad (4.2)$$

(Dwell is the time set for accumulation of pulse returns to constitute an adequate total signal.) Therefore, the actual pulse volume is an ellipse, 90 m deep, with volume:

$$V = \pi\ (0.007\ R)[0.007\ R + (\partial\theta_r/\partial t)\ \text{dwell} \cdot R/2]\ (90\ \text{m}). \qquad (4.3)$$

The second factor can be easily comparable in magnitude to the first given average antenna speeds and dwell times. (Typical dwell times multiplied by $d\theta_r/dt$ during CONDORS were 1.2°.)

Pulse volumes are acquired along a radial continuously to form a beam, and a beam of processed data is acquired approximately five times per second. A sweep is made up of all the beams acquired as the antenna sweeps at a constant elevation through an azimuth sector. A volume scan consists of a set of several sweeps at increasing elevations. In CONDORS, the plumes studied required between 9 and 27 volume scans to cover the period of interest. Each volume scan lasted approximately two minutes.

4.2 Clutter and Blockage

Ground clutter, or reflectivity from the topography and other objects surrounding the radar, is apparent at fixed locations in the lower elevation sweeps. Treatment of the ground clutter is discussed in Sec. 4.5. Blockage, a related problem, is caused by the physical shadowing of a portion of the beam by terrain. The site for the radar was purposely chosen so that the nearby horizon blocked the beam below approximately 0.5°. This was done to minimize ground clutter at the ranges where the plume would be located. However, this necessary constraint resulted in lost data below 0.5°; each beam in the lowest (0.5°) sweep was approximately 50% blocked. This caused an underestimate of plume concentrations near the ground.

4.3 Chaff Tracer

Chaff is composed of microwave reflecting filaments of aluminized mylar cut to 1.6 cm lengths to maximize the return for the X-band radar. The chaff cutter (see Fig. 4.2) produces 38,000 filaments/s, dispersed in a small air jet; however, a large fraction of these filaments clump together and fall quickly to

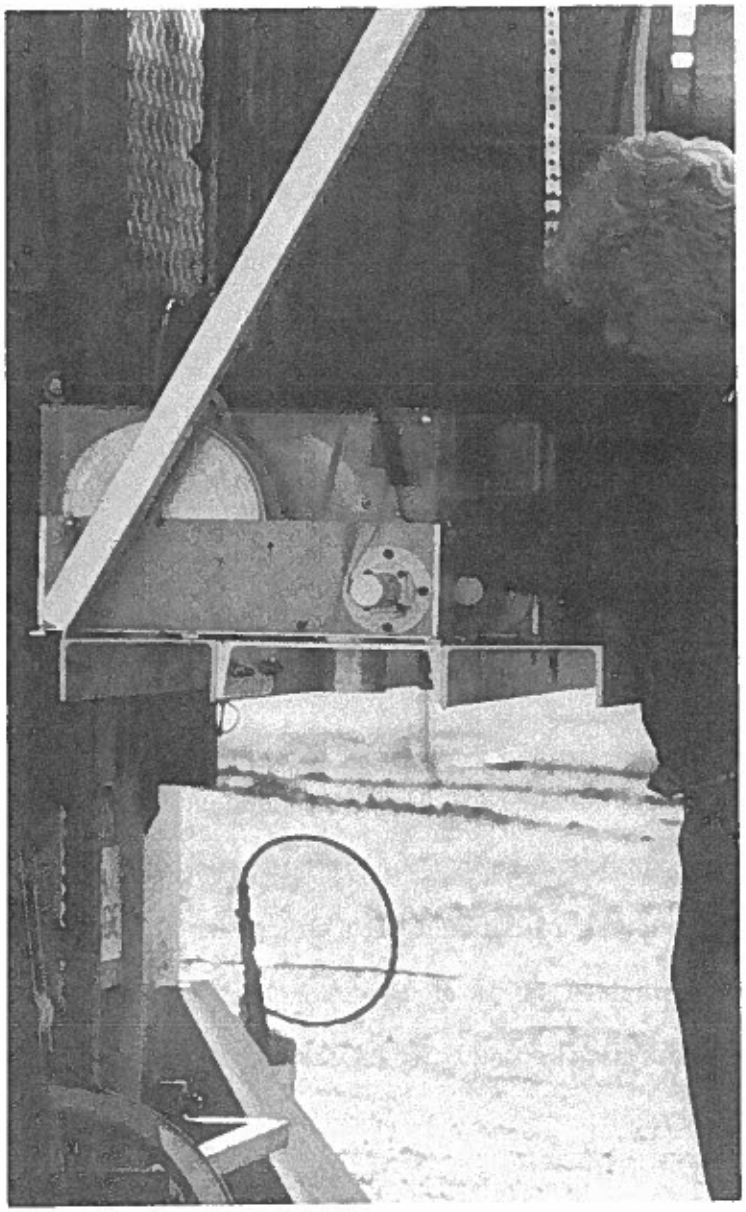

Figure 4.2. Chaff cutter being installed on the carriage for chaff release at elevated point on the BAO tower.

the ground. This clumping seemed to be more serious for the ground releases than for the elevated ones, probably because the wind blowing by the cutter is stronger for elevated releases. These clumps quickly fall out of the plume and do not contaminate the data significantly.

Gravitational settling makes chaff a less than perfect tracer. The terminal velocity of a chaff filament is about 30 cm/s. In this daytime study, convective turbulence was sufficient to keep the chaff aloft and the effects of settling are relatively small compared with those during less vigorous turbulence conditions. However, the observed chaff plumes tended to reach the ground somewhat sooner than oil fog plumes released from the same tower platform, and there was some evidence of deposition loss of chaff after 1 or 2 km of travel.

4.4 Radar Scan Modes

The plumes in the CONDORS experiment were tracked by the radar operator. Therefore, as the plume spread vertically and horizontally and moved as a function of changing wind fields, adjustments were made to the azimuth sector width and to the number of elevation sweeps that the radar performed to fully cover the plume. Changes in the number of elevation sweeps affected the elevation increment between sweeps, thus affecting the resolution of data. The elevation increment was generally between 0.6° and 1.0°.

4.5 Data Processing

4.5.1 Processing

In order to put the radar data in a useful form for analysis, a number of steps must be performed. Briefly, these steps are: 1) "thresholding", 2) conversion of reflectivity to chaff density, 3) interpolation to a Cartesian grid, 4) removal of ground clutter, and 5) averaging of individual volume scans. These steps are discussed in detail below.

1) Thresholding. A preset threshold on received power was used to ensure that signals too weak to be reliable did not become part of the data set. This threshold was set at -85.5 dBm (85.5 dB below 1 mW). This translated into an equivalent reflectivity factor of -3.0 dBZ at 3 km range from the radar and 5.0 dBZ at 7.5 km range. Using the relationship between equivalent reflectivity factor and spatial chaff density discussed in Sec. 3 below, these reflectivity factors translate into minimum required chaff densities of 0.09 filaments per $(50m)^3$ at 3 km range, and 0.58 filaments per $(50m)^3$ at 7.5 km range. In fact, things are slightly better than this. At ranges closer than 4.3 km (0.8 km downwind of the tower), the radar beam dimensions are sufficiently small that the radar can pick up one chaff filament per pulse volume; that is, the radar can see every chaff filament. Beyond this range, the minimum chaff densities mentioned above are required.

In two cases (Periods 8-83 and 9-83) the preset power threshold still allowed some extraneous data. In these cases, an additional reflectivity threshold of 3 dBZ was applied to the data. This translated into a minimum spatial chaff density of 0.4 filaments per $(50m)^3$, independent of range. This threshold, combined with the power threshold previously mentioned, resulted in a minimum

required chaff density of 0.4 filaments per $(50m)^3$ for ranges less that 6 km. Beyond that range, the minimum chaff densities were determined by the power threshold.

2) Cartesian interpolation. For ease of analysis, reflectivity data from each volume scan were interpolated onto a Cartesian grid. The grid was rotated so that the negative x axis lay along the approximate mean wind direction for each averaging period. Tables 4.1 and 4.2 show the Cartesian grids used for each case. To produce a smoother field of Cartesian data, new interpolated sweeps were created between every two actual sweeps. Both radar data and interpolated data that fell within each grid cell were averaged together to produce Cartesian data.

3) Conversion of reflectivity to chaff density. Radar data presented in this report are in the form of χ, the number of chaff filaments per unit volume. In all cases, the unit of volume for χ is $(50m)^3$. This rather odd unit was chosen because it is the size of a Cartesian cell for the grids used in most cases. Reflectivity data were converted to χ by starting with the relation

$$N = \eta \, (0.18 \, \lambda^2)^{-1} \tag{4.4}$$

from Schlessinger (1961, p 130), where N is in filaments/m^3, η is radar reflectivity in m^{-1} and λ is radar wavelength in m. η is related to radar reflectivity factor Z by

$$\eta = 0.93 \, \pi^5 \, \lambda^{-4} \, Z \tag{4.5}$$

from Battan (1973, p 44), where Z is in $(mm)^6/m^3$. The resulting relationship between Z and χ is

$$\chi = 0.184 \, Z \, . \tag{4.6}$$

Table 4.1 Parameters used in radar data processing, 1982

Period	Time	# Vols	Speed for thresholding m/s	True direction of x axis	grid size (km)	Radar location (x,y,z) in rotated coordinate system (km)
0-82	10 Sept 82, 1143	12	2.0	295°	x: -0.25 to 3.75 by 0.05 y: -2.0 to 2.0 by 0.05 z: 0 to 0.8 by 0.05	(3.16, 1.51, -0.01)
1-82	16 Sept 82, 1304	9	2.0	250°	x: -0.25 to 3.75 by 0.05 y: -2.0 to 2.0 by 0.05 z: 0 to 0.8 by 0.05	(3.30, -1.18, -0.01)
2-82	16 Sept 82, 1411	11	2.0	250°	x: -0.06 to -4.8 by 0.06 y: -2.4 to 2.4 by 0.06 z: 0 to 0.95 by 0.05	(3.30, -1.18, -0.01)
3-82	18 Sept 82, 1354	22	2.0	290°	x: -0.25 to +3.75 by 0.05 y: -2.0 to +2.0 by 0.05 z: 0 to 0.9 by 0.05	(3.30, 1.17, -0.01)
4-82	20 Sept 82, 1153	11	0.5	250°	x: -0.25 to +3.75 by 0.05 y: -2.0 to +2.0 by 0.05 z: 0 to 1.2 by 0.05	(3.30, -1.18, -0.01)
5-82	20 Sept 82, 1312	11	0.51	250°	x: -0.25 to 3.75 by 0.05 y: -2.0 to 2.0 by 0.05 z: 0 to 1.5 by 0.05	(3.30, -1.18, -0.01)

Table 4.2 Parameters used in radar data processing, 1983

Period	Time	# Vols	Speed for thresholding m/s	True direction of x axis	grid size (km)	Radar location (x,y,z) in rotated coordinate system (km)
2-83	28 Aug 83, 1129	15	1.0	297°	x: -0.05 to 3.95 by 0.05 y: -4.0 to 4.0 by 0.10 z: 0 to 1.35 by 0.05	(3.11, 1.60, -0.01)
4-83	31 Aug 83, 1055	18	1.0	302°	x: -0.15 to 3.95 by 0.05 y: -3.96 to 3.94 by 0.10 z: 0 to 1.35 by 0.05	(2.95, 1.87, -0.01)
5,6-83	6 Sept 83, 1050	27	1.1	309°	x: -0.05 to 3.95 by 0.05 y: -4.4 to 6.0 by 0.13 z: 0 to 1.35 by 0.05	(2.70, 2.22, -0.01)
7-83	6 Sept 83, 1210	12	1.1	300°	x: -0.05 to 3.95 by 0.05 y: -2.0 to 6.0 by 0.10 z: 0 to 1.35 by 0.05	(3.02, 1.77, -0.01)
8-83	7 Sept 83, 1229	19	2.5	264°	x: -0.05 to 3.95 by 0.05 y: -2.0 to 2.0 by 0.05 z: 0 to 1.35 by 0.05	(3.48, -0.34, -0.01)
9-83	7 Sept 83, 1310	21	2.8	266°	x: -0.05 to 3.95 by 0.05 y: -2.0 to 2.0 by 0.05 z: 0 to 1.35 by 0.05	(3.49, -0.22, -0.01)

4) Ground clutter removal. Ground clutter was present in the lowest few planes of data. This clutter was removed by comparing the data taken during chaff releases with data taken by the radar when no chaff was present. Plume data having a signal strength greater than 10 dB above the clutter alone was retained. Some clutter-contaminated data were still obvious in grid points adjacent to points that had been removed. We therefore prepared a "spread out" clutter map. In this map, in each horizontal level, the clutter signal strength at each grid point was set to the maximum of the clutter strengths in any of the four adjacent grid points; i.e., if G is the ground clutter signal strength,

$$GS(x,y) = \max[G(x,y),G(x+dx,y),G(x-dx,y),G(x,y+dy),G(x,y-dy)] \; . \qquad (4.7)$$

If the data signal was less than 10 dB above GS, the data were kept only if the Doppler velocity was greater than some value. This value depended on the mean wind for the day and varied between 0.5 and 2.8 m/s. The values used for each case are shown in Tables 4.1 and 4.2. This velocity test was added because most data well away from clutter-contaminated points had velocities near the mean wind speed, and most data known to be contaminated had velocities biased to nearly zero by the presence of clutter.

These two tests together--signal strength and velocity--removed nearly all evidence of clutter in the data. Occasional spurious data points remained, however. These were most likely due to vehicles and aircraft. Such points were removed by hand on an individual basis.

5) Volume scan averaging. The number of individual volume scans for each averaging period, as shown in Tables 4.1 and 4.2, varied from 9 to 27. For each

averaging period, the individual volume scans were averaged. This resulted in a single volume of averaged data; all subsequent analysis was performed on the averaged volume.

4.6 Data analysis

For each averaging period, ten products, showing various statistical properties of the plume, are generally available. These are discussed below, with the equations used to calculate them. All products are available for the processed cases of 1983; however, some of the products are missing for some of the 1982 cases. The products are presented in Chapter 9.

1) Plume concentration, integrated vertically (χ_z). Although data are available for every (x,y) grid column, data shown in Chapter 9 are averaged along 250 m intervals in x, in order to produce a more readable data set. In much of the 1983 data, the χ_y are normalized to sum to 1000 along each vertical column; these data are identified by the superscript n.

$$\chi_z(x,y) = \int_0^{z_{max}} \chi(x,y,z)dz \tag{4.8}$$

$$\chi_z^n(x,y) = 1000 \frac{\chi_z(x,y)}{\int_{y_{min}}^{y_{max}} \chi_z(x,y)dy} \tag{4.9}$$

2) Plume concentration integrated along the y (crosswind) direction (χ_y). Data are available for every (x,z) grid column; however, as with χ_z data shown in Chapter 9 are averaged along 250 m intervals in x. In much of the 1983 data, the χ_y are normalized to sum to 1000 along each vertical column; these data are identified by the superscript n.

$$\chi_y(x,z) = \int_{y_{min}}^{y_{max}} \chi(x,y,z)dy \tag{4.10}$$

$$\chi_y^n(x,z) = 1000 \frac{\chi_y(x,z)}{\int_0^{z_{max}} \chi(x,z)dz} \quad . \tag{4.11}$$

3) Plume concentration integrated along both y and z, hence, the total plume material at each downwind distance interval χ_{yz}. For a conservative tracer, this should be a constant. For our data, however, this quantity is highly variable. We attribute this to the following: a) Variability of the chaff cutter output rate, b) chaff being carried below the minimum field of view of the radar, and then back into the field of view, c) chaff settling out, d) small bunches of chaff breaking up as they travel downwind, resulting in increased radar reflectivity, and e) chaff diffusing until it is below the minimum detectable signal of the radar.

$$\chi_{yz}(x) = \int_{y_{min}}^{y_{max}} dy \int_0^{z_{max}} dz\ \chi(x,y,z) \quad . \tag{4.12}$$

4) Mean plume height ($\bar{z}$).

$$\bar{z}(x) = \frac{\int_0^{z_{max}} z\ \chi_y(x,z)dz}{\int_0^{z_{max}} \chi_y(x,z)dz} \quad . \tag{4.13}$$

5) Vertical variance of the crosswind integrated plume (σ_z^2)

$$\sigma_z^2(x) = \frac{\int_0^{z_{max}} z^2 \chi_y(x,z)dz}{\int_0^{z_{max}} \chi_y(x,z)dz} - [\bar{z}(x)]^2 . \qquad (4.14)$$

6) Mean crosswind plume position for each downwind distance ($\bar{y}$).

$$\bar{y}(x) = \frac{\int_{y_{min}}^{y_{max}} y\ \chi_z(x,y)dy}{\int_{y_{min}}^{y_{max}} \chi_z(x,y)dy} . \qquad (4.15)$$

7) Horizontal standard deviation of the vertically integrated plume (σ_y^2).

$$\sigma_y^2(x) = \frac{\int_{y_{min}}^{y_{max}} y^2\ \chi_z(x,y)dy}{\int_{y_{min}}^{y_{max}} \chi_z(x,y)dy} - [\bar{y}(x)]^2 . \qquad (4.16)$$

8) Maximum concentration observed in the crosswind-integrated plume ($(\chi_y)_{max}$).

9) Height at which the maximum concentration occurred in the crosswind-integrated plume (z of $(\chi_y)_{max}$). This is not necessarily the height of the three-dimensional point of maximum concentration, but it does correspond to the heights of maximum concentration presented by Willis and Deardorff (1976a, 1978, 1981) and other investigators.

10) Crosswind location at which the maximum concentration occurred in the vertically integrated plume (y of $(\chi_z)_{max}$).

5. IN SITU SAMPLING OF GAS TRACERS

G. A. Briggs and G. E. Start

The specific objective of the CONDORS experiment was to determine the geometry of plumes from surface and elevated releases in the atmosphere during convective conditions in order to compare them with the surprising results of laboratory and numerical modeling. However, an important ultimate objective is to develop improved models of surface concentration, χ. In Sec. 2.6 we discussed how the ratio χ/Q, where Q is the release rate, can be estimated from the fields of relative concentration of oil fog or chaff by assuming uniform depletion of source material at any given value of x. It is simply taken as the ratio of local concentration to the downwind flux of local concentration at that distance. However, this assumption is imperfect. For instance, the percentage reduction of chaff due to surface deposition is not likely to be uniform with height, and slightly more evaporation of oil fog droplets may occur near the ground because of smaller $\bar{u}$ and larger travel time. It is difficult to make a priori estimates of the magnitude of these factors. Therefore, it seemed worthwhile to do some "ground truth" testing of these χ/Q estimates using proven methods of surface sampling of quite conservative, gaseous tracers. In situ sampling was carried out in CONDORS 83 by the NOAA Air Resources Laboratory Field Research Division (ARLFRD).

5.1 Siting

Budget and accessability considerations limited the in situ effort to one line of 29 samplers spaced at 5° intervals of azimuth from the BAO tower, the

primary release point (see Fig. 5.1). This spacing was adequate to define the approximate lateral distribution of X in convective conditions, as most plumes were about 40° wide at the sampling arc. A N-S road located 1.22 km west of the tower provided easy access to the largest segment of the sampling arc, in the most favorable plume direction, and at a desirable distance from the source (near or no more than twice the distance of expected maximum surface impact from the elevated releases--see Sec. 2.6 and 2.7). A circular arc was not possible, because of houses to the north and fields under cultivation; most of the samplers were set a few meters from the inside edges of the roads

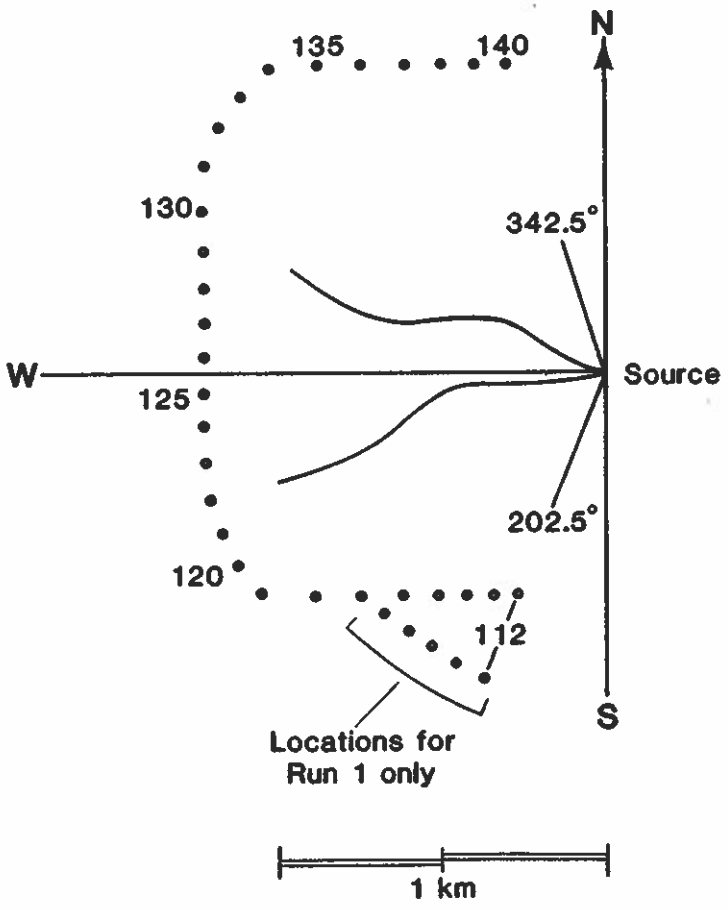

Figure 5.1. Location of sampler stations for tracer gases shown in relationship to release point at the BAO tower.

defining the "square mile" in which the BAO tower stands, with some rounding of the corners. The E-W road 0.92 km to the north was considered an acceptable arc segment, while the one 0.67 km to the south was considered too close to the source. Therefore, the five most southerly samplers were initially placed 1000 m from the tower, across an open field. However, they had to be relocated to the north edge of the road immediately after the run of August 27 because plowing was in progress.

An error in the supposed azimuth positions of the samplers was discovered. A survey of the west road alignment showed that it lay within 0.2° of true N-S alignment, as indicated by USGS maps; 2.5° had to be subtracted from the nominal azimuth positions to make the straight-line segments of the sampling arc nearly N-S and E-W. This correction is reflected in the positions indicated in Fig. 5.1 and in Table 5.1.

Table 5.1 Gas sampler locations for CONDORS 83

Location number	Bearing* (degrees azimuth) from tower base	Range (km) Test 1	Range (km) Test 2-6	Comments
112	202.5	1.000	0.726	
113	207.5	1.000	0.756	Locations
114	212.5	1.000	0.796	changed
115	217.5	1.000	0.846	
116	222.5	1.000	0.910	
117	227.5	0.994	0.994	
118	232.5	1.104	1.104	
119	237.5	1.249	1.249	
120	242.5	1.249	1.249	
121	247.5	1.249	1.249	
122	252.5	1.249	1.249	
123	257.5	1.247	1.247	
124	262.5	1.227	1.227	
125	267.5	1.217	1.217	
126	272.5	1.217	1.217	

* Corrected for 2.5° offset in the nominal azimuth positions.

Table 5.1 Gas sampler locations for CONDORS 83 (continued)

Location number	Bearing* (degrees azimuth) from tower base	Range (km) Test 1	Range (km) Test 2-6	Comments
127	277.5	1.226	1.226	
128	282.5	1.245	1.245	
129	287.5	1.274	1.274	
130	292.5	1.314	1.314	
131	297.5	1.364	1.364	
132	302.5	1.364	1.364	
133	307.5	1.364	1.364	
134	312.5	1.364	1.364	
135	317.5	1.252	1.252	
136	322.5	1.162	1.162	
137	327.5	1.094	1.094	
138	332.5	1.041	1.041	
139	337.5	0.996	0.996	
140	342.5	0.965	0.965	

* Corrected for 2.5° offset in the nominal azimuth positions.

5.2 Tracers

Two tracer gases were employed, SF_6 and Freon 13B1 (CF_3Br). The SF_6 was always released near the chaff generator on the elevated carriage mounted on the west side of the tower. The 13B1 was released a few meters from the oil fog generators when they operated from the surface release site, 141 m WNW of the tower; during the two runs with elevated oil fog, September 6 and 7, it was released from the west corner of the tower base. The releases were initiated about 10 min before the samplers were turned on, to allow time for the transport of the tracer to the sampling arc. The tracers were stored in compressed gas cylinders and were piped through linearized mass flow meters to the release nozzles, with strip chart recording of the release rates and digital readouts of the total release volumes. The release rates during each run were quite steady. The pre- and post-test weights of each gas cylinder served

as checks on the flow meter measurements; these needed only a -4% to +1% adjustment, except for a +7% and +10% adjustment for one run (August 27). The adjusted release rates for the successful runs are shown in Table 5.2.

Table 5.2 Gas tracer release data

Test no.	Sampling period		SF_6		13B1	
	Date	Time (MST)	Release rate (g/s)	Amount released (g)	Release rate (g/s)	Amount released (g)
1	27 Aug 83	1230-1430	0.191	1492	1.25	9730
2	28 Aug 83	1130-1330	0.185	1443	----	----
3	31 Aug 83	1055-1255	0.201	1504	----	----
4	2 Sept 83	1150-1220*	----	----	----	----
5	6 Sept 83	1050-1250	0.192	1498	----	----
6	7 Sept 83	1210-1410	0.195	1519	----	----

*Run aborted

Note: Density of SF_6 : 6515 g/m^3 at STP
Density of 13B1 : 6644 g/m^3 at STP

5.3 Samplers

The samplers at each position were modified EMI ASQII air samplers; each housed 12 separate pumps and external tubes to draw ambient air into 12 two-liter Tedlar bags. Each sampler is battery powered and is electronically programmed using a crystal-controlled clock accurate within ±0.002% to turn on the pumps for sequential sampling. In this experiment, 10 min samples were taken over 120 min sampling periods. This allowed some flexibility in the choice of averaging periods for analysis; these were generally chosen for steadiness of meteorological variables, but sometimes were set to avoid the

short lapses that occurred in radar or lidar data acquisition. The pumps were actually cycled on and off about every five seconds to achieve the desired sampling volume (about 1.7 liters), as they performed best at full power. Although the sampling initiation time could be preset, this was impractical in this experiment because the onset time of favorable wind speed, wind direction, and mixing depth could not be predicted. Instead, the samplers were connected by a wire that was switched to "on" if conditions remained favorable after the start of the tracer releases, about 10 min earlier.

5.4 Analysis

The 12 bags from the 29 samplers were collected soon after each run by persons who had not been near the release points. The bags were placed in separate 12-compartment boxes for shipping to the ARLFRD laboratory in Idaho Falls for analysis. However, all samples from the last three of the eight runs of CONDORS 83 were found to be highly contaminated (measured concentrations appeared to be randomly distributed across the entire arc and were 100 to 1000 times as large as expected plume centerline concentrations). It is believed that contamination occurred during shipping because partly filled gas cylinders accompanied the boxes of samples in the same truck. In addition, the remaining 13B1 samples, except the August 27 ones, showed similar levels of contamination. This was possibly due to improper storage of the bags in a van or building with some source of 13B1 prior to use.

The bag samplers were analyzed in the laboratory using electron capture gas chromatographs (GC's). These were automated adaptations of Lovelock's 1972 prototype GCs. Careful check-in and handling procedures were followed,

and the calibrations of the GCs were tested before and after each gas analysis shift using five reference mixtures each of SF_6 and 13B1. Past checks on these mixtures by other laboratories indicated less than 10% uncertainties in the concentrations of these mixtures, as claimed by the manufacturer.

5.5 Error Estimates

This experiment did not include cross-checks such as collocated samplers or independent audits. However, the methods and equipment were similar to those used by ARLFRD in the Small Hill Impaction Study No. 2 (SHIS2), for which such checks were made (Greene, 1985). The SHIS2 measured and calibration concentrations were generally much higher than those observed in CONDORS 83 because the former experiment was made in stable conditions. For reference, typical plume centerline levels of SF_6 in CONDORS 83 were 30 to 50 ppt (parts per trillion) and background levels were about 2 ppt. Plume centerline levels of 13B1 for the only usable period were about 70 ppt and background levels were too small to be resolvable.

The standard deviation of repeated measurements of standard mixtures for SHIS2 averaged over all GCs was 14% for the most dilute 13B1 mixture, 58 ppt; it improved to 8% at 150 ppt. The standard deviation for the SF_6 tests was smaller, 10% at 3 ppt improving to 6.5% at 10 ppt and to 3% at 500 ppt. The average errors of four GCs compared to audits of standard mixtures by the Research Triangle Institute, North Carolina, ranged from -12% to +3% for 13B1 at 2000 ppt and from -11% to -2% for SF_6 at 100 ppt. The sign of the errors reversed at higher test concentrations, but there was no significant trend in the absolute values of the errors.

The SHIS2 experiment included two pairs of collocated samplers. For SF_6, the average absolute disagreement between the collocated samplers was only 6%; this did not vary appreciably with concentration range. However, for 13B1 concentrations of less than 1000 ppt, the average disagreement was almost 70% (i.e., a factor of 2 difference in the readings). This improved markedly for higher concentrations, to 16%, but the CONDORS 83 plume concentrations were much smaller than 1000 ppt. This result and the large inconsistencies beween our 10 min samples adjacent in time or space (see Table 10.2) tend to reduce confidence in the CONDORS 13B1 measurements. On the other hand, the total error in concentrations measured from uncontaminated SF_6 samples was probably less than 10%.

6. OPERATIONAL SCENARIO

G. A. Briggs, W. L. Eberhard and W. R. Moninger

It is apparent from the preceding sections that the prerequisites for a good run included an acceptable range and slow growth of z_i, steady insolation, wind speed in a suitable range, and wind direction in the chosen sector. To avoid scheduling runs during days and hours that the above meteorological criteria were not met, we identified possible run days about a day in advance so that needed personnel would be on hand. The starting time for the two-hour runs was set nominally at 1200 MST but could be called as early as 1100 MST if an accelerated midday mixing layer growth was anticipated, based on the early morning sounding. We therefore established a decision time (0830 MST) to give people enough time to get to their duty stations and to make preparations for the run. From 0930 MST onward, z_i was closely monitored with rawinsonde, lidar, radar and acoustic sounder; just prior to the beginning of the elevated release, the carriage height was adjusted according to the z_i forecast for the middle of the run.

Thus, it was recognized from the outset that the success of the experiment depended on some skill at short-term predictions of meteorological variables at the BAO site. It seemed prudent to develop such skills before the main experiment CONDORS 83. The following learning program was followed for CONDORS 82.

On the basis of National Weather Service projections for 1200 GMT (0700 MST), we had to decide whether the following day looked favorable. Based on preliminary evidence from BAO records and weather maps from previous years, the criteria for a "favorable" day were:

1. Clear or partly cloudy sky.
2. The state of Colorado more under the influence of a surface high than a surface low.
3. Light to moderate geostrophic winds over Colorado.

On days deemed favorable, a rawinsonde was released at about 0530 MST before mixing layer development began, and tracked with double theodolites to about 3000 m height. Temperature, humidity, wind speed, and wind direction profiles were developed with the best resolution possible up to this height. Wind speed and wind direction at the tower top were monitored throughout the morning and midday hours. Through the same hours, determinations of z_i were made at the site at least every 30 min.

The above information was forwarded as soon as it was available to several people designated as 'forecasters' for the experiment. Using 1200 GMT NWS synoptic maps and the above measurements at the site, mostly intuitive methods were used for predicting midday wind speed, wind direction, and z_i behavior for the site during CONDORS 82. The procedure was made more objective for CONDORS 83 through the use of Wilczak and Phillips (1984) boundary layer height prediction model, which provided a z_i forecast for the day based on the predawn sounding at the BAO. The model predictions were compared with z_i values determined from the rawinsonde data and from periodic soundings made by the lidar and the radar. Because the most convenient source of above-tower meteorology was the radiosonde, at least three releases were scheduled before and during each run, including a release at 1000 MST. Usually, only two radiosondes were released during each run. The lidar and radar soundings for z_i were made on a regular basis approximately every 20 min until the start of

the run, after which they were made only as needed to avoid undue interruptions in the data sampling. The z_i information, along with other parameters from the tower, were plotted as the run progressed to provide a realistic assessment of the quality of the run. At run initiation time (RIT) minus 30 min, a revised estimate of z_i at RIT + 1 hr was made and the elevated source height adjusted accordingly, to 1/4 or 1/2 z_i. This z_i estimate, current wind speed and direction at upper tower levels, and the distance scale $z_i\bar{u}/w_*$ were used to advise the lidar crew of desired azimuth settings for this run and the maximum elevation angles needed to encompass the plumes. The radar crew was given wind direction and z_i estimates to determine the range of azimuth and the desired elevation angles for the radar sweeps. Sources (oil fog, chaff, gases) were turned on at about 10 to 20 min before the declared run initiation time; this allowed time for the materials to reach about X = 1 by the time measurements actually began (see Fig. 2.5).

Lidar and radar measurements of the plume were conducted from RIT + 0 hr to RIT + 2 hr and occasionally longer. They were recorded throughout this period, to be subdivided later for averaging according to periods of steadiest meteorological conditions. While frequent repetition of lidar scans and radar sweeps was desirable for obtaining good ensemble averaging, there was little little to be gained statistically by repeating them much more often than every $z_i/\bar{u}$, because consecutive realizations of plume concentrations at any given position would then be highly correlated. This period ranged from 100 to 400 s, so a scan cycle every 2 to 4 min was typical.

During CONDORS 83, ground sampling of gas tracers also extended from 0 to 2 hr past RIT. Two gas tracers were released: SF_6 from the elevated release

point on the tower and Freon 13B1 from the base of the tower. While most of the SF_6 concentrations were measured and evaluated with sufficient accuracy, only one of the 13B1 releases could be evaluated successfully because of sampler bag contamination.

7. METEOROLOGICAL DATA SUMMARIES FOR OBSERVING PERIODS

G. A. Briggs and J. E. Gaynor

The choice of periods for analysis depended very much on the vagaries of the experimental conditions, including operation of the measuring equipment. The BAO meteorological tower measurements, which were already well automated with eight levels of measurement, were looked at first to screen out periods of sudden changes in wind direction, $\bar{u}$ or $\overline{w'T'}$, or periods of wind direction or speed outside of the suitable ranges. Selected variables were processed into 5 min averages, in addition to the customary 20 min real-time averaging period employed at the BAO tower. Lidar and radar data during the run periods were examined to provide frequent estimates of z_i. Time plots of z_i, wind direction, wind speed, and $\overline{w'T'}$ (see Fig. 7.1) were inspected in order to define periods during each 2 hr run with the least variability in z_i, $w_*/\bar{u}$, and 5 min averaged wind direction. Emphasis was placed on steadiness rather than on length in choosing averaging periods. Typically the chosen periods were of 40 min duration; most of the 2 hr runs furnished two adequate averaging periods. Since typical large eddies in convective turbulence are 1.5 z_i across (Willis and Deardorff 1976b) and eddies pass by a point at about the mean wind speed, each average will be an "ensemble" of about (40 min) ÷ $(1.5z_i/\bar{u})$ eddy passages; this number ranged from 2 to 13 in these experiments.

All lidar scans and radar sweeps were averaged over the chosen periods; data outside those periods were not analyzed. For each averaging period, values of the meteorological parameters were selected for the purpose of nondimensionalizing the results. The mean wind direction, $\bar{\theta}_A$, averaged over the

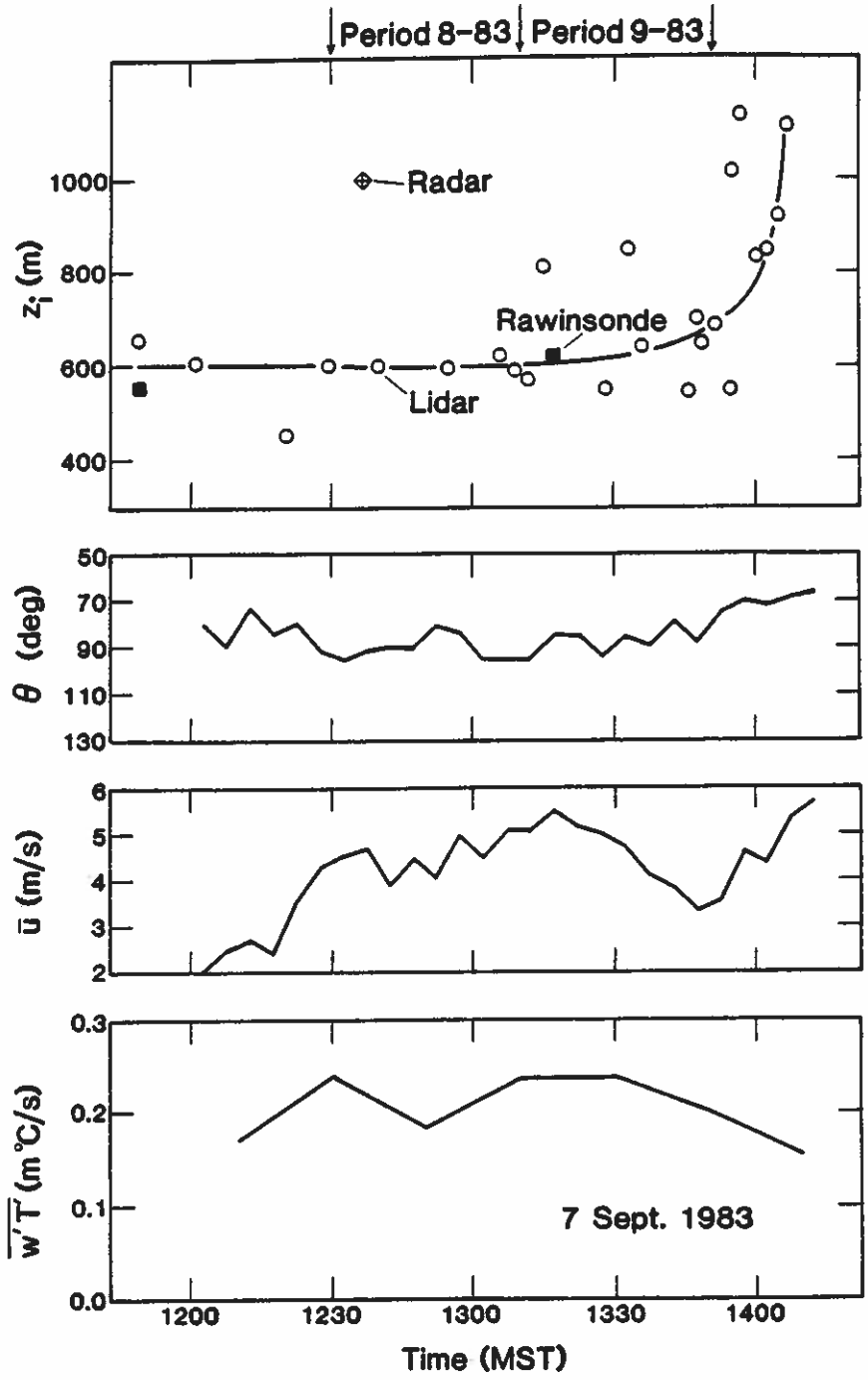

Figure 7.1. Mixing depth, wind direction, wind speed and heat flux for the observing period on 7 Sept. 1983, plotted as a function of time. Periods selected for analysis are indicated on the mixing depth plot.

upper four tower layers was used to orient the radar coordinate system along the plume centerline. The wind speed was averaged through the same layers to get $\bar{u}$. Consistent with previous findings (Kaimal et al., 1976), the mixed layer wind speeds and wind directions at the four levels above 100 m showed little variation with height. To calculate w_*, the estimated value of z_i was used with $(g/T)\overline{w'T'}$ values determined from the time averages at the lowest two levels on the tower. Accurate determination of z_i is less straightforward; our methods are discussed in some detail below.

The summary data for CONDORS 82 and CONDORS 83 are given in Table 7.1. In this table we define $\bar{u}$ and $\overline{\theta_A}$ as the average of the wind speed and direction, respectively, at the top four levels on the tower (150, 200, 250 and 300 m) and $\overline{w'T'}$ as the vertical temperature flux from the 10 and 22 m levels. The source height for the tracer is designated as z_s and the chosen averaging period duration as τ.

Because CONDORS was designed to compare field measurements of diffusion with laboratory and numerical results using convective scaling, adequate determinations of the mixing depth, z_i, are particularly important. Preliminary estimates made during the runs and for initial data analyses were derived from the rawinsonde profiles of temperature and humidity; these were supplemented by reports of the haze top elevation by the lidar team and of the highest chaff elevation by the radar team (the chaff reports probably represented the most penetrative thermals, and tended to be several hundred meters higher than the other indicators). When the processed profiles of $\int x dy$ for the chaff returns during CONDORS 82 became available, z_i was estimated using 0.92 times the projected height of zero concentration for each averaging period

Table 7.1 Data summaries for CONDORS 82 and CONDORS 83

Period No.	Date	Start Time (MST)	Duration τ (min)	z_s (m) Oil fog	Chaff	SF_6	13B1	z_i (m)	$\bar{u}$ (m/s)	$\bar{\theta}_A$ (deg)	$\overline{w'T'}$ (m°C/s)	w_* (m/s)	$z_i\bar{u}/w_*$ (m)	$\bar{u}/w_*$	$\tau\bar{u}/z_i$
0-82	10 Sept 82	1143	36	-	3	-	-	1000	3.65	114	0.271	2.07	1770	1.77	7.9
1-82	16 Sept 82	1304	29	235	235	-	-	520	5.80	52	0.186	1.46	2060	3.97	19.4
2-82	16 Sept 82	1411	35	235	235	-	-	730	6.23	50	0.124	1.43	3180	4.36	17.9
3-82	18 Sept 82	1354	40	167	167	-	-	960	2.76	89	0.117	1.54	1720	1.79	6.9
4-82	20 Sept 82	1153	44	3	3	-	-	980	2.40	52	0.186	1.81	1300	1.33	6.5
5-82	20 Sept 82	1312	42	3	3	-	-	1260	1.59	59	0.148	1.82	1100	0.87	3.2
1-83	27 Aug 83	1330	30	3	265	265	3	1600	3.15	121	0.158	2.00	2518	1.57	3.5
2-83	28 Aug 83	1130	30	3	235	235	-	1240	1.91	117	0.207	2.01	1178	0.95	2.8
3-83	28 Aug 83	1230	60	3	235	235	-	1400	2.57	107	0.179	1.99	1806	1.29	6.6
4-83	31 Aug 83	1055	50	3	280	280	-	1100	1.90	127	0.189	1.88	1110	1.01	5.2
5-83	6 Sept 83	1050	40	280	280	280	-	880	2.52	122	0.152	1.64	1356	1.54	6.9
6-83	6 Sept 83	1130	30	280	280	280	-	880	2.59	140	0.184	1.74	1310	1.49	5.3
7-83	6 Sept 83	1210	30	280	280	280	-	880	3.34	122	0.158	1.65	1778	2.02	6.8
8-83	7 Sept 83	1230	40	265	265	265	-	640	4.45	91	0.130	1.38	2065	3.22	16.7
9-83	7 Sept 83	1310	40	265	265	265	-	780	4.59	87	0.133	1.48	2416	3.10	14.1
10-83	13 Sept 83	1140	30	3	-	-	-	900	2.09	102	0.200	1.80	1042	1.16	4.2
11-83	13 Sept 83	1240	40	3	-	-	-	870	1.57	56	0.227	1.86	734	0.84	4.3

(for details, see Moninger et al., 1983). These determinations showed considerable constancy with distance when $x > 2$ km. The oil fog profiles obtained during CONDORS 82 did not extend far enough downwind to show this, and were not used for z_i determinations.

During CONDORS 83, a heavier, less volatile type of oil was used, which extended the maximum ranges at which the lidar could distinguish the oil fog plume from background haze by more than 20%. Furthermore, for the surface releases in 1983, the source strength was doubled by using two oil fog generators (these were too bulky to mount more than one on the tower carriage). For these releases, the maximum source-plume distance of processed scans was about 80% larger than in 1982. The processed scan distances ranged from 1100 to 1850 m in 1982, from 1500 to 2000 m for elevated releases in 1983, and from 2100 to 2900 m for the surface releases in 1983. Except for period 7-83, an elevated release, oil fog scans made in 1983 were useful for determining z_i. In addition to the "zero projection" method used in 1982, a second method was applied to both chaff and oil fog profiles of $\int \chi dy$ vs. z. A peak or a "shelf" of nearly constant $\int \chi dy$ was chosen from the upper part of the profile, and z_i was assumed to be the height above this level where $\int \chi dy$ drops to 40% of this concentration. Because a few of the profiles were complex and showed more than one peak or shelf in the upper layers, an arbitrary choice sometimes had to be made; the z_i value most consistent with profiles at neighboring values of x was the usual choice, unless the profile strongly suggested otherwise. The z_i values from this method differed from that given by the "zero projection" method by no more than -99 to +35 m for the chaff, and by no more than -40 to +38 m for the oil fog in periods 1, 3, 4, and 8 through 11 of

1983. In periods 2, 5, and 6 of 1983 the "zero projection" method applied to oil fog was at variance with the other indicators, and in period 7 the oil fog simply did not reach the z_i elevation indicated by the chaff and the rawinsonde profiles (the maximum X, as in Eq. (2.7), was 0.94 for oil fog and 2.1 for chaff).

A comparison of z_i estimates, along with recommended values, is shown for CONDORS 83 in Table 7.2. The $\int X dy$ profiles of chaff and oil fog were considered the primary indicators of mixing depth in the most literal sense. They were given weight especially when they yielded an approximately constant z_i over a large range of x and when they showed a sharp drop-off near the top of the distribution (one measure of this is the "profile fuzziness index" defined in the table; 0.9 or greater means z_i is very ambiguous, while 0.25 or less indicates a well-defined cutoff). The lidar-determined haze tops were instantaneous measures that agree best with other measures only when they agree well with each other, which probably occurs when undulations in z_i are small (e.g., this occurred 6 September 1983). The rawinsonde measurements can also be considered instantaneous. The rawinsonde profiles were given more weight when there was a steep increase in virtual potential temperature or a steep decrease in dewpoint in a layer above a nearly uniform layer. For instance, in period 1-83, the potential temperature profile was quite ambiguous. The dew point showed definite drops at two different levels; however, the layer of greatest wind speed and direction shear, which is another coarse indicator of z_i, encompassed only the lower dew point drop layer, near 1600 m. This was in good agreement with the sharply defined oil fog profile at x = 2.14 km, so z_i was assumed to be 1600 m. For the other 10 periods, there was

Table 7.2. Mixing depth estimates for CONDORS 83

Period	1-83	2-83	3-83	4-83	5-83	6-83	7-83	8-83	9-83	10-83	11-83
Time center of averaging period	1345	1145	1300	1120	1110	1145	1230	1250	1330	1155	1300
Time nearest rawinsonde(s), at z_i	1320	1131	1233	1109	1030	1143	1245	1148	1318	1134	1251
z_i estimates from rawinsonde (m):											
Virtual potential temperature	2400	1100	1430	770, 1050	910	900	930	600	600	800	700, 1000
Dew point profile	1600, 2400	1000	1100 to 1500	not clear	950	900	930	550	550	850	700, 1050
Relative humidity profile	1600, 2400	1000	1450	not clear	910	900	930	550	550	850	700, 1050
Wind velocity shear	1200 to 2050	1000 to 1200	1400 to 1800	850, 1250	600 to 1000	750 to 1000	800 to 1000	500 to 600	550 to 730	940	800
z_i estimates from $\int x dy$ profiles											
I. Zero projection × 0.92											
Chaff	----	1216	----	1110	900	-----	900	886	708	799	----	----
Oil fog	1565	835	1374	1110	1015	varies		485	655	812	883	868
II. 40% of upper peak/shoulder											
Chaff	----	1251	----	1024	880	-----	880	876	611	700	----	----
Oil fog	1586	1256	1412	1090	890	875		685	615	780	916	865
Quality factors for $\int x dy$ methods											
Profile fuzziness index*, large x											
Chaff	----	1.0	----	0.5	0.25	----	0.25	0.3	0.5	0.6	----	
Oil fog	0.15	0.7	0.9	0.55	1.4	0.75		0.9	0.33	0.5	0.13	0.23
x range z_i nearly const., 10^2 m											
Chaff - method I	----	19-26	----	9-36	6-36	6-36		21-36	21-36	16-34	----	----
method II	----	16-26	----	29-36	16-36	16-36		14-36	16-36	19-36	----	----
Oil fog - method I	-21-	11-21	-28-	10-21	13-16	none		13-17	12-15	15-20	8-26	11-29
method II	16-21	21-27	-28-	6-14	13-16	10-19		12-17	12-15	15-20	8-26	8-29
Haze dropoff midpoints, lidar	----	730 to 1330	1310 to 1970	940 to 1140	860	860		860	550	570	840	935
Consensus estimate of z_i	1600 m	1240 m--1400 m		1100 m	880 m	---880 m	---880 m		640 m	---780 m	900 m	---870 m

* $3(z_{1/6} - z_{1/2})/z_{zp}$, where z_{zp} = "zero projection" height = $z_{1/6} + (z_{1/6} - z_{1/2})/2$.

a larger array of supporting evidence for the recommended z_i values. The accuracy of these values can be roughly estimated as ±20 m on 6 September and 13 September, and as ±50 m on other days.

Much valuable statistical information on wind velocity was obtained from the fast-response u-v-w measurements from sonic anemometers at eight tower levels (10 m, 22 m, 50 m, and every 50 m to 300 m). One example is shown in Tables 7.3 and 7.4, which list frequencies of occurrence of wind azimuth and elevation angles, by 5° bins, for each CONDORS 83 period at z = 250 m (near the height of elevated releases). These distributions will be useful for comparison with the observed near-source chaff and oil fog distributions. Table 7.3, which shows azimuth angle distributions, shows predominantly Gaussian-like distributions, with a skew towards one flank or secondary peaks during some periods. The square root of variance, σ_a, ranges from 11° to 39°, and is predominantly controlled by wind speed; $\sigma_a \simeq \sigma_v/\overline{u}$, when σ_a is expressed in radians, and $\sigma_v \simeq 0.6\ w^*$ have been observed in convective boundary-layer experiments at all z/z_i for averaging periods of about 1 hr (Hicks, 1985). For CONDORS 83 periods, $\sigma_a\ \overline{u}/w^* \simeq 0.6$ for most periods and ranges from 0.37 to 0.77; the smallest and largest values coincide with the smallest and largest dimensionless period durations, 2.8 and 16.7, respectively, but the correlation is imperfect as there is considerable scatter. Period 11-83, with the smallest $\overline{u}/w^*$ (0.87), had 10-s average θ_a values scattered all around the compass, but the relationship $\sigma_a \simeq 0.6\ w^*/\overline{u}$ held true. This small $\overline{u}/w^*$ marks the lowest useable value in our experiment, because we could observe plumes only within a certain sector of wind direction. Furthermore, at lower $\overline{u}/w^*$, upwind diffusion of the oil fog tended to threaten both personnel and delicate instrumentation.

Table 7.3 Frequency distributions of wind azimuth angles, z = 250 m, BAO Tower, CONDORS 83 (from 10 s averages), percent × 10^{-3}

Period / Direction	1-83	2-83	3-83	4-83	5-83	6-83	7-83	8-83	9-83	10-83	11-83*
40°-45°			3		4					6	8
45°-50°			8	3	4		6				8
50°-55°		8	6				6	8	8	6	4
55°-60°		4	8		4		6	12		6	21
60°-65°			3	13	8	6		12	12	44	4
65°-70°		4	3	3	17	6	6	29	17	28	17
70°-75°	6	12	11	3	17	6	6	50	25	11	33
75°-80°	6	4	19	3	17			71	75	17	46
80°-85°	6	4	25	7	29	17	6	125	196	22	4
85°-90°		8	31	23	25	22	17	117	213	100	38
90°-95°	39	29	64	10	38	11	11	154	171	89	67
95°-100	33	29	103	20	62	11	17	113	125	89	58
100°-105	61	38	119	30	46	11	22	108	71	106	87
105°-110°	72	108	119	37	58	28	67	117	54	83	87
110°-115°	106	146	69	40	50	22	89	58	17	72	108
115°-120°	122	108	108	90	46	50	167	17	8	67	83
120°-125°	128	129	83	93	54	56	139	8	8	28	83
125°-130°	89	67	72	113	62	100	78			50	75
130°-135°	83	46	61	113	62	111	144			39	42
135°-140°	83	62	36	110	79	72	78			33	25
140°-145°	28	50	28	73	67	106	56			11	
145°-150°	17	33	17	33	92	50	61			17	17
150°-155°	11	25	3	47	25	61	11			28	8
155°-160°	22	29		47	50	78					4
160°-165°	11	17		33	38	72	11				4
165°-170°	33	8		13	29	50				11	8
170°-175°	17	4		7	8	22				6	4
175°-180°	11	4			4	17					4
180°-185°	17	12		7	4	11				17	4
185°-190°				3							
190°-195°		8		7		6					
σ_a	21°	22°	19°	23°	28°	24°	18°	14°	11°	29°	39°
$\sigma_a \bar{u}/w^*$	0.58	0.37	0.43	0.41	0.75	0.62	0.64	0.77	0.59	0.60	0.57

*50° added to period 11 azimuths - mean wind direction was 56°

Table 7.4 Frequency distributions of wind elevation angles, z = 250 m, BAO Tower, CONDORS 83 (from 10 s averages), percent × 10^3

Period / Elevation	1-83	2-83	3-83	4-83	5-83	6-83	7-83	8-83	9-83	10-83	11-83
75°-80°											8
70°-75°				3							
65°-70°				13							
60°-65°				7						6	8
55°-60°		4		7	4	6				6	21
50°-55°		8	3	23	8	17					8
45°-50°		8		13	8	6	11			11	8
40°-45°		17	6	47	21	6	6			22	8
35°-40°	6	4	6	43	33	11	22	4		44	17
30°-35°		4	11	33	50	6	11	8		39	21
25°-30°	6	33	11	43	58	17	17	4	17	6	21
20°-25°	17	38	11	17	29	28	11	46	29	17	42
15°-20°	28	21	19	47	54	6	44	79	75	17	12
10°-15°	67	38	22	37	75	17	67	146	100	44	21
5°-10°	89	12	17	37	50	56	94	154	142	39	17
+ 0°- 5°	83	29	22	27	92	39	61	142	175	72	12
- 5°- 0°	94	42	61	47	42	39	78	125	154	56	46
10°- 5°	122	75	61	63	92	61	161	117	129	78	67
15°-10°	94	87	56	60	117	61	100	92	92	78	38
20°-15°	89	67	117	83	100	167	78	71	54	100	104
25°-20°	89	87	181	80	83	156	78	8	21	117	104
30°-25°	78	138	142	40	33	139	56	4	12	72	79
35°-30°	50	117	139	57	33	94	50			78	75
40°-35°	44	62	72	37	12	56	11			39	83
45°-40°	17	50	25	40	4	17	28			39	50
50°-45°	6	25	14	40			6			11	33
55°-50°	11	17	6	7			6				38
60°-55°	6			10			6				17
65°-60°		8		13						6	8
70°-65°		8		10							12
75°-70°				3						6	8
80°-75°	6			7							4
85°-80°				3							4
90°-85°				3							4
Mean θ_e	-11°	-15°	-18°	-5°	+1°	-13°	-6°	+2°	+1°	-8°	-16°
σ_e	18°	24°	18°	33°	21°	21°	20°	12°	12°	25°	31°
$\sigma_e \bar{u}/w^*$	0.50	0.40	0.40	0.58	0.58	0.54	0.69	0.67	0.62	0.50	0.45
250 m/z_i	0.16	0.20	0.18	0.23	0.28	0.28	0.28	0.39	0.32	0.28	0.29

Table 7.4, which shows elevation angle distributions, reveals surprisingly large skewness in some periods, with mean θ_e as low as -18° and the mode of θ_e as low as -28°. The most negative mean θ_e values tended to correlate with the lowest wind speeds, and two of the three slightly positive values occurred during the highest wind speed periods. This trend could be due to a site effect, or could be due to a bias towards downdraft-dominated periods in our attempt to exclude large wind direction changes from averaging periods (this is especially a problem at low wind speeds). This question needs further investigation. The $\sigma_e \, \overline{u}/w^*$ values, with σ_e in radians, fall within the range observed in other convective boundary-layer experiments, with a slight trend to smaller values both at smaller dimensionless period durations ($\tau\overline{u}/z_i$) and at smaller dimensionless measurement heights (250 m/z_i).

Much more statistical information has been obtained than could be included in this volume. The type of information in Tables 7.3 and 7.4 has been obtained for each tower level for each CONDORS 83 period; in addition, we have calculated the mean wind speeds for each 5° bin of θ_a and of θ_e, and the joint distribution of θ_a and θ_e for each averaging period. For each of the five days with SF_6 sampling, for the entire release period, we have calculated 5-min averages and distributions for a number of quantities; these include $\overline{w'T'}$, solar radiation, $\overline{u}$ and $\overline{\theta}_a$ at 50 m and 250 m, the distribution of θ_a at 250 m by 5° bins, and the percent of negative 10 s $\overline{w}$ events at 50 and 250 m; in addition, the $\overline{u}$, $\overline{\theta}_a$, and θ_a distribution were conditionally sampled during negative $\overline{w}$ events for comparisons with tracer distributions impacting the surface from elevated sources.

8. OIL FOG PLUME STATISTICS FROM LIDAR OBSERVATIONS

S. W. Troxel and W. L. Eberhard

8.1 Description of Data

This chapter presents a summary description of the average behavior of the oil fog plume for each analysis period. The tables in Sec. 8.3 include parameters such as the coordinates of plume's centroid, second moments of the horizontal and vertical profiles, and the empirical conversion factor that relates optical backscatter coefficient to mass loading. Each parameter was calculated after the two-dimensional distributions from the individual scans were averaged together at each lidar azimuth (there were typically about 11 scans in an averaging period). Section 8.2 defines the algebraic symbols for these plume parameters and the relevant coordinate systems (Fig. 8.1) for the lidar data.

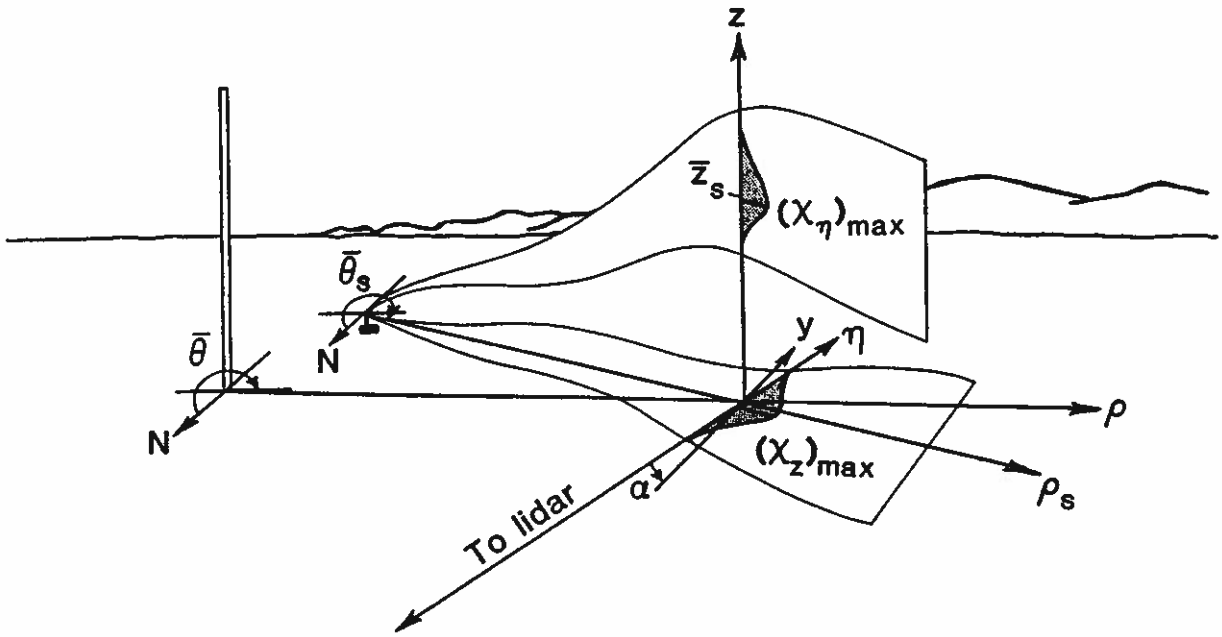

Figure 8.1. Conceptual diagram illustrating coordinates and symbols defined in Sec. 8.2.

Some aspects of these data require clarification. The oil fog release rate changed during some of the periods; K_0 is based on a time-averaged rate for the period. Since the surface releases were about 0.1 km west of the tower, the centroid locations relative to the source (subscripted with an s) are more rigorous. Centroid locations that have no subscripts are relative to the base of the tower. They are useful for comparing lidar data with those from the radar and gas samplers. (The value of $\overline{z} - \overline{z}_s$ differs slightly from the nominal release height z_s because minor, uncoordinated approximations were applied to each type of data. The difference is insignificant.) The parameter z of $(\chi_\eta)_{max}$ is the only one that incorporates the adjustments (Eq. 3.12) to the lowest usable data point. For more detailed data, see Appendix A.

8.2 Lidar Coordinates and Symbols

K_0	conversion factor from χ to optical backscatter coefficient ($m^2\ g^{-1}\ sr^{-1}$).
y	horizontal coordinate normal to $\overline{\rho}_s$ (m).
z	vertical coordinate referenced to tower base (m).
$\overline{z}$	height of plume centroid from tower base ($\simeq \overline{z}_s$ for surface release) (m).
$\overline{z}_s$	height of plume centroid from source (m).
z of $(\chi_\eta)_{max}$	height referenced to tower base of maximum in χ_η (m).
α	acute angle between η and y axes (°).
η	horizontal coordinate in the scan plane (m).
$\overline{\theta}$	azimuth angle of plume centroid from tower base (°).
$\overline{\theta}_s$	azimuth angle of plume centroid from source (°).
θ_L	lidar scan azimuth (°).

ρ	horizontal coordinate referenced to tower base (m).
$\overline{\rho}$	horizontal distance from tower to centroid (m).
ρ_s	horizontal coordinate referenced to source (m).
$\overline{\rho}_s$	horizontal distance from source to centroid (m).
σ_y	standard deviation of χ_z projection on y axis (m).
σ_z	standard deviation of χ_η along z axis (m).
χ_η	horizontally integrated oil fog concentration (sr^{-1}).
χ_z	vertically integrated oil fog concentration (sr^{-1}).
χ_η^n, χ_z^n	normalized concentrations usually total 1000 (see Eqs. 3.4, 3.5).
$\chi_{\eta z}$	horizontally and vertically integrated oil fog concentration ($m\ sr^{-1}$).
χ/Q	inferred normalized concentration based on empirical calibration (see Eq. 3.13) ($s\ m^{-3}$).

A pictorial representation of the above symbols is given in Fig. 8.1.

8.3 Average Oil Fog Plume Statistics for CONDORS 82 and CONDORS 83

Table 8.1 CONDORS 82 averaged plume statistics, Period 1-82
Release height: 235 m

θ_L	150.0°	154.9°	162.5°	176.6°
Start time (MST)	1304	1304	1304	1304
End time (MST)	1333	1333	1333	1333
$\overline{\rho_s}$	274	540	950	1745
$\overline{\rho}$	274	540	950	1745
$\overline{\theta_s}$	232.6	231.9	236.3	241.5
$\overline{\theta}$	232.6	231.9	236.3	241.5
σ_y	38.1	51.1	132.9	358.7
$\overline{z_s}$	-2.2	17.6	13.9	4.8
$\overline{z}$	233.7	253.5	249.8	240.8
σ_z	36.6	56.1	116.9	146.9
z of $(x_n)_{max}$	207	219	288	38
K_0	0.1204	0.0707	0.0782	0.0295
α	7.4	13.1	16.2	25.2

Table 8.2 CONDORS 82 averaged plume statistics, Period 2-82
Release height: 235 m

θ_L	150.0°	154.9°	162.5°	176.6°
Start time (MST)	1411	1411	1411	1411
End time (MST)	1446	1446	1446	1446
$\overline{\rho_s}$	275	538.3	1026	1911
$\overline{\rho}$	275	538.3	1026	1911
$\overline{\theta_s}$	231.7	232.6	225.2	232.4
$\overline{\theta}$	231.7	232.6	225.2	232.4
σ_y	32.1	65.2	100.1	317.4
$\overline{z_s}$	2.7	-15.7	46.2	25.1
$\overline{z}$	238.6	220.3	282.1	261.0
σ_z	36.8	50.4	115.1	146.3
z of $(\chi_\eta)_{max}$	207	226	238	288
K_0	0.1457	0.0682	0.0655	0.0296
α	8.3	12.3	27.3	34.2

Table 8.3 CONDORS 82 averaged plume statistics, Period 3-82
Release height: 167 m

θ_L	147.8°	150.0°	154.9°	165.0°
Start time (MST)	1354	1354	1354	1354
End time (MST)	1434	1434	1434	1434
$\overline{\rho_s}$	183	321	575	1086
$\overline{\rho}$	183	321	575	1086
$\overline{\theta_s}$	268.4	272.1	268.8	272.6
$\overline{\theta}$	268.4	272.1	268.8	272.6
σ_y	64.2	55.2	118.6	268.7
$\overline{z_s}$	20.5	46.7	71.9	126.0
$\overline{z}$	188.4	214.6	239.8	293.9
σ_z	48.1	85.0	138.1	206.8
z of $(\chi_\eta)_{max}$	176	126	188	38
K_0	0.1400	0.0637	0.0647	0.0302
α	30.6	32.1	24.0	17.6

Table 8.4 CONDORS 82 averaged plume statistics, Period 4-82
Release height: surface

θ_L	150.0°	154.9°	159.7°
Start time (MST)	1153	1153	1153
End time (MST)	1237	1237	1237
$\overline{\rho_s}$	182	444	693
$\overline{\rho}$	290	526	779
$\overline{\theta_s}$	239.0	229.1	233.0
$\overline{\theta}$	260.3	242.1	241.4
σ_y	123.7	195.2	277.7
$\overline{z_s}$	135.6	364.3	504.4
$\overline{z}$	136.6	365.3	505.4
σ_z	109.6	193.5	250.7
z of $(\chi_\eta)_{max}$	38	438	538
K_0	0.0841	0.0716	0.0358
α	1.0	15.9	16.7

Table 8.5 CONDORS 82 averaged plume statistics, Period 5-82
Release height: surface

θ_L	150.0°	154.9°	159.7°
Start time (MST)	1312	1312	1312
End time (MST)	1354	1354	1354
$\overline{\rho_s}$	207	463	677
$\overline{\rho}$	272	532	772
$\overline{\theta_s}$	211.2	222.4	238.7
$\overline{\theta}$	240.8	236.1	246.5
σ_y	139.7	199.5	306.6
$\overline{z_s}$	224.0	374.8	557.5
$\overline{z}$	225.0	375.7	558.5
σ_z	180.0	270.1	260.9
z of $(x_n)_{max}$	26	88	488
K_0	0.0567	0.0495	0.0398
α	28.8	22.5	11.0

Table 8.6 CONDORS 83 averaged plume statistics, Period 1-83
Release height: surface

θ_L	169.9°	174.0°	181.1°	190.0°	200.1°*	200.1°**
Start time (MST)	1330	1330	1330	1330	1330	1330
End time (MST)	1400	1400	1400	1400	1400	1400
$\overline{\rho_s}$	391	576	1078	1565	2144	2155
$\overline{\rho}$	510	712	1214	1704	2284	2295
$\overline{\theta_s}$	325.0	302.3	301.0	293.5	286.7	283.3
$\overline{\theta}$	315.6	299.6	299.6	293.1	286.8	283.6
σ_y	62.5	134.0	249.6	322.0	435.8	471.1
$\overline{z_s}$	100.5	169.9	377.0	667.7	896.1	888.2
$\overline{z}$	98.3	167.7	374.8	665.5	893.9	886.1
σ_z	88.3	104.8	256.9	345.5	441.2	456.9
z of $(\chi_\eta)_{max}$	20	20	133	583	733	733
K_0	0.0145	0.0497	0.0455	0.0548	0.0283	0.0361
α	65.2	38.3	29.9	13.5	3.4	6.8

* Smoke from fire was excluded. May have omitted some oil fog.
** Some smoke from fire included.

Table 8.7 CONDORS 83 averaged plume statistics, Period 2-83
Release height: surface

θ_L	169.9°	174.0°	181.1°	190.0°	200.1°	210.1°
Start time (MST)	1140	1130	1130	1130	1130	1130
End time (MST)	1200	1200	1200	1200	1200	1200
$\overline{\rho_s}$	219	540	1049	1604	2161	2691
$\overline{\rho}$	357	678	1187	1742	2298	2830
$\overline{\theta_s}$	300.6	297.4	298.0	298.5	297.8	296.2
$\overline{\theta}$	295.8	295.5	296.9	297.7	297.2	295.8
σ_y	74.5	173.9	229.7	323.5	443.9	581.3
$\overline{z_s}$	59.0	225.3	342.9	364.0	391.1	488.1
$\overline{z}$	56.9	223.2	340.7	361.9	388.9	485.9
σ_z	41.8	174.4	231.2	248.9	256.6	319.9
z of $(x_\eta)_{max}$	14	95	183	133	333	283
K_0	0.0331	0.0712	0.0603	0.0492	0.0468	0.0397
α	40.7	33.3	26.9	18.5	7.7	3.8

Table 8.8 CONDORS 83 averaged plume statistics, Period 3-83
Release height: surface

θ_L	169.9°	174.0°	181.1°	190.0°	200.1°	210.0°
Start time (MST)	1230	1230	1230	1230	1230	1230
End time (MST)	1330	1330	1330	1330	1330	1330
$\overline{\rho_s}$	168	471	949	1539	2146	2786
$\overline{\rho}$	305	609	1088	1679	2285	2925
$\overline{\theta_s}$	272.1	280.8	281.1	288.8	286.8	284.6
$\overline{\theta}$	279.4	282.5	282.0	288.7	286.8	284.7
σ_y	112.6	235.5	339.3	548.7	686.6	745.6
$\overline{z_s}$	59.4	153.9	269.4	358.4	429.6	522.6
$\overline{z}$	57.2	151.7	267.7	356.2	427.4	520.5
σ_z	60.7	123.4	186.6	255.6	308.0	349.1
z of $(\chi_\eta)_{max}$	14	45	83	183	133	183
K_0	0.0590	0.0729	0.0717	0.0757	0.0839	0.0955
α	12.2	16.8	10.0	8.8	3.4	15.5

Table 8.9 CONDORS 83 averaged plume statistics, Period 4-83
Release height: surface

θ_L	169.9°	173.0°	177.5°	183.1°	195.0°
Start time (MST)	1055	1055	1055	1055	1055
End time (MST)	1145	1145	1145	1145	1145
$\overline{\rho_s}$	339	639	993	1410	2143
$\overline{\rho}$	463	765	1121	1537	2267
$\overline{\theta_s}$	320.8	316.4	313.8	313.8	316.1
$\overline{\theta}$	311.5	311.4	310.7	311.5	314.4
σ_y	137.6	220.9	288.0	345.9	384.8
$\overline{z_s}$	199.7	357.9	485.4	528.7	493.7
$\overline{z}$	197.5	355.7	483.2	526.5	491.5
σ_z	185.0	256.7	282.3	283.9	285.1
z of $(\chi_\eta)_{max}$	33	233	483	533	433
K_0	0.0378	0.0420	0.0464	0.0380	0.0334
α	60.9	53.4	46.4	40.7	31.1

Table 8.10 CONDORS 83 averaged plume statistics, Period 5-83
Release height: 280 m

θ_L	169.9°	174.0°	178.9°	183.1°	188.0°
Start time (MST)	1050	1050	1050	1050	1050
End time (MST)	1130	1130	1130	1130	1130
$\overline{\rho s}$	369	757	1045	1275	1555
$\overline{\rho}$	369	757	1045	1275	1555
$\overline{\theta s}$	300.4	305.1	298.2	293.3	289.3
$\overline{\theta}$	300.4	305.1	298.2	293.3	289.3
σy	163.2	257.0	328.7	352.7	441.1
$\overline{z_s}$	-17.0	0.2	-17.9	33.6	2.1
$\overline{z}$	264.0	281.1	263.1	314.6	283.1
σz	152.0	210.1	203.8	239.4	240.9
z of $(x_\eta)_{max}$	283	33	83	83	33
K_0	0.0385	0.0299	0.0341	0.0301	0.0215
α	40.5	41.1	29.2	20.2	11.2

Table 8.11 CONDORS 83 averaged plume statistics, Period 6-83
Release height: 280 m

θ_L	169.9°	174.0°	178.9°	183.1°	188.0°
Start time (MST)	1130	1130	1130	1130	1130
End time (MST)	1200	1200	1200	1200	1200
$\overline{\rho_s}$	600	963	1330	1592	1922
$\overline{\rho}$	600	963	1330	1592	1922
$\overline{\theta_s}$	322.0	317.7	315.7	314.2	315.6
$\overline{\theta}$	322.0	317.7	315.7	314.2	315.6
σ_y	144.6	265.4	344.8	441.8	387.3
$\overline{z_s}$	-75.7	-33.1	8.5	-22.1	48.4
$\overline{z}$	205.3	247.9	289.5	258.9	329.4
σ_z	157.8	202.0	195.5	174.6	203.3
z of $(x_\eta)_{max}$	133	33	33	133	333
K_0	0.0312	0.0306	0.0315	0.0373	0.0365
α	62.1	53.7	46.8	41.0	37.6

Table 8.12 CONDORS 83 averaged plume statistics, Period 7-83
Release height: 280 m

θ_L	169.9°	174.0°	178.9°	183.1°	188.0°
Start time (MST)	1210	1210	1210	1210	1214
End time (MST)	1240	1240	1240	1240	1240
$\overline{\rho_s}$	484	821	1155	1336	1681
$\overline{\rho}$	484	821	1155	1336	1681
$\overline{\theta_s}$	314.2	310.0	306.9	299.4	303.1
$\overline{\theta}$	314.2	310.0	306.9	299.4	303.1
σ_y	120.3	224.4	276.3	386.7	448.8
$\overline{z_s}$	-24.0	-53.1	-1.8	-103.2	-78.2
$\overline{z}$	257.0	227.9	279.2	177.7	202.8
σ_z	105.5	151.7	197.4	125.9	156.1
z of $(\chi_\eta)_{max}$	220	33	33	83	83
K_0	0.0305	0.0305	0.0261	0.0284	0.0219
α	54.3	46.0	38.0	26.0	25.1

Table 8.13 CONDORS 83 averaged plume statistics, Period 8-83
Release height: 265 m

θ_L	168.4°	172.3°	176.1°	178.9°	183.1°	188.0°
Start time (MST)	1230	1230	1230	1230	1230	1230
End time (MST)	1310	1310	1310	1310	1310	1310
$\overline{\rho_s}$	178	462	723	915	1197	1526
$\overline{\rho}$	178	462	723	915	1197	1526
$\overline{\theta_s}$	267.9	274.3	273.8	274.6	272.9	273.7
$\overline{\theta}$	267.9	274.3	273.8	274.6	272.9	273.7
σ_y	54.9	100.9	123.2	143.2	200.9	271.7
$\overline{z_s}$	8.8	58.3	90.6	99.6	83.4	64.1
$\overline{z}$	274.9	324.4	356.7	365.7	349.5	330.2
σ_z	36.3	88.8	114.1	136.7	129.7	163.4
z of $(x_n)_{max}$	301	395	420	433	333	283
K_0	0.1142	0.1194	0.1239	0.0851	0.0778	0.0747
α	9.5	12.0	7.7	5.7	0.2	4.3

Table 8.14 CONDORS 83 averaged plume statistics, Period 9-83
Release height: 265 m

θ_L	168.4°	172.3°	176.1°	178.9°	183.1°	188.0°	195.0°
Start time (MST)	1310	1310	1310	1310	1310	1310	1329
End time (MST)	1323	1350	1350	1350	1350	1350	1350
$\overline{\rho_s}$	177	452	718	911	1197	1527	1998
$\overline{\rho}$	177	452	718	911	1197	1527	1998
$\overline{\theta_s}$	268.2	267.7	266.1	269.8	273.7	273.5	275.1
$\overline{\theta}$	268.2	267.7	266.1	269.8	273.7	273.5	275.1
σ_y	36.9	63.0	164.3	188.3	271.2	228.0	333.4
$\overline{z_s}$	19.8	40.2	91.3	80.8	28.1	79.1	123.0
$\overline{z}$	285.8	306.2	357.3	346.8	294.1	345.2	389.1
σ_z	22.7	100.1	159.2	160.3	219.8	204.2	226.2
z of $(\chi_\eta)_{max}$	276	270	283	333	33	133	433
K_0	0.1372	0.1066	0.0932	0.0708	0.0648	0.0618	0.0634
α	9.8	5.4	0.0	0.9	0.6	4.5	9.9

Table 8.15 CONDORS 83 averaged plume statistics, Period 10-83
Release height: surface

θ_L	172.3°	175.0°	178.9°	183.1°	190.0°	205.0°
Start time (MST)	1140	1140	1140	1140	1140	1140
End time (MST)	1210	1210	1210	1210	1210	1210
$\overline{\rho_s}$	407	588	821	1084	1526	2597
$\overline{\rho}$	545	727	961	1223	1663	2732
$\overline{\theta_s}$	298.0	293.2	285.8	282.6	275.7	273.7
$\overline{\theta}$	295.5	292.2	286.1	283.3	276.7	274.4
σ_y	221.2	345.9	428.7	461.9	488.0	500.6
$\overline{z_s}$	238.0	334.2	420.4	469.3	524.4	433.8
$\overline{z}$	235.9	332.0	418.2	467.2	522.2	431.7
σ_z	207.1	235.6	271.1	252.4	249.5	250.7
z of $(\chi_n)_{max}$	33	183	133	333	783	183
K_0	0.0828	0.0606	0.0626	0.0543	0.0375	0.0102
α	35.7	28.2	16.9	9.5	4.4	21.3

Table 8.16 CONDORS 83 averaged plume statistics, Period 11-83
Release height: surface

θ_L	172.3°	175.0°	178.9°	183.1°	190.0°	205.0°
Start time (MST)	1240	1240	1240	1240	1240	1240
End time (MST)	1320	1320	1320	1320	1320	1320
$\overline{\rho_s}$	335	538	811	1134	1707	2930
$\overline{\rho}$	456	654	931	1251	1823	3054
$\overline{\theta_s}$	252.2	250.0	254.8	253.8	253.0	260.7
$\overline{\theta}$	262.5	257.6	259.5	257.4	255.5	261.9
σ_y	141.6	212.9	215.6	299.3	464.0	571.6
$\overline{z_s}$	164.1	312.7	344.8	438.0	490.1	469.1
$\overline{z}$	161.9	310.5	342.6	435.9	487.9	467.0
σ_z	139.1	198.9	230.4	241.0	221.9	226.3
z of $(\chi_n)_{max}$	83	133	183	233	633	483
K_0	0.1038	0.0615	0.0553	0.0412	0.0335	0.0119
α	10.1	15.0	14.1	19.3	27.0	34.4

9. CHAFF PLUME STATISTICS FROM RADAR OBSERVATIONS

T. Uttal and W. R. Moninger

9.1 Data Format

Radar observations for the 12 periods chosen for the CONDORS study are presented in this section. For each period, up to nine parameters describing the statistical properties of the observed average plumes are tabulated in Sec. 9.3 (there were typically about 17 volume scans in an averaging period). These calculations are discussed in Sec. 4.4. It should be noted that the first period, designated 0-82, was not included in any subsequent analysis or in the radar-lidar intercomparison. However, the radar data alone are of sufficient interest that we include them here. Periods 1, 3, 10 and 11 of 1983 were processed for the lidar, but have not been processed for the radar. Therefore, data for these periods are not included here. Also, periods 5 and 6 of 1983 were combined into one averaging period in the radar data analysis.

Most of the statistical parameters presented in the following tables can also be viewed in graphical form in Appendix B.

9.2 Radar Coordinates and Symbols

x	horizontal downwind coordinate referenced to tower base (m).
y	horizontal crosswind coordinate referenced to tower base (m).
$\bar{y}$	centroid of X_z (m).
y of $(X_z)_{max}$	crosswind position of maximum X_z (m).
z	vertical coordinate referenced to tower base (m).
$\bar{z}$	centroid of X_y (m).

z of $(x_y)_{max}$	height of maximum x_y (m).
σ_y	standard deviation of x_z along y axis (m).
σ_z	standard deviation of x_y along z axis (m).
x	chaff concentration (filament/(50 m)^3).
x_y	horizontally crosswind integrated chaff concentration (filament/(50 m)^2 horizontal column).
x_z	vertically integrated chaff concentration (filament/(50 m)^2 vertical column).
x_y^n, x_z^n	integrated concentrations normalized to total 1000, (see Eqs. 4.3, 4.5).
x_{yz}	horizontally (crosswind) and vertically integrated chaff concentration (filament/50 m thick slab normal to plume axis).

A pictorial representation of the above symbols is given in Fig. 9.1.

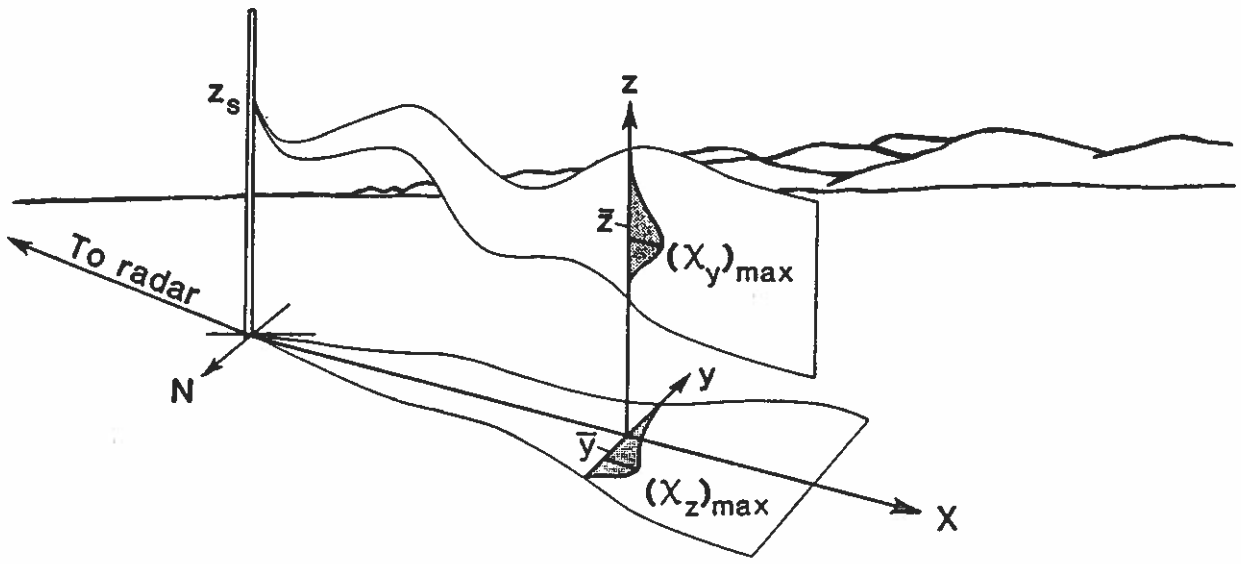

Fig. 9.1. Conceptual diagram illustrating coordinates and symbols defined in Sec. 9.2.

9.3 Average Chaff Plume Statistics for CONDORS 82 and CONDORS 83

Table 9.1 CONDORS 82 averaged plume statistics, Period 0-82
Release height: 3 m, direction x axis: 295°

x	$\bar{y}$	σ_y	y of $(x_z)_{max}$	$\bar{z}$	σ_z	z of $(x_y)_{max}$	$(x_y)_{max}$	x_{yz}
125	0	0	0	155	124	85	1	2
375	0	0	0	95	84	65	1	3
625	0	0	0	112	70	75	16	47
875	0	0	0	189	88	215	43	191
1125	0	0	0	342	194	215	31	233
1375	0	0	0	335	199	265	36	250
1625	0	0	0	378	267	185	25	188
1875	0	0	0	407	255	85	31	342
2125	0	0	0	479	255	565	19	273
2375	0	0	0	509	268	535	16	203
2625	0	0	0	489	283	255	16	223
2875	0	0	0	491	286	205	21	252
3125	0	0	0	498	264	465	13	185
3375	0	0	0	439	239	315	16	173
3625	0	0	0	473	245	515	15	176

Table 9.2 CONDORS 82 averaged plume statistics, Period 1-82
Release height: 235 m, direction x axis: 250°

x	$\bar{y}$	σ_y	y of $(x_z)_{max}$	$\bar{z}$	σ_z	z of $(x_y)_{max}$	$(x_y)_{max}$	x_{yz}
125	-11	132	15	220	34	225	5474	8786
375	-53	76	-35	201	53	195	5706	14626
625	-126	128	-125	213	87	185	3461	13849
875	-239	177	-345	243	126	195	3603	20969
1125	-249	151	-225	199	118	125	4622	21919
1375	-268	283	-255	209	141	85	3608	16785
1625	-331	345	-405	195	136	75	3066	13949
1875	-525	290	-495	181	126	75	2619	11367
2125	-528	357	-495	221	132	125	2306	14216
2375	-527	391	-615	246	124	215	2356	15484
2625	-342	441	-255	255	113	285	1769	11111
2875	-493	383	-655	214	127	115	2050	10917
3125	-656	442	-885	246	132	135	1702	11260
3375	-608	619	-815	265	127	195	1444	9919
3625	-636	675	-1045	265	124	225	1590	10676

Table 9.3 CONDORS 82 averaged plume statistics, Period 2-82
Release height: 235 m, direction x axis: 250°

x	$\bar{y}$	σ_y	y of $(\chi_z)_{max}$	$\bar{z}$	σ_z	z of $(\chi_y)_{max}$	$(\chi_y)_{max}$	χ_{yz}
150	14	139	-6	204	38	205	----	----
450	-117	121	-102	230	82	185	6026	19991
750	-441	501	-594	184	109	105	5195	16804
1050	-486	350	-716	203	129	105	6292	23807
1350	-528	285	-702	217	147	95	5390	27807
1650	-566	346	-726	245	156	125	2595	16298
1950	-663	356	-738	199	148	95	3651	17296
2250	-805	433	-918	243	170	75	3886	21550
2550	-838	529	-870	281	177	155	2315	15959
2850	-865	559	-666	290	188	125	2230	17111
3150	-1090	552	-1098	266	169	175	2789	18256
3450	-1136	704	-1350	308	187	195	1680	13707
3750	-1138	758	-1878	323	186	125	1329	11273
4050	-1235	663	-1242	312	175	155	1694	13615
4350	-1222	751	-1578	348	182	155	1191	11432

Table 9.4 CONDORS 82 averaged plume statistics, Period 3-82
Release height: 167 m, direction x axis: 290°

x	$\bar{y}$	σ_y	y of $(\chi_z)_{max}$	$\bar{z}$	σ_z	z of $(\chi_y)_{max}$	$(\chi_y)_{max}$	χ_{yz}
225	6	63	35	141	60	95	11780	35536
475	-29	116	5	161	109	75	10768	46034
725	-43	175	15	207	142	115	8487	45819
975	-34	223	95	252	169	125	7640	52478
1225	-82	256	-155	294	190	125	6102	52752
1475	-76	296	-275	339	199	245	5024	52709
1725	-29	334	45	386	210	345	4906	50629
1975	26	381	175	431	223	295	4392	49594
2225	77	403	25	460	231	415	4009	47851
2475	125	411	175	475	236	455	3385	41560
2725	177	432	305	479	242	495	3087	38186
2975	225	452	335	474	246	445	2763	32850
3225	282	456	415	467	249	455	2299	28511
3475	280	451	335	443	242	315	2104	25105
3725	9	310	135	412	235	265	1231	13989

Table 9.5 CONDORS 82 averaged plume statistics, Period 4-82
Release height: 3 m, direction x axis: 250°

x	$\bar{y}$	σ_y	y of $(x_z)_{max}$	$\bar{z}$	σ_z	z of $(x_y)_{max}$	$(x_y)_{max}$	x_{yz}
275	-4	183	35	160	116	135	428	1424
525	-122	250	-115	340	181	285	146	1070
775	-228	457	-395	439	236	245	137	886
1025	-188	446	85	566	230	635	118	1114
1275	-300	563	-765	578	247	575	140	1303
1525	-276	541	-105	579	241	705	107	1312
1775	-313	595	-155	598	241	765	106	1305
2025	-385	652	-625	590	261	725	96	1156
2275	-450	635	-435	548	267	675	91	1140
2525	-540	637	-725	538	239	645	82	1018
2775	-645	664	-855	544	246	675	78	909
3025	-678	713	-925	532	248	655	65	834
3275	-734	757	-965	546	249	615	62	727
3525	-806	768	-1175	546	257	645	50	620

Table 9.6 CONDORS 82 averaged plume statistics, Period 5-82
Release height: 3 m, direction x axis: 250°

x	$\bar{y}$	σ_y	y of $(\chi_z)_{max}$	$\bar{z}$	σ_z	z of $(\chi_y)_{max}$	$(\chi_y)_{max}$	χ_{yz}
275	-76	241	-45	257	204	85	607	3998
525	39	376	305	319	215	155	1503	5251
775	119	470	355	352	230	245	2530	6341
1025	-48	445	-45	572	270	565	321	3827
1275	-21	589	-55	651	323	435	313	4090
1525	92	573	195	706	317	665	239	4068
1775	94	645	605	708	319	765	219	3692
2025	77	711	425	723	314	665	194	3205
2275	96	752	255	681	306	715	178	2659
2525	149	790	35	650	304	745	157	2394
2775	136	834	-55	613	309	745	131	2148
3025	118	863	75	581	309	635	128	2065
3275	54	939	-55	585	297	625	122	1786
3525	72	951	275	595	310	655	88	1333

Table 9.7 CONDORS 83 averaged plume statistics, Period 2-83
Release height: 235 m, direction x axis: 297°

x	$\bar{y}$	σ_y	y of $(\chi_z)_{max}$	$\bar{z}$	σ_z	z of $(\chi_y)_{max}$	$(\chi_y)_{max}$	χ_{yz}
135	61	192	-110	177	93	135	5388	13811
385	52	105	50	161	127	65	4517	19639
635	38	154	30	167	135	35	3656	16299
885	41	193	-39	197	192	25	5346	18551
1135	57	226	130	300	238	115	2187	17258
1385	49	266	90	343	257	185	1625	15967
1635	66	290	130	399	304	165	1429	14841
1885	41	345	190	439	307	125	1075	13397
2135	54	393	250	434	292	155	935	11560
2385	54	454	270	432	289	165	825	10192
2635	74	491	150	468	309	265	694	9292
2885	96	552	210	512	326	245	532	8006
3135	73	607	190	540	339	235	454	6881
3385	70	621	250	575	342	365	359	5290
3635	37	645	290	583	332	435	300	4489

Table 9.8 CONDORS 83 averaged plume statistics, Period 4-83
Release height: 280 m, direction x axis: 302°

x	$\bar{y}$	σ_y	y of $(\chi_z)_{max}$	$\bar{z}$	σ_z	z of $(\chi_y)_{max}$	$(\chi_y)_{max}$	χ_{yz}
135	65	124	40	333	121	255	2495	9405
385	126	149	60	284	224	115	2390	16548
635	184	211	120	312	252	75	2405	18222
885	185	284	120	339	279	75	3643	20829
1135	280	335	320	410	270	185	1590	20906
1385	374	390	400	452	273	325	1463	20952
1635	432	394	440	452	266	365	1318	19522
1885	475	406	540	443	256	335	1140	16738
2135	506	435	420	442	260	375	944	14413
2385	541	483	520	472	274	415	822	12807
2635	570	509	520	510	283	465	768	11710
2885	634	536	580	534	285	485	673	10792
3135	651	567	640	532	289	485	570	9189
3385	672	609	580	538	287	535	478	8032
3635	674	638	600	541	285	385	426	6896

Table 9.9 CONDORS 83 averaged plume statistics, Period 5,6-83
Release height: 280 m, direction x axis: 309°

x	$\bar{y}$	σ_y	y of $(\chi_z)_{max}$	$\bar{z}$	σ_z	z of $(\chi_y)_{max}$	$(\chi_y)_{max}$	χ_{yz}
135	31	103	59	253	99	225	2661	5404
385	13	225	59	206	157	135	1744	7861
635	-42	284	85	217	186	105	1622	9475
885	-124	386	-227	228	205	25	1656	8453
1135	-141	464	-175	300	228	85	1040	8513
1385	-153	543	-253	355	241	105	760	8477
1635	-146	596	-279	385	242	165	613	7899
1885	-117	668	-253	412	240	225	553	7823
2135	-77	728	-71	423	239	295	542	7610
2385	-22	788	-123	440	240	295	462	6790
2635	-3	851	-123	445	236	305	439	6304
2885	13	888	137	452	232	375	404	5682
3135	24	938	397	453	234	385	359	5094
3385	76	965	215	449	231	405	348	4731
3635	145	942	423	443	231	365	310	4182

Table 9.10 CONDORS 83 averaged plume statistics, Period 7-83
Release height: 280 m, direction x axis: 300°.

x	$\bar{y}$	σ_y	y of $(\chi_z)_{max}$	$\bar{z}$	σ_z	z of $(\chi_y)_{max}$	$(\chi_y)_{max}$	χ_{yz}
125	46	73	30	214	53	205	4250	8711
375	83	120	110	179	106	105	2313	10707
625	112	176	110	216	125	175	1853	11156
875	152	296	90	153	156	35	6199	13997
1125	228	372	330	242	200	35	2559	12272
1375	252	467	310	302	223	65	1536	11272
1625	447	586	510	312	245	35	1185	9746
1875	519	701	150	349	241	155	919	9533
2125	631	777	10	385	233	175	648	8328
2375	767	832	110	399	232	145	618	7600
2625	826	865	170	419	227	225	614	7901
2875	921	915	110	440	224	295	553	7363
3125	991	961	190	450	224	445	537	7048
3375	1128	957	670	455	229	425	484	6965
3625	1212	960	950	452	230	435	457	6294

Table 9.11 CONDORS 83 averaged plume statistics, Period 8-83
Release height: 265 m, direction x axis: 264°

x	$\bar{y}$	σ_y	y of $(\chi_z)_{max}$	$\bar{z}$	σ_z	z of $(\chi_y)_{max}$	$(\chi_y)_{max}$	χ_{yz}
135	48	162	45	263	74	285	1244	3160
385	73	102	55	287	89	265	2354	10836
635	146	128	175	275	123	255	1932	12253
885	147	172	95	272	154	215	1572	12403
1135	210	178	245	282	153	205	1638	13958
1385	253	228	275	277	169	205	1373	12610
1635	279	258	285	306	174	335	1295	12714
1885	348	305	365	312	171	285	1358	12702
2135	382	321	385	320	174	275	1515	12995
2385	428	352	425	329	177	285	1302	12253
2635	476	364	465	324	179	265	1154	10858
2885	497	414	465	327	181	305	996	9867
3135	564	458	445	316	182	325	958	9238
3385	591	487	625	302	180	195	928	9190
3635	603	498	605	303	183	225	950	8957

Table 9.12 CONDORS 83 averaged plume statistics, Period 9-83
Release height: 265 m, direction x axis: 266°

x	$\bar{y}$	σ_y	y of $(\chi_z)_{max}$	$\bar{z}$	σ_z	z of $(\chi_y)_{max}$	$(\chi_y)_{max}$	χ_{yz}
135	65	75	55	265	44	275	4326	8185
385	78	96	85	278	85	265	2666	11049
635	101	126	105	286	132	285	2505	13850
885	157	189	195	279	179	155	2168	12873
1135	168	208	165	308	167	295	1902	14108
1385	219	250	175	302	205	125	1226	10623
1635	267	262	255	304	191	225	1343	12289
1885	260	287	185	303	198	195	1123	10441
2135	328	304	315	299	196	145	1088	10321
2385	337	342	265	333	205	155	927	9986
2635	366	367	325	319	207	235	974	9218
2885	415	378	325	341	198	255	894	8777
3135	466	411	345	337	211	235	723	8012
3385	484	423	415	345	211	185	743	7983
3635	522	431	505	357	210	225	674	7460

10. IN SITU OBSERVATIONS FROM GAS SAMPLERS

G. A. Briggs and G. E. Start

Normalized concentrations of the two tracer gases, SF_6 and Freon 13B1, measured along the 29 points on the sampling arc for the duration of the 1983 data averaging periods are presented in Table 10.1. As mentioned in Chapter 5, each 120 min diffusion run is separated into twelve 10 min sampling periods referred to as "fields" in the table. For example, Period 1-83 comprises Fields 7, 8 and 9. The bearings of the 29 stations listed are the corrected values with the 2.5° offset removed from the nominal azimuth positions. Superscripts in parenthesis indicate the number of missing 10 min samples in the average. If more than half the 10 min samples are missing, no average is given.

The "background" values of X/Q listed in Table 10.1 do not necessarily represent the actual background level of the tracers. They represent the high side of the range of measured X/Q values that occurs most frequently outside the obvious plume boundaries. These and lesser values seem to be randomly distributed with respect to sampler positions. The background values are suggested on the basis of frequency distributions for the 10 min samples for each entire run; these distributions are shown here in Fig. 10.1. (Values that were outside the scale ranges are credited in the highest and lowest log(X/Q) ranges in these figures.) For SF_6 there was a clear peak in the low-level X/Q frequency for four of the runs; for the remaining one, Test 2 (28 August 1983, Periods 2-83 and 3-83), there were two peaks in the distribution, one near 60×10^{-9} and one near 120×10^{-9} s/m^3; we chose the smaller X/Q as

Table 10.1 Average X/Q, 10^{-9} s/m^3, measured along sampling arc during CONDORS 83 averaging periods

Period	1-83	1-83	2-83	3-83	4-83	5-83	6-83	7-83	8-83	9-83
Tracer	131I	SF_6	SF_6	SF_6	SF_6	SF_6	SF_6	SF_6	SF_6	SF_6
Duration (min)	30	30	30	60	50	40	30	30	40	40
Fields	7-9	7-9	13-15	19-24	25-29	49-52	53-55	57-59	63-66	67-70
Background	52	52	72	72	100	72	72	72	100	100
Bearing										
202.5°	21	38	20	66	64(1)	79	45	71	---	---
207.5°	954	45	72	98	67(2)	100	33	47	---	---
212.5°	---	---	48	46(1)	91(1)	168(1)	88	90(1)	52(2)	---
217.5°	334	18	39	36	24	165	123	86	37(2)	---
222.5°	6(1)	21(1)	28	75(1)	112	29	21(1)	504	151(2)	---
227.5°	511	29	25	24(1)	57	105(1)	46	21	26(2)	---
232.5°	---	---	33	39	182	69	89	75	42(2)	140
237.5°	---	---	49	24	98(1)	52	70	446	96	229(1)
242.5°	---	---	6(1)	21	34	476	---	11(1)	126	88
247.5°	95(1)	5(1)	72	210	65	69	38	78	60	265
252.5°	---	---	62	370	50(1)	106	738	419	124(1)	37
257.5°	---	---	33	313	70	175	67	72	310	120
262.5°	---	---	70	463	103	177(1)	296	119(1)	324(1)	895
267.5°	21	56	745	91(1)	73(1)	752(1)	60	290	728	968
272.5°	90	52	200	1567	49(1)	1064	242	563	1445	1838
277.5°	145	27	312	1598	103	784	364	673	1112	689
282.5°	---	---	792	835	157	1250	312	774	237	166
287.5°	133	46	1018	412	259	736	240	1318	2337	2659
292.5°	405	294	314	148(1)	362	720(1)	264	703	221	36(1)
297.5°	205	364	1090	399	348	793	239(1)	682	191(1)	32
302.5°	364	215	1160	267	267	818	698	1064	45	58
307.5°	335	143	461	192(1)	774(1)	650	1010	681	149	155
312.5°	348	141	369	149(1)	1018	451	900	967(1)	31	60
317.5°	158	183	138	144(2)	540(1)	182(1)	6606	887	74	151
322.5°	101	212	348	136(3)	546	852(1)	---	659	71	140(2)
327.5°	52	51	95(1)	---	253(1)	12495(1)	2756	12532	680	230
332.5°	49	52	54(1)	139(3)	2725(1)	84	1338(1)	467	67(1)	23
337.5°	42	29	---	---	116	744	636	548	70(1)	117
342.5°	7	32	---	---	144	93	414	272	66	94

Note: Superscripts in parenthesis indicate number of missing 10 min samples (no avg. if >50% missing).

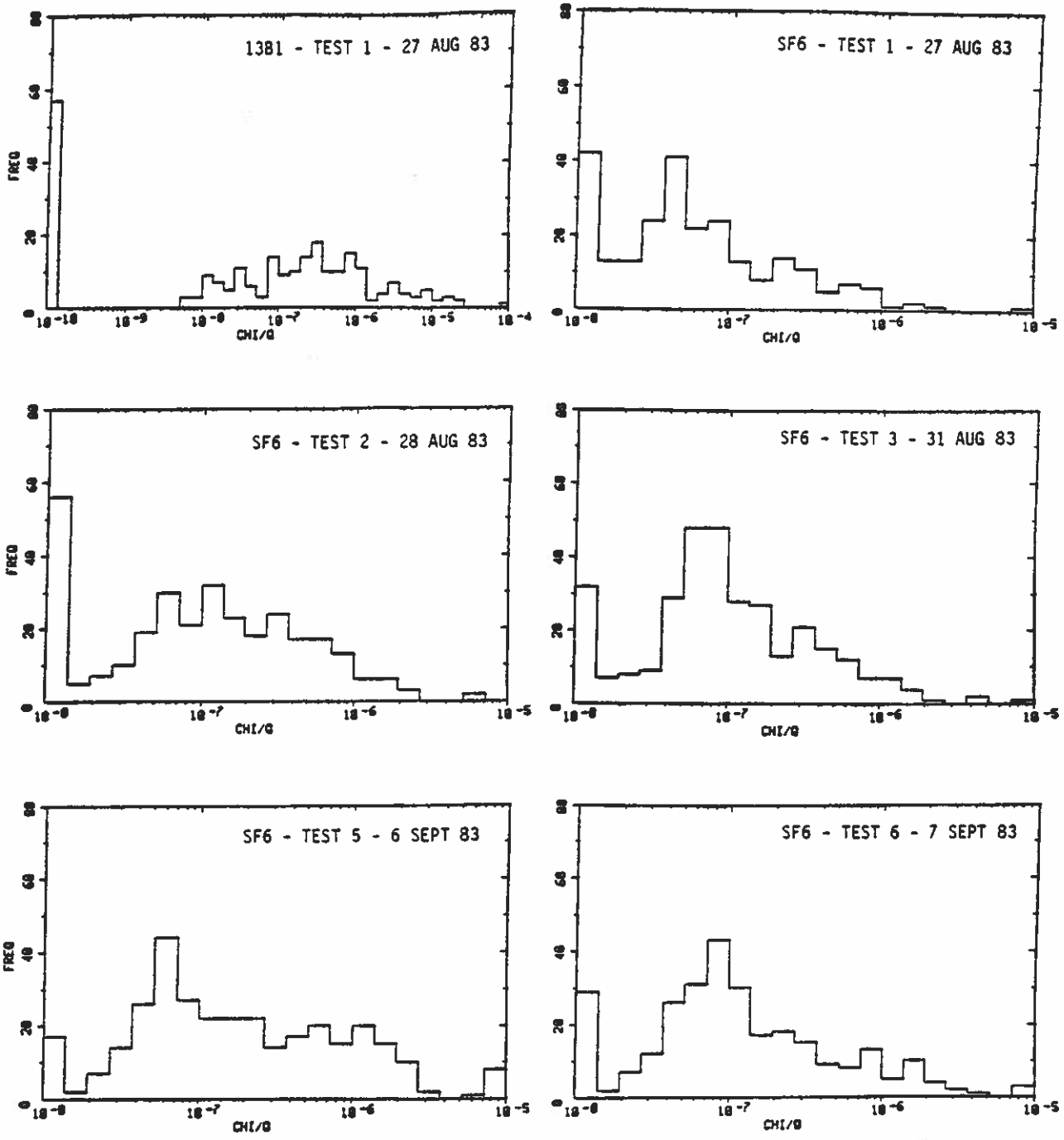

Figure 10.1 Frequency of occurrence of 10 min samples by log (X/Q) categories, 7 per decade, for each tracer in each successful run of CONDORS 83. X/Q in s/m^3. Out-of-range values placed in highest or lowest ranges within each figure abscissa.

"background" in this case. The 13B1 distribution has a number of peaks broadly distributed; the background value in this case is partly chosen on the basis of Period 1-83 (fields 7-9), the only data averaging period for that run.

Tables 10.2 to 10.7 show all the 10 min χ/Q values measured for the five successful runs during CONDORS 83. All five had acceptable ranges of values for the elevated-release SF_6, but only the first run gave reasonable magnitudes for the surface-release 13B1 tracer. The remainder of the measurements are not shown because strong contamination of the samples is suspected, as mentioned in Section 5.4. The suspected causes of the contamination are discussed at length in Appendix C.

It is evident in Tables 10.2 - 10.7 and in Fig. 10.1 that there are infrequent "spikes" of very large 10 min χ/Q compared to that measured at nearby samplers. (In Tests 1 and 5, some of these occurred slightly off the high end of the scales in Fig. 10.1) It is difficult to accept all of these as real, rather than as products of sporadic contamination. For instance, the largest χ/Q, $(8000\ m^3/s)^{-1}$ for 13B1 in Field 12 at 247.5° azimuth, implies the equivalent of a plume only 50 m wide and high impacting on only that particular sampler for 10 min, at x = 1250 m during highly dispersive conditions (Pasquill "B" stability category). For SF_6, during Test 5 (6 Sept. 1983) there were three spikes of about 1/4 this magnitude and four spikes of lesser magnitude for 10 min samples at a single sampler, 327.5° azimuth; the extreme case, Field 60, had 578 times the average χ/Q of its two nearest neighbors in azimuth. It is particularly difficult to imagine that such spikes of very high χ/Q could repeatedly hit the same sampler during noncongruent sampling

Table 10.2 13B1 X/Q, 10^{-9} s/m^3, for 27 August 1983, 1230-1430 MST

Field	1	2	3	4	5	6	7	8	9	10	11	12
Bearing												
202.5°	52	0	117	328	0	0	36	0	25	9	996	---
207.5°	1290	1297	1116	---	1019	911	726	1221	915	---	2766	4126
212.5°	---	---	---	---	---	---	---	---	---	---	---	---
217.5°	896	1096	1034	1034	524	883	0	1001	0	7592	919	517
222.5°	12	0	---	76	0	0	0	12	---	494	5999	---
227.5°	569	46	825	0	1063	424	607	563	365	---	---	---
232.5°	0	20	191	---	25	---	---	---	---	---	---	---
237.5°	179	0	6	75	37	---	---	---	---	---	---	---
242.5°	779	9	18	19855	19101	---	---	---	---	---	---	---
247.5°	527	974	0	0	---	---	---	0	189	7597	1627	125130
252.5°	---	0	0	0	---	---	---	---	---	---	---	---
257.5°	19	53	35	---	87	---	---	---	---	---	---	---
262.5°	0	---	876	0	---	---	---	---	---	---	---	---
267.5°	15	225	109	74	0	49	7	41	14	10903	---	---
272.5°	0	384	455	590	6	231	76	78	114	3262	---	---
277.5°	0	894	---	1001	883	321	169	0	265	2597	---	---
282.5°	0	---	268	17	342	692	---	---	---	---	---	---
287.5°	222	247	673	117	42	0	0	118	282	3072	---	---
292.5°	310	327	113	0	479	0	575	278	361	4304	---	---
297.5°	13	59	43	78	30	0	30	298	287	17854	---	---
302.5°	---	0	467	220	372	327	485	294	312	2648	---	---
307.5°	11	17	43	13	0	0	0	216	788	5739	4844	171
312.5°	99	216	0	29	19	252	664	380	0	7459	---	---
317.5°	175	0	0	0	302	212	311	164	0	2229	---	---
322.5°	0	0	19	72	72	28	93	211	0	21893	18442	2513
327.5°	0	0	---	0	91	842	84	37	35	8329	10909	2910
332.5°	174	111	35	36	11	0	8	126	13	9526	1777	6617
337.5°	262	0	96	311	0	166	0	0	127		392	2793
342.5°	252	14	0	152	0	0	0	0	21		4106	26
							Period 1-83					

Table 10.3 SF_6 X/Q, 10^{-9} s/m^3, for 27 August 1983, 1230-1430 MST

Field	1	2	3	4	5	6	7	8	9	10	11	12
Bearing												
202.5°	26	54	22	48	36	38	35	50	28	46	10	---
207.5°	92	72	13	---	8	14	50	39	45	---	32	40
212.5°	---	---	---	---	---	---	---	---	---	---	---	---
217.5°	16	946	79	75	70	1	32	16	5	34	5	1
222.5°	183	18	---	31	56	19	1	42	---	26	72	---
227.5°	781	556	195	9	64	62	18	19	51	---	---	---
232.5°	232	42	83	---	70	---	---	---	---	---	---	---
237.5°	580	4	48	17	25	---	---	---	---	---	---	---
242.5°	546	1	68	103	72	---	---	---	---	---	---	---
247.5°	206	240	41	42	---	---	---	10	1	259	77	22476
252.5°	---	72	24	36	---	---	---	---	---	---	---	---
257.5°	114	21	53	---	44	---	---	---	---	---	---	---
262.5°	323	---	128	2396	---	---	---	---	---	---	---	---
267.5°	59	84	1639	1745	932	50	34	124	10	106	---	---
272.5°	150	1	983	1335	24	76	60	59	35	111	---	---
277.5°	46	602	---	144	674	19	23	6	51	63	---	---
282.5°	38	---	54	46	197	46	---	---	---	---	---	---
287.5°	835	21	39	177	91	41	56	10	72	81	---	---
292.5°	60	172	17	38	179	83	313	126	442	296	---	---
297.5°	28	4	11	64	83	441	511	231	352	524	---	---
302.5°	---	1	50	11	209	328	215	227	203	541	---	---
307.5°	1	31	4	49	41	337	73	1	356	287	268	130
312.5°	44	76	30	36	4	50	315	1	105	138	---	---
317.5°	10	44	1	1	52	32	152	332	66	124	---	---
322.5°	12	13	13	41	50	9	44	79	512	175	43	113
327.5°	21	33	---	78	4	109	15	82	55	284	6	37
332.5°	26	58	14	1	34	50	41	38	78	259	14	41
337.5°	38	34	34	98	19	65	37	31	18		95	79
342.5°	23	4	1	12	33	16	3	37	57	---	242	45

Period 1-83

Table 10.4 SF_6 X/Q, 10^{-9} s/m^3, for 28 August 1983, 1130-1330 MST

Field	13	14	15	16	17	18	19	20	21	22	23	24
Bearing												
202.5°	1	1	59	1	1	55	13	135	49	22	58	119
207.5°	65	131	19	1	1	1	175	8	192	157	1	55
212.5°	56	48	39	49	4	24	30	58	60	---	73	11
217.5°	1	21	95	65	111	1	91	74	35	18	1	1
222.5°	82	1	1	1	6	1	250	111	1	13	1	---
227.5°	58	15	1	36	1	5	72	34	11	---	1	1
232.5°	51	1	47	49	49	27	18	59	63	10	53	30
237.5°	43	66	39	136	140	41	119	1	1	24	1	1
242.5°	1	---	11	1	1	1	1	37	8	1	76	1
247.5°	208	1	8	31	110	49	189	178	364	193	11	323
252.5°	52	51	83	7	7	54	781	206	789	79	224	139
257.5°	22	76	1	24	60	1	1	792	675	93	215	102
262.5°	44	88	79	8	96	---	1522	147	157	191	429	334
267.5°	1916	288	29	1079	80	187	276	15	44	74	---	49
272.5°	126	346	127	58	114	312	315	4508	791	152	1996	739
277.5°	283	366	288	111	48	277	718	6010	770	247	1459	385
282.5°	1291	918	166	189	242	499	473	2636	472	667	485	277
287.5°	1894	515	645	523	185	679	371	488	221	285	742	363
292.5°	302	56	584	537	641	107	245	160	167	74	---	94
297.5°	1019	1092	1161	980	1042	602	101	293	259	558	607	399
302.5°	2234	908	339	469	807	1591	79	126	209	305	883	1
307.5°	622	131	629	494	459	1475	135	60	228	473	---	65
312.5°	131	360	616	356	379	638	138	71	---	153	276	108
317.5°	122	32	260	536	486	207	330	20	113	113	---	---
322.5°	173	741	129	348	500	57	110	95	201	---	---	---
327.5°	---	59	130	120	177	150	---	56	100	---	---	---
332.5°	---	59	49	234	148	54	119	---	229	68	---	---
337.5°	---	---	135	119	85	64	---	---	---	---	---	---
342.5°	---	---	43	6	171	85	---	---	---	---	---	---
	Period 2-83						Period 3-83					

Table 10.5 SF_6 X/Q, 10^{-9} s/m^3, for 31 August 1983, 1055-1255 MST

Field	25	26	27	28	29	30	31	32	33	34	35	36
Bearing												
202.5°	56	96	---	66	39	---	---	40	52	15	58	1
207.5°	122	---	1	---	79	97	48	1	1	1	---	1
212.5°	70	96	21	---	175	52	1	16	84	1	42	1
217.5°	38	24	26	1	31	31	55	47	53	74	41	90
222.5°	1	137	156	216	50	1	1	1	---	1	12	---
227.5°	159	1	38	88	1	89	90	116	80	83	490	65
232.5°	84	142	62	55	567	49	67	---	63	107	64	213
237.5°	88	122	85	97	---	---	1	53	83	88	64	39
242.5°	63	46	18	40	4	76	---	102	46	8	58	80
247.5°	90	75	49	63	49	54	77	1	71	34	57	14
252.5°	58	43	22	74	---	---	---	---	9	63	32	40
257.5°	100	1	64	167	19	64	45	156	40	78	93	73
262.5°	84	69	1	302	61	96	6	60	29	117	21	28
267.5°	39	116	57	79	---	170	749	92	65	100	270	165
272.5°	50	---	22	63	61	102	330	71	238	180	195	126
277.5°	44	73	17	316	65	1	63	68	27	1	4700	1296
282.5°	375	33	287	64	25	151	176	274	50	256	160	145
287.5°	141	282	367	88	416	154	127	244	84	179	392	220
292.5°	268	509	618	45	368	86	57	---	124	114	85	219
297.5°	237	293	611	116	484	1015	71	48	127	11	472	624
302.5°	114	689	290	150	93	242	90	54	64	96	444	332
307.5°	900	1009	---	259	929	370	171	66	54	132	908	70
312.5°	2521	1421	368	438	343	598	76	93	---	174	599	103
317.5°	353	396	---	577	834	470	134	151	732	169	91	291
322.5°	27	1270	56	241	1136	179	---	131	359	---	91	377
327.5°	43	162	114	692	---	288	42	203	855	391	97	682
332.5°	76	1589	8817	---	417	190	4483	1709	127	1495	63	1280
337.5°	5	113	109	181	173	16	188	71	---	---	103	1123
342.5°	95	1	167	138	321	97	336	123	633	391	63	692
	Period 4-83											

Table 10.6 SF_6 X/Q, 10^{-9} s/m^3, for 6 September 1983, 1050-1250 MST

Field	49	50	51	52	53	54	55	56	57	58	59	60
Bearing												
202.5°	70	117	65	63	36	91	9	41	70	93	51	65
207.5°	129	114	65	90	1	63	36	1	61	31	49	18
212.5°	313	148	44	---	169	59	36	61	105	76	---	56
217.5°	356	239	1	64	46	257	67	233	59	176	23	10
222.5°	58	1	1	56	1	---	41	58	44	78	1389	829
227.5°	65	91	159	---	64	39	35	35	1	57	6	148
232.5°	69	48	73	85	64	63	140	23	36	43	146	1
237.5°	2	37	133	35	80	60	72	457	608	665	65	122
242.5°	235	1475	187	8	---	33	---	42	20	1	---	---
247.5°	190	63	23	1	56	55	1	49	79	56	98	20
252.5°	118	202	51	52	59	2060	96	490	677	502	79	60
257.5°	133	56	462	50	63	64	70	188	75	108	33	21
262.5°	122	311	---	100	30	278	580	281	194	45	---	220
267.5°	229	767	1262	---	63	84	33	---	756	76	39	175
272.5°	574	1726	1031	924	238	364	121	67	1041	42	606	658
277.5°	825	429	344	1539	54	175	864	121	417	84	1518	554
282.5°	1682	1219	1063	1034	271	453	213	98	964	100	1258	225
287.5°	1429	253	707	556	284	265	173	---	728	1286	1939	451
292.5°	1512	480	167	---	247	393	151	81	129	864	1116	148
297.5°	790	225	619	1537	---	222	256	58	357	1230	460	123
302.5°	434	273	1541	1023	398	911	784	124	1149	1956	88	596
307.5°	161	88	640	1710	465	563	2003	262	1001	889	153	226
312.5°		48	615	1443	904	534	1262	303	1359	576	---	542
317.5°	252	160	133	---	8371	8093	3356	42	556	1998	107	8010
322.5°	1952	39	566	---	---	---	2725	74	1409	468	99	44
327.5°	1286	186	---	36012	285	6015	1967	16445	27155	9402	1038	32078
332.5°	28	84	89	137	155	---	2521	2052	930	423	46	67
337.5°	43	2655	65	214	127	104	1677	1696	1472	121	50	40
342.5°	17	---	12	248	23	52	1168	1230	358	414	42	65
	Period 5-83				Period 6-83				Period 7-83			

Table 10.7 SF_6 X/Q, 10^{-9} s/m^3, for 7 September 1983, 1210-1410 MST

Field	61	62	63	64	65	66	67	68	69	70	71	72
Bearing												
202.5°	70	1	38	---	---	---	---	---	---	---	---	---
207.5°	77	29	230	---	---	---	---	---	---	---	---	---
212.5°	12	250	85	20	---	---	---	---	---	---	---	---
217.5°	1	31	55	20	---	---	---	---	---	---	---	---
222.5°	75	16	136	166	---	---	---	---	---	---	---	---
227.5°	1	76	50	1	---	---	---	---	---	---	---	---
232.5°	84	1	---	26	66	33	264	61	183	51	778	81
237.5°	430	954	59	48	183	94	491	---	24	172	47	102
242.5°	205	635	63	349	93	1	115	40	105	93	56	289
247.5°	427	341	1	21	178	38	1	316	58	685	117	1407
252.5°	---	---	260	57	---	55	1	1	31	117	205	231
257.5°	854	84	849	65	233	94	210	186	67	19	123	51
262.5°	422	813	344	---	564	65	27	2493	916	145	340	---
267.5°	836	576	1898	343	490	182	46	746	1097	1984	90	107
272.5°	659	228	2533	1201	572	1475	917	1112	1514	3810	179	9981
277.5°	2487	1004	1398	1433	855	763	459	216	226	1856	107	66
282.5°	62	413	328	375	180	64	105	118	359	82	58	83
287.5°	40	470	85	144	40	9079	9227	1289	20	102	3137	3289
292.5°	47	85	1	537	41	304	10	40	57	---	90	42
297.5°	68	82	277	---	146	150	34	94	1	1	1660	44
302.5°	78	47	123	52	1	5	57	68	106	1	100	124
307.5°	1	74	102	28	265	199	80	166	295	80	86	67
312.5°	101	1	37	41	46	1	123	60	10	46	95	77
317.5°	60		48	133	27	87	90	53	275	186	198	37
322.5°	131	73	75	111	97	1	---	238	41	---	103	89
327.5°	105	48	299	71	879	1471	260	22	519	117	864	1435
332.5°	101	41	107	---	59	36	1	87	1	2	50	87
337.5°	53	96	139	71	---	1	84	63	226	97	304	105
342.5°	39	1	72	78	29	86	1	169	102	104	79	141
			Period 8-83				Period 9-83					

intervals, while entirely missing the nearest samplers, about 110 m away. In these cases contamination of the particular sampler is easily suspected, although no cause of this type of contamination has been uncovered.

Tables 10.8 and 10.9 are provided here to identify the most suspect 10-min spikes of large χ/Q values affecting our averaging periods. Table 10.8 identifies cases of multiple spikes occurring at the same sampler during the same run. A spike is defined here as more than 5 times both the background χ/Q and the average χ/Q of the nearest two neighbors. If the neighboring χ/Q is missing, the designated background value for the run is used in its place. Table 10.9 identifies cases of single spikes of 10- or 20-min high χ/Q values using a slightly more restrictive criterion. A spike is defined here as more than 10 times both the background χ/Q and the average χ/Q of the nearest two neighbors, with the same fallback for missing neighbors.

These tables are presented for convenience, but we hesitate to recommend discarding all of these data samples. Some could be real, especially the less extreme cases like Fields 70 and 72 of SF_6 at 247.5°. The incidence of these suspect samples ranges from none for SF_6 during Period 1-83 to 16.4% for 13B1 during the same period. The average incidence for all 871 measured SF_6 samples during the averaging periods is 3.1%. The recomputed period average χ/Q's with removal of all spikes listed in Tables 10.8 and 10.9 are listed in Table 10.10 and plotted in Fig. 10.2. These averages give much improved appearance to the χ/Q cross sections compared with the untouched averages in Table 10.1. Except when the spikes occur outside the azimuth range of the plume, this filtering should have only small effects on computed σ_y values. However, inclusion or removal of the spikes has a large effect on crosswind-

Table 10.8. Multiple spikes in tracer x affecting averaging periods

Period(s) Affected	Bearing	Fields	Avg. x/Q, 10^{-9} s/m^3 Spikes	Neigbors	Ratio
13B1: 1-83	207.5°	1,2,3,5,6,7,8,9,12	1403	42	34
"	217.5°	1,2,3,4,5,6,8,10	1758	66	26
"	227.5°	1,3,5,6,7,8,9	631	39	16
"	292.5°	5,7	527	26	21
"	302.5°	3,5,6,7	413	24	17
SF_6: 2-83	267.5°	13,16	1498	59	25
4	332.5°	26,27,31,32	4150	125	33
7	237.5°	56,57,58	577	28	21
6,7	252.5°	54,57,58	1080	73	15
6	317.5°	53,54,60	8158	361	23
5,6,7	327.5°	52,54,56,57,58,59,60	18306	426	43
9	247.5°	70,72	1046	182	6
8,9	287.5°	66,67,68,71,72	5204	91	57
8,9	327.5°	65,66,69,71,72	1034	56	18

Note: A "spike" in this context means that each x field listed exceeded both the background and the average of the two neighboring samplers by at least a factor of 5. If a neighboring sample is missing, background x is assumed.

Table 10.9. Single spikes in tracer x affecting averaging periods.

Period(s) Affected	Bearing	Fields	Avg. x/Q, 10^{-9} s/m^3 Spikes	Neigbors	Ratio
SF_6: 2-83	322.5°	14	741	46	16
3	262.5°	19	1522	138	11
5	242.5°	50	1475	50	30
5	337.5°	50	2655	78	34
7	222.5°	59-60	1109	47	24

Note: A "spike" in this context means that each x field listed exceeded both the background and the average of the two neighboring samplers by at least a factor of 10. If a neighboring sample is missing, background x is assumed.

Table 10.10 Average X/Q, 10^{-9} s/m^3, measured along sampling arc during CONDORS 83 averaging periods, spikes removed

Period	1-83	1-83	2-83	3-83	4-83	5-83	6-83	7-83	8-83	9-83
Tracer	1381	SF_6	SF_6	SF_6	SF_6	SF_6	SF_6	SF_6	SF_6	SF_6
Duration (min)	30	30	30	60	50	40	30	30	40	40
Fields	7-9	7-9	13-15	19-24	25-29	49-52	53-55	57-59	63-66	67-70
Background	52	52	72	72	100	72	72	72	100	100
Bearing										
202.5°	21	38	20	66	64(1)	79	45	71	---	---
207.5°	---	45	72	98	67(2)	100	33	47	---	---
212.5°	---	---	48	46(1)	91(1)	168(1)	88	90(1)	52(2)	---
217.5°	0(1)	18	39	36	24	165	123	86	37(2)	---
222.5°	6(1)	21(1)	28	75(1)	112	29	21(1)	61(1)	151(2)	---
227.5°	---	29	25	24(1)	57	105(1)	46	21	26(2)	---
232.5°	---	---	33	39	182	69	89	75	42(2)	140
237.5°	---	---	49	24	98(1)	52	70	---	96	229(1)
242.5°	---	---	6(1)	21	34	143(1)	---	11(1)	126	88
247.5°	95(1)	5(1)	72	210	65	69	38	78	60	125(1)
252.5°	---	---	62	370	50(1)	106	78(1)	---	124(1)	37
257.5°	---	---	33	313	70	175	67	72	310	120
262.5°	---	---	70	252(1)	103	177(1)	296	119(1)	324(1)	895
267.5°	21	56	158(1)	91(1)	73(1)	752(1)	60	290	728	968
272.5°	90	52	200	1567	49(1)	1064	242	563	1445	1838
277.5°	145	27	312	1598	103	784	364	673	1112	689
282.5°	---	---	792	835	157	1250	312	774	237	166
287.5°	133	46	1018	412	259	736	240	1318	90(1)	61(1)
292.5°	320(1)	294	314	148(1)	362	720(1)	264	703	221	36(1)
297.5°	205	364	1090	399	348	793	239(1)	682	191(1)	32
302.5°	303(1)	215	1160	267	267	818	698	1064	45	58
307.5°	335	143	461	192(1)	774(1)	650	1010	681	149	155
312.5°	348	141	369	149(1)	1018	451	900	967(1)	31	60
317.5°	158	183	138	144(2)	540(1)	182(1)	---	887	74	151
322.5°	101	212	151(1)	136(3)	546	852(1)	---	659	71	140(2)
327.5°	52	51	95(1)	---	253(1)	736(2)	1126(1)	---	185(2)	133(1)
332.5°	49	52	54(1)	139(3)	---	84	1338(1)	467	67(1)	23
337.5°	42	29	---	---	116	107(1)	636	548	70(1)	117
342.5°	7	32	---	---	144	93))1)	414	272	66	94

Note: Superscripts in parenthesis indicate number of missing 10 min samples (no avg. if >50% missing).

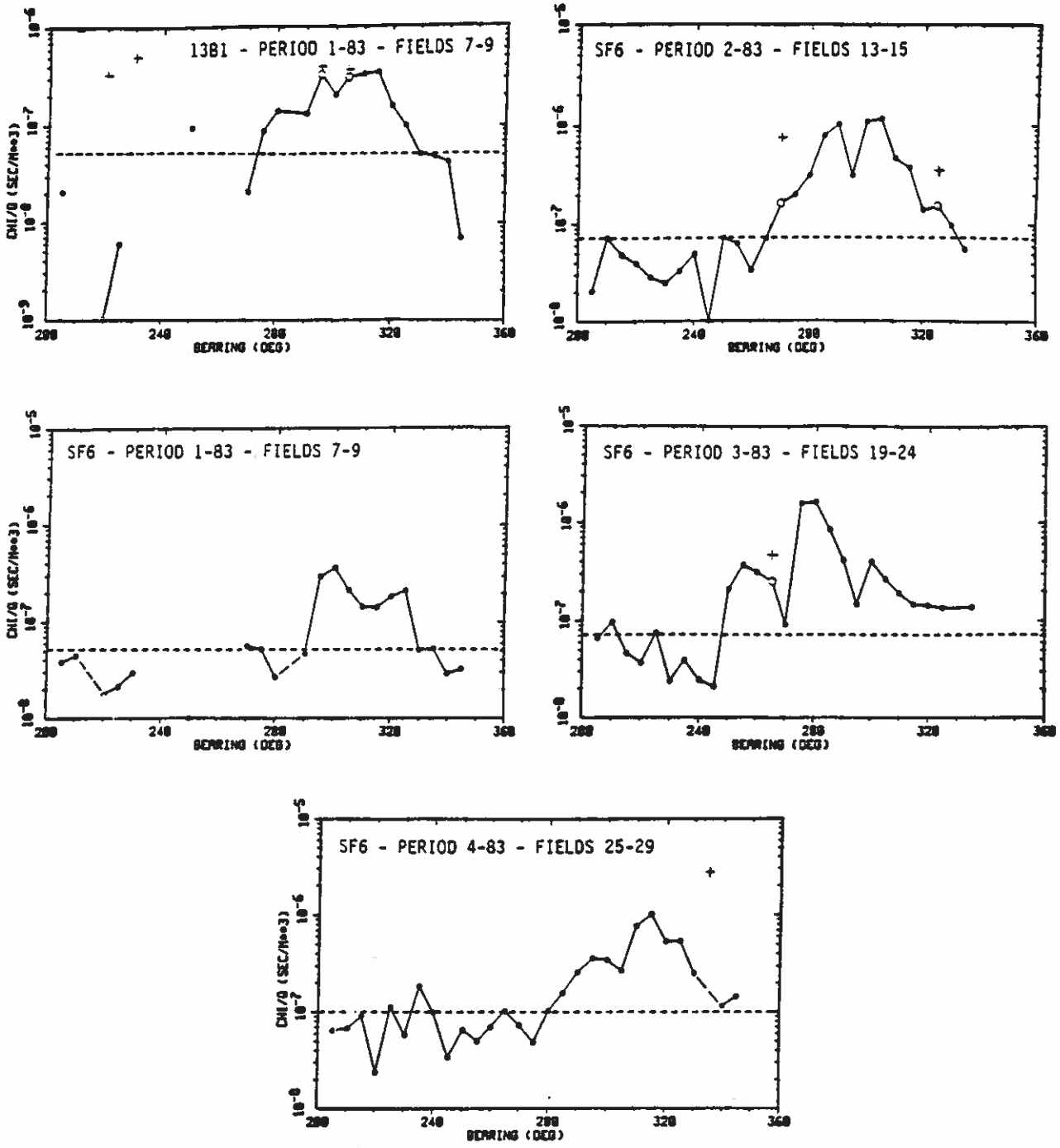

Figure 10.2. Log ($\overline{X}$/Q) at each measured azimuth for each tracer in each successful averaging period of CONDORS 83. X/Q in s/m^3. Bearings are nominal; actual bearings from BAO tower are 2.5° less. Horizontal dashed line is designated background concentration. Long dashed lines are interpolations through azimuth of missing or doubtful measurements. Open circles are averages listed in Table 10.10, obtained after removal of "spikes" listed in Tables 10.8 and 10.9. Plus are averages listed in Table 10.1, which are inclusive of spikes.

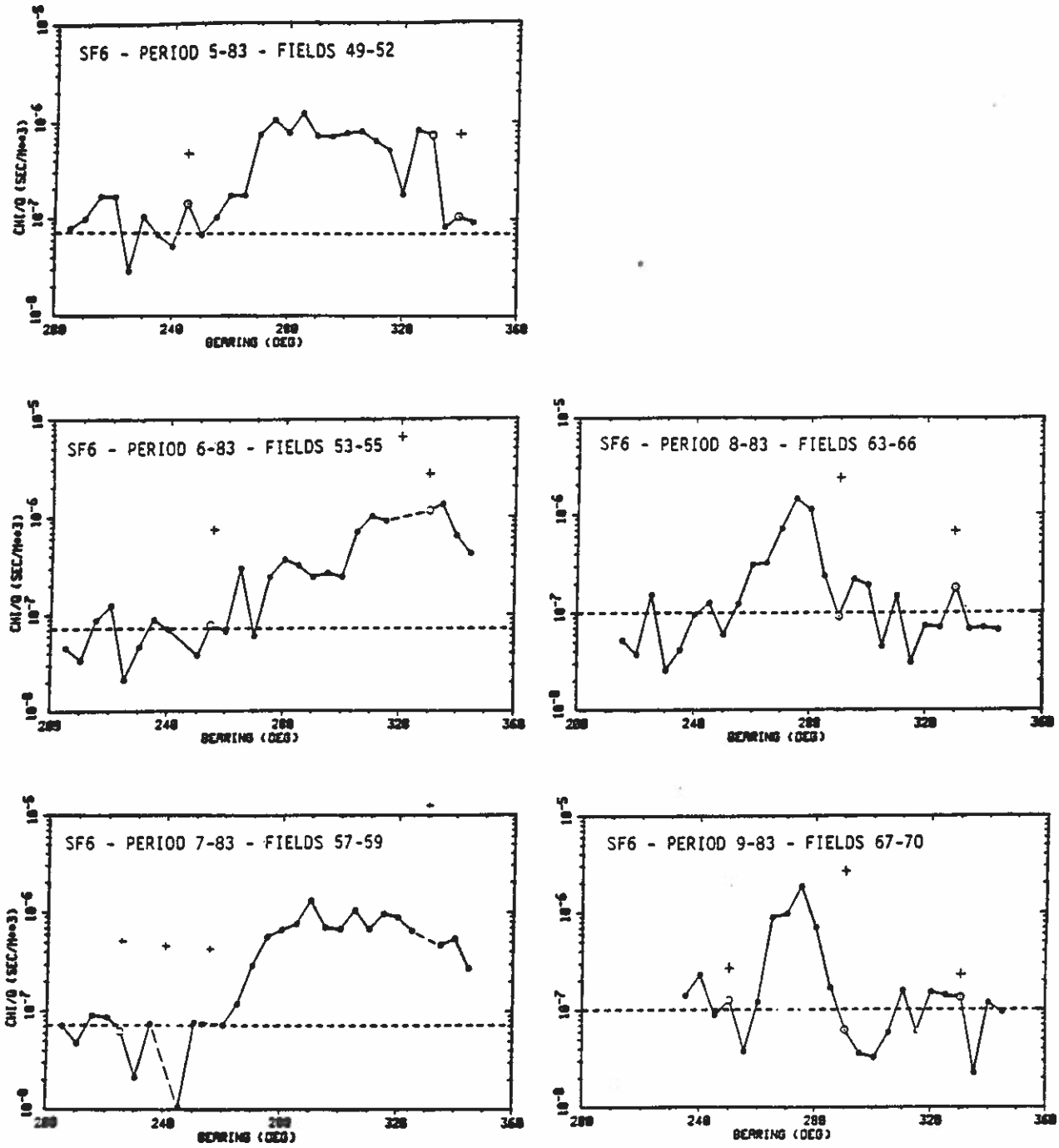

Figure 10.2. Continued.

integrated or summed values of X/Q for most periods. For instance, the inclusion of the single 10 min spike from Field 52 at 327.5° more than doubles the summed 40 min averages of SF_6 for Period 5-83.

Removal of these spikes generally does not affect the completeness of the cross sections shown in Fig. 10.2, if 1) we accept an average at one sampler if half or more of the 10 min samples remain and 2) we accept interpolation across a single sampler lacking adequate measurements. However, for SF_6 in Period 6-83 we lose two adjacent samplers near the midpoint of the plume, while inclusion of the spikes gives average X/Q's with unlikely magnitudes. The 13B1 readings for Test 1, which affect Period 1-83, are another special case. Here we find in Table 10.2 many very large X samples in the southwest sector, especially at 207.5°, 217.5°, and 227.5°. The wind direction was initially toward 240° during this run, but shifted to the range 270° - 340° within 20 min of run initiation time. Thus, we would not expect to find substantial plume concentrations in the SW sector. However, these samplers were only 400 to 600 m west of a storage area that contained cylinders of 13B1 not in service at the time, and it has been established that some of these cylinders have valves with substantial leakage (see Appendix C). While the leakage rate would have to be quite large to produce such high X values, the stored 13B1 cylinders are a conceivable source. This explanation still leaves the puzzle of very small values of X/Q at 202.5° and 222.5° for most fields, and a few extremely large values near 245°. Considering these enigmas and the many missing samples at azimuths less than 265°, it is convenient to pretend that there were no 13B1 samplers captured in the SW sector. The removal of spikes screened by the criterion in Table 10.8 effectively does this.

11. DISCUSSION OF EXPERIMENTAL RESULTS

W. L. Eberhard, G. A. Briggs, W. R. Moninger, and J. C. Kaimal

11.1 Assessment of Observations

The results presented in the three previous chapters and Appendices A and B comprise an extensive data set useful for verifying diffusion models developed for the convective boundary layer. Although taken one year apart, the data from CONDORS 82 and CONDORS 83 can be viewed as the product of a single experiment; the sensor configuration was essentially the same for both years. CONDORS 82, as stated earlier in this report, was designed to test the feasibility of the oil fog and chaff tracer techniques. CONDORS 83 served to complete the experiment with tracer releases separated in height and augmented by the addition of conventional gas sampling techniques.

Processing and tabulation of the data required considerable investment in personnel time. Data manipulations for model comparisons have only begun. Some preliminary results have been presented at conferences (Moninger et al., 1983; Eberhard and Lavery, 1984; Eberhard et al., 1985), highlighting some of the more general characteristics observed during data processing. With data now processed for all the selected periods, the findings of CONDORS 82 can be summarized as follows:

1. The field results qualitatively support the plume behavior observed in laboratory tank (Willis and Deardorff, 1978) and numerical model (Lamb, 1978) experiments. Excellent agreement is found (Moninger et al., 1983) between the crosswind integrated dimensionless chaff concentrations

observed during Period 1-82 and the results from laboratory tank experiments. The height of maximum concentration for Period 1-82 dropped with downwind distance as observed in the tank and predicted by the numerical model.

2. The oil fog and chaff data show good agreement in the horizontal profiles of vertically integrated concentrations; the horizontal edges agree to within 100 m of each other (Moninger et al., 1983). However, the vertical profiles of crosswind integrated concentrations did not agree as well. This is probably because of settling of the chaff, which has a terminal velocity of 0.3 m/s. Such settling was generally small with respect to statistical variations in the vertical behavior of plumes. (Buoyancy of the hot oil fog was considered in Eberhard et al., 1985, and was estimated to cause no more than a 13 m rise in the height of the oil fog plume.)

3. Neither the oil fog nor the chaff can be considered fully conserved, but the losses can be reasonably compensated for within the distance range of greatest interest (prior to uniform vertical mixing) by using the local mass flux in place of source strength in x/Q calculations.

4. Extinction of the laser radiation by the haze and self-shielding by the plume is not a serious problem. The data can be adequately corrected for this attenuation, at least for plume-source distances of greatest interest. Ground clutter present in the lowest 200 m of radar data can be removed by comparing with clutter data obtained in the absence of chaff and retaining only data with Doppler velocities or reflectivity above predetermined thresholds.

In terms of meteorology and signal-to-noise ratios encountered, conditions for CONDORS 83 were even more favorable than for CONDORS 82. The loss of most gas sampler information through contamination of the sampler bags was indeed a disappointment. But there were more periods with steady wind directions, wind speeds, and boundary layer depths in 1983. The excellent agreement between the horizontal profiles of oil fog, chaff and SF_6 gas for Period 9-83 reported by Eberhard et al. (1985) was in part due to the steady conditions prevailing at the time. Some small but significant departures from the laboratory tank observations were noted in the behavior of the height of maximum concentration, but confirmation from analyses of other periods listed is needed prior to final conclusions concerning this behavior.

A comprehensive study of all the data is beyond the scope of this report. In the sections to follow, we limit ourselves to a case study of Period 9-83 to demonstrate some characteristics of the data presented in this report. The period is an ideal one for this purpose: the oil fog, chaff, and SF_6 gas were all released from the same elevated point, allowing direct comparison of sampled results.

11.2 Meteorological Conditions for Period 9-83

Figure 7.1 shows the preliminary meteorological data that formed the basis for selecting Period 9-83 for analysis. The mixed layer heights in the figure were derived from essentially real-time data. Temperature and humidity profiles obtained from the radiosonde data determined the inversion heights plotted in the figure. The lidar heights reported were the tops (above the lidar) of the surface-based haze layer. The radar heights reported were the

top of a layer of natural targets, thought to be insects. The agreement between the reported mixed layer heights is surprisingly good, as is the relative constancy of that height through the afternoon. (Most other periods show a small but steady increase in the mixed layer height with time.) Only toward the end of Period 9-83 did the mixed layer show signs of rising rapidly. The procedure used for establishing the value of z_i are described in Chapter 7.

The wind speeds and wind directions in Fig. 7.1 are 5 min averages processed a few weeks after the field experiment. The wind directions during Period 9-83 remained well within the design range for tracer sampling. The direction showed a small, gradual trend toward a more northerly component. Period 9-83 had less variation in wind direction than most of the other periods. The behavior of heat flux in Fig. 7.1 was typical for that time of day.

11.3 Tracers

Oil fog and chaff were released during Period 9-83 from the carriage at 265 m above the surface. The SF_6 was released from the personnel elevator inside the tower structure at essentially the same height. (Freon 13B1 was dispensed from the surface, but its measurements were invalidated by contamination.)

Load capacity of the carriage allowed only one fogger to be operated during Period 9-83, at an oil flow rate of about 26 g/s (see Table A1 in Appendix A). Surface releases during 1983 from the dual foggers were typically twice this rate. The chaff cutter operated in the usual manner (Sec.

4.3) during Period 9-83 without interruption. SF_6 was released during Period 9-83 at a rate of 0.195 g/s (Table 5.2).

11.4 Tracer Sampling

During Period 9-83 the lidar scanned in the seven vertical planes shown in Fig. 3.4. During the first 15 min of the period, only the six planes closest to the source were scanned. At 1326 MST the scan closest to the source was discontinued and replaced by the farthest downwind scan shown in Fig. 3.4 because we desired measurements at larger X, and the oil fog signal seemed adequate for detection there. Such rare instances of azimuth change can be identified by the times listed in Tables 8.1 through 8.16. The scan at azimuth 183.1° was closest to the north-south midsection of the sampling arc. During Period 9-83, which lasted 40 min, the lidar successfully completed 13 scans at 183.1°, as listed in the heading for this period in Fig. A.1. Averaged over all the periods, the lidar completed the azimuth sequence once every 210 s.

The domain of the radar scan was selected according to the mean wind direction from the tower (with generous allowance for fluctuations in wind direction) and mixed layer height. When the wind changed direction, the radar scan was sometimes adjusted during a run to include all of the chaff plume to at least 4 km downwind of the tower. Figure 3.4 shows the azimuth limits of the radar scan for Period 9-83. The radar swept in azimuth at each of a series of discrete elevation angles. During Period 9-83, the radar used 15 elevation angles, ranging from 0.5° to 10.1°, at 0.7° increments. This sequence was completed 21 times (Table 4.2) during the period. Averaged over

all periods, the radar completed a sequence of elevation sweeps once every 135 s.

Table 11.1 lists typical tracer sampling resolutions and intervals for CONDORS. The vertical and crosswind parameters for the lidar and radar tended to be somewhat finer near the source and coarser at the greatest reported distances downwind. The vertical sampling intervals also scaled roughly with mixed layer height.

Table 11.1. Typical tracer sampling resolutions and intervals

Item	Vertical	Crosswind	Downwind	Time
Lidar				
resolution	2 m	6 m	2 m	instantaneous
interval	10 m	3 m	380 m	210 s
Radar				
resolution	70 m	160 m	90 m	instantaneous
interval	70 m	90 m	37.5 m	135 s
Gas				
resolution	point	point	point	continuous
interval	---	100 m	---	600 s

The sampling intervals for the lidar and the radar (210 s and 135 s) have to be examined in the context of typical eddy passage times. The eddies in the convective boundary layer are typically 1.5 z_i (Willis and Deardorff, 1976b; Kaimal et al., 1976), so the eddy passage time is about 1.5 z_i/U which was 255 s for Period 9-83. Thus, the sampling rates for the lidar and the radar are not rapid enough to fully resolve the individual eddy passages. Some aliasing in the data may be present. The radar data are probably more representative of the ensemble average than the lidar data, since the radar scan fills the entire volume of the plume rather than only taking slices at discrete distances downwind like the lidar.

The total sampling time for Period 9-83, τ = 40 min, corresponds to a nondimensional interval $\tau\bar{u}/z_i$ = 14.1 (Table 7.1). This represents 9 to 10 typical eddy passages, which can be considered a statistically meaningful "ensemble" of events (individual scans). However, the comparable nondimensional interval for the laboratory tank experiments was 28, allowing a better approximation to a true average.

11.5 Comparisons of Tracer Measurements

Since the oil fog, chaff, and SF_6 releases were collocated during Period 9-83, the results can be examined for internal consistency and for discrepancies due to differences in the techniques. Moninger et al. (1983) performed such a comparison for Period 1-82, while Eberhard et al. (1985) examined Periods 5-83 and 9-83. In this report we expand somewhat our analysis of these results, including more comparisons with data from the tank experiments of Willis and Deardorff (1978 and 1981).

While SF_6 is known to be a highly conservative tracer, the behaviors of oil fog and chaff are less well known. This point is discussed in Sec. 3.5 and 4.6 of this report. For oil fog, a decrease in the value of K_0 with downwind distance would imply loss of oil fog. We find a modest (50%) decline in K_0 at x = 1.2 to 2.0 km in Table 8.14 for Period 9-83. (Declines in K_0 measured in CONDORS 83 at x ≈ 1.5 km ranged from 0 to 65%.) The value of χ_{yz} for chaff in Fig. B.8 (Appendix B) shows an initial increase to a maximum at x ≈ 1 km, followed by an exponential decline with downwind distance of about 20% per km. From these results we conclude that the oil fog and chaff could be considered, at least in the range of maximum surface impact (x ~ 1 km

for Period 9-83), semiconservative. It is, therefore, reasonable to account for gradual changes by normalizing oil fog profiles with K_0 and chaff profiles by χ_{yz}. This is the main reason for normalizing profiles in Appendices A and B to total 1000.

The horizontal profiles of vertically integrated concentrations of oil fog are quite consistent with those of chaff, as exemplified in Fig. 11.1. Oil fog data are from the Period 9-83 entries of Table A.1 with normal (50 m) grid spacing. (Figure A.1 includes plots of the same profiles.) The horizontal profile of oil fog in Fig. 11.1 has been projected from the n plane

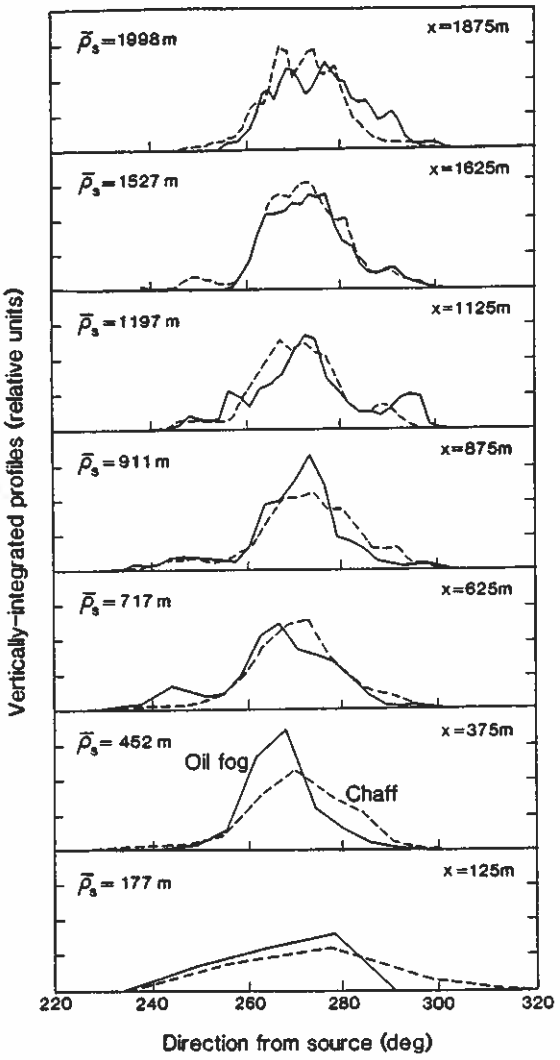

Figure 11.1. Horizontal profiles of χ_z^n for Period 9-83: oil fog (solid line) and chaff (dashed line).

onto a plane normal to the plume axis, which is defined by $\bar{\theta}_s$ in Table 8.14. Chaff data are from the Period 9-83 entry in Table B.1, where the y coordinate has been aligned approximately normal to the mean wind direction as listed in Table 4.2. The gross features of the profiles of the two tracers are similar, although differences do exist in detail. Such minor differences can be expected because the plume is patchy and the two instruments were not precisely synchronized in time and space. The similarity of the horizontal profiles instills confidence in the oil fog and chaff.

Figure 11.2 is a plot in nondimensional coordinates of σ_y for Period 9-83 for chaff (Fig. B.3), oil fog (Table 8.14), and from Willis and

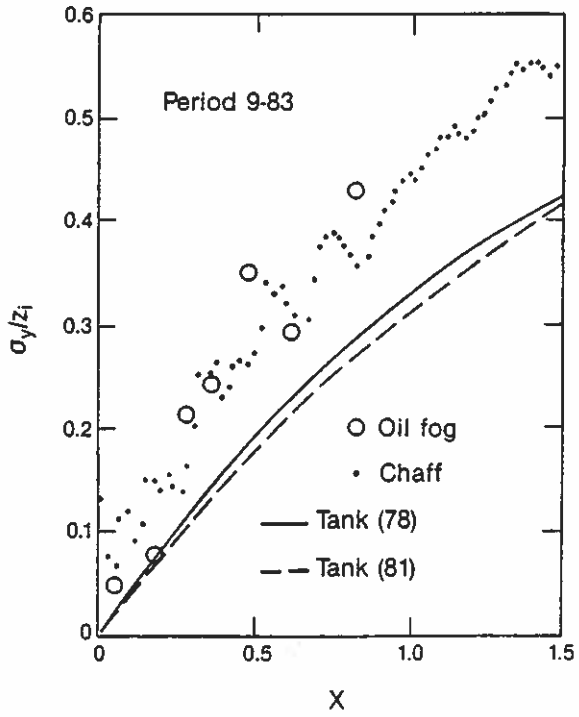

Figure 11.2. Horizontal dispersion parameter for oil fog (circles) and chaff (dots) for Period 9-83 (z/z_i = 0.34), plotted as a function of the nondimensional downwind distance, X. The solid line represents the water tank results of Willis and Deardorff (1978) for z_s/z_i = 0.24 and the dashed line, Willis and Deardorff (1981) for z_s/z_i = 0.49.

Deardorff's (Fig. 2, 1978, and Fig. 2, 1981) convective tank experiment. The oil fog and chaff match well, except near the source where the cruder resolution of the radar introduces an artificial spread, also evident in Fig. 11.1. The tracer in the tank spread more slowly in the horizontal than did the tracer in the field; a similar observation was made by Nieuwstadt (1980) in his analysis of the Prairie Grass field data. Wind direction shear and mesoscale changes in wind direction are absent in the tank; this may be one cause of the difference. Other possible causes include differences in how the scaling parameters were determined and the restrictive influence of the tank's sidewalls. The release heights in the tank were different than in the field, but the effect of z_s on σ_y appears not to be large.

A comparison of oil fog and gas concentrations provides another check of the integrity of these tracers. Since gas samplers operated at the surface, and the lidar could scan only as low as a few tens of meters above the surface, some type of extrapolation of measured oil fog concentrations to the surface is necessary. A near-surface profile of oil fog (azimuth 183.1° of Period 9-83 from Table A.3) is plotted in Fig. 11.3, along with nearby SF_6 measurements from Table 10.1. This lidar scan is the one closest to the west side of the sampler arc (Fig. 3.4). The average oil fog concentration in the lowest scanned 50 m deep layer, between about 22 and 72 m above the ground, is assumed to represent oil fog concentrations at the surface. The empirical calibration factor K_0 for this scan from Table 8.14 was used in (3.13) to convert backscatter coefficient to mass concentration. The SF_6 data has had a background value of 0.09×10^{-6} s m^{-3} subtracted from it and a suspect data point at 287.5° removed. The agreement in Fig. 11.3 is very good, considering

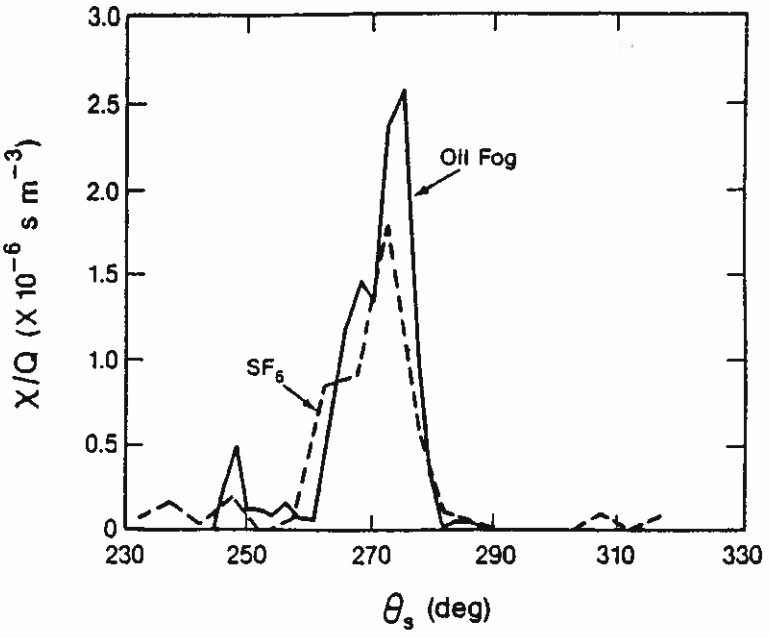

Figure 11.3. Surface concentration distribution of tracers for Period 9-83 on and near sampling arc shown as a function of azimuth direction from release point. Oil fog and SF_6 concentrations are represented by solid and dashed lines respectively.

the differences in tracer and sampling techniques; the integral of the oil fog profile is only 16% greater than that of the SF_6 profile.

Vertical profiles of the the horizontally integrated concentrations of the oil fog and chaff should likewise be similar for Period 9-83, except for the effect of the settling velocity of the chaff. Figure 11.4 shows vertical profiles in nondimensional spatial coordinates. Similarities in the gross features are again apparent. Overall, the chaff in this example is slightly lower than the oil fog. The plots of mean tracer height in Fig. 11.5 also clearly illustrate the tendency of oil fog to maintain greater heights than chaff during this period. Chaff fall velocity certainly must contribute to the differences in $\overline{z}$, but imperfect synchronization in the sampling could also cause random differences. The whole body of data for collocated chaff and oil

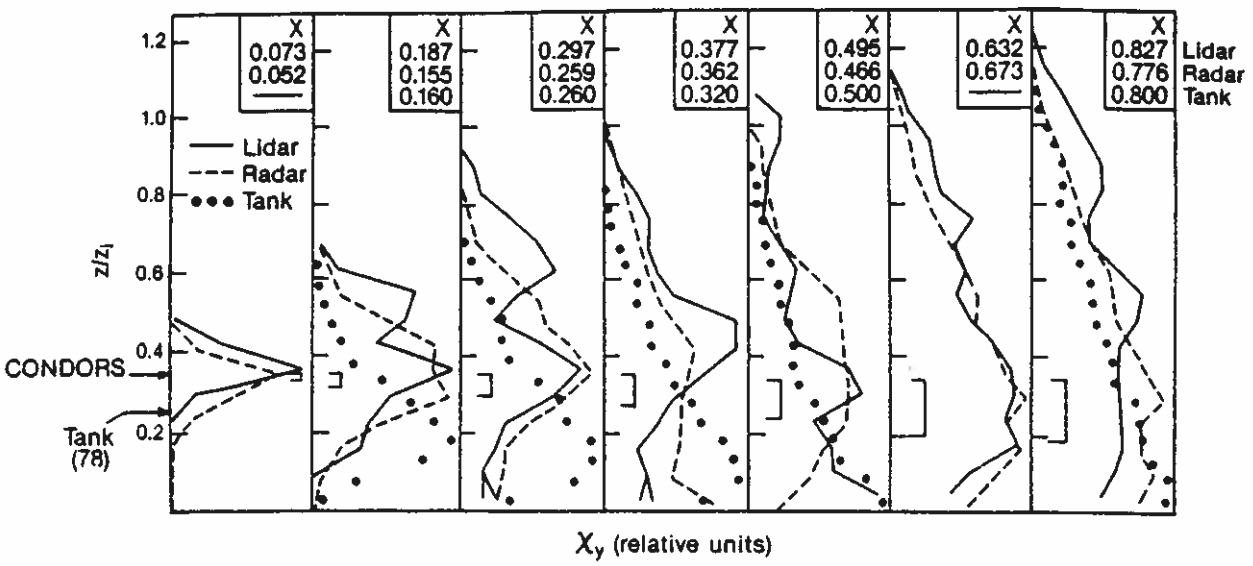

Figure 11.4. Vertical profiles of X_y in nondimensional coordinates. Oil fog (solid line) and chaff (dashed line) are from Period 9-83, while large dots are from tank results (Willis and Deardorff, 1978). Downwind distances X for lidar, radar, and tank, are shown at the top. The data at X = 0.16 for the tank are an average of results published for X = 0.12 and 0.20. The brackets, whose tops are at BAO release height, show predicted chaff fall distance assuming 30 cm/s settling rate and horizontal transport at the mean wind speed. Arrows along the ordinate indicate release heights.

fog releases should be considered in determining the effect of gravitational settling on chaff vertical profiles.

The loss of signal from chaff and oil fog near the surface biases $\overline{z}$ slightly toward larger values. Table A.1 explicitly shows the cutoff height for x_n^n in the lidar vertical profile. The branches at the bottom of the oil fog profiles in Fig. 11.4 show the adjustments to the lowest data points as listed in Table A.2. Low-level blockage of the radar is discussed in Sec. 4.2 and in Appendix C.

The profiles in Fig. 11.4 from the tank are noticeably smoother than the field results, which may be partly attributed to the shorter nondimensional

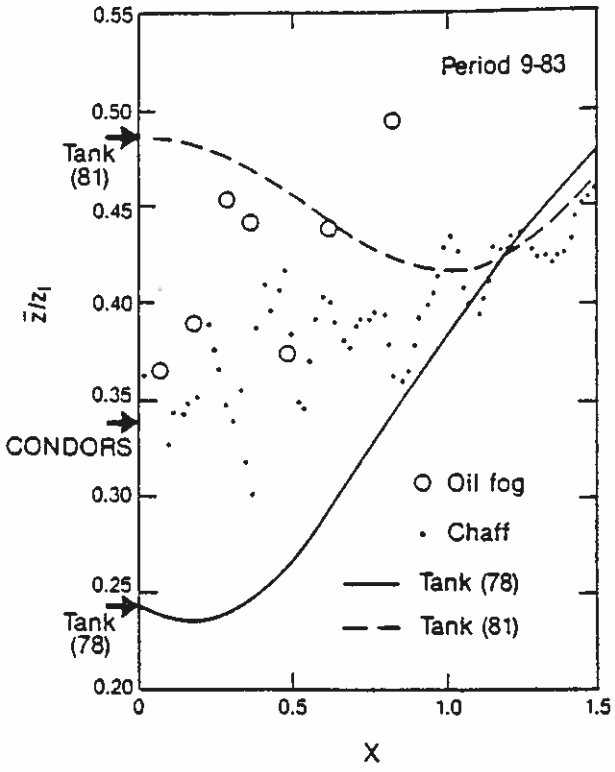

Figure 11.5. Mean tracer height plotted as a function of X for Period 9-83.

duration of the latter. It should be noted also that the curves from the tank were obtained from smoothed contour plots (Deardorff, 1982, personal communication).

Nondimensionalized mean tracer heights versus X are compared with Willis and Deardorff's (1978, 1981) tank results in Fig. 11.5. Except for the lack of a slight initial dip in $\bar{z}/z_i$, the chaff values approximate an interpolation between the two tank experiments for z_s/z_i = 0.24 and 0.49 (z_s/z_i = 0.34 in Period 9-83). Half of the oil fog scans roughly agree, and half give $\bar{z}/z_i$ values 0.05 to 0.1 larger. These increments are also the order of the scatter between adjacent radar volumes and lidar scans. The tank data were subjected to smoothing procedures. Later analyses of CONDORS data will

attempt to combine similar periods and to apply some smoothing to reduce stochastic noise.

Figure 11.6 shows σ_z plotted in nondimensional coordinates. The chaff near the source has larger σ_z than the oil fog, presumably as a result of coarser instrument resolution. There is also a hint of slightly larger σ_z for the oil fog farther downwind. These differences notwithstanding, the agreement among the chaff, the oil fog, and the tank results is very good.

The behavior of the height of $(X_y)_{max}$ shown in Fig. 11.7 departs somewhat from behavior observed in the tank experiments. In the water tank, this

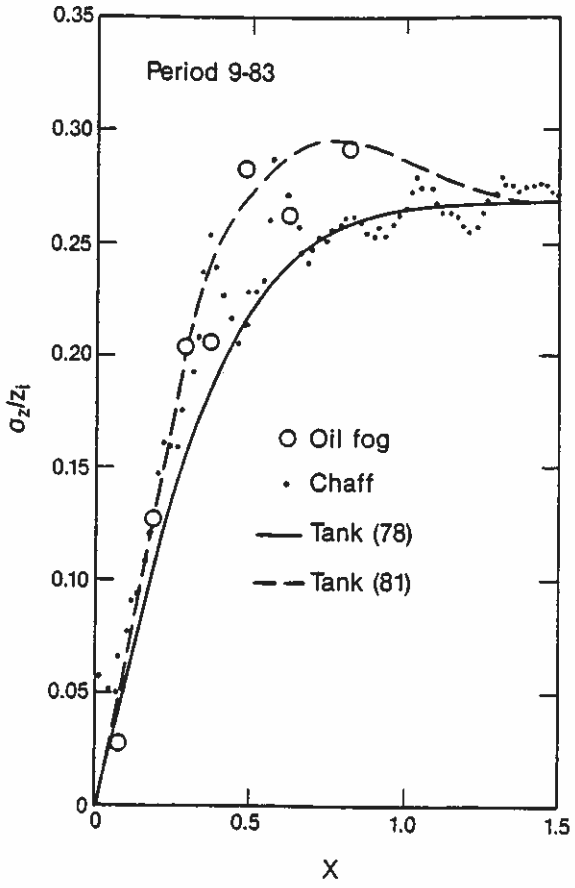

Figure 11.6. Vertical dispersion parameter shown as a function of X for Period 9-83.

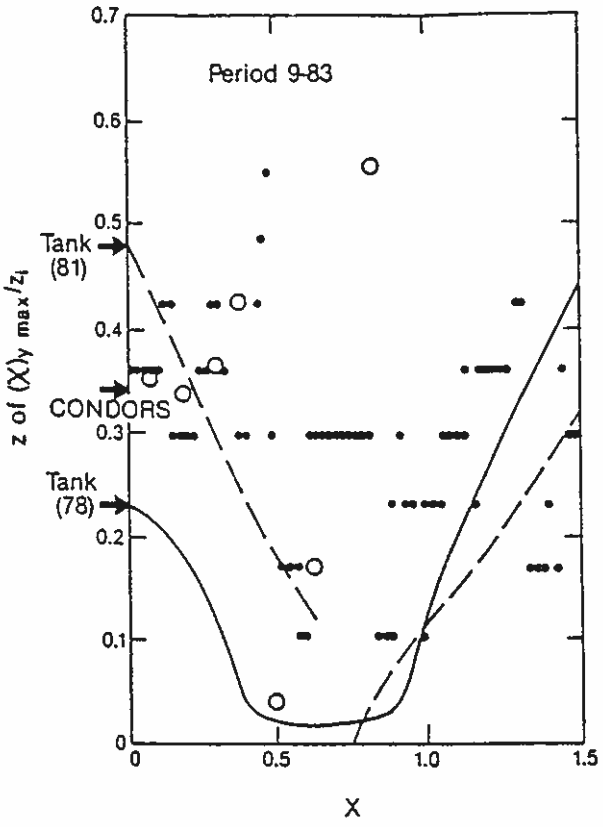

Figure 11.7. Height of maximum horizontally integrated concentration shown as a function of X for Period 9-83. Symbols and lines are as defined in Fig. 11.2.

height dropped quickly to the surface, while the oil fog and the chaff showed an initial increase before starting to descend. It should be pointed out that in some of the other CONDORS periods analyzed (Eberhard et al., 1985; Moninger et al., 1983), behavior of z of $(x_y)_{max}$ had shown striking resemblance to the tank results. The shorter dimensionless sampling time compared with the tank experiments and the lack of smoothing in the field data make the results for oil and chaff in Fig. 11.7 considerably more erratic than the laboratory results. Much more agreeable comparisons are obtained using mean quantities or standard deviations, as in Figs. 11.2, 11.5, and 11.6.

11.6 Strengths and Limitations of Data Set

The CONDORS data set viewed in its entirety is one of good quality, containing unique information on dispersion in the convectively mixed boundary layer.

The meteorological data from the BAO tower is comprehensive and accurate. The height of the mixed layer, which is a crucial scaling parameter, was determined by a consensus of several methods.

The gas tracers provide information on surface concentrations in the vicinity where high concentrations are predicted by the water tank results. This tracer is conservative and is a well-established methodology. It therefore serves also as a benchmark for establishing the validity of the oil fog and chaff measurements. The gas data were carefully screened and bad periods rejected, but a small number of data points reported here are still suspect. The gas tracers also offer no information on the vertical distribution of tracer that is the central theme of CONDORS.

The lidar measured the distribution of oil fog in cross sections through the plume, supplying the required data on vertical profiles of a tracer. Blockage by intervening terrain and eye safety restrictions prevented us from monitoring oil fog within the first few tens of meters above the surface. The small diameters of the fog droplets make them excellent passive tracers of air motion. One disadvantage of the oil fog was the lack of adequate signal beyond 1-3 km downwind, depending on fogger and meteorological conditions. The oil fog also was not fully conserved, but we consider the relative profiles to be trustworthy. Empirical calibration factors can correct for the losses and allow computation of dilution factors.

The radar measurements of chaff throughout the volume of the plume also provide vertical profiles. The chaff data are more comprehensive than the lidar data because the latter were obtained only at a few discrete, thin planes. Chaff signal was also sufficient for measurements to 4 km downwind during all periods. The greatest disadvantage of the chaff is its settling velocity, for which a compensation scheme must yet be applied. The radar also endured more terrain blockage than the lidar, but this is a major problem only for the surface releases of chaff. Removal of ground clutter was extremely successful; residual contamination is of little consequence in the data reported here.

REFERENCES

Battan, L. J., 1973: Radar Observations of the Atmosphere. Univ. of Chicago Press, Chicago, IL, 324 pp.

Briggs, G. A., 1977: Some theoretical notes on sigma curves and stability classification (unpublished manuscript). Atmospheric Turbulence and Diffusion Laboratory, P.O. Box E, Oak Ridge, TN 37830.

Briggs, G. A., 1982: Similarity forms for ground source surface layer diffusion. Boundary-Layer Meteorol., 23, 489-502.

Collis, R. T. H., and P. B. Russell, 1976: Lidar measurements of particles and gases by elastic backscattering and differential absorption. pp 71-151 in Laser Monitoring of the Atmosphere, E. D. Hinkley, ed., Springer-Verlag, 380 pp.

Deardorff, J. W., 1972: Numerical investigation of neutral and unstable planetary boundary layers. J. Atmos. Sci., 29, 91-115.

Deardorff, J. W. and G. E. Willis, 1975: A parameterization of diffusion into the mixed layer. J. Appl. Meteor., 14, 1451-1458.

Eberhard, W. L., 1983: Eye-safe tracking of oil fog plumes by UV lidar. Appl. Opt., 22, 2282-2285.

Eberhard, W. L., and T. F. Lavery, 1984: Participation of NOAA lidar in experiments guiding development of air quality models. Proceedings of the 77th APCA Annual Meeting, Vol. 3, San Francisco, California, June 24-29, 1984, Paper # 84-51.1. Air Pollut. Control Association, Pittsburgh, PA.

Eberhard, W. L., W. R. Moninger, T. Uttal, S. W. Troxel, J. E. Gaynor, and G. A. Briggs, 1985: Field measurements in three dimensions of plume dispersion in the highly convective boundary layer. Preprints, 7th Symposium on Turbulence and Diffusion, November 12-15, 1985, Boulder, Colorado. American Meteorological Society, Boston, 115-118.

Greene, B. R., 1985: Complex terrain model development: quality assurance project report for small hill impaction study no. 1. ERT Document No. P-B876-350, August 1985. Environmental Research and Technology, Inc., Concord, MA 01742.

Gudiksen, P. H., G. J. Ferber, M. M. Fowler, W. L. Eberhard, M. A. Fosberg, and W. R. Knuth, 1984: Field studies of transport and dispersion of atmospheric tracers in nocturnal drainage flows. Atmos. Environ., 18, 713-731.

Hicks, B. B., 1985: Behavior of turbulent statistics in the convective boundary layer. J. Clim. Appl. Meteorol., 24, 607-614.

Hooke, W. H., ed., 1979: Project Phoenix: the September 1978 Field Operation. Report Number One, December 1979. NOAA/ERL, Boulder, CO 80303.

Kaimal, J. C., N. L. Abshire, R. B. Chadwick, M. T. Decker, W. H. Hooke, R. A. Kropfli, W. D. Neff, F. Pasqualucci, and P. H. Hildebrand, 1980: Convective boundary layer thickness estimated by in-situ and remote probes. Preprints, Nineteenth Conference on Radar Meteorology, April 1980, Miami. American Meteorological Society, Boston, 633-636.

Kaimal, J. C., N. L. Abshire, R. B. Chadwick, M. T. Decker, W. H. Hooke, R. A. Kropfli, W. D. Neff, and F. Pasqualucci, 1982: Estimating the depth of the convective boundary layer. J. Appl. Meteor., 21, 1123-1129.

Kaimal, J. C., and J. E. Gaynor, 1983: The Boulder Atmospheric Observatory. J. Clim. Appl. Meteor., 22, 863-880.

Kaimal, J. C., J. C. Wyngaard, D. A. Haugen, O. R. Cote, Y. Izumi, S. J. Caughey, and C. J. Readings, 1976: Turbulence structure of the convective boundary layer. J. Atmos. Sci., 33, 2152-2169.

Lamb, R. G., 1978: A numerical simulation of dispersion from an elevated point source in the convective planetary boundary layer. Atmos. Environ., 12, 1297-1304.

Lamb, R. G., 1979: The effects of release height on material dispersion in the convective planetary boundary layer. Preprints, Fourth Symposium on Turbulence, Diffusion and Air Pollution, January 15-18, 1979, Reno, Nevada. American Meteorological Society, Boston, 27-33.

Moninger, W. R., and R. A. Kropfli, 1982: Radar observations of a plume from an elevated continuous point source. J. Appl. Meteorol., 21, 1685-1697.

Moninger, W. R., W. L. Eberhard, G. A. Briggs, R. A. Kropfli, and J. C. Kaimal 1983: Simultaneous radar and lidar observations of plumes from continuous point sources. Preprints, 21st Conference on Radar Meteorology, Edmonton, Alta. Canada, American Meteorological Society, Boston, 246-250.

Nieuwstadt, F. T. M., 1980: Application of mixed-layer similarity to the observed dispersion from a ground-level source. J. Appl. Meteor., 19, 157-162.

Schiessinger, R. J., 1961: Principles of Electronic Warfare. Prentice-Hall, 213 pp.

Uthe, E. E., W. B. Johnson, and H. Till, 1979: Vertical plume diffusion parameters derived by lidar for the Rancho Seco generating station. Preprints, Fourth Symposium on Turbulence, Diffusion, and Air Pollution, January 15-18, 1979, Reno, Nevada. American Meteorological Society, Boston, 536-540.

Venkatram, A., D. Strimaitis, and W. Eberhard, 1983: Dispersion of elevated releases in the stable boundary layer. Extended Abstracts, Sixth Symposium on Turbulence and Diffusion, March 22-25, 1983, Boston, Massachusetts. American Meteorological Society, Boston, 297-299.

Wilczak, J. M., and M. S. Phillips, 1984: Indirect Estimation of Convective Boundary Layer Structure for Use in Routine Dispersion Models. EPA Report No. EPA/600/3-84/091. EPA Research Triangle Park, NC, 27711, 80 pp.

Willis, G. E., and J. W. Deardorff, 1976a: A laboratory model of diffusion into the convective planetary boundary layer. Quart. J. Roy. Meteorol. Soc., 102, 427-445.

Willis, G. E., and J. W. Deardorff, 1976b: Visual observations of horizontal planforms of penetrative convection. Third Symposium on Atmospheric Turbulence, Diffusion, and Air Quality, Raleigh, North Carolina. October 19-22, 1976. American Meteorological Society, Boston, 9-12.

Willis, G. E., and J. W. Deardorff, 1978: A laboratory study of dispersion from an elevated source within a modeled convective planetary boundary layer. Atmos. Environ., 12, 1305-1311.

Willis, G. E., and J. W. Deardorff, 1981: A laboratory study of dispersion from a source in the middle of the convectively mixed layer. Atmos. Environ., 15, 109-117.

APPENDIX A

HORIZONTAL AND VERTICAL PROFILES OF OIL FOG CONCENTRATION

The profiles presented in Table A.1 are identified by period, lidar azimuth for the cross section, and resolution (for complete definition of the symbols see Sec. 8.2). Each normalized oil fog concentration value is the average over a length interval centered at the coordinate listed. For the horizontal profile of vertically integrated concentration, χ^{η}_{z}, this coordinate is horizontal distance to the release point, ρ_s (η is the horizontal distance from the lidar and θ_s is the azimuth angle from the source). For the vertical profile of horizontally integrated concentration, χ^{η}_{η}, it is height relative to the base of the tower, z. For the standard 50 m resolution, the profile values total 1000. For some azimuths near the source, the profiles are first given at finer resolution, with a normalized total equal to an integer multiple of 1000. The solid hash mark shows the height in the vertical profile of the lower scan limit; data values at lower z are erroneously small. The dashed hash mark, when present, indicates that a correction has been calculated for the lowest usable data point; this and the additive adjustment are listed in Table A.2.

The average of the scans at each lidar azimuth for each analysis period are presented in Fig. A.1. Each plot corresponds to a profile set in Table A.1 with the same data spacing. As in Table A.1, some of the averaged scans near the source appear twice, first with fine resolution, followed by the standard 50 m × 50 m grid spacing. These plots reveal the general behavior of the plumes more completely than do the tabulated profiles in Table A.1. They

also illustrate the "lumpiness" of the plume, which is often apparent even after the averaging of many scans. They reveal instances where the near-surface portion of the plume is displaced horizontally with respect to the body of the plume aloft.

Table A.2 lists the adjustments to the vertical profiles of X_n^n to compensate for incomplete coverage of the plume at scan bottom. These adjustments, when added to the appropriate data points in Table A.1, alter the normalized total to a number larger than 1000.

Near-surface profiles in the form of dilution factors, X/Q, are presented in Table A.3. These are horizontal profiles within a vertically narrow strip whose height limits relative to the base of the tower are listed in each table. The minimum elevation was chosen to avoid regions where significant signal would have been lost because of the lower limit of any of the scans. The coordinates of the data point are the distance and direction from the source to the center of the horizontal cell. These profiles can be used as an estimate of the concentration at the surface, although with less confidence when strong vertical gradients exist near the surface. The dilution factors were calculated using the empirical calibration factors, K_Q, in Tables 8.1 to 8.16 (in effect, Q is replaced by the estimated total downwind flux of optical backscatter from the plume in each scan, taken individually).

Slight contamination of the oil fog plume by smoke from a stubble fire occurred during Period 1-83. Two versions of processing, one which removes the smoke and the other which does not, were applied to the contaminated azimuth (θ = 200.1°). Both the results are presented in Table A.1 and Fig. A.1.

Table A.3 includes only the version from which smoke (and a bit of oil fog) was removed. The oil release rate listed in Table A.1 is the most prevalent rate for each period of lidar data. The average rate for each period was slightly different.

Table A.1 Fine and standard resolution profiles of vertically integrated and horizontally integrated oil fog concentrations for CONDORS 82 and CONDORS 83. For definitions, see opening paragraph of this appendix (they are also listed in Sec. 8.2). Profiles tabulated chronologically by period, within periods by increasing lidar azimuth.

Period 1-82, θ_L =150.0° (fine)

CONDORS '82 AVERAGED OIL FOG PROFILES Period # 1
Release Rate: 35.3 g/s Azimuth 150.0
Release Height: 235.9 m

Horizontal Profile (12.5 m res.)				Vertical Profile (12.5 m res.)	
η(m)	ρ_s(m)	θ_s(°)	χ^n_z	z(m)	χ^n_η
2906	283	256.0	.0	119	.0
2919	280	253.6	.0	132	1.7
2931	277	251.0	4.6	144	13.6
2944	275	248.5	93.0	157	27.6
2956	273	245.9	248.6	169	31.1
2969	272	243.3	230.5	182	322.0
2981	272	240.6	139.7	194	565.3
2994	272	238.0	360.4	207	572.3
3006	273	235.4	729.7	219	208.5
3019	274	232.8	625.7	232	318.5
3031	276	230.2	463.1	244	453.9
3044	278	227.7	284.9	257	466.8
3056	281	225.2	150.1	269	404.2
3069	285	222.7	262.6	282	345.7
3081	289	220.4	251.5	294	203.3
3094	293	218.1	91.3	307	54.9
3106	298	215.8	37.6	319	5.8
3119	303	213.7	11.8	332	-.4
3131	309	211.6	5.2	344	.0
3144	315	209.6	4.4	357	.0
3156	322	207.7	2.4		
3169	328	205.8	2.6		
3181	336	204.1	.0		
3194	343	202.4	.0		

Period 1-82, θ_L =150.0° (normal)

CONDORS '82 AVERAGED OIL FOG PROFILES Period # 1
Release Rate: 35.3 g/s Azimuth 150.0
Release Height: 235.9 m

Horizontal Profile (50.0 m res.)				Vertical Profile (50.0 m res.)	
η(m)	ρ_s(m)	θ_s(°)	χ^n_z	z(m)	χ^n_η
2875	293	261.9	.0	88	.0
2925	278	252.3	24.4	138	12.0
2975	272	242.0	244.8	188	372.6
3025	275	231.5	525.8	238	362.0
3075	286	221.5	198.8	288	252.0
3125	306	212.6	14.8	338	1.4
3175	332	204.9	1.3	388	.0
3225	363	198.5	.0		

Period 1-82, θ_L =154.9° (fine)

CONDORS '82 AVERAGED OIL FOG PROFILES Period # 1
Release Rate: 35.3 g/s Azimuth 154.9
Release Height: 235.9 m

Horizontal Profile (12.5 m res.)				Vertical Profile (12.5 m res.)	
η(m)	ρ_s(m)	θ_s(°)	χ^n_z	z(m)	χ^n_η
2906	528	249.7	.0	119	.0
2919	527	248.3	.0	132	.5
2931	527	247.0	.0	144	13.4
2944	526	245.6	.2	157	92.8
2956	526	244.2	1.3	169	198.1
2969	527	242.9	13.5	182	191.5
2981	527	241.5	24.6	194	262.2
2994	528	240.2	42.8	207	348.8
3006	529	238.8	172.4	219	392.3
3019	531	237.5	488.4	232	274.2
3031	533	236.1	561.2	244	376.9
3044	535	234.8	409.0	257	294.5
3056	537	233.5	320.1	269	222.4
3069	540	232.2	304.1	282	173.0
3081	542	230.9	352.1	294	164.5
3094	546	229.6	353.2	307	214.2
3106	549	228.4	176.9	319	226.5
3119	553	227.1	90.8	332	194.3
3131	557	225.9	73.2	344	216.2
3144	561	224.7	95.2	357	102.0
3156	565	223.5	141.8	369	28.5
3169	570	222.4	160.3	382	20.5
3181	575	221.2	125.7	394	2.5
3194	580	220.1	59.4	407	.1
3206	585	219.0	23.6	419	.0
3219	591	217.9	7.8	432	.0
3231	597	216.8	2.1	444	.0
3244	603	215.8	.3	457	.0
3256	609	214.7	.0		
3269	615	213.7	.0		
3281	622	212.7	.0		
3294	629	211.8	.0		

Period 1-82, θ_L =154.9° (normal)

CONDORS '82 AVERAGED OIL FOG PROFILES Period # 1
Release Rate: 35.3 g/s Azimuth 154.9
Release Height: 235.9 m

Horizontal Profile (50.0 m res.)				Vertical Profile (50.0 m res.)	
η(m)	ρ_s(m)	θ_s(°)	χ^n_z	z(m)	χ^n_η
2875	532	253.0	.0	88	.0
2925	527	247.6	.1	138	26.7
2975	527	242.2	20.5	188	247.6
3025	532	236.8	407.7	238	334.5
3075	541	231.6	332.3	288	193.5
3125	555	226.5	109.1	338	184.8
3175	572	221.8	121.8	388	12.9
3225	594	217.3	8.4	438	.0
3275	619	213.2	.0		

Table A.1 (1-82/150° to 154.9°)

Period 1-82, θ_L =162.5° (normal)

CONDORS '82 AVERAGED OIL FOG PROFILES — Period # 1
Release Rate: 35.3 g/s — Azimuth 162.5
Release Height: 235.9 m

Horizontal Profile (50.0 m res.)				Vertical Profile (50.0 m res.)	
η(m)	ρ_s(m)	θ_s(°)	χ^n_z	z(m)	χ^n_η
2775	915	257.5	.0	-12	.0
2825	912	254.4	.1	38	36.6
2875	912	251.2	20.7	88	143.8
2925	915	248.1	53.5	138	97.3
2975	920	245.0	107.8	188	73.2
3025	928	241.9	255.7	238	162.1
3075	938	238.9	117.5	288	199.5
3125	951	236.0	49.8	338	116.2
3175	967	233.2	62.0	388	58.3
3225	984	230.4	86.7	438	93.2
3275	1004	227.8	110.4	488	19.9
3325	1026	225.2	85.7	538	-.1
3375	1050	222.8	37.1	588	.0
3425	1076	220.5	12.0		
3475	1103	218.3	.9		
3525	1132	216.2	.0		

Period 1-82, θ_L =176.6° (normal)

CONDORS '82 AVERAGED OIL FOG PROFILES — Period # 1
Release Rate: 35.3 g/s — Azimuth 176.6
Release Height: 235.9 m

Horizontal Profile (50.0 m res.)				Vertical Profile (50.0 m res.)	
η(m)	ρ_s(m)	θ_s(°)	χ^n_z	z(m)	χ^n_η
2425	1584	271.0	.0	-12	.0
2475	1581	269.2	.0	38	146.4
2525	1579	267.4	2.7	88	134.4
2575	1579	265.6	9.5	138	46.6
2625	1581	263.8	15.6	188	109.3
2675	1584	262.0	24.2	238	117.5
2725	1589	260.2	44.0	288	145.2
2775	1595	258.4	69.9	338	86.3
2825	1603	256.6	56.6	388	73.6
2875	1613	254.9	52.8	438	49.4
2925	1624	253.1	42.4	488	49.3
2975	1636	251.4	34.9	538	34.8
3025	1650	249.8	13.9	588	7.2
3075	1665	248.1	9.7	638	.1
3125	1682	246.5	15.2	688	.0
3175	1699	244.9	19.0		
3225	1719	243.4	32.5		
3275	1739	241.8	25.3		
3325	1760	240.4	17.5		
3375	1783	238.9	10.7		
3425	1807	237.5	12.1		
3475	1832	236.2	29.4		
3525	1858	234.8	57.6		
3575	1884	233.5	100.0		
3625	1912	232.3	71.9		
3675	1941	231.1	69.1		
3725	1970	229.9	55.7		
3775	2001	228.7	40.7		
3825	2032	227.6	49.5		
3875	2063	226.5	16.9		
3925	2096	225.5	9.8		
3975	2129	224.5	-1.3		
4025	2163	223.5	-3.2		
4075	2197	222.5	-1.6		
4125	2233	221.6	-.9		
4175	2268	220.7	-.2		
4225	2304	219.9	-1.2		
4275	2341	219.0	-.4		
4325	2378	218.2	.0		
4375	2416	217.4	.0		

Period 2-82, θ_L =150.0° (fine)

CONDORS '82 AVERAGED OIL FOG PROFILES — Period # 2
Release Rate: 35.3 g/s — Azimuth 150.0
Release Height: 235.9 m

Horizontal Profile (25.0 m res.)				Vertical Profile (12.5 m res.)	
η(m)	ρ_s(m)	θ_s(°)	χ^n_z	z(m)	χ^n_η
2863	298	264.1	.0	119	.0
2888	289	259.6	.0	132	-.1
2913	281	254.8	.2	144	.4
2938	276	249.8	.2	157	5.4
2963	273	244.6	56.6	169	57.6
2988	272	239.3	332.5	182	182.3
3013	274	234.1	719.7	194	382.5
3038	277	228.9	592.0	207	599.7
3063	283	224.0	232.5	219	546.1
3088	291	219.2	30.9	232	393.8
3113	301	214.8	9.8	244	260.8
3138	312	210.6	6.7	257	365.2
3163	325	206.8	6.2	269	445.4
3188	340	203.3	5.4	282	291.4
3213	355	200.0	4.3	294	261.7
3238	372	197.1	1.6	307	130.8
3263	389	194.4	.3	319	26.2
3288	407	191.9	.2	332	.7
3313	426	189.7	.3	344	.0
3338	446	187.6	.2	357	.0
3363	466	185.7	.2		
3388	487	184.0	.0		
3413	507	182.4	.0		
3438	529	181.0	.0		

Period 2-82, θ_L =150.0° (normal)

CONDORS '82 AVERAGED OIL FOG PROFILES — Period # 2
Release Rate: 35.3 g/s — Azimuth 150.0
Release Height: 235.9 m

Horizontal Profile (50.0 m res.)				Vertical Profile (50.0 m res.)	
η(m)	ρ_s(m)	θ_s(°)	χ^n_z	z(m)	χ^n_η
2875	293	261.9	.0	88	.0
2925	279	252.3	.2	138	1.4
2975	272	242.0	194.5	188	305.5
3025	275	231.5	655.8	238	391.5
3075	287	221.6	131.7	288	294.8
3125	306	212.7	8.3	338	6.7
3175	332	205.0	5.8	388	.0
3225	363	198.5	3.0		
3275	398	193.1	.2		
3325	436	188.6	.2		
3375	476	184.9	.1		
3425	518	181.7	.0		

Table A.1 (1-82/162.5° to 2-82/150°)

Period 2-82, θ_L =154.9° (fine)

CONDORS '82 AVERAGED OIL FOG PROFILES — Period # 2
Release Rate: 35.3 g/s — Azimuth 154.9
Release Height: 235.9 m

Horizontal Profile (25.0 m res.)				Vertical Profile (25.0 m res.)	
η(m)	ρ_s(m)	θ_s(°)	χ^n_z	z(m)	χ^n_η
2813	544	259.6	.0	76	.0
2838	538	257.0	-.0	101	.0
2863	533	254.4	-.1	126	26.0
2888	530	251.7	3.8	151	242.7
2913	527	249.0	12.1	176	320.4
2938	526	246.3	18.0	201	247.9
2963	526	243.6	95.1	226	535.9
2988	527	240.8	289.4	251	345.7
3013	530	238.1	222.4	276	118.9
3038	533	235.5	201.6	301	66.6
3063	538	232.8	226.5	326	13.7
3088	544	230.3	338.7	351	50.9
3113	550	227.7	249.3	376	25.8
3138	558	225.3	145.8	401	5.4
3163	567	222.9	79.5	426	.0
3188	577	220.6	37.7	451	.0
3213	588	218.4	64.2		
3238	599	216.2	14.1		
3263	612	214.2	1.7		
3288	625	212.2	.3		
3313	639	210.3	.0		
3338	653	208.5	.0		

Period 2-82, θ_L =154.9° (normal)

CONDORS '82 AVERAGED OIL FOG PROFILES — Period # 2
Release Rate: 35.3 g/s — Azimuth 154.9
Release Height: 235.9 m

Horizontal Profile (50.0 m res.)				Vertical Profile (50.0 m res.)	
η(m)	ρ_s(m)	θ_s(°)	χ^n_z	z(m)	χ^n_η
2775	554	263.3	.0	-12	.0
2825	541	258.3	.0	38	.0
2875	531	253.0	1.8	88	.0
2925	526	247.6	15.0	138	134.4
2975	526	242.2	192.3	188	234.2
3025	531	236.8	212.0	238	440.8
3075	540	231.5	282.6	288	92.8
3125	554	226.5	197.6	338	32.3
3175	572	221.8	58.6	388	15.6
3225	593	217.3	39.2	438	.0
3275	618	213.2	1.0	488	.0
3325	646	209.4	.0	538	.0

Period 2-82, θ_L =176.6° (normal)

CONDORS '82 AVERAGED OIL FOG PROFILES — Period # 2
Release Rate: 35.3 g/s — Azimuth 176.6
Release Height: 235.9 m

Horizontal Profile (50.0 m res.)				Vertical Profile (50.0 m res.)	
η(m)	ρ_s(m)	θ_s(°)	χ^n_z	z(m)	χ^n_η
2725	1590	260.2	.0	-12	.0
2775	1396	258.4	.0	38	44.1
2825	1604	256.6	1.1	88	129.1
2875	1614	254.9	5.2	138	125.9
2925	1624	253.1	24.2	188	100.7
2975	1637	251.4	27.8	238	107.9
3025	1651	249.8	25.5	288	161.6
3075	1666	248.1	27.9	338	145.5
3125	1682	246.5	24.3	388	79.1
3175	1700	244.9	15.3	438	33.6
3225	1719	243.4	8.7	488	20.5
3275	1740	241.9	16.6	538	7.4
3325	1761	240.4	58.1	588	7.9
3375	1784	238.9	60.4	638	9.7
3425	1808	237.5	68.6	688	16.9
3475	1832	236.2	84.4	738	8.3
3525	1858	234.8	65.5	788	2.8
3575	1885	233.5	44.0	838	.0
3625	1913	232.3	26.1		
3675	1941	231.1	9.2		
3725	1971	229.9	8.1		
3775	2001	228.7	9.6		
3825	2032	227.6	21.6		
3875	2064	226.5	35.5		
3925	2097	225.5	81.3		
3975	2130	224.5	68.8		
4025	2164	223.5	47.2		
4075	2198	222.6	30.6		
4125	2233	221.6	29.8		
4175	2269	220.7	21.0		
4225	2305	219.9	10.0		
4275	2342	219.0	9.8		
4325	2379	218.2	7.8		
4375	2416	217.4	9.7		
4425	2455	216.7	8.0		
4475	2493	215.9	4.0		
4525	2532	215.2	2.7		
4575	2571	214.5	1.3		
4625	2611	213.8	.4		
4675	2651	213.2	.0		
4725	2691	212.6	.0		
4775	2732	211.9	.0		
4825	2773	211.3	.0		
4875	2814	210.8	.0		

Period 2-82, θ_L =162.5° (normal)

CONDORS '82 AVERAGED OIL FOG PROFILES — Period # 2
Release Rate: 35.3 g/s — Azimuth 162.5
Release Height: 235.9 m

Horizontal Profile (50.0 m res.)				Vertical Profile (50.0 m res.)	
η(m)	ρ_s(m)	θ_s(°)	χ^n_z	z(m)	χ^n_η
2775	915	257.5	.0	-12	.0
2825	912	254.4	.0	38	1.2
2875	912	251.2	.0	88	31.4
2925	914	248.1	.1	138	99.6
2975	920	245.0	5.1	188	99.2
3025	928	241.9	14.9	238	339.5
3075	938	238.9	36.6	288	97.1
3125	951	236.0	31.5	338	105.7
3175	966	233.1	37.2	388	96.8
3225	984	230.4	90.7	438	74.0
3275	1004	227.8	142.4	488	7.4
3325	1026	225.2	163.9	538	12.0
3375	1050	222.8	211.4	588	18.3
3425	1075	220.5	182.9	638	14.7
3475	1103	218.3	54.3	688	2.9
3525	1132	216.2	19.6	738	.0
3575	1162	214.2	4.8		
3625	1194	212.3	4.3		
3675	1227	210.5	.1		
3725	1261	208.8	-.0		
3775	1296	207.2	.0		

Table A.1 (2-82/154.9° to 176.6°)

Period 3-82, θ_L =147.8° (fine)

CONDORS '82 AVERAGED OIL FOG PROFILES — Period # 3
Release Rate: 35.3 g/s — Azimuth 147.8
Release Height: 168.0 m

Horizontal Profile (25.0 m res.)				Vertical Profile (25.0 m res.)	
η(m)	ρ_s(m)	θ_s(°)	χ^n_z	z(m)	χ^n_η
2663	366	302.3	.0	26	.0
2688	343	300.6	.0	51	12.5
2713	321	298.5	.0	76	181.3
2738	300	296.2	17.4	101	201.6
2763	279	293.5	89.9	126	176.4
2788	259	290.4	116.0	151	458.2
2813	239	286.7	164.5	176	530.8
2838	221	282.4	45.3	201	238.4
2863	204	277.4	235.5	226	64.8
2888	189	271.6	342.0	251	90.3
2913	177	264.9	336.8	276	33.3
2938	167	257.2	144.4	301	12.5
2963	160	248.7	268.5	326	.0
2988	157	239.7	21.6	351	.0
3013	158	230.7	44.1		
3038	163	221.9	137.4		
3063	172	213.9	29.5		
3088	184	206.7	4.7		
3113	198	200.5	2.3		
3138	214	195.2	.0		

Period 3-82, θ_L =147.8° (normal)

CONDORS '82 AVERAGED OIL FOG PROFILES — Period # 3
Release Rate: 35.3 g/s — Azimuth 147.8
Release Height: 168.0 m

Horizontal Profile (50.0 m res.)				Vertical Profile (50.0 m res.)	
η(m)	ρ_s(m)	θ_s(°)	χ^n_z	z(m)	χ^n_η
2675	355	301.5	.0	12	.0
2725	311	297.4	8.7	38	6.2
2775	269	292.0	103.0	88	191.3
2825	230	284.7	104.9	138	317.4
2875	196	274.6	298.8	188	384.6
2925	171	261.1	240.6	238	77.5
2975	158	244.3	145.0	288	22.9
3025	161	226.2	90.8	338	.0
3075	177	210.2	17.1	388	.0
3125	205	197.7	1.1		
3175	241	188.6	.0		

Period 3-82, θ_L =150.0° (fine)

CONDORS '82 AVERAGED OIL FOG PROFILES — Period # 3
Release Rate: 35.3 g/s — Azimuth 150.0
Release Height: 168.0 m

Horizontal Profile (25.0 m res.)				Vertical Profile (25.0 m res.)	
η(m)	ρ_s(m)	θ_s(°)	χ^n_z	z(m)	χ^n_η
2363	679	306.4	.0	1	.0
2388	656	305.5	.0	26	30.8
2413	633	304.6	.0	51	109.8
2438	611	303.6	.4	76	174.2
2463	589	302.5	.6	101	214.6
2488	567	301.3	1.4	126	246.3
2513	545	300.1	1.8	151	81.2
2538	523	298.7	1.9	176	133.6
2563	502	297.2	6.9	201	151.0
2588	481	295.6	3.7	226	169.8
2613	461	293.9	7.3	251	227.0
2638	441	292.9	4.9	276	225.8
2663	421	289.8	35.7	301	141.0
2688	403	287.5	36.9	326	74.5
2713	385	285.0	51.8	351	17.8
2738	367	282.3	146.9	376	2.5
2763	351	279.2	185.2	401	.2
2788	336	275.9	245.7	426	.0
2813	322	272.3	284.3		
2838	309	268.4	389.3		
2863	298	264.2	269.6		
2888	289	259.7	209.2		
2913	281	254.8	77.9		
2938	276	249.8	33.7		
2963	273	244.6	4.7		
2988	272	239.4	.0		
3013	273	234.1	.0		
3038	277	229.0	.0		

Period 3-82, θ_L =150.0° (normal)

CONDORS '82 AVERAGED OIL FOG PROFILES — Period # 3
Release Rate: 35.3 g/s — Azimuth 150.0
Release Height: 168.0 m

Horizontal Profile (50.0 m res.)				Vertical Profile (50.0 m res.)	
η(m)	ρ_s(m)	θ_s(°)	χ^n_z	z(m)	χ^n_η
2375	667	306.0	.0	12	.0
2425	622	304.1	.2	38	70.3
2475	578	301.9	1.0	88	194.4
2525	534	299.4	1.8	138	163.7
2575	492	296.4	5.3	188	142.3
2625	451	292.9	6.1	238	198.4
2675	412	288.7	36.3	288	183.4
2725	376	283.7	99.4	338	46.1
2775	343	277.6	215.5	388	1.3
2825	315	270.4	336.9	438	.0
2875	293	262.0	239.3		
2925	278	252.4	55.8		
2975	272	242.0	2.4		
3025	275	231.5	.0		

Table A.1 (3-82/147.8° to 150°)

Period 3-82, θ_L =154.9° (normal)

CONDORS '82 AVERAGED OIL FOG PROFILES — Period # 3
Release Rate: 35.3 g/s — Azimuth 154.9
Release Height: 168.0 m

Horizontal Profile (50.0 m res.)				Vertical Profile (50.0 m res.)	
η(m)	ρ_s(m)	θ_s(°)	χ^n_z	z(m)	χ^n_η
2125	979	302.4	.0	-12	1.1
2175	937	300.8	.0	38	116.0
2225	896	299.0	.1	88	145.2
2275	856	297.0	.5	138	164.9
2325	817	294.9	1.2	188	168.3
2375	779	292.5	5.0	238	157.8
2425	743	289.9	17.9	288	73.5
2475	709	287.0	44.0	338	32.6
2525	676	283.9	54.8	388	21.5
2575	646	280.4	57.0	438	31.8
2625	618	276.7	114.8	488	37.7
2675	593	272.6	76.6	538	33.4
2725	572	268.1	197.9	588	11.2
2775	554	263.4	205.6	638	4.8
2825	540	258.3	75.2	688	.2
2875	531	253.1	70.2	738	.0
2925	526	247.7	54.9	788	.0
2975	526	242.2	16.5	838	.0
3025	531	236.8	7.3		
3075	540	231.6	.5		
3125	554	226.5	.0		

Period 3-82, θ_L =165.0° (normal)

CONDORS '82 AVERAGED OIL FOG PROFILES — Period # 3
Release Rate: 35.3 g/s — Azimuth 165.0
Release Height: 168.0 m

Horizontal Profile (50.0 m res.)				Vertical Profile (50.0 m res.)	
η(m)	ρ_s(m)	θ_s(°)	χ^n_z	z(m)	χ^n_η
1375	1771	309.3	.0	-12	25.7
1425	1731	308.3	.0	38	164.1
1475	1691	307.3	.4	88	114.0
1525	1652	306.2	.9	138	112.7
1575	1613	305.1	2.0	188	94.6
1625	1575	303.9	2.3	238	78.7
1675	1538	302.7	2.1	288	57.3
1725	1501	301.4	2.2	338	50.0
1775	1465	300.1	.9	388	38.9
1825	1430	298.7	-.1	438	48.6
1875	1396	297.2	4.5	488	52.5
1925	1363	295.6	7.3	538	48.9
1975	1331	294.0	14.5	588	44.3
2025	1300	292.3	40.7	638	38.5
2075	1271	290.5	49.2	688	15.6
2125	1242	288.6	29.7	738	4.5
2175	1215	286.6	31.7	788	3.1
2225	1190	284.6	34.4	838	2.5
2275	1166	282.5	28.1	888	2.8
2325	1144	280.2	29.5	938	2.4
2375	1124	277.9	82.7	988	.2
2425	1105	275.5	84.3	1038	.0
2475	1089	273.1	53.8		
2525	1074	270.5	43.9		
2575	1062	267.9	41.2		
2625	1052	265.3	60.2		
2675	1044	262.6	85.2		
2725	1039	259.8	99.0		
2775	1036	257.1	65.5		
2825	1035	254.3	44.8		
2875	1037	251.5	15.2		
2925	1041	248.8	10.1		
2975	1048	246.1	14.8		
3025	1056	243.4	14.1		
3075	1068	240.8	4.6		
3125	1081	238.2	.4		
3175	1096	235.7	.0		

Period 4-82, θ_L =150.0° (normal)

CONDORS '82 AVERAGED OIL FOG PROFILES — Period # 4
Release Rate: 35.3 g/s — Azimuth 150.0
Release Height: Surface

Horizontal Profile (50.0 m res.)				Vertical Profile (50.0 m res.)	
η(m)	ρ_s(m)	θ_s(°)	χ^n_z	z(m)	χ^n_η
2575	356	299.4	.0	-12	5.8
2625	314	294.7	.0	38	321.5
2675	274	288.6	.2	88	214.5
2725	239	280.7	52.3	138	140.3
2775	210	270.3	270.7	188	119.5
2825	190	257.2	156.7	238	69.5
2875	181	241.9	170.4	288	38.1
2925	187	226.4	119.7	338	26.4
2975	204	212.6	68.0	388	27.7
3025	232	201.6	27.3	438	34.0
3075	266	193.1	45.1	488	1.4
3125	304	186.6	35.6	538	.2
3175	345	181.7	36.6	588	.7
3225	389	177.8	16.1	638	.3
3275	434	174.7	1.3	688	.0
3325	480	172.2	.0		

Period 4-82, θ_L =154.9° (normal)

CONDORS '82 AVERAGED OIL FOG PROFILES — Period # 4
Release Rate: 35.3 g/s — Azimuth 154.9
Release Height: Surface

Horizontal Profile (50.0 m res.)				Vertical Profile (50.0 m res.)	
η(m)	ρ_s(m)	θ_s(°)	χ^n_z	z(m)	χ^n_η
2475	571	286.6	.0	-12	1.8
2525	540	282.6	.9	38	48.9
2575	510	278.2	9.6	88	30.4
2625	485	273.2	25.8	138	63.8
2675	463	267.8	54.8	188	67.7
2725	446	261.8	36.0	238	105.0
2775	434	255.5	40.2	288	92.4
2825	428	248.9	75.3	338	107.0
2875	427	242.2	142.0	388	105.0
2925	433	235.6	155.7	438	115.8
2975	443	229.2	101.0	488	102.7
3025	459	223.2	54.6	538	49.8
3075	480	217.6	42.2	588	17.6
3125	505	212.6	41.0	638	6.0
3175	533	208.0	36.9	688	12.5
3225	565	204.0	47.4	738	17.6
3275	599	200.4	52.8	788	25.1
3325	635	197.1	35.0	838	16.7
3375	673	194.3	24.5	888	6.6
3425	712	191.7	19.8	938	1.4
3475	753	189.4	4.0	988	2.5
3525	794	187.4	.3	1038	3.1
3575	837	185.6	.0	1088	.4

Table A.1 (3-82/154.9° to 4-82/154.9°)

Period 4-82, θ_L =159.7° (normal)

CONDORS '82 AVERAGED OIL FOG PROFILES — Period # 4
Release Rate: 35.3 g/s — Azimuth 159.7
Release Height: Surface

Horizontal Profile (50.0 m res.)				Vertical Profile (50.0 m res.)	
η(m)	ρ_s(m)	θ_s(°)	χ^n_z	z(m)	χ^n_η
2225	884	291.0	.0	-12	1.8
2275	852	288.5	.0	38	53.2
2325	822	285.8	2.4	88	50.0
2375	793	282.9	9.0	138	27.8
2425	767	279.8	11.2	188	23.4
2475	743	276.4	14.3	238	30.4
2525	722	272.9	11.5	288	42.0
2575	704	269.1	13.5	338	63.0
2625	689	265.2	21.0	388	59.3
2675	677	261.1	40.4	438	61.5
2725	669	256.9	43.3	488	74.0
2775	665	252.7	64.5	538	84.9
2825	664	248.3	101.4	588	62.0
2875	667	244.1	92.5	638	54.7
2925	674	239.8	73.6	688	64.1
2975	684	235.7	49.6	738	62.7
3025	698	231.7	39.0	788	68.2
3075	715	227.9	44.8	838	53.1
3125	735	224.3	50.1	888	39.4
3175	758	220.9	56.1	938	19.8
3225	783	217.7	38.4	988	4.8
3275	811	214.7	25.3	1038	.0
3325	841	211.9	31.6	1088	.0
3375	872	209.3	39.8	1138	.0
3425	905	206.9	31.8		
3475	940	204.6	34.4		
3525	976	202.6	32.4		
3575	1013	200.6	17.5		
3625	1052	198.8	7.7		
3675	1091	197.2	2.2		
3725	1131	195.6	.5		
3775	1172	194.2	.0		

Period 5-82, θ_L =150.0° (fine)

CONDORS '82 AVERAGED OIL FOG PROFILES — Period # 5
Release Rate: 35.3 g/s — Azimuth 150.0
Release Height: Surface

Horizontal Profile (50.0 m res.)				Vertical Profile (25.0 m res.)	
η(m)	ρ_s(m)	θ_s(°)	χ^n_z	z(m)	χ^n_η
2325	585	311.9	.0	-24	.0
2375	538	310.3	.0	1	.4
2425	491	308.3	.0	26	270.6
2475	445	305.9	.0	51	214.1
2525	400	303.0	.8	76	112.4
2575	356	299.4	3.1	101	86.0
2625	314	294.7	8.1	126	112.6
2675	274	288.7	15.6	151	128.9
2725	239	280.7	36.5	176	112.2
2775	210	270.3	53.2	201	84.5
2825	190	257.2	42.7	226	86.6
2875	181	241.9	174.1	251	91.8
2925	187	226.4	93.4	276	84.1
2975	204	212.6	152.8	301	69.3
3025	232	201.6	124.1	326	52.4
3075	266	193.1	114.2	351	47.9
3125	304	186.6	68.4	376	56.3
3175	345	181.7	25.9	401	48.8
3225	389	177.8	20.4	426	47.6
3275	434	174.7	14.7	451	37.2
3325	480	172.2	19.7	476	35.5
3375	526	170.2	22.5	501	44.1
3425	573	168.4	6.2	526	43.4
3475	621	167.0	1.3	551	29.0
3525	669	165.7	.8	576	21.5
3575	717	164.6	.7	601	18.7
3625	766	163.7	.4	626	12.4
3675	814	162.9	.2	651	8.6
3725	863	162.1	.1	676	9.5
3775	912	161.5	.0	701	7.7
				726	6.5
				751	5.3
				776	3.9
				801	3.2
				826	3.7
				851	2.1
				876	.6
				901	.2
				926	.1
				951	.0

Period 5-82, θ_L =150.0° (normal)

CONDORS '82 AVERAGED OIL FOG PROFILES — Period # 5
Release Rate: 35.3 g/s — Azimuth 150.0
Release Height: Surface

Horizontal Profile (50.0 m res.)				Vertical Profile (50.0 m res.)	
η(m)	ρ_s(m)	θ_s(°)	χ^n_z	z(m)	χ^n_η
2325	585	311.9	.0	-12	.2
2375	538	310.3	.0	38	242.4
2425	491	308.3	.0	88	99.2
2475	445	305.9	.0	138	120.8
2525	400	303.0	.9	188	98.4
2575	356	299.4	3.1	238	89.2
2625	314	294.7	8.1	288	76.7
2675	274	288.7	15.6	338	50.2
2725	239	280.7	36.5	388	52.5
2775	210	270.3	53.1	438	42.4
2825	190	257.2	42.7	488	39.8
2875	181	241.9	174.2	538	36.2
2925	187	226.4	93.4	588	20.1
2975	204	212.6	152.9	638	10.5
3025	232	201.6	124.1	688	8.6
3075	266	193.1	114.2	738	5.9
3125	304	186.6	68.4	788	3.6
3175	345	181.7	25.9	838	2.9
3225	389	177.8	20.4	888	.4
3275	434	174.7	14.7	938	.0
3325	480	172.2	19.7	988	.0
3375	526	170.2	22.5		
3425	573	168.4	6.2		
3475	621	167.0	1.3		
3525	669	165.7	.8		
3575	717	164.6	.7		
3625	766	163.7	.4		
3675	814	162.9	.2		
3725	863	162.1	.1		
3775	912	161.5	.0		

Table A.1 (4-82/159.7° to 5-82/150°)

Period 5-82, θ_L =154.9° (normal)

CONDORS '82 AVERAGED OIL FOG PROFILES — Period # 5
Release Rate: 35.3 g/s — Azimuth 154.9
Release Height: Surface

Horizontal Profile (50.0 m res.)				Vertical Profile (50.0 m res.)	
η(m)	ρ_s(m)	θ_s(°)	χ^n_z	z(m)	χ^n_η
2125	846	304.6	.0	-12	4.2
2175	803	302.8	.0	38	66.8
2225	761	300.8	.2	88	153.7
2275	720	298.5	.4	138	128.1
2325	681	296.0	1.1	188	52.8
2375	643	293.2	3.6	238	38.2
2425	606	290.1	3.3	288	29.9
2475	572	286.6	2.5	338	39.9
2525	540	282.6	2.7	388	43.3
2575	511	278.1	6.0	438	44.5
2625	485	273.2	9.0	488	55.4
2675	464	267.8	19.6	538	52.7
2725	447	261.8	34.3	588	61.2
2775	435	255.5	61.2	638	65.8
2825	428	248.9	60.6	688	46.4
2875	428	242.2	42.4	738	36.5
2925	433	235.6	57.3	788	28.1
2975	444	229.2	99.7	838	14.8
3025	460	223.2	134.1	888	9.3
3075	481	217.7	138.0	938	6.6
3125	505	212.6	76.6	988	7.2
3175	534	208.1	63.8	1038	5.1
3225	565	204.0	65.6	1088	3.2
3275	599	200.4	37.2	1138	2.5
3325	635	197.2	19.3	1188	2.0
3375	673	194.3	12.9	1238	1.6
3425	712	191.8	9.0	1288	.1
3475	753	189.5	7.1	1338	.0
3525	795	187.4	9.6	1388	.0
3575	837	185.6	5.9	1438	.0
3625	881	183.9	4.4		
3675	925	182.4	6.5		
3725	969	181.1	5.1		
3775	1014	179.8	1.3		
3825	1060	178.7	.0		

Period 5-82, θ_L =159.7° (normal)

CONDORS '82 AVERAGED OIL FOG PROFILES — Period # 5
Release Rate: 35.3 g/s — Azimuth 159.7
Release Height: Surface

Horizontal Profile (50.0 m res.)				Vertical Profile (50.0 m res.)	
η(m)	ρ_s(m)	θ_s(°)	χ^n_z	z(m)	χ^n_η
1925	1106	302.8	.0	-12	.5
1975	1067	301.2	.0	38	15.0
2025	1028	299.4	.3	88	19.6
2075	990	297.6	1.1	138	29.8
2125	954	295.5	1.8	188	43.7
2175	919	293.4	2.5	238	38.2
2225	885	291.0	2.9	288	52.1
2275	853	288.5	5.2	338	52.0
2325	822	285.8	8.6	388	50.1
2375	794	282.9	14.6	438	69.3
2425	768	279.7	17.6	488	84.2
2475	744	276.4	21.9	538	72.6
2525	723	272.9	28.3	588	66.8
2575	705	269.1	34.0	638	66.6
2625	690	265.2	41.4	688	51.7
2675	678	261.1	46.4	738	40.4
2725	670	256.9	52.6	788	42.4
2775	666	252.7	54.7	838	43.8
2825	665	248.3	57.1	888	47.1
2875	668	244.1	48.7	938	44.5
2925	675	239.8	48.2	988	35.6
2975	685	235.7	71.2	1038	20.1
3025	699	231.7	93.8	1088	11.1
3075	716	227.9	78.2	1138	2.3
3125	736	224.3	52.5	1188	.3
3175	759	220.9	44.7	1238	.1
3225	784	217.7	36.0	1288	.0
3275	812	214.7	32.4	1338	.0
3325	841	211.9	22.5	1388	.0
3375	873	209.3	16.2	1438	.0
3425	906	206.9	12.0		
3475	941	204.7	9.7		
3525	977	202.6	7.8		
3575	1014	200.7	7.0		
3625	1052	198.9	3.8		
3675	1092	197.2	3.5		
3725	1132	195.7	3.2		
3775	1172	194.2	4.6		
3825	1214	192.9	4.9		
3875	1256	191.7	4.9		
3925	1299	190.5	1.7		
3975	1342	189.4	.9		
4025	1386	188.4	.7		
4075	1430	187.4	.1		
4125	1474	186.5	.0		

Table A.1 (5-82/154.9° to 159.7°)

Period 1-83, θ_L =169.9° (fine)

CONDORS '83 AVERAGED OIL FOG PROFILES — Period # 1
Release Rate: 58.6 g/s — Azimuth 169.9
Release Height: Surface

Horizontal Profile (50.0 m res.)				Vertical Profile (25.0 m res.)	
η(m)	ρ_s(m)	θ_s(°)	χ^n_z	z(m)	χ^n_η
3125	860	338.9	.0	-30	.0
3175	811	338.2	.0	-5	3.6
3225	762	337.4	-.1	20	624.5
3275	714	336.6	1.3	45	421.1
3325	665	335.6	21.0	70	116.8
3375	617	334.4	46.0	95	92.8
3425	569	333.1	87.1	120	110.9
3475	521	331.5	134.6	145	86.9
3525	474	329.6	105.8	170	132.6
3575	427	327.2	44.0	195	137.3
3625	382	324.4	95.7	220	101.1
3675	337	320.7	143.5	245	33.8
3725	295	315.9	127.0	270	29.8
3775	255	309.7	88.7	295	44.9
3825	219	301.2	50.6	320	46.9
3875	190	289.7	37.5	345	12.3
3925	170	275.0	14.0	370	4.4
3975	164	257.9	2.4	395	.0
4025	174	241.2	.7	420	.0
4075	195	227.2	.0	445	.0

Period 1-83, θ_L =169.9° (normal)

CONDORS '83 AVERAGED OIL FOG PROFILES — Period # 1
Release Rate: 58.6 g/s — Azimuth 169.9
Release Height: Surface

Horizontal Profile (50.0 m res.)				Vertical Profile (50.0 m res.)	
η(m)	ρ_s(m)	θ_s(°)	χ^n_z	z(m)	χ^n_η
3125	860	338.9	.0	-17	1.8
3175	811	338.2	.0	33	522.7
3225	762	337.4	-.1	83	104.8
3275	714	336.6	1.3	133	98.9
3325	665	335.6	21.0	183	135.0
3375	617	334.4	46.0	233	67.5
3425	569	333.1	87.1	283	37.4
3475	521	331.5	134.6	333	29.6
3525	474	329.6	105.8	383	2.2
3575	427	327.2	44.0	433	.0
3625	382	324.4	95.7		
3675	337	320.7	143.5		
3725	295	315.9	127.0		
3775	255	309.7	88.7		
3825	219	301.2	50.6		
3875	190	289.7	37.5		
3925	170	275.0	14.0		
3975	164	257.9	2.4		
4025	174	241.2	.7		
4075	195	227.2	.0		

Period 1-83, θ_L =174.0° (fine)

CONDORS '83 AVERAGED OIL FOG PROFILES — Period # 1
Release Rate: 58.6 g/s — Azimuth 174.0
Release Height: Surface

Horizontal Profile (50.0 m res.)				Vertical Profile (25.0 m res.)	
η(m)	ρ_s(m)	θ_s(°)	χ^n_z	z(m)	χ^n_η
2925	1117	330.2	.0	-30	.0
2975	1072	329.1	.0	-5	.1
3025	1027	327.9	.1	20	94.4
3075	982	326.6	2.7	45	189.1
3125	938	325.2	7.4	70	197.9
3175	894	323.7	10.1	95	200.5
3225	852	322.0	17.1	120	197.2
3275	810	320.1	32.5	145	188.6
3325	769	318.0	36.2	170	175.5
3375	729	315.7	38.1	195	157.0
3425	690	313.2	50.4	220	112.2
3475	653	310.3	82.0	245	80.3
3525	618	307.1	96.2	270	73.7
3575	585	303.5	90.5	295	61.2
3625	555	299.5	130.8	320	88.4
3675	527	295.1	114.2	345	88.4
3725	503	290.2	120.3	370	43.8
3775	483	284.9	74.1	395	19.4
3825	468	279.1	83.0	420	11.1
3875	457	273.1	5.6	445	5.6
3925	452	266.8	1.1	470	2.0
3975	453	260.5	2.4	495	2.2
4025	458	254.2	2.6	520	3.1
4075	469	248.2	1.0	545	3.0
4125	485	242.5	1.0	570	3.5
4175	506	237.2	.3	595	1.7
4225	530	232.4	.0	620	.1
4275	558	228.0	.0	645	.0
4325	589	224.1	.0	670	.0
4375	622	220.6	.0	695	.0

Period 1-83, θ_L =174.0° (normal)

CONDORS '83 AVERAGED OIL FOG PROFILES — Period # 1
Release Rate: 58.6 g/s — Azimuth 174.0
Release Height: Surface

Horizontal Profile (50.0 m res.)				Vertical Profile (50.0 m res.)	
η(m)	ρ_s(m)	θ_s(°)	χ^n_z	z(m)	χ^n_η
2925	1117	330.2	.0	-17	.0
2975	1072	329.1	.0	33	141.8
3025	1027	327.9	.1	83	199.2
3075	982	326.6	2.7	133	192.9
3125	938	325.2	7.4	183	166.2
3175	894	323.7	10.1	233	96.2
3225	852	322.0	17.1	283	67.4
3275	810	320.1	32.5	333	88.4
3325	769	318.0	36.2	383	31.6
3375	729	315.7	38.1	433	8.4
3425	690	313.2	50.4	483	2.1
3475	653	310.3	82.0	533	3.1
3525	618	307.1	96.2	583	2.6
3575	585	303.5	90.5	633	.0
3625	555	299.5	130.8	683	.0
3675	527	295.1	114.2		
3725	503	290.2	120.3		
3775	483	284.9	74.1		
3825	468	279.1	83.0		
3875	457	273.1	5.6		
3925	452	266.8	1.1		
3975	453	260.5	2.4		
4025	458	254.2	2.6		
4075	469	248.2	1.0		
4125	485	242.5	1.0		
4175	506	237.2	.3		
4225	530	232.4	.0		
4275	558	228.0	.0		
4325	589	224.1	.0		
4375	622	220.6	.0		

Table A.1 (1-83/169.9° to 174°)

Period 1-83, θ_L =181.1° (normal)

CONDORS '83 AVERAGED OIL FOG PROFILES — Period # 1
Release Rate: 58.6 g/s — Azimuth 181.1
Release Height: Surface

Horizontal Profile (50.0 m res.)				Vertical Profile (50.0 m res.)	
η(m)	ρ_s(m)	θ_s(°)	χ^n_z	z(m)	χ^n_η
2525	1631	326.1	.0	-17	2.5
2575	1590	325.1	.0	33	73.4
2625	1550	324.0	.1	83	81.2
2675	1510	322.9	.5	133	102.7
2725	1471	321.7	1.0	183	85.7
2775	1433	320.4	3.9	233	81.7
2825	1395	319.1	8.4	283	63.0
2875	1359	317.7	22.1	333	54.7
2925	1323	316.2	38.1	383	46.2
2975	1288	314.6	36.6	433	41.2
3025	1254	312.9	41.5	483	41.6
3075	1221	311.2	45.8	533	52.7
3125	1190	309.3	87.9	583	41.6
3175	1159	307.4	105.0	633	46.5
3225	1130	305.4	67.0	683	49.2
3275	1103	303.2	61.4	733	35.5
3325	1077	301.0	63.5	783	30.7
3375	1053	298.6	57.6	833	34.5
3425	1031	296.1	56.7	883	21.7
3475	1011	293.6	63.0	933	7.2
3525	993	290.9	50.9	983	2.4
3575	977	288.1	54.4	1033	1.4
3625	964	285.3	37.8	1083	1.1
3675	953	282.4	24.4	1133	.7
3725	944	279.4	14.8	1183	-.0
3775	938	276.4	2.5	1233	-.0
3825	935	273.3	1.1	1283	.0
3875	934	270.3	2.3	1333	.0
3925	936	267.2	3.4	1383	.0
3975	941	264.2	3.8	1433	.0
4025	948	261.2	7.1		
4075	958	258.2	5.9		
4125	971	255.3	7.0		
4175	985	252.5	14.9		
4225	1002	249.8	7.7		
4275	1022	247.2	1.8		
4325	1043	244.7	.0		
4375	1066	242.3	.0		
4425	1091	240.0	.0		
4475	1118	237.8	.0		

Period 1-83, θ_L =190.0° (normal)

CONDORS '83 AVERAGED OIL FOG PROFILES — Period # 1
Release Rate: 58.6 g/s — Azimuth 190.0
Release Height: Surface

Horizontal Profile (50.0 m res.)				Vertical Profile (50.0 m res.)	
η(m)	ρ_s(m)	θ_s(°)	χ^n_z	z(m)	χ^n_η
2425	1966	319.3	.0	-17	1.5
2475	1935	318.2	-.0	33	17.6
2525	1904	317.0	.1	83	28.2
2575	1875	315.8	.7	133	28.9
2625	1846	314.5	1.2	183	22.3
2675	1818	313.2	2.2	233	29.4
2725	1791	311.9	6.7	283	32.7
2775	1765	310.5	15.1	333	27.5
2825	1741	309.1	24.0	383	36.1
2875	1717	307.6	31.1	433	39.8
2925	1694	306.1	38.6	483	51.4
2975	1673	304.6	44.3	533	62.2
3025	1653	303.0	45.9	583	69.3
3075	1634	301.4	53.7	633	64.8
3125	1616	299.7	64.1	683	50.6
3175	1600	298.0	81.0	733	50.9
3225	1585	296.3	89.9	783	56.1
3275	1572	294.6	79.9	833	68.2
3325	1560	292.8	67.8	883	59.5
3375	1550	291.0	61.6	933	46.8
3425	1541	289.2	47.7	983	31.3
3475	1534	287.3	32.9	1033	22.7
3525	1529	285.5	25.4	1083	16.6
3575	1525	283.6	19.7	1133	11.0
3625	1522	281.7	20.0	1183	10.3
3675	1522	279.8	16.7	1233	9.2
3725	1523	277.9	14.1	1283	8.0
3775	1525	276.1	15.2	1333	8.4
3825	1530	274.2	17.0	1383	8.2
3875	1536	272.3	14.4	1433	6.7
3925	1543	270.5	14.4	1483	6.3
3975	1552	268.7	12.3	1533	4.9
4025	1563	266.9	6.4	1583	3.3
4075	1575	265.1	4.9	1633	1.8
4125	1588	263.4	5.5	1683	.7
4175	1603	261.7	5.8	1733	.2
4225	1620	260.0	6.4	1783	.2
4275	1638	258.3	4.8	1833	.3
4325	1657	256.7	3.6	1883	.5
4375	1677	255.2	1.8	1933	.7
4425	1699	253.6	1.7	1983	1.1
4475	1722	252.1	1.0	2033	1.2
4525	1746	250.7	.2	2083	1.1
4575	1771	249.3	.0	2133	1.0
4625	1797	247.9	.0	2183	.4
				2233	.1
				2283	.0
				2333	.0
				2383	.0
				2433	.0

Table A.1 (1-83/181.1° to 190°)

Period 1-83,* $\theta_L = 200.1°$ (normal)

CONDORS '83 AVERAGED OIL FOG PROFILES — Period # 1
Release Rate: 58.6 g/s — Azimuth 200.1
Release Height: Surface

Horizontal Profile (50.0 m res.)				Vertical Profile (50.0 m res.)	
η(m)	ρ_s(m)	θ_s(°)	χ^n_z	z(m)	χ^n_η
1925	2570	323.7	.0	-17	1.5
1975	2542	322.8	.0	33	6.1
2025	2516	321.8	.0	83	12.5
2075	2490	320.8	.3	133	18.9
2125	2465	319.8	.8	183	24.3
2175	2440	318.8	.9	233	26.1
2225	2417	317.8	1.1	283	37.0
2275	2394	316.7	.9	333	36.9
2325	2372	315.6	.4	383	30.5
2375	2351	314.5	.1	433	25.4
2425	2331	313.4	.5	483	18.0
2475	2311	312.3	1.1	533	18.1
2525	2293	311.1	1.2	583	27.2
2575	2275	309.9	2.6	633	34.7
2625	2259	308.7	3.9	683	38.3
2675	2243	307.5	5.0	733	44.4
2725	2229	306.3	5.5	783	40.8
2775	2216	305.1	5.9	833	35.5
2825	2203	303.8	9.1	883	28.6
2875	2192	302.5	10.9	933	30.7
2925	2182	301.3	15.7	983	30.9
2975	2172	300.0	24.3	1033	32.0
3025	2164	298.7	30.6	1083	32.8
3075	2158	297.3	41.8	1133	33.2
3125	2152	296.0	56.3	1183	31.3
3175	2147	294.7	64.1	1233	29.3
3225	2144	293.4	46.0	1283	35.6
3275	2142	292.0	42.2	1333	40.1
3325	2141	290.7	38.2	1383	40.9
3375	2141	289.3	38.8	1433	43.3
3425	2142	288.0	44.6	1483	42.7
3475	2144	286.7	55.3	1533	39.2
3525	2148	285.3	54.6	1583	18.5
3575	2153	284.0	60.4	1633	10.0
3625	2158	282.7	68.3	1683	4.7
3675	2165	281.4	65.6	1733	.7
3725	2174	280.1	52.3	1783	-.6
3775	2183	278.8	26.2	1833	-.2
3825	2193	277.5	14.0	1883	.0
3875	2205	276.2	6.8	1933	.0
3925	2217	275.0	3.6	1983	.0
3975	2231	273.7	2.2	2033	.0
4025	2245	272.5	4.1	2083	.0
4075	2261	271.3	1.9	2133	.0
4125	2277	270.1	.7	2183	.0
4175	2295	268.9	1.0		
4225	2314	267.8	3.0		
4275	2333	266.7	6.4		
4325	2353	265.5	9.0		
4375	2375	264.4	9.7		
4425	2397	263.4	9.5		
4475	2419	262.3	7.0		
4525	2443	261.3	6.8		
4575	2468	260.3	8.3		
4625	2493	259.3	9.2		
4675	2519	258.3	8.3		
4725	2546	257.3	6.4		
4775	2573	256.4	3.4		
4825	2601	255.5	1.3		
4875	2630	254.6	.7		
4925	2659	253.7	.6		
4975	2689	252.8	.4		
5025	2720	252.0	-.0		
5075	2751	251.2	.0		
5125	2783	250.4	.0		

*Fire smoke removed

Period 1-83,* $\theta_L = 200.1°$ (normal)

CONDORS '83 AVERAGED OIL FOG PROFILES — Period # 1
Release Rate: 58.6 g/s — Azimuth 200.1
Release Height: Surface

Horizontal Profile (50.0 m res.)				Vertical Profile (50.0 m res.)	
η(m)	ρ_s(m)	θ_s(°)	χ^n_z	z(m)	χ^n_η
1925	2570	323.7	.0	-17	3.0
1975	2542	322.8	.0	33	10.8
2025	2516	321.8	.0	83	14.0
2075	2490	320.8	.3	133	19.5
2125	2465	319.8	.7	183	22.9
2175	2440	318.8	.7	233	23.5
2225	2417	317.8	.8	283	32.7
2275	2394	316.7	.7	333	34.3
2325	2372	315.6	.2	383	31.2
2375	2351	314.5	.1	433	28.5
2425	2331	313.4	.4	483	24.7
2475	2311	312.3	.8	533	28.5
2525	2293	311.1	1.0	583	34.2
2575	2275	309.9	2.0	633	34.8
2625	2259	308.7	3.1	683	34.9
2675	2243	307.5	4.0	733	39.3
2725	2229	306.3	4.4	783	38.3
2775	2216	305.1	4.7	833	35.6
2825	2203	303.8	7.3	883	30.1
2875	2192	302.5	8.9	933	31.0
2925	2182	301.3	12.6	983	31.2
2975	2172	300.0	19.3	1033	32.5
3025	2164	298.7	24.3	1083	33.3
3075	2158	297.3	33.0	1133	32.6
3125	2152	296.0	44.9	1183	29.7
3175	2147	294.7	51.0	1233	26.8
3225	2144	293.4	37.1	1283	31.4
3275	2142	292.0	33.7	1333	33.7
3325	2141	290.7	30.8	1383	33.3
3375	2141	289.3	31.7	1433	35.7
3425	2142	288.0	36.7	1483	36.1
3475	2144	286.7	45.2	1533	33.6
3525	2148	285.3	45.0	1583	17.2
3575	2153	284.0	49.3	1633	11.6
3625	2158	282.7	56.6	1683	9.4
3675	2165	281.4	55.5	1733	7.2
3725	2174	280.1	47.7	1783	5.4
3775	2183	278.8	30.2	1833	3.9
3825	2193	277.5	20.5	1883	2.5
3875	2205	276.2	15.2	1933	.9
3925	2217	275.0	14.2	1983	.1
3975	2231	273.7	14.7	2033	.0
4025	2245	272.5	14.4	2083	.0
4075	2261	271.3	13.3	2133	.0
4125	2277	270.1	15.9	2183	.0
4175	2295	268.9	18.2		
4225	2314	267.8	20.2		
4275	2333	266.7	21.5		
4325	2353	265.5	20.6		
4375	2375	264.4	19.1		
4425	2397	263.4	16.8		
4475	2419	262.3	11.4		
4525	2443	261.3	7.6		
4575	2468	260.3	7.6		
4625	2493	259.3	7.5		
4675	2519	258.3	6.5		
4725	2546	257.3	5.0		
4775	2573	256.4	2.7		
4825	2601	255.5	1.0		
4875	2630	254.6	.5		
4925	2659	253.7	.5		
4975	2689	252.8	.3		
5025	2720	252.0	-.0		
5075	2751	251.2	.0		
5125	2783	250.4	.0		

*Fire smoke not removed

Table A.1 (1-83/200.1° with and without fire-smoke contaminated plume area)

Period 2-83, θ_L =169.9° (fine)

CONDORS '83 AVERAGED OIL FOG PROFILES — Period # 2
Release Rate: 44.6 g/s — Azimuth 169.9
Release Height: Surface

Horizontal Profile (25.0 m res.)				Vertical Profile (12.5 m res.)	
η(m)	ρ_s(m)	θ_s(°)	χ^n_z	z(m)	χ^n_η
3413	581	333.3	.0	-36	.0
3438	557	332.5	.1	-24	.0
3463	533	331.7	.6	-11	.0
3488	510	330.9	.3	1	.6
3513	486	329.9	.5	14	620.2
3538	463	328.8	.3	26	706.1
3563	440	327.7	.6	39	596.8
3588	416	326.4	.2	51	515.8
3613	394	324.9	9.0	64	482.7
3638	371	323.3	40.1	76	307.7
3663	349	321.4	61.7	89	208.2
3688	327	319.3	87.2	101	168.8
3713	306	317.0	198.1	114	92.5
3738	285	314.2	167.3	126	63.1
3763	265	311.1	140.1	139	47.7
3788	246	307.4	115.5	151	32.3
3813	229	303.2	99.5	164	40.1
3838	212	298.3	259.3	176	30.0
3863	198	292.6	119.1	189	21.2
3888	185	286.1	38.3	201	13.7
3913	176	278.8	124.4	214	15.0
3938	169	270.7	405.1	226	18.3
3963	166	262.2	104.0	239	17.7
3988	167	253.7	12.4	251	1.3
4013	172	245.3	7.3		
4038	180	237.6	4.9		
4063	191	230.6	2.8		
4088	204	224.5	1.1		
4113	219	219.2	.0		
4138	237	214.6	.0		

Period 2-83, θ_L =169.9° (normal)

CONDORS '83 AVERAGED OIL FOG PROFILES — Period # 2
Release Rate: 44.6 g/s — Azimuth 169.9
Release Height: Surface

Horizontal Profile (50.0 m res.)				Vertical Profile (50.0 m res.)	
η(m)	ρ_s(m)	θ_s(°)	χ^n_z	z(m)	χ^n_η
3425	569	332.9	.1	-17	.1
3475	522	331.3	.5	33	609.7
3525	474	329.4	.4	83	291.8
3575	428	327.0	.4	133	58.9
3625	382	324.1	24.6	183	26.2
3675	338	320.4	74.5	233	13.1
3725	296	315.6	182.7		
3775	256	309.3	127.8		
3825	220	300.8	179.4		
3875	191	289.5	78.7		
3925	172	274.8	264.7		
3975	166	257.9	58.2		
4025	175	241.4	6.1		
4075	197	227.5	1.9		
4125	228	216.8	.0		

Period 2-83, θ_L =174.0° (fine)

CONDORS '83 AVERAGED OIL FOG PROFILES — Period # 2
Release Rate: 44.6 g/s — Azimuth 174.0
Release Height: Surface

Horizontal Profile (25.0 m res.)				Vertical Profile (25.0 m res.)	
η(m)	ρ_s(m)	θ_s(°)	χ^n_z	z(m)	χ^n_η
2613	1409	335.3	.0	-30	.0
2638	1385	335.0	.0	-5	.8
2663	1362	334.7	.0	20	76.9
2688	1338	334.3	.0	45	149.9
2713	1314	333.9	.1	70	175.2
2738	1291	333.6	.4	95	196.0
2763	1268	333.2	.4	120	190.4
2788	1244	332.8	.5	145	159.9
2813	1221	332.3	1.1	170	118.0
2838	1198	331.9	2.4	195	93.5
2863	1175	331.4	3.8	220	86.4
2888	1152	331.0	5.3	245	90.5
2913	1129	330.5	5.5	270	81.7
2938	1106	329.9	4.3	295	75.4
2963	1083	329.4	4.0	320	67.6
2988	1060	328.8	4.4	345	61.7
3013	1038	328.2	4.8	370	56.5
3038	1015	327.6	4.7	395	41.9
3063	993	327.0	4.6	420	36.4
3088	971	326.3	3.9	445	36.6
3113	949	325.6	4.6	470	34.1
3138	927	324.9	5.9	495	22.8
3163	905	324.1	6.4	520	17.0
3188	884	323.3	7.6	545	14.7
3213	862	322.5	9.3	570	11.9
3238	841	321.6	10.8	595	13.3
3263	820	320.6	14.0	620	15.9
3288	799	319.6	17.4	645	11.1
3313	779	318.6	23.2	670	9.4
3338	758	317.5	27.4	695	8.8
3363	738	316.4	30.0	720	9.4
3388	719	315.1	35.3	745	8.4
3413	700	313.9	37.3	770	6.1
3438	681	312.5	36.8	795	4.1
3463	662	311.1	39.0	820	2.4
3488	644	309.5	39.3	845	2.0
3513	627	307.9	48.7	870	2.1
3538	609	306.3	59.0	895	2.5
3563	593	304.5	70.4	920	2.9
3588	577	302.6	76.5	945	2.7
3613	562	300.6	73.1	970	2.2
3638	547	298.5	69.2	995	.7
3663	534	296.3	80.2	1020	.0
3688	521	293.9	99.0	1045	.0
3713	509	291.5	139.7	1070	.0
3738	498	288.9	170.7	1095	.0
3763	488	286.3	155.5	1120	.0
3788	479	283.5	125.3	1145	.0
3813	471	280.6	107.3	1170	.0
3838	464	277.7	77.7	1195	.0
3863	459	274.6	56.1		
3888	455	271.5	60.8		
3913	453	268.4	67.0		
3938	451	265.2	35.6		
3963	452	262.1	19.6		
3988	453	258.9	10.2		
4013	456	255.8	3.0		
4038	460	252.7	.7		
4063	466	249.7	.0		
4088	473	246.7	.0		

Table A.1 (2-83/169.9° to 174°/fine)

Period 2-83, θ_L =174.0° (normal)

CONDORS '83 AVERAGED OIL FOG PROFILES — Period # 2
Release Rate: 44.6 g/s — Azimuth 174.0
Release Height: Surface — Tape File # 69

Horizontal Profile (50.0 m res.)				Vertical Profile (50.0 m res.)	
η(m)	ρ_s(m)	θ_s(°)	χ^n_z	z(m)	χ^n_η
2625	1397	335.2	.0	-17	.4
2675	1350	334.5	.0	33	113.4
2725	1303	333.8	.2	83	185.6
2775	1256	333.0	.5	133	175.1
2825	1209	332.1	1.8	183	105.8
2875	1163	331.2	4.6	233	88.5
2925	1117	330.2	4.9	283	78.6
2975	1072	329.1	4.2	333	64.7
3025	1027	327.9	4.7	383	49.2
3075	982	326.7	4.3	433	36.5
3125	938	325.3	5.3	483	28.4
3175	894	323.7	7.0	533	15.9
3225	851	322.0	10.1	583	12.6
3275	810	320.1	15.7	633	13.5
3325	769	318.1	25.3	683	9.1
3375	729	315.8	32.6	733	8.9
3425	690	313.2	37.1	783	5.1
3475	653	310.3	39.2	833	2.2
3525	618	307.1	53.8	883	2.3
3575	585	303.5	73.5	933	2.8
3625	554	299.5	71.2	983	1.4
3675	527	295.1	89.6	1033	.0
3725	503	290.2	155.2	1083	.0
3775	483	284.9	140.4	1133	.0
3825	467	279.2	92.5	1183	.0
3875	457	273.1	58.5		
3925	452	266.8	51.3		
3975	452	260.5	14.9		
4025	458	254.2	1.8		
4075	469	248.2	.0		

Period 2-83, θ_L =181.1° (normal)

CONDORS '83 AVERAGED OIL FOG PROFILES — Period # 2
Release Rate: 44.6 g/s — Azimuth 181.1
Release Height: Surface

Horizontal Profile (50.0 m res.)				Vertical Profile (50.0 m res.)	
η(m)	ρ_s(m)	θ_s(°)	χ^n_z	z(m)	χ^n_η
2125	1972	332.8	.0	-17	.1
2175	1928	332.1	.0	33	62.6
2225	1885	331.4	.0	83	88.8
2275	1841	330.6	.1	133	94.9
2325	1799	329.8	.2	183	96.2
2375	1756	328.9	.4	233	88.3
2425	1714	328.0	1.0	283	82.9
2475	1672	327.1	1.7	333	81.4
2525	1631	326.1	2.8	383	80.1
2575	1590	325.1	2.9	433	70.2
2625	1550	324.0	2.3	483	45.5
2675	1511	322.9	2.6	533	34.7
2725	1472	321.7	6.3	583	32.9
2775	1433	320.4	7.2	633	31.7
2825	1396	319.0	6.9	683	23.0
2875	1359	317.6	6.1	733	22.2
2925	1323	316.1	8.0	783	16.9
2975	1289	314.6	10.9	833	13.9
3025	1255	312.9	17.7	883	8.4
3075	1222	311.2	20.5	933	6.9
3125	1190	309.3	30.2	983	7.9
3175	1160	307.4	42.7	1033	7.6
3225	1131	305.3	65.2	1083	2.8
3275	1104	303.2	83.7	1133	.2
3325	1078	300.9	108.3	1183	.0
3375	1054	298.6	120.4		
3425	1032	296.1	100.3		
3475	1012	293.5	84.7		
3525	994	290.9	58.7		
3575	978	288.1	42.1		
3625	965	285.3	30.7		
3675	954	282.4	27.4		
3725	945	279.4	21.5		
3775	939	276.4	18.7		
3825	936	273.3	21.7		
3875	936	270.3	13.8		
3925	938	267.2	10.3		
3975	942	264.2	9.7		
4025	950	261.2	6.4		
4075	960	258.2	3.3		
4125	972	255.4	1.0		
4175	987	252.6	.7		
4225	1004	249.9	.6		
4275	1023	247.3	.3		
4325	1044	244.7	-.0		
4375	1067	242.3	-.0		
4425	1092	240.0	.0		
4475	1119	237.8	.0		
4525	1147	235.8	.0		
4575	1177	233.8	.0		

Table A.1 (2-83/174°/normal to 181.1°)

Period 2-83, θ_L =190.0° (normal)

CONDORS '83 AVERAGED OIL FOG PROFILES — Period # 2
Release Rate: 44.6 g/s — Azimuth 190.0
Release Height: Surface

Horizontal Profile (50.0 m res.)				Vertical Profile (50.0 m res.)	
η(m)	ρ_s(m)	θ_s(°)	χ^n_z	z(m)	χ^n_η
1825	2391	330.5	.0	-17	5.2
1875	2353	329.7	.0	33	72.0
1925	2315	328.9	.0	83	84.1
1975	2277	328.1	.0	133	84.7
2025	2240	327.3	.0	183	76.5
2075	2204	326.4	.0	233	76.1
2125	2168	325.5	.0	283	75.7
2175	2133	324.5	.2	333	74.9
2225	2098	323.5	.3	383	68.8
2275	2064	322.5	.5	433	67.6
2325	2030	321.5	1.0	483	61.6
2375	1998	320.4	1.1	533	54.1
2425	1966	319.3	2.0	583	43.0
2475	1934	318.2	3.1	633	32.0
2525	1904	317.0	4.4	683	27.7
2575	1874	315.8	6.3	733	19.3
2625	1845	314.5	12.1	783	13.3
2675	1818	313.2	20.2	833	11.1
2725	1791	311.9	31.7	883	12.2
2775	1765	310.5	42.9	933	12.0
2825	1740	309.1	55.1	983	13.1
2875	1716	307.6	62.1	1033	5.0
2925	1694	306.1	61.6	1083	3.1
2975	1672	304.6	64.8	1133	4.3
3025	1652	303.0	64.4	1183	2.7
3075	1633	301.4	59.8	1233	-.1
3125	1616	299.7	59.6	1283	.0
3175	1600	298.0	52.7	1333	.0
3225	1585	296.3	50.1	1383	.0
3275	1571	294.6	45.7	1433	.0
3325	1560	292.8	35.4		
3375	1549	291.0	30.7		
3425	1541	289.2	28.5		
3475	1533	287.3	20.1		
3525	1528	285.5	18.1		
3575	1524	283.6	21.9		
3625	1522	281.7	25.3		
3675	1521	279.8	25.4		
3725	1522	277.9	23.2		
3775	1525	276.1	20.5		
3825	1529	274.2	15.6		
3875	1535	272.3	10.8		
3925	1542	270.5	9.5		
3975	1551	268.7	6.6		
4025	1562	266.9	3.7		
4075	1574	265.1	2.2		
4125	1588	263.4	.7		
4175	1603	261.6	.1		
4225	1619	260.0	-.0		
4275	1637	258.3	.0		

Period 2-83, θ_L =200.1° (normal)

CONDORS '83 AVERAGED OIL FOG PROFILES — Period # 2
Release Rate: 44.6 g/s — Azimuth 200.1
Release Height: Surface

Horizontal Profile (50.0 m res.)				Vertical Profile (50.0 m res.)	
η(m)	ρ_s(m)	θ_s(°)	χ^n_z	z(m)	χ^n_η
1875	2598	324.6	.0	-17	9.6
1925	2570	323.7	.0	33	59.7
1975	2543	322.8	.6	83	68.1
2025	2516	321.8	.7	133	70.2
2075	2490	320.8	1.3	183	70.7
2125	2465	319.8	3.6	233	72.6
2175	2441	318.8	6.1	283	75.7
2225	2417	317.8	8.4	333	77.9
2275	2394	316.7	10.3	383	70.1
2325	2372	315.6	12.7	433	65.4
2375	2351	314.5	14.8	483	64.6
2425	2331	313.4	15.3	533	59.2
2475	2312	312.3	17.6	583	48.7
2525	2293	311.1	19.5	633	40.1
2575	2276	309.9	21.7	683	39.6
2625	2260	308.7	31.5	733	26.4
2675	2244	307.5	38.4	783	16.9
2725	2230	306.3	44.5	833	12.7
2775	2216	305.1	49.9	883	9.3
2825	2204	303.8	49.8	933	8.1
2875	2193	302.5	49.2	983	7.1
2925	2182	301.2	47.7	1033	7.2
2975	2173	300.0	47.7	1083	6.0
3025	2165	298.6	47.8	1133	4.8
3075	2158	297.3	48.1	1183	4.3
3125	2153	296.0	47.7	1233	3.7
3175	2148	294.7	44.0	1283	1.5
3225	2145	293.4	38.4	1333	-.3
3275	2142	292.0	33.3	1383	.0
3325	2141	290.7	27.2	1433	.0
3375	2141	289.3	18.9		
3425	2143	288.0	15.0		
3475	2145	286.7	15.1		
3525	2149	285.3	17.9		
3575	2153	284.0	20.4		
3625	2159	282.7	18.4		
3675	2166	281.4	14.1		
3725	2175	280.1	12.6		
3775	2184	278.8	11.6		
3825	2194	277.5	11.6		
3875	2206	276.2	11.6		
3925	2218	275.0	10.4		
3975	2232	273.8	9.3		
4025	2246	272.5	8.7		
4075	2262	271.3	7.5		
4125	2278	270.1	6.8		
4175	2296	269.0	4.6		
4225	2315	267.8	3.4		
4275	2334	266.7	2.5		
4325	2354	265.6	1.3		
4375	2376	264.5	.5		
4425	2398	263.4	.2		
4475	2421	262.3	-.0		
4525	2444	261.3	-.0		
4575	2469	260.3	.0		

Table A.1 (2-83/190° to 200.1°)

Period 2-83, θ_L = 210.0° (normal)

CONDORS '83 AVERAGED OIL FOG PROFILES — Period # 2
Release Rate: 44.6 g/s — Azimuth 210.0
Release Height: Surface

Horizontal Profile (50.0 m res.)				Vertical Profile (50.0 m res.)	
η(m)	ρ_s(m)	θ_s(°)	χ^n_z	z(m)	χ^n_η
1725	2942	324.2	.0	-17	5.3
1775	2922	323.3	.3	33	42.8
1825	2903	322.4	.7	83	50.1
1875	2884	321.4	2.0	133	57.0
1925	2867	320.5	5.1	183	62.5
1975	2849	319.6	5.1	233	64.8
2025	2833	318.6	5.6	283	66.6
2075	2818	317.6	6.3	333	64.4
2125	2803	316.7	6.8	383	61.6
2175	2789	315.7	8.4	433	56.4
2225	2776	314.7	9.7	483	50.1
2275	2764	313.7	12.2	533	50.6
2325	2752	312.7	13.7	583	51.5
2375	2742	311.7	15.0	633	45.2
2425	2732	310.6	16.9	683	42.1
2475	2723	309.6	19.2	733	33.4
2525	2715	308.6	23.2	783	27.2
2575	2708	307.5	26.1	833	24.6
2625	2702	306.5	27.3	883	20.6
2675	2697	305.4	31.7	933	18.2
2725	2693	304.3	38.8	983	19.0
2775	2690	303.3	44.7	1033	17.7
2825	2687	302.2	46.1	1083	15.9
2875	2686	301.2	47.2	1133	15.6
2925	2685	300.1	47.6	1183	11.8
2975	2686	299.0	48.8	1233	8.6
3025	2687	298.0	47.2	1283	6.9
3075	2689	296.9	41.9	1333	5.8
3125	2693	295.8	35.8	1383	3.6
3175	2697	294.8	26.2	1433	.6
3225	2702	293.7	20.7	1483	-.0
3275	2708	292.7	16.8	1533	.0
3325	2715	291.6	13.4	1583	.0
3375	2722	290.6	11.8	1633	.0
3425	2731	289.5	11.1	1683	.0
3475	2741	288.5	12.6		
3525	2751	287.5	11.5		
3575	2762	286.5	11.7		
3625	2774	285.5	11.3		
3675	2787	284.5	14.0		
3725	2801	283.5	15.9		
3775	2816	282.5	16.9		
3825	2831	281.6	17.8		
3875	2848	280.6	18.3		
3925	2865	279.7	18.5		
3975	2882	278.7	18.3		
4025	2901	277.8	14.3		
4075	2920	276.9	13.9		
4125	2940	276.0	13.8		
4175	2961	275.1	12.9		
4225	2982	274.2	10.4		
4275	3004	273.4	10.3		
4325	3027	272.5	8.4		
4375	3051	271.7	6.5		
4425	3075	270.9	3.9		
4475	3099	270.1	2.0		
4525	3125	269.3	2.0		
4575	3150	268.5	1.4		
4625	3177	267.7	.1		
4675	3204	267.0	.0		

Period 3-83, θ_L = 169.9° (fine)

CONDORS '83 AVERAGED OIL FOG PROFILES — Period # 3
Release Rate: 41.3 g/s — Azimuth 169.9
Release Height: Surface

Horizontal Profile (25.0 m res.)				Vertical Profile (12.5 m res.)	
η(m)	ρ_s(m)	θ_s(°)	χ^n_z	z(m)	χ^n_η
3113	873	339.0	.0	-36	.0
3138	848	338.7	.0	-24	.0
3163	823	338.4	.0	-11	.0
3188	799	338.0	.0	1	70.2
3213	775	337.6	.0	14	721.6
3238	750	337.2	.0	26	831.8
3263	726	336.8	.0	39	647.0
3288	701	336.3	.0	51	473.8
3313	677	335.8	.1	64	345.6
3338	653	335.3	.0	76	267.9
3363	629	334.7	.3	89	143.3
3388	605	334.1	.7	101	104.0
3413	581	333.4	1.6	114	72.3
3438	557	332.7	4.4	126	46.6
3463	533	331.9	12.9	139	9.3
3488	509	331.0	16.8	151	5.6
3513	486	330.1	10.6	164	7.0
3538	462	329.0	7.6	176	20.2
3563	439	327.9	3.6	189	55.5
3588	416	326.6	.9	201	39.7
3613	393	325.1	.6	214	15.2
3638	370	323.5	.3	226	6.7
3663	348	321.7	.2	239	5.1
3688	326	319.6	.1	251	8.6
3713	305	317.2	.1	264	8.2
3738	284	314.5	.2	276	8.1
3763	264	311.4	9.1	289	8.5
3788	245	307.7	64.8	301	8.8
3813	227	303.5	99.4	314	8.2
3838	211	298.6	123.6	326	10.4
3863	196	292.9	187.9	339	12.7
3888	184	286.3	118.6	351	15.8
3913	174	279.0	161.9	364	10.0
3938	168	270.8	83.0	376	3.3
3963	165	262.3	294.9	389	1.6
3988	165	253.6	254.4	401	.7
4013	170	245.2	256.6	414	.5
4038	178	237.4	93.8	426	.6
4063	189	230.4	45.6	439	2.0
4088	203	224.2	64.0	451	1.7
4113	218	218.9	45.7	464	.9
4138	235	214.3	19.4	476	.3
4163	254	210.3	10.1	489	.2
4188	273	206.9	3.8	501	.0
4213	294	204.0	1.2	514	.0
4238	315	201.4	.9	526	.0
4263	336	199.2	.2	539	.0
4288	358	197.2	.1	551	.0
4313	380	195.5	.0	564	.0
4338	403	194.0	.0	576	.0
				589	.0
				601	.0
				614	.0
				626	.0
				639	.0
				651	.0
				664	.0
				676	.0
				689	.0
				701	.0

Table A.1 (2-83/210° to 3-83/169.9°/fine)

Period 3-83, θ_L =169.9° (normal)

CONDORS '83 AVERAGED OIL FOG PROFILES — Period # 3
Release Rate: 41.3 g/s — Azimuth 169.9
Release Height: Surface

Horizontal Profile (50.0 m res.)				Vertical Profile (50.0 m res.)	
η(m)	ρ_s(m)	θ_s(°)	χ^n_z	z(m)	χ^n_η
3125	860	338.8	.0	-17	17.5
3175	811	338.2	.0	33	668.6
3225	762	337.4	.0	83	215.2
3275	714	336.5	.0	133	33.5
3325	665	335.6	.1	183	30.6
3375	617	334.4	.5	233	8.9
3425	569	333.1	3.0	283	8.4
3475	521	331.5	14.9	333	11.8
3525	474	329.6	9.1	383	3.9
3575	427	327.2	2.2	433	1.2
3625	382	324.3	.4	483	.4
3675	337	320.7	.1	533	.0
3725	295	315.9	.2	583	.0
3775	255	309.6	36.9	633	.0
3825	219	301.1	111.5	683	.0
3875	190	289.7	153.3		
3925	170	275.0	122.4		
3975	165	257.9	274.6		
4025	174	241.2	175.2		
4075	195	227.2	54.8		
4125	226	216.5	32.6		
4175	263	208.5	7.0		
4225	304	202.6	1.0		
4275	347	198.2	.1		
4325	392	194.7	.0		

Period 3-83, θ_L =174.0° (fine)

CONDORS '83 AVERAGED OIL FOG PROFILES — Period # 3
Release Rate: 41.3 g/s — Azimuth 174.0
Release Height: Surface

Horizontal Profile (25.0 m res.)				Vertical Profile (25.0 m res.)	
η(m)	ρ_s(m)	θ_s(°)	χ^n_z	z(m)	χ^n_η
2413	1599	337.7	.0	-30	.0
2438	1575	337.4	.0	-5	.0
2463	1552	337.1	.0	20	145.1
2488	1528	336.9	.1	45	316.2
2513	1504	336.6	.5	70	306.9
2538	1480	336.3	.7	95	212.3
2563	1456	336.0	.6	120	155.6
2588	1432	335.7	.4	145	136.0
2613	1409	335.4	.3	170	116.4
2638	1385	335.0	.3	195	95.4
2663	1361	334.7	.3	220	69.5
2688	1338	334.3	.4	245	70.8
2713	1314	334.0	.4	270	64.1
2738	1291	333.6	.4	295	52.3
2763	1267	333.2	.5	320	46.9
2788	1244	332.8	.6	345	54.1
2813	1221	332.4	1.0	370	46.6
2838	1198	331.9	.8	395	27.9
2863	1175	331.5	.6	420	11.4
2888	1151	331.0	.9	445	6.3
2913	1129	330.5	.9	470	7.3
2938	1106	330.0	.3	495	11.3
2963	1083	329.4	-.0	520	6.3
2988	1060	328.9	-.1	545	5.0
3013	1038	328.3	-.1	570	6.1
3038	1015	327.7	-.1	595	7.7
3063	993	327.0	-.0	620	4.8
3088	971	326.4	.1	645	2.1
3113	949	325.7	.7	670	1.1
3138	927	324.9	2.1	695	1.4
3163	905	324.1	3.5	720	1.1
3188	883	323.3	5.3	745	.7
3213	862	322.5	7.6	770	.5
3238	841	321.6	9.8	795	.5
3263	820	320.7	10.4	820	.3
3288	799	319.7	22.0	845	.0
3313	778	318.6	27.9	870	-.0
3338	758	317.5	25.7	895	.0
3363	738	316.4	20.0	920	.0
3388	718	315.2	20.6	945	.0
3413	699	313.9	20.2		
3438	680	312.5	22.6		
3463	662	311.1	19.4		
3488	644	309.6	22.1		
3513	626	308.0	37.1		
3538	609	306.3	33.9		
3563	592	304.5	32.5		
3588	576	302.6	26.2		
3613	561	300.6	26.1		
3638	547	298.5	47.9		
3663	533	296.3	56.4		
3688	520	294.0	53.8		
3713	508	291.5	49.2		
3738	497	289.0	34.8		
3763	487	286.3	30.9		
3788	478	283.5	68.3		
3813	470	280.7	98.7		
3838	464	277.7	114.9		
3863	458	274.7	99.2		
3888	454	271.6	91.8		
3913	452	268.4	107.2		
3938	451	265.2	106.4		
3963	451	262.1	80.5		
3988	452	258.9	83.1		
4013	455	255.8	92.4		
4038	460	252.7	92.8		
4063	465	249.7	82.5		
4088	472	246.7	48.1		
4113	480	243.9	44.4		
4138	489	241.1	37.8		
4163	499	238.5	38.0		
4188	511	235.9	24.5		
4213	523	233.5	8.5		
4238	536	231.2	2.3		
4263	550	229.0	.2		
4288	565	226.9	.0		
4313	580	225.0	.0		
4338	596	223.1	.0		
4363	613	221.3	.0		
4388	630	219.7	.0		

Table A.1 (3-83/169.9°/normal to 174°/fine)

Period 3-83, θ_L =174.0° (normal)

CONDORS '83 AVERAGED OIL FOG PROFILES — Period # 3
Release Rate: 41.3 g/s — Azimuth 174.0
Release Height: Surface

Horizontal Profile (50.0 m res.)				Vertical Profile (50.0 m res.)	
η(m)	ρ_s(m)	θ_s(°)	X_z^n	z(m)	X_η^n
2425	1587	337.5	.0	-17	.0
2475	1540	337.0	.1	33	230.6
2525	1492	336.4	.6	83	259.6
2575	1444	335.8	.5	133	150.8
2625	1397	335.2	.3	183	105.9
2675	1350	334.5	.3	233	70.2
2725	1303	333.8	.4	283	58.2
2775	1256	333.0	.6	333	50.5
2825	1209	332.1	.9	383	37.2
2875	1163	331.2	.8	433	8.9
2925	1117	330.2	.6	483	9.3
2975	1071	329.1	-.1	533	5.6
3025	1026	328.0	-.1	583	6.9
3075	982	326.7	.0	633	3.5
3125	938	325.3	1.4	683	1.2
3175	894	323.7	4.4	733	.9
3225	851	322.1	8.7	783	.5
3275	809	320.2	16.2	833	.2
3325	768	318.1	26.8	883	-.0
3375	728	315.8	20.3	933	.0
3425	690	313.2	21.4		
3475	653	310.4	20.7		
3525	617	307.1	35.5		
3575	584	303.6	29.3		
3625	554	299.6	37.0		
3675	526	295.1	55.1		
3725	502	290.3	42.0		
3775	482	284.9	49.6		
3825	467	279.2	106.8		
3875	456	273.1	95.5		
3925	451	266.8	106.8		
3975	451	260.5	81.8		
4025	457	254.2	92.6		
4075	468	248.2	65.3		
4125	484	242.5	41.1		
4175	505	237.2	31.2		
4225	529	232.4	5.4		
4275	557	228.0	.1		
4325	588	224.0	.0		
4375	621	220.5	.0		

Period 3-83, θ_L =181.1° (normal)

CONDORS '83 AVERAGED OIL FOG PROFILES — Period # 3
Release Rate: 41.3 g/s — Azimuth 181.1
Release Height: Surface

Horizontal Profile (50.0 m res.)				Vertical Profile (50.0 m res.)	
η(m)	ρ_s(m)	θ_s(°)	X_z^n	z(m)	X_η^n
1825	2241	336.5	.0	-17	3.9
1875	2195	335.9	.0	33	107.2
1925	2150	335.3	.0	83	132.6
1975	2105	334.7	.0	133	111.5
2025	2060	334.1	.1	183	103.0
2075	2016	333.5	.2	233	82.4
2125	1972	332.8	.1	283	81.8
2175	1928	332.1	.0	333	80.4
2225	1884	331.4	.0	383	74.2
2275	1841	330.6	.0	433	60.8
2325	1798	329.8	.1	483	46.0
2375	1756	328.9	.9	533	30.8
2425	1714	328.1	2.3	583	28.8
2475	1672	327.1	3.1	633	17.9
2525	1631	326.1	1.9	683	11.9
2575	1590	325.1	2.1	733	10.4
2625	1550	324.0	2.6	783	7.0
2675	1510	322.9	4.0	833	5.9
2725	1471	321.7	3.3	883	3.1
2775	1433	320.4	2.2	933	.4
2825	1396	319.1	2.1	983	.1
2875	1359	317.6	3.2	1033	-.0
2925	1323	316.2	3.8	1083	.0
2975	1288	314.6	3.1	1133	.0
3025	1254	312.9	2.7	1183	.0
3075	1221	311.2	7.0		
3125	1190	309.3	22.2		
3175	1160	307.4	24.8		
3225	1131	305.4	24.8		
3275	1103	303.2	22.8		
3325	1078	301.0	19.9		
3375	1054	298.6	19.9		
3425	1032	296.1	22.8		
3475	1011	293.6	32.2		
3525	993	290.9	36.0		
3575	978	288.1	43.3		
3625	964	285.3	55.6		
3675	953	282.4	63.4		
3725	945	279.4	77.1		
3775	939	276.4	76.8		
3825	935	273.3	66.4		
3875	935	270.3	51.6		
3925	937	267.2	54.2		
3975	942	264.2	56.8		
4025	949	261.2	54.4		
4075	959	258.2	44.0		
4125	971	255.4	32.6		
4175	986	252.6	20.8		
4225	1003	249.8	17.1		
4275	1022	247.2	7.6		
4325	1043	244.7	2.8		
4375	1067	242.3	1.1		
4425	1092	240.0	1.9		
4475	1118	237.8	1.4		
4525	1146	235.7	.7		
4575	1176	233.7	.2		
4625	1207	231.9	.0		
4675	1239	230.1	.0		
4725	1273	228.4	.0		
4775	1307	226.8	.0		

Table A.1 (3-83/174°/normal to 181.1°)

Period 3-83, θ_L =190.0° (normal)

CONDORS '83 AVERAGED OIL FOG PROFILES — Period # 3
Release Rate: 41.3 g/s — Azimuth 190.0
Release Height: Surface

Horizontal Profile (50.0 m res.)				Vertical Profile (50.0 m res.)	
η(m)	ρ_s(m)	θ_s(°)	χ^n_z	z(m)	χ^n_η
1425	2712	335.9	.0	-17	7.9
1475	2671	335.3	.0	33	75.1
1525	2630	334.7	.2	83	87.6
1575	2589	334.0	.5	133	87.7
1625	2549	333.4	.4	183	91.1
1675	2509	332.7	.5	233	81.5
1725	2469	332.0	.5	283	68.8
1775	2430	331.3	.8	333	65.2
1825	2391	330.5	.8	383	67.1
1875	2353	329.7	1.0	433	63.0
1925	2315	328.9	1.4	483	57.5
1975	2277	328.1	2.1	533	45.3
2025	2241	327.3	2.2	583	37.2
2075	2204	326.4	1.9	633	31.8
2125	2168	325.5	2.1	683	26.9
2175	2133	324.5	2.6	733	23.6
2225	2098	323.5	3.7	783	20.4
2275	2064	322.5	7.3	833	14.2
2325	2030	321.5	9.8	883	9.8
2375	1998	320.4	8.3	933	8.7
2425	1966	319.3	7.9	983	8.6
2475	1934	318.2	7.4	1033	6.8
2525	1904	317.0	9.3	1083	5.6
2575	1874	315.8	10.3	1133	4.2
2625	1845	314.5	10.2	1183	2.5
2675	1818	313.2	12.5	1233	1.1
2725	1791	311.9	16.1	1283	.4
2775	1765	310.5	20.7	1333	.1
2825	1740	309.1	23.6	1383	.0
2875	1716	307.6	24.2	1433	.0
2925	1694	306.1	24.7	1483	.0
2975	1672	304.6	22.9	1533	.0
3025	1652	303.0	21.4	1583	.0
3075	1633	301.4	23.8	1633	.0
3125	1616	299.7	26.2	1683	.0
3175	1600	298.0	29.6	1733	-.0
3225	1585	296.3	31.4	1783	.0
3275	1572	294.6	29.1	1833	.0
3325	1560	292.8	24.2	1883	.0
3375	1549	291.0	21.2	1933	.0
3425	1541	289.2	19.2		
3475	1534	287.3	21.0		
3525	1528	285.5	22.2		
3575	1524	283.6	27.6		
3625	1522	281.7	35.3		
3675	1521	279.8	39.2		
3725	1522	277.9	39.4		
3775	1525	276.1	40.9		
3825	1529	274.2	43.4		
3875	1535	272.3	47.0		
3925	1542	270.5	41.5		
3975	1551	268.7	38.4		
4025	1562	266.9	33.1		
4075	1574	265.1	26.3		
4125	1588	263.4	18.8		
4175	1603	261.6	12.8		
4225	1619	260.0	10.7		
4275	1637	258.3	7.9		
4325	1656	256.7	5.4		
4375	1676	255.1	5.9		
4425	1698	253.6	7.1		
4475	1721	252.1	7.2		
4525	1745	250.7	3.3		
4575	1770	249.3	1.3		
4625	1796	247.9	.8		
4675	1823	246.6	.5		
4725	1851	245.3	.4		
4775	1880	244.0	.1		
4825	1910	242.8	-.1		
4875	1940	241.6	-.1		
4925	1972	240.5	.0		
4975	2004	239.4	.0		
5025	2037	238.3	.0		
5075	2071	237.3	.0		
5125	2105	236.3	.0		

Period 3-83, θ_L =200.1° (normal)

CONDORS '83 AVERAGED OIL FOG PROFILES — Period # 3
Release Rate: 41.3 g/s — Azimuth 200.1
Release Height: Surface

Horizontal Profile (50.0 m res.)				Vertical Profile (50.0 m res.)	
η(m)	ρ_s(m)	θ_s(°)	χ^n_z	z(m)	χ^n_η
1625	2748	328.9	.0	-17	11.3
1675	2717	328.1	.0	33	59.5
1725	2686	327.2	.1	83	70.2
1775	2656	326.4	.4	133	74.8
1825	2627	325.5	.7	183	73.8
1875	2598	324.6	1.7	233	70.2
1925	2570	323.7	2.3	283	66.4
1975	2543	322.7	3.2	333	59.3
2025	2516	321.8	4.4	383	54.4
2075	2491	320.8	5.0	433	50.8
2125	2465	319.8	4.9	483	49.4
2175	2441	318.8	5.3	533	49.9
2225	2417	317.8	7.7	583	48.7
2275	2395	316.7	9.5	633	42.3
2325	2373	315.6	10.4	683	37.6
2375	2352	314.5	12.5	733	36.5
2425	2331	313.4	13.7	783	31.7
2475	2312	312.3	13.0	833	26.3
2525	2294	311.1	13.6	883	19.4
2575	2276	309.9	14.9	933	13.6
2625	2260	308.7	15.2	983	8.8
2675	2244	307.5	17.6	1033	8.0
2725	2230	306.3	19.5	1083	7.7
2775	2217	305.1	19.9	1133	6.4
2825	2204	303.8	20.6	1183	3.8
2875	2193	302.5	22.2	1233	2.9
2925	2183	301.2	20.6	1283	2.7
2975	2174	300.0	20.7	1333	2.1
3025	2166	298.6	20.5	1383	1.9
3075	2159	297.3	22.2	1433	1.7
3125	2153	296.0	21.3	1483	1.6
3175	2149	294.7	19.3	1533	1.3
3225	2145	293.4	20.3	1583	1.4
3275	2143	292.0	23.8	1633	1.2
3325	2142	290.7	23.8	1683	.9
3375	2142	289.3	21.5	1733	.7
3425	2143	288.0	20.1	1783	.5
3475	2146	286.7	20.1	1833	.2
3525	2149	285.3	20.3	1883	.0
3575	2154	284.0	22.0	1933	-.0
3625	2160	282.7	22.4	1983	-.0
3675	2167	281.4	25.0	2033	.0
3725	2175	280.1	27.9	2083	.0
3775	2184	278.8	29.5	2133	.0
3825	2195	277.5	29.2	2183	.0
3875	2206	276.3	25.4		
3925	2219	275.0	23.0		
3975	2232	273.8	22.4		
4025	2247	272.5	23.3		
4075	2262	271.3	24.2		
4125	2279	270.1	24.3		
4175	2297	269.0	25.4		
4225	2315	267.8	24.5		
4275	2335	266.7	20.8		
4325	2355	265.6	17.1		
4375	2376	264.5	15.2		
4425	2398	263.4	13.4		
4475	2421	262.3	12.4		
4525	2445	261.3	11.7		
4575	2469	260.3	11.2		
4625	2495	259.3	10.7		
4675	2521	258.3	8.3		
4725	2547	257.3	6.3		
4775	2575	256.4	5.4		
4825	2603	255.5	3.7		
4875	2632	254.6	1.8		
4925	2661	253.7	.6		
4975	2691	252.9	.2		
5025	2721	252.0	.1		
5075	2753	251.2	.0		

Table A.1 (3-83/190° to 200.1°)

Period 3-83, $\theta_L = 210.0°$ (normal)

CONDORS '83 AVERAGED OIL FOG PROFILES — Period # 3
Release Rate: 41.3 g/s — Azimuth 210.0
Release Height: Surface

Horizontal Profile (50.0 m res.)				Vertical Profile (50.0 m res.)	
η(m)	ρ_s(m)	θ_s(°)	χ^n_z	z(m)	χ^n_η
1225	3180	332.4	-.0	-17	7.4
1275	3153	331.6	.0	33	45.0
1325	3127	330.9	.1	83	52.2
1375	3102	330.1	.2	133	55.3
1425	3077	329.3	.5	183	57.5
1475	3053	328.4	.4	233	55.5
1525	3030	327.6	.3	283	53.2
1575	3007	326.8	.5	333	52.6
1625	2985	325.9	.7	383	53.3
1675	2963	325.0	1.1	433	53.8
1725	2942	324.2	1.5	483	52.7
1775	2922	323.3	1.9	533	50.0
1825	2903	322.4	2.2	583	48.6
1875	2884	321.4	2.5	633	47.0
1925	2866	320.5	3.3	683	42.7
1975	2849	319.6	4.3	733	39.1
2025	2833	318.6	5.3	783	33.8
2075	2817	317.6	6.2	833	27.1
2125	2803	316.7	6.2	883	24.7
2175	2789	315.7	6.7	933	22.8
2225	2776	314.7	7.1	983	20.3
2275	2763	313.7	7.5	1033	18.2
2325	2752	312.7	7.9	1083	15.4
2375	2741	311.7	8.0	1133	12.8
2425	2732	310.6	8.5	1183	12.2
2475	2723	309.6	9.7	1233	10.9
2525	2715	308.6	10.1	1283	8.8
2575	2708	307.5	9.5	1333	7.2
2625	2702	306.5	8.3	1383	5.9
2675	2697	305.4	8.0	1433	4.5
2725	2693	304.3	9.4	1483	3.4
2775	2689	303.3	11.1	1533	2.8
2825	2687	302.2	12.2	1583	2.0
2875	2686	301.2	13.0	1633	1.0
2925	2685	300.1	13.3	1683	.4
2975	2686	299.0	13.7	1733	.0
3025	2687	298.0	14.2	1783	-.2
3075	2689	296.9	15.7	1833	-.0
3125	2692	295.8	16.7	1883	.0
3175	2696	294.8	17.5	1933	.0
3225	2701	293.7	17.7		
3275	2707	292.7	17.9		
3325	2714	291.6	17.9		
3375	2722	290.6	17.6		
3425	2731	289.5	18.7		

η(m)	ρ_s(m)	θ_s(°)	χ^n_z	z(m)	χ^n_η
3475	2740	288.5	20.1		
3525	2751	287.5	21.3		
3575	2762	286.5	21.2		
3625	2774	285.5	23.1		
3675	2787	284.5	25.8		
3725	2801	283.5	26.3		
3775	2816	282.5	26.7		
3825	2831	281.5	27.0		
3875	2847	280.6	28.5		
3925	2864	279.7	29.0		
3975	2882	278.7	27.6		
4025	2901	277.8	25.3		
4075	2920	276.9	25.0		
4125	2940	276.0	25.2		
4175	2961	275.1	26.1		
4225	2982	274.2	26.9		
4275	3004	273.4	25.6		
4325	3027	272.5	23.9		
4375	3050	271.7	23.6		
4425	3074	270.9	22.1		
4475	3099	270.1	19.1		
4525	3124	269.3	16.4		
4575	3150	268.5	14.0		
4625	3176	267.7	12.6		
4675	3203	267.0	10.7		
4725	3231	266.2	9.4		
4775	3259	265.5	8.5		
4825	3288	264.8	8.5		
4875	3317	264.1	7.7		
4925	3346	263.4	5.7		
4975	3376	262.7	4.7		
5025	3407	262.0	3.7		
5075	3438	261.4	3.0		
5125	3469	260.7	2.8		
5175	3501	260.1	3.2		
5225	3534	259.5	3.6		
5275	3566	258.9	3.4		
5325	3599	258.3	2.8		
5375	3633	257.7	2.1		
5425	3667	257.1	1.2		
5475	3701	256.5	.8		
5525	3735	256.0	.6		
5575	3770	255.4	.5		
5625	3806	254.9	.2		
5675	3841	254.4	.1		

Table A.1 (3-83/210°)

Period 4-83, θ_L =169.9° (normal)

CONDORS '83 AVERAGED OIL FOG PROFILES — Period # 4
Release Rate: 44.5 g/s — Azimuth 169.9
Release Height: Surface

Horizontal Profile (50.0 m res.)				Vertical Profile (50.0 m res.)	
η(m)	ρ_s(m)	θ_s(°)	χ^n_z	z(m)	χ^n_η
1825	2151	345.5	.0	-17	.8
1875	2101	345.4	.0	33	196.8
1925	2051	345.3	.1	83	200.6
1975	2001	345.2	.2	133	173.0
2025	1951	345.0	.3	183	129.9
2075	1902	344.9	.2	233	57.8
2125	1852	344.8	.2	283	36.8
2175	1802	344.6	.3	333	31.1
2225	1752	344.5	.4	383	27.1
2275	1702	344.3	.6	433	34.6
2325	1653	344.2	.8	483	35.1
2375	1603	344.0	.8	533	20.2
2425	1553	343.8	1.0	583	13.8
2475	1503	343.6	1.3	633	9.6
2525	1454	343.4	2.0	683	7.9
2575	1404	343.1	2.5	733	6.6
2625	1354	342.9	2.1	783	4.9
2675	1305	342.6	2.2	833	3.5
2725	1255	342.3	2.1	883	2.3
2775	1206	342.0	2.8	933	2.5
2825	1156	341.7	2.9	983	2.5
2875	1107	341.3	3.1	1033	1.7
2925	1057	340.9	5.2	1083	.5
2975	1008	340.5	6.7	1133	.3
3025	959	340.0	6.9	1183	.0
3075	909	339.4	6.2		
3125	860	338.8	5.6		
3175	811	338.2	7.8		
3225	762	337.4	9.4		
3275	714	336.5	14.4		
3325	665	335.5	15.6		
3375	617	334.4	18.7		
3425	569	333.0	25.3		
3475	521	331.4	39.1		
3525	474	329.5	57.5		
3575	427	327.2	57.5		
3625	382	324.3	62.4		
3675	337	320.6	49.2		
3725	295	315.9	69.8		
3775	255	309.6	137.8		
3825	219	301.1	132.9		
3875	190	289.7	71.8		
3925	171	274.9	64.1		
3975	165	257.9	91.2		
4025	174	241.2	17.4		
4075	196	227.2	1.0		
4125	227	216.5	.4		
4175	264	208.6	.1		
4225	304	202.7	.0		
4275	347	198.2	.0		

Period 4-83, θ_L =173.0° (normal)

CONDORS '83 AVERAGED OIL FOG PROFILES — Period # 4
Release Rate: 44.5 g/s — Azimuth 173.0
Release Height: Surface

Horizontal Profile (50.0 m res.)				Vertical Profile (50.0 m res.)	
η(m)	ρ_s(m)	θ_s(°)	χ^n_z	z(m)	χ^n_η
1625	2360	343.7	.0	-17	.7
1675	2311	343.5	.0	33	56.4
1725	2262	343.3	.0	83	85.6
1775	2213	343.1	.1	133	97.8
1825	2163	342.9	.2	183	100.5
1875	2114	342.6	.4	233	106.8
1925	2065	342.4	.5	283	82.1
1975	2016	342.1	.9	333	75.1
2025	1967	341.8	1.1	383	66.0
2075	1918	341.5	1.3	433	48.6
2125	1869	341.2	1.3	483	42.7
2175	1820	340.9	1.2	533	39.5
2225	1771	340.6	1.2	583	37.2
2275	1722	340.2	1.1	633	25.3
2325	1673	339.8	1.8	683	21.4
2375	1625	339.4	2.5	733	21.1
2425	1576	339.0	3.1	783	20.2
2475	1528	338.6	3.8	833	11.2
2525	1479	338.1	4.5	883	10.9
2575	1431	337.6	5.1	933	12.7
2625	1383	337.0	6.1	983	14.5
2675	1335	336.4	6.8	1033	8.6
2725	1287	335.8	6.6	1083	5.8
2775	1240	335.1	7.5	1133	5.7
2825	1192	334.4	9.7	1183	2.5
2875	1145	333.6	11.6	1233	1.1
2925	1098	332.7	11.7	1283	.0
2975	1051	331.7	17.1	1333	.0
3025	1005	330.7	22.7	1383	.0
3075	959	329.6	27.1	1433	.0
3125	913	328.3	31.0		
3175	868	326.9	34.8		
3225	823	325.4	42.6		
3275	779	323.7	50.6		
3325	736	321.8	56.9		
3375	694	319.7	61.4		
3425	652	317.2	54.6		
3475	613	314.5	43.2		
3525	574	311.4	36.8		
3575	538	307.9	34.2		
3625	504	303.8	38.1		
3675	473	299.2	47.7		
3725	445	294.0	61.3		
3775	421	288.2	76.9		
3825	403	281.8	64.3		
3875	389	274.8	35.9		
3925	382	267.4	41.5		
3975	382	259.9	24.6		
4025	388	252.5	4.5		
4075	400	245.5	1.8		
4125	418	238.9	.2		
4175	440	233.0	.0		
4225	467	227.6	.0		
4275	498	223.0	.0		
4325	532	218.8	.0		

Table A.1 (4-83/169.9° to 173°)

Period 4-83, θ_L =177.5° (normal)

CONDORS '83 AVERAGED OIL FOG PROFILES — Period # 4
Release Rate: 44.5 g/s — Azimuth 177.4
Release Height: Surface

Horizontal Profile (50.0 m res.)				Vertical Profile (50.0 m res.)	
η(m)	ρ_s(m)	θ_s(°)	χ^n_z	z(m)	χ^n_η
1625	2389	340.8	.0	-17	4.1
1675	2341	340.4	.1	33	36.2
1725	2293	340.0	.6	83	55.8
1775	2245	339.7	1.4	133	56.1
1825	2198	339.3	1.7	183	50.1
1875	2150	338.9	1.5	233	52.1
1925	2103	338.4	1.7	283	51.9
1975	2056	338.0	1.8	333	55.8
2025	2009	337.5	1.8	383	63.6
2075	1962	337.0	1.8	433	64.6
2125	1915	336.5	2.4	483	65.1
2175	1868	335.9	2.8	533	62.1
2225	1822	335.3	4.0	583	51.9
2275	1776	334.7	5.6	633	50.4
2325	1730	334.1	7.6	683	49.3
2375	1684	333.4	8.1	733	49.9
2425	1638	332.7	10.0	783	38.7
2475	1593	332.0	13.7	833	27.5
2525	1548	331.2	17.2	883	24.6
2575	1503	330.3	19.8	933	23.9
2625	1459	329.4	19.4	983	23.4
2675	1415	328.5	18.7	1033	20.8
2725	1372	327.5	16.8	1083	11.6
2775	1328	326.4	15.2	1133	6.2
2825	1286	325.2	19.5	1183	3.2
2875	1244	324.0	24.5	1233	.8
2925	1202	322.7	29.4	1283	.2
2975	1162	321.3	33.9	1333	-.0
3025	1122	319.8	40.3	1383	.0
3075	1082	318.2	42.9	1433	.0
3125	1044	316.4	43.5		
3175	1007	314.6	47.4		
3225	971	312.6	55.4		
3275	936	310.4	51.0		
3325	903	308.1	46.4		
3375	871	305.6	49.8		
3425	841	302.9	51.6		
3475	813	300.1	46.2		
3525	787	297.0	42.7		
3575	764	293.7	34.9		
3625	743	290.3	27.9		
3675	725	286.6	31.4		
3725	710	282.8	29.4		
3775	699	278.8	32.8		
3825	690	274.8	19.3		
3875	686	270.6	11.6		
3925	685	266.4	8.1		
3975	688	262.3	5.8		
4025	694	258.2	.6		
4075	704	254.1	.0		

Period 4-83, θ_L =183.1° (normal)

CONDORS '83 AVERAGED OIL FOG PROFILES — Period # 4
Release Rate: 44.5 g/s — Azimuth 183.1
Release Height: Surface

Horizontal Profile (50.0 m res.)				Vertical Profile (50.0 m res.)	
η(m)	ρ_s(m)	θ_s(°)	χ^n_z	z(m)	χ^n_η
1625	2447	337.2	.2	-17	6.5
1675	2402	336.7	1.0	33	31.1
1725	2358	336.1	2.3	83	37.4
1775	2313	335.6	3.7	133	42.1
1825	2269	335.0	4.5	183	43.0
1875	2225	334.4	5.2	233	44.0
1925	2181	333.8	5.4	283	47.4
1975	2138	333.1	6.3	333	51.5
2025	2095	332.4	7.8	383	57.6
2075	2052	331.7	9.4	433	57.1
2125	2009	331.0	10.4	483	60.5
2175	1967	330.2	14.1	533	67.1
2225	1925	329.4	17.4	583	66.2
2275	1884	328.5	19.5	633	58.2
2325	1843	327.7	22.1	683	54.2
2375	1803	326.7	25.6	733	51.1
2425	1763	325.8	26.5	783	41.6
2475	1723	324.8	27.7	833	35.9
2525	1684	323.7	29.4	883	36.8
2575	1646	322.6	28.9	933	33.3
2625	1608	321.4	27.2	983	26.9
2675	1571	320.2	26.9	1033	21.7
2725	1535	319.0	27.3	1083	15.3
2775	1499	317.6	33.1	1133	9.4
2825	1465	316.2	39.2	1183	3.6
2875	1431	314.8	41.1	1233	.4
2925	1398	313.2	39.7	1283	.0
2975	1367	311.6	40.2	1333	.0
3025	1336	310.0	42.5	1383	.0
3075	1307	308.2	43.6	1433	.0
3125	1279	306.4	46.0		
3175	1252	304.5	44.0		
3225	1227	302.5	39.2		
3275	1203	300.4	33.2		
3325	1181	298.2	31.5		
3375	1161	296.0	28.4		
3425	1142	293.7	27.6		
3475	1125	291.3	24.8		
3525	1111	288.8	21.6		
3575	1098	286.3	18.4		
3625	1088	283.8	18.0		
3675	1080	281.2	15.8		
3725	1074	278.5	10.4		
3775	1070	275.9	6.0		
3825	1069	273.2	4.1		
3875	1070	270.5	2.1		
3925	1074	267.8	.5		
3975	1080	265.2	.0		
4025	1088	262.6	.0		
4075	1098	260.0	.0		

Table A.1 (4-83/177.4° to 183.1°)

Period 4-83, θ_L =195.0° (normal)

CONDORS .'83 AVERAGED OIL FOG PROFILES — Period # 4
Release Rate: 44.5 g/s — Azimuth 195.0
Release Height: Surface

Horizontal Profile (50.0 m res.)				Vertical Profile (50.0 m res.)	
η(m)	ρ_s(m)	θ_s(°)	χ^n_z	z(m)	χ^n_η
1025	3100	338.7	.0	-17	16.0
1075	3060	338.2	.2	33	39.5
1125	3020	337.6	.5	83	43.2
1175	2981	337.0	1.1	133	43.9
1225	2941	336.4	1.5	183	48.4
1275	2902	335.8	1.6	233	51.3
1325	2864	335.2	1.4	283	53.7
1375	2826	334.5	2.3	333	54.4
1425	2788	333.8	3.4	383	60.3
1475	2750	333.2	4.6	433	60.8
1525	2713	332.4	6.5	483	59.3
1575	2677	331.7	8.9	533	60.2
1625	2641	331.0	11.3	583	59.9
1675	2605	330.2	12.4	633	57.1
1725	2570	329.4	16.2	683	53.8
1775	2535	328.6	20.0	733	46.1
1825	2501	327.8	22.2	783	42.3
1875	2467	326.9	24.2	833	35.6
1925	2434	326.1	25.3	883	28.8
1975	2401	325.2	27.3	933	24.7
2025	2369	324.2	29.4	983	19.8
2075	2338	323.3	31.7	1033	14.9
2125	2308	322.3	35.5	1083	11.1
2175	2278	321.3	37.3	1133	7.2
2225	2248	320.3	37.4	1183	4.0
2275	2220	319.2	37.1	1233	2.6
2325	2192	318.2	38.9	1283	1.0
2375	2165	317.0	39.9	1333	.6
2425	2139	315.9	39.5	1383	-.4
2475	2114	314.7	42.5	1433	-.2
2525	2090	313.6	43.7		
2575	2066	312.3	40.2		
2625	2044	311.1	35.5		
2675	2022	309.8	34.1		
2725	2002	308.5	34.0		
2775	1982	307.2	37.2		
2825	1964	305.8	37.0		
2875	1947	304.5	33.5		
2925	1931	303.1	29.6		
2975	1916	301.7	25.6		
3025	1902	300.2	19.3		
3075	1890	298.7	14.2		
3125	1878	297.3	8.9		
3175	1868	295.8	7.4		
3225	1860	294.2	7.7		
3275	1852	292.7	7.6		
3325	1846	291.2	6.7		
3375	1842	289.6	5.6		
3425	1838	288.1	3.5		
3475	1836	286.5	3.1		
3525	1836	285.0	2.9		
3575	1836	283.4	1.7		
3625	1838	281.8	.7		
3675	1842	280.3	.0		
3725	1847	278.7	.0		

Period 5-83, θ_L =169.9° (normal)

CONDORS .'83 AVERAGED OIL FOG PROFILES — Period # 5
Release Rate: 10.2 g/s — Azimuth 169.9
Release Height: 286.0 m

Horizontal Profile (50.0 m res.)				Vertical Profile (50.0 m res.)	
η(m)	ρ_s(m)	θ_s(°)	χ^n_z	z(m)	χ^n_η
2125	1931	341.5	.0	-17	.0
2175	1882	341.3	.0	33	14.6
2225	1833	341.1	.0	83	126.9
2275	1783	340.8	.0	133	90.2
2325	1734	340.6	-.0	183	183.2
2375	1684	340.3	-.0	233	121.4
2425	1635	340.0	.0	283	183.3
2475	1586	339.7	.0	333	83.5
2525	1537	339.4	.1	383	47.0
2575	1488	339.0	.5	433	50.3
2625	1439	338.6	.3	483	29.4
2675	1390	338.2	.4	533	15.7
2725	1341	337.8	.6	583	10.9
2775	1292	337.3	.5	633	11.8
2825	1243	336.8	-.1	683	7.3
2875	1194	336.3	.8	733	10.6
2925	1146	335.7	2.2	783	11.2
2975	1097	335.1	.4	833	2.5
3025	1049	334.4	.4	883	.0
3075	1001	333.6	.5	933	.0
3125	953	332.8	1.5		
3175	906	331.8	3.7		
3225	858	330.8	6.3		
3275	811	329.6	9.4		
3325	764	328.3	10.0		
3375	718	326.9	7.7		
3425	672	325.2	10.9		
3475	627	323.3	19.3		
3525	583	321.1	40.3		
3575	540	318.5	59.8		
3625	498	315.6	56.1		
3675	457	312.0	62.8		
3725	419	307.8	66.0		
3775	383	302.8	77.0		
3825	351	296.8	116.2		
3875	323	289.7	84.4		
3925	302	281.5	99.1		
3975	287	272.1	92.6		
4025	281	262.1	65.4		
4075	283	252.0	91.7		
4125	294	242.3	10.9		
4175	313	233.5	2.1		
4225	338	225.9	.0		
4275	369	219.5	.0		
4325	403	214.0	.0		

Table A.1 (4-83/195° to 5-83/169.9°)

Period 5-83, θ_L =174.0° (normal)

CONDORS '83 AVERAGED OIL FOG PROFILES — Period # 5
Release Rate: 10.2 g/s — Azimuth 174.0
Release Height: 286.0 m

Horizontal Profile (50.0 m res.)				Vertical Profile (50.0 m res.)	
η(m)	ρ_s(m)	θ_s(°)	χ^n_z	z(m)	χ^n_η
2125	1965	337.1	.0	-17	.0
2175	1917	336.7	.0	33	104.2
2225	1869	336.2	.4	83	118.0
2275	1822	335.8	.8	133	121.9
2325	1775	335.3	1.0	183	102.9
2375	1727	334.7	1.6	233	111.2
2425	1680	334.2	1.8	283	59.9
2475	1633	333.6	3.2	333	55.0
2525	1586	332.9	6.3	383	45.0
2575	1540	332.3	4.5	433	40.4
2625	1494	331.5	5.0	483	40.1
2675	1447	330.8	7.8	533	32.6
2725	1402	330.0	8.5	583	29.6
2775	1356	329.1	9.4	633	30.0
2825	1311	328.2	10.2	683	26.1
2875	1266	327.2	12.3	733	24.2
2925	1222	326.2	11.7	783	15.9
2975	1178	325.0	8.7	833	10.4
3025	1134	323.8	10.3	883	2.5
3075	1091	322.5	17.3	933	-.0
3125	1049	321.1	21.7	983	.0
3175	1007	319.5	24.1	1033	.0
3225	967	317.8	30.4	1083	.0
3275	927	316.0	28.0	1133	.0
3325	888	314.0	39.7	1183	.0
3375	850	311.9	53.5		
3425	814	309.5	59.3		
3475	779	306.9	46.8		
3525	746	304.1	63.4		
3575	715	301.0	60.8		
3625	686	297.7	41.9		
3675	659	294.1	32.7		
3725	636	290.2	52.6		
3775	615	286.0	66.6		
3825	598	281.5	129.8		
3875	585	276.9	89.5		
3925	576	272.0	26.4		
3975	571	267.0	8.5		
4025	571	262.0	2.4		
4075	575	257.0	.6		
4125	583	252.2	.2		
4175	595	247.4	.0		
4225	611	242.9	.0		
4275	631	238.7	.0		
4325	654	234.7	.0		

Period 5-83, θ_L =178.9° (normal)

CONDORS '83 AVERAGED OIL FOG PROFILES — Period # 5
Release Rate: 10.2 g/s — Azimuth 178.9
Release Height: 286.0 m

Horizontal Profile (50.0 m res.)				Vertical Profile (50.0 m res.)	
η(m)	ρ_s(m)	θ_s(°)	χ^n_z	z(m)	χ^n_η
1875	2259	335.1	.0	-17	6.0
1925	2213	334.6	.1	33	119.7
1975	2168	334.1	.2	83	145.0
2025	2122	333.5	.6	133	123.1
2075	2077	332.9	.7	183	99.7
2125	2033	332.3	.8	233	96.6
2175	1988	331.6	1.0	283	72.3
2225	1944	331.0	1.1	333	56.8
2275	1900	330.2	.6	383	59.0
2325	1856	329.5	.2	433	56.8
2375	1813	328.7	.1	483	33.3
2425	1770	327.9	1.6	533	24.9
2475	1727	327.1	5.5	583	18.8
2525	1685	326.2	7.3	633	22.4
2575	1643	325.2	7.9	683	18.8
2625	1601	324.2	9.1	733	18.1
2675	1561	323.2	9.9	783	15.0
2725	1520	322.1	10.9	833	9.4
2775	1481	320.9	11.6	883	4.3
2825	1442	319.7	17.0	933	-.0
2875	1403	318.4	22.2	983	-.0
2925	1366	317.0	16.9	1033	.0
2975	1329	315.6	17.5	1083	.0
3025	1293	314.1	20.9	1133	.0
3075	1258	312.5	24.3	1183	.0
3125	1224	310.8	30.7		
3175	1191	309.0	30.4		
3225	1160	307.1	30.4		
3275	1129	305.1	36.4		
3325	1101	303.0	42.5		
3375	1073	300.8	41.9		
3425	1048	298.5	52.4		
3475	1024	296.0	59.0		
3525	1002	293.5	60.1		
3575	983	290.8	65.7		
3625	965	288.1	63.0		
3675	950	285.2	57.8		
3725	937	282.3	42.8		
3775	927	279.3	34.9		
3825	919	276.2	34.8		
3875	914	273.1	38.2		
3925	912	270.0	31.9		
3975	912	266.8	25.9		
4025	915	263.7	16.3		
4075	921	260.6	9.0		
4125	930	257.6	5.6		
4175	941	254.6	2.0		
4225	955	251.7	.8		
4275	971	248.8	-.0		
4325	989	246.1	-.3		
4375	1009	243.5	-.1		
4425	1032	241.0	-.0		
4475	1056	238.6	.0		
4525	1082	236.3	.0		
4575	1110	234.1	.0		

Table A.1 (5-83/174° to 178.9°)

Period 5-83, θ_L =183.1° (normal)

CONDORS '83 AVERAGED OIL FOG PROFILES — Period # 5
Release Rate: 10.2 g/s — Azimuth 183.1
Release Height: 286.0 m

Horizontal Profile (50.0 m res.)				Vertical Profile (50.0 m res.)	
η(m)	ρ_s(m)	θ_s(°)	χ^n_z	z(m)	χ^n_η
1875	2322	332.1	.0	-17	4.6
1925	2279	331.4	.1	33	100.4
1975	2237	330.8	.4	83	118.5
2025	2195	330.1	.3	133	103.0
2075	2153	329.3	.2	183	101.8
2125	2112	328.6	.2	233	88.7
2175	2071	327.8	.2	283	74.5
2225	2030	327.0	-.2	333	62.1
2275	1990	326.1	-.2	383	47.5
2325	1950	325.2	.3	433	38.8
2375	1911	324.3	1.0	483	37.8
2425	1872	323.4	2.3	533	33.8
2475	1834	322.4	2.7	583	32.5
2525	1796	321.3	5.0	633	28.9
2575	1759	320.2	6.1	683	29.6
2625	1723	319.1	7.6	733	31.1
2675	1688	317.9	11.4	783	24.9
2725	1653	316.7	12.3	833	18.5
2775	1619	315.4	14.8	883	14.1
2825	1585	314.1	12.1	933	6.9
2875	1553	312.7	10.1	983	1.9
2925	1522	311.2	16.0	1033	.0
2975	1491	309.7	23.3	1083	.0
3025	1462	308.2	31.5	1133	.0
3075	1434	306.5	41.0	1183	.0
3125	1407	304.8	39.7		
3175	1381	303.1	40.8		
3225	1357	301.2	42.0		
3275	1334	299.3	42.4		
3325	1313	297.4	46.9		
3375	1293	295.4	55.7		
3425	1275	293.3	56.8		
3475	1259	291.1	48.3		
3525	1244	288.9	39.4		
3575	1231	286.7	37.7		
3625	1221	284.4	42.5		
3675	1212	282.1	43.4		
3725	1205	279.8	41.2		
3775	1200	277.4	40.5		
3825	1198	275.0	41.1		
3875	1197	272.6	41.0		
3925	1198	270.2	38.2		
3975	1202	267.8	25.4		
4025	1208	265.5	13.4		
4075	1215	263.1	7.5		
4125	1225	260.8	7.1		
4175	1237	258.6	3.6		
4225	1250	256.4	1.8		
4275	1265	254.2	1.3		
4325	1282	252.1	1.3		
4375	1301	250.0	1.5		
4425	1322	248.0	.7		
4475	1344	246.1	.1		
4525	1367	244.2	.0		
4575	1392	242.4	.0		

Period 5-83, θ_L =188.0° (normal)

CONDORS '83 AVERAGED OIL FOG PROFILES — Period # 5
Release Rate: 10.2 g/s — Azimuth 188.0
Release Height: 286.0 m

Horizontal Profile (50.0 m res.)				Vertical Profile (50.0 m res.)	
η(m)	ρ_s(m)	θ_s(°)	χ^n_z	z(m)	χ^n_η
1775	2493	330.3	.0	-17	14.2
1825	2454	329.6	.1	33	148.5
1875	2415	328.9	.9	83	124.1
1925	2376	328.1	1.3	133	108.5
1975	2338	327.3	1.4	183	101.7
2025	2301	326.5	1.8	233	88.3
2075	2263	325.7	1.4	283	69.0
2125	2227	324.8	1.1	333	49.4
2175	2191	323.9	.6	383	43.3
2225	2155	323.0	1.2	433	43.3
2275	2120	322.0	2.0	483	27.4
2325	2086	321.0	3.2	533	20.7
2375	2052	320.0	5.1	583	18.6
2425	2019	319.0	3.6	633	19.2
2475	1986	317.9	2.9	683	22.9
2525	1955	316.7	3.9	733	30.0
2575	1924	315.6	6.9	783	29.7
2625	1894	314.4	9.1	833	24.1
2675	1865	313.1	7.5	883	11.7
2725	1836	311.9	6.2	933	6.4
2775	1809	310.6	7.5	983	-1.0
2825	1783	309.2	11.3	1033	.0
2875	1757	307.8	14.5	1083	.0
2925	1733	306.4	14.5	1133	.0
2975	1710	304.9	21.0	1183	.0
3025	1688	303.4	26.1		
3075	1667	301.8	36.2		
3125	1648	300.2	37.6		
3175	1629	298.6	48.5		
3225	1612	296.9	45.9		
3275	1597	295.2	48.1		
3325	1583	293.5	51.0		
3375	1570	291.8	43.3		
3425	1559	290.0	41.2		
3475	1550	288.2	44.8		
3525	1542	286.3	41.9		
3575	1535	284.5	29.8		
3625	1531	282.6	38.0		
3675	1527	280.8	40.9		
3725	1526	278.9	43.9		
3775	1526	277.0	42.8		
3825	1528	275.1	40.3		
3875	1531	273.3	35.4		
3925	1536	271.4	37.7		
3975	1543	269.6	25.6		
4025	1551	267.7	17.6		
4075	1561	265.9	10.9		
4125	1572	264.1	8.0		
4175	1585	262.4	4.2		
4225	1599	260.7	3.0		
4275	1614	259.0	2.6		
4325	1631	257.3	1.5		
4375	1650	255.7	1.0		
4425	1670	254.1	1.2		
4475	1690	252.5	1.3		
4525	1713	251.0	2.2		
4575	1736	249.6	3.4		
4625	1760	248.1	2.6		
4675	1786	246.7	2.5		
4725	1812	245.4	2.2		
4775	1840	244.1	1.9		
4825	1868	242.8	1.0		
4875	1897	241.6	2.0		
4925	1928	240.4	2.1		
4975	1958	239.2	.8		
5025	1990	238.1	.0		
5075	2023	237.0	.0		

Table A.1 (5-83/183.1° to 188.1°)

Period 6-83, θ_L =169.9° (normal)

CONDORS '83 AVERAGED OIL FOG PROFILES — Period # 6
Release Rate: 9.3 g/s — Azimuth 169.9
Release Height: 286.0 m

Horizontal Profile (50.0 m res.)				Vertical Profile (50.0 m res.)	
η(m)	ρ_s(m)	θ_s(°)	χ^n_z	z(m)	χ^n_η
2225	1833	341.1	.0	-17	.5
2275	1783	340.8	.0	33	39.1
2325	1734	340.6	-.0	83	170.1
2375	1684	340.3	1.7	133	309.5
2425	1635	340.0	2.4	183	165.5
2475	1586	339.7	.8	233	88.6
2525	1537	339.4	.0	283	74.7
2575	1488	339.0	.4	333	54.4
2625	1439	338.6	.6	383	19.2
2675	1390	338.2	.6	433	3.4
2725	1341	337.8	4.3	483	4.0
2775	1292	337.3	11.3	533	14.6
2825	1243	336.8	11.5	583	10.1
2875	1194	336.3	11.8	633	11.9
2925	1146	335.7	22.5	683	11.1
2975	1097	335.1	20.9	733	2.8
3025	1049	334.4	17.0	783	3.4
3075	1001	333.6	8.9	833	8.2
3125	953	332.8	13.8	883	8.4
3175	905	331.8	17.7	933	.5
3225	858	330.8	20.5		
3275	811	329.6	68.2		
3325	764	328.3	86.7		
3375	718	326.9	52.1		
3425	672	325.2	31.1		
3475	627	323.3	44.3		
3525	583	321.1	44.5		
3575	540	318.6	32.4		
3625	498	315.6	35.7		
3675	457	312.0	77.4		
3725	419	307.8	122.8		
3775	383	302.8	66.8		
3825	351	296.8	85.9		
3875	323	289.7	40.2		
3925	302	281.5	18.7		
3975	287	272.1	11.8		
4025	281	262.1	13.7		
4075	283	252.0	.7		
4125	294	242.3	.0		
4175	313	233.5	.0		

Period 6-83, θ_L =174.0° (normal)

CONDORS '83 AVERAGED OIL FOG PROFILES — Period # 6
Release Rate: 9.3 g/s — Azimuth 174.0
Release Height: 286.0 m

Horizontal Profile (50.0 m res.)				Vertical Profile (50.0 m res.)	
η(m)	ρ_s(m)	θ_s(°)	χ^n_z	z(m)	χ^n_η
1225	2838	342.4	.0	-17	1.0
1275	2789	342.2	.2	33	150.3
1325	2740	342.0	.4	83	147.1
1375	2691	341.8	.5	133	122.8
1425	2643	341.5	1.0	183	102.3
1475	2594	341.3	1.1	233	93.0
1525	2545	341.1	1.7	283	87.0
1575	2496	340.8	2.0	333	68.8
1625	2448	340.5	2.3	383	45.9
1675	2399	340.2	2.7	433	32.7
1725	2351	340.0	2.7	483	30.4
1775	2302	339.7	2.0	533	19.8
1825	2254	339.3	1.8	583	22.1
1875	2209	339.0	1.4	633	18.3
1925	2157	338.7	1.1	683	13.1
1975	2109	338.3	1.5	733	13.1
2025	2061	337.9	2.5	783	13.2
2075	2013	337.5	1.8	833	10.4
2125	1965	337.1	3.2	883	4.7
2175	1917	336.7	3.0	933	4.2
2225	1869	336.2	2.2	983	.1
2275	1822	335.8	2.7	1033	-.1
2325	1775	335.2	3.7	1083	.0
2375	1727	334.7	5.1	1133	.0
2425	1680	334.2	3.8	1183	.0
2475	1633	333.6	3.6		
2525	1586	332.9	6.7		
2575	1540	332.3	22.4		
2625	1494	331.5	21.9		
2675	1448	330.8	21.2		
2725	1402	330.0	20.4		
2775	1356	329.1	19.3		
2825	1311	328.2	18.4		
2875	1266	327.2	21.9		
2925	1222	326.2	30.1		
2975	1178	325.0	27.6		
3025	1134	323.8	23.6		
3075	1091	322.5	30.6		
3125	1049	321.1	34.0		
3175	1007	319.5	31.4		
3225	967	317.8	30.8		
3275	927	316.0	42.0		
3325	888	314.0	47.4		
3375	850	311.8	76.2		
3425	814	309.5	66.4		
3475	779	306.9	52.5		
3525	746	304.1	50.9		
3575	715	301.0	51.0		
3625	686	297.7	48.4		
3675	659	294.1	44.6		
3725	636	290.2	38.4		
3775	615	286.0	33.9		
3825	599	281.5	17.0		
3875	585	276.9	8.7		
3925	576	272.0	5.7		
3975	572	267.0	1.8		
4025	571	262.0	.6		
4075	575	257.0	.1		
4125	583	252.2	.0		
4175	595	247.4	-.0		

Table A.1 (6-83/169.9° to 174°)

Period 6-83, θ_L =178.9° (normal)

CONDORS '83 AVERAGED OIL FOG PROFILES — Period # 6
Release Rate: 9.3 g/s — Azimuth 178.9
Release Height: 286.0 m

Horizontal Profile (50.0 m res.)				Vertical Profile (50.0 m res.)	
η(m)	ρ_s(m)	θ_s(°)	χ^n_z	z(m)	χ^n_η
1125	2960	341.0	.0	-17	11.3
1175	2913	340.7	.0	33	106.7
1225	2865	340.4	.1	83	108.6
1275	2818	340.1	.2	133	105.1
1325	2771	339.7	.7	183	89.7
1375	2724	339.4	1.0	233	70.0
1425	2676	339.0	1.2	283	61.8
1475	2630	338.7	1.4	333	65.5
1525	2583	338.3	2.3	383	77.1
1575	2536	337.9	2.5	433	77.2
1625	2489	337.5	2.8	483	87.4
1675	2443	337.0	2.7	533	42.5
1725	2397	336.6	1.9	583	29.9
1775	2350	336.1	1.6	633	28.3
1825	2304	335.6	1.8	683	18.3
1875	2259	335.1	2.6	733	11.5
1925	2213	334.6	3.2	783	5.7
1975	2167	334.1	7.3	833	2.1
2025	2122	333.5	8.9	883	1.2
2075	2077	332.9	8.9	933	.2
2125	2032	332.3	11.0	983	-.0
2175	1988	331.6	13.2	1033	.0
2225	1943	331.0	12.9	1083	.0
2275	1899	330.3	11.6	1133	.0
2325	1856	329.5	10.5	1183	.0
2375	1812	328.8	8.3		
2425	1769	327.9	11.2		
2475	1726	327.1	28.1		
2525	1684	326.2	38.6		
2575	1642	325.2	35.2		
2625	1601	324.3	35.8		
2675	1560	323.2	37.1		
2725	1520	322.1	32.4		
2775	1480	321.0	38.6		
2825	1441	319.7	46.4		
2875	1402	318.4	37.0		
2925	1365	317.1	33.6		
2975	1328	315.6	30.8		
3025	1292	314.1	32.8		
3075	1257	312.5	29.6		
3125	1223	310.8	21.7		
3175	1190	309.0	18.1		
3225	1159	307.1	17.2		
3275	1128	305.1	25.5		
3325	1100	303.0	36.7		
3375	1072	300.8	39.7		
3425	1047	298.5	30.2		
3475	1023	296.1	43.6		
3525	1001	293.5	41.2		
3575	981	290.9	35.7		
3625	964	288.1	32.5		
3675	948	285.3	28.8		
3725	936	282.3	20.3		
3775	925	279.3	15.2		
3825	918	276.2	5.6		
3875	913	273.1	2.4		
3925	910	270.0	.2		
3975	911	266.8	.0		
4025	914	263.7	.0		
4075	920	260.6	.0		

Period 6-83, θ_L =183.1° (normal)

CONDORS '83 AVERAGED OIL FOG PROFILES — Period # 6
Release Rate: 9.3 g/s — Azimuth 183.1
Release Height: 286.0 m

Horizontal Profile (50.0 m res.)				Vertical Profile (50.0 m res.)	
η(m)	ρ_s(m)	θ_s(°)	χ^n_z	z(m)	χ^n_η
1125	2990	339.5	.0	-17	15.5
1175	2944	339.1	.2	33	96.4
1225	2899	338.7	.3	83	109.3
1275	2853	338.3	.3	133	116.5
1325	2808	337.8	.5	183	111.4
1375	2763	337.4	.9	233	101.2
1425	2718	336.9	1.3	283	92.3
1475	2673	336.5	1.6	333	87.5
1525	2629	336.0	2.4	383	74.8
1575	2584	335.5	3.6	433	59.9
1625	2540	335.0	4.4	483	42.3
1675	2496	334.4	4.5	533	30.0
1725	2452	333.8	7.2	583	21.0
1775	2409	333.3	12.1	633	14.2
1825	2366	332.7	12.7	683	12.5
1875	2323	332.0	13.0	733	8.0
1925	2280	331.4	15.3	783	3.5
1975	2238	330.7	19.3	833	2.2
2025	2196	330.0	21.6	883	1.4
2075	2154	329.3	25.3	933	.3
2125	2113	328.5	27.5	983	.0
2175	2072	327.7	22.6	1033	.0
2225	2031	326.9	19.4	1083	.0
2275	1991	326.1	18.5	1133	.0
2325	1952	325.2	23.0	1183	.0
2375	1912	324.3	25.5		
2425	1874	323.3	25.3		
2475	1836	322.3	25.1		
2525	1798	321.3	25.4		
2575	1761	320.2	20.8		
2625	1725	319.0	17.6		
2675	1689	317.9	16.1		
2725	1655	316.6	18.3		
2775	1621	315.4	18.4		
2825	1588	314.0	19.4		
2875	1555	312.6	20.7		
2925	1524	311.2	22.7		
2975	1494	309.7	27.3		
3025	1465	308.1	29.3		
3075	1436	306.5	32.7		
3125	1410	304.8	34.1		
3175	1384	303.0	35.1		
3225	1360	301.2	38.0		
3275	1337	299.3	35.5		
3325	1316	297.3	37.7		
3375	1296	295.3	34.1		
3425	1278	293.2	36.4		
3475	1262	291.1	32.8		
3525	1248	288.9	30.5		
3575	1235	286.7	19.7		
3625	1224	284.4	13.6		
3675	1216	282.1	13.6		
3725	1209	279.7	11.3		
3775	1204	277.4	9.7		
3825	1201	275.0	5.7		
3875	1201	272.6	4.3		
3925	1202	270.2	4.3		
3975	1206	267.9	1.1		
4025	1212	265.5	.0		
4075	1219	263.2	.0		

TAble A.1 (6-83/178.9° to 183.1°)

Period 6-83, θ_L =188.0° (normal)

CONDORS.'83 AVERAGED OIL FOG PROFILES — Period # 6
Release Rate: 9.3 g/s — Azimuth 188.0
Release Height: 286.0 m

Horizontal Profile (50.0 m res.)				Vertical Profile (50.0 m res.)	
η(m)	ρ_s(m)	θ_s(°)	χ^n_z	z(m)	χ^n_η
1325	2862	335.9	.0	-17	14.5
1375	2820	335.3	.1	33	60.0
1425	2778	334.8	.6	83	86.5
1475	2736	334.2	1.3	133	82.6
1525	2695	333.6	2.5	183	74.8
1575	2654	333.0	5.6	233	83.9
1625	2613	332.4	8.7	283	87.4
1675	2573	331.7	10.2	333	89.2
1725	2532	331.0	11.6	383	82.2
1775	2493	330.3	13.2	433	74.2
1825	2453	329.6	17.3	483	66.5
1875	2414	328.9	18.8	533	53.0
1925	2376	328.1	19.7	583	41.5
1975	2338	327.3	25.2	633	31.0
2025	2300	326.5	30.6	683	22.7
2075	2263	325.7	25.1	733	21.8
2125	2226	324.8	23.0	783	15.1
2175	2190	323.9	26.7	833	10.2
2225	2154	323.0	31.4	883	2.9
2275	2119	322.1	33.1	933	-.0
2325	2085	321.1	35.8	983	.0
2375	2051	320.0	41.0	1033	.0
2425	2018	319.0	48.5	1083	.0
2475	1985	317.9	46.8	1133	.0
2525	1954	316.8	39.0	1183	.0
2575	1923	315.6	31.1		
2625	1893	314.4	26.0		
2675	1863	313.2	25.9		
2725	1833	311.9	25.2		
2775	1808	310.6	23.1		
2825	1781	309.2	23.0		
2875	1756	307.8	20.9		
2925	1732	306.6	28.3		
2975	1708	304.9	32.1		
3025	1686	303.4	32.2		
3075	1666	301.9	37.3		
3125	1646	300.3	34.7		
3175	1628	298.6	29.2		
3225	1611	297.0	24.8		
3275	1595	295.3	19.5		
3325	1581	293.5	16.3		
3375	1568	291.8	16.2		
3425	1557	290.0	14.5		
3475	1548	288.2	11.8		
3525	1540	286.3	7.4		
3575	1533	284.5	4.3		
3625	1528	282.6	.4		
3675	1525	280.8	.0		
3725	1524	278.9	.0		
3775	1524	277.0	.0		

Period 7-83, θ_L =169.9° (fine)

CONDORS.'83 AVERAGED OIL FOG PROFILES — Period # 7
Release Rate: 9.3 g/s — Azimuth 169.9
Release Height: 286.0 m

Horizontal Profile (50.0 m res.)				Vertical Profile (25.0 m res.)	
η(m)	ρ_s(m)	θ_s(°)	χ^n_z	z(m)	χ^n_η
2775	1292	337.3	.0	-30	.0
2825	1243	336.8	.0	-5	.2
2875	1195	336.2	-.0	20	21.9
2925	1146	335.6	1.4	45	50.5
2975	1098	335.0	4.1	70	50.6
3025	1050	334.3	4.7	95	66.1
3075	1002	333.5	14.1	120	77.0
3125	954	332.7	27.6	145	83.2
3175	906	331.7	16.5	170	114.8
3225	859	330.7	6.2	195	150.1
3275	812	329.5	6.2	220	202.3
3325	765	328.2	10.3	245	171.2
3375	719	326.7	19.3	270	199.5
3425	673	325.1	25.9	295	174.6
3475	628	323.2	36.1	320	144.7
3525	584	320.9	66.4	345	117.4
3575	541	318.4	85.6	370	173.0
3625	499	315.4	120.6	395	96.7
3675	458	311.8	96.5	420	31.0
3725	420	307.6	115.9	445	10.7
3775	385	302.6	134.4	470	12.5
3825	353	296.6	85.1	495	29.1
3875	325	289.5	84.6	520	10.8
3925	304	281.3	28.4	545	9.8
3975	289	272.0	3.5	570	2.1
4025	283	262.1	2.3	595	.0
4075	285	252.0	1.8	620	.0
4125	296	242.4	1.7	645	.0
4175	315	233.7	.5	670	.0
4225	340	226.1	.4	695	.0
4275	370	219.7	-.2		
4325	404	214.3	-.0		
4375	442	209.7	.0		
4425	481	205.9	.0		
4475	522	202.7	.0		

Table A.1 (6-83/188° to 7-83/169.9°/fine)

Period 7-83, θ_L =169.9° (normal)

CONDORS '83 AVERAGED OIL FOG PROFILES — Period # 7
Release Rate: 9.3 g/s — Azimuth 169.9
Release Height: 286.0 m

Horizontal Profile (50.0 m res.)				Vertical Profile (50.0 m res.)	
η(m)	ρ_s(m)	θ_s(°)	χ^n_z	z(m)	χ^n_η
2775	1292	337.3	.0	-17	.1
2825	1243	336.8	.0	33	36.2
2875	1195	336.2	-.0	83	58.4
2925	1146	335.6	1.4	133	80.1
2975	1098	335.0	4.1	183	132.4
3025	1050	334.3	4.7	233	186.7
3075	1002	333.5	14.1	283	187.1
3125	954	332.7	27.6	333	131.1
3175	906	331.7	16.5	383	134.9
3225	859	330.7	6.2	433	20.8
3275	812	329.5	6.2	483	20.8
3325	765	328.2	10.3	533	10.3
3375	719	326.7	19.3	583	1.1
3425	673	325.1	25.9	633	.0
3475	628	323.2	36.1	683	.0
3525	584	320.9	66.3		
3575	541	318.4	85.6		
3625	499	315.4	120.6		
3675	458	311.8	96.5		
3725	420	307.6	116.0		
3775	385	302.6	134.4		
3825	353	296.6	89.1		
3875	325	289.5	84.6		
3925	304	281.3	28.4		
3975	289	272.0	3.5		
4025	283	262.1	2.3		
4075	285	252.0	1.8		
4125	296	242.4	1.7		
4175	315	233.7	.5		
4225	340	226.1	.4		
4275	370	219.7	-.2		
4325	404	214.3	-.0		
4375	442	209.7	.0		
4425	481	205.9	.0		
4475	522	202.7	.0		

Period 7-83, θ_L =174.0° (normal)

CONDORS '83 AVERAGED OIL FOG PROFILES — Period # 7
Release Rate: 9.3 g/s — Azimuth 174.0
Release Height: 286.0 m

Horizontal Profile (50.0 m res.)				Vertical Profile (50.0 m res.)	
η(m)	ρ_s(m)	θ_s(°)	χ^n_z	z(m)	χ^n_η
2325	1774	335.3	.0	-17	.7
2375	1727	334.7	.5	33	132.6
2425	1680	334.2	.8	83	143.6
2475	1633	333.6	1.1	133	108.9
2525	1586	332.9	.8	183	102.5
2575	1540	332.3	1.0	233	96.7
2625	1493	331.6	2.2	283	131.4
2675	1447	330.8	3.2	333	103.3
2725	1402	330.0	3.8	383	59.7
2775	1356	329.1	7.5	433	45.9
2825	1311	328.2	14.1	483	29.2
2875	1266	327.2	32.6	533	12.9
2925	1222	326.2	31.2	583	14.0
2975	1178	325.0	31.4	633	6.5
3025	1134	323.8	29.8	683	4.1
3075	1091	322.5	42.9	733	7.3
3125	1049	321.1	60.3	783	.5
3175	1007	319.5	47.9	833	.0
3225	967	317.8	40.0	883	.0
3275	927	316.0	25.8	933	.0
3325	888	314.0	24.3		
3375	850	311.9	22.5		
3425	814	309.5	32.8		
3475	779	306.9	41.3		
3525	746	304.1	78.7		
3575	714	301.0	84.2		
3625	685	297.7	63.7		
3675	659	294.1	59.0		
3725	635	290.2	53.7		
3775	615	286.0	52.3		
3825	598	281.5	43.9		
3875	585	276.9	37.7		
3925	576	272.0	21.9		
3975	571	267.0	6.9		
4025	571	262.0	.2		

Period 7-83, θ_L =178.9° (normal)

CONDORS '83 AVERAGED OIL FOG PROFILES — Period # 7
Release Rate: 9.3 g/s — Azimuth 178.9
Release Height: 286.0 m

Horizontal Profile (50.0 m res.)				Vertical Profile (50.0 m res.)	
η(m)	ρ_s(m)	θ_s(°)	χ^n_z	z(m)	χ^n_η
2125	2032	332.3	.0	-17	2.2
2175	1988	331.6	.3	33	138.1
2225	1943	331.0	.9	83	104.5
2275	1899	330.3	.6	133	92.6
2325	1856	329.5	1.3	183	105.6
2375	1812	328.8	1.3	233	76.2
2425	1769	327.9	1.7	283	86.2
2475	1726	327.1	3.0	333	79.2
2525	1684	326.2	3.3	383	51.1
2575	1642	325.2	5.7	433	48.3
2625	1601	324.3	10.3	483	45.7
2675	1560	323.2	18.0	533	54.4
2725	1520	322.1	31.3	583	41.6
2775	1480	321.0	34.3	633	38.0
2825	1441	319.7	36.6	683	16.6
2875	1402	318.4	42.8	733	11.2
2925	1365	317.1	61.7	783	5.9
2975	1328	315.6	54.0	833	2.3
3025	1292	314.1	57.1	883	.4
3075	1257	312.5	47.1	933	.0

η(m)	ρ_s(m)	θ_s(°)	χ^n_z	z(m)	χ^n_η
3125	1223	310.8	44.1		
3175	1190	309.0	41.1		
3225	1159	307.1	37.4		
3275	1128	305.1	38.5		
3325	1100	303.0	37.0		
3375	1072	300.8	31.3		
3425	1047	298.5	32.6		
3475	1023	296.1	34.2		
3525	1001	293.5	39.7		
3575	981	290.9	56.0		
3625	964	288.1	66.1		
3675	948	285.3	43.5		
3725	936	282.3	24.9		
3775	925	279.3	21.6		
3825	918	276.2	17.2		
3875	913	273.1	10.2		
3925	910	270.0	9.4		
3975	911	266.8	3.2		
4025	914	263.7	.8		
4075	920	260.6	.0		

Table A.1 (7-83/169.9°/normal to 178.9°)

Period 7-83, θ_L =183.1° (normal)

CONDORS '83 AVERAGED OIL FOG PROFILES — Period # 7
Release Rate: 9.3 g/s — Azimuth 183.1
Release Height: 286.0 m

Horizontal Profile (50.0 m res.)				Vertical Profile (50.0 m res.)	
η(m)	ρ_s(m)	θ_s(°)	χ^n_z	z(m)	χ^n_η
2125	2112	328.6	.2	-17	11.9
2175	2071	327.8	1.7	33	152.0
2225	2030	327.0	6.4	83	189.6
2275	1990	326.1	6.6	133	171.5
2325	1950	325.2	4.8	183	136.4
2375	1911	324.3	6.7	233	102.9
2425	1872	323.4	9.5	283	83.1
2475	1834	322.4	9.8	333	45.3
2525	1797	321.3	14.8	383	41.9
2575	1760	320.2	18.6	433	32.3
2625	1723	319.1	24.5	483	19.3
2675	1688	317.9	31.6	533	6.6
2725	1653	316.7	34.8	583	3.0
2775	1619	315.4	27.1	633	3.7
2825	1586	314.1	25.9	683	.3
2875	1553	312.7	20.5	733	.0
2925	1522	311.2	23.6	783	.0
2975	1492	309.7	22.7	833	.0
3025	1462	308.1	17.8	883	.0
3075	1434	306.5	14.1	933	.0
3125	1407	304.8	21.3		
3175	1382	303.0	34.8		
3225	1357	301.2	37.2		
3275	1335	299.3	40.3		
3325	1313	297.4	33.4		
3375	1294	295.3	35.6		
3425	1275	293.3	31.9		
3475	1259	291.1	42.9		
3525	1245	288.9	67.9		
3575	1232	286.7	53.2		
3625	1221	284.4	42.5		
3675	1212	282.1	54.2		
3725	1205	279.8	61.5		
3775	1201	277.4	50.8		
3825	1198	275.0	39.2		
3875	1197	272.6	23.9		
3925	1199	270.2	6.8		
3975	1202	267.8	.8		
4025	1208	265.5	.1		
4075	1216	263.1	.0		

Period 7-83, θ_L =188.0° (normal)

CONDORS '83 AVERAGED OIL FOG PROFILES — Period # 7
Release Rate: 9.3 g/s — Azimuth 188.0
Release Height: 286.0 m

Horizontal Profile (50.0 m res.)				Vertical Profile (50.0 m res.)	
η(m)	ρ_s(m)	θ_s(°)	χ^n_z	z(m)	χ^n_η
1825	2453	329.6	.0	-17	25.7
1875	2414	328.9	.0	33	150.5
1925	2375	328.1	.0	83	159.8
1975	2337	327.4	.2	133	138.6
2025	2299	326.5	1.9	183	117.6
2075	2262	325.7	3.4	233	93.2
2125	2226	324.8	5.2	283	85.2
2175	2189	323.9	7.8	333	75.8
2225	2154	323.0	13.4	383	49.8
2275	2119	322.1	20.3	433	32.3
2325	2084	321.1	28.5	483	18.4
2375	2050	320.1	29.2	533	13.8
2425	2017	319.0	29.6	583	13.3
2475	1985	317.9	29.5	633	11.8
2525	1953	316.8	29.2	683	10.3
2575	1922	315.6	28.3	733	3.5
2625	1892	314.4	31.0	783	.2
2675	1863	313.2	37.4	833	.0
2725	1834	311.9	36.3	883	.0
2775	1807	310.6	34.0	933	.0
2825	1781	309.2	40.8		
2875	1755	307.8	37.3		
2925	1731	306.4	41.0		
2975	1708	304.9	31.1		
3025	1685	303.4	26.8		
3075	1665	301.9	28.6		
3125	1645	300.3	25.5		
3175	1627	298.6	26.6		
3225	1610	297.0	33.8		
3275	1594	295.3	22.9		
3325	1580	293.5	18.1		
3375	1567	291.8	18.7		
3425	1556	290.0	17.1		
3475	1547	288.2	23.3		
3525	1539	286.4	29.1		
3575	1532	284.5	29.2		
3625	1527	282.6	26.6		
3675	1524	280.8	26.8		
3725	1523	278.9	29.5		
3775	1523	277.0	34.6		
3825	1524	275.1	30.4		
3875	1528	273.2	22.1		
3925	1533	271.4	11.5		
3975	1539	269.5	3.4		
4025	1547	267.7	.0		

Table A.1 (7-83/183.1° to 188°)

Period 8-83, θ_L =168.4° (fine)

CONDORS '83 AVERAGED OIL FOG PROFILES — Period # 8
Release Rate: 23.5 g/s — Azimuth 168.4
Release Height: 266.1 m

Horizontal Profile (25.0 m res.)				Vertical Profile (12.5 m res.)	
η(m)	ρ_s(m)	θ_s(°)	χ^n_z	z(m)	χ^n_η
3813	289	310.9	.0	164	.0
3838	269	307.6	.0	176	.0
3863	251	303.9	.0	189	5.0
3888	234	299.6	.0	201	115.8
3913	218	294.7	20.5	214	235.6
3938	204	289.0	232.4	226	302.9
3963	193	282.6	344.3	239	200.4
3988	184	275.5	279.9	251	556.7
4013	178	267.7	344.0	264	363.5
4038	176	259.7	429.5	276	293.3
4063	177	251.6	134.8	289	456.5
4088	182	243.7	31.6	301	674.7
4113	190	236.4	35.2	314	372.5
4138	200	229.7	121.7	326	325.6
4163	213	223.8	23.5	339	95.5
4188	228	218.7	2.6	351	1.7
4213	245	214.2	.0	364	.0
4238	263	210.3	.0	376	.0
4263	282	206.9	.0	389	.0
4288	302	203.9	.0	401	.0

Period 8-83, θ_L =168.4° (normal)

CONDORS '83 AVERAGED OIL FOG PROFILES — Period # 8
Release Rate: 23.5 g/s — Azimuth 168.4
Release Height: 266.1 m

Horizontal Profile (50.0 m res.)				Vertical Profile (50.0 m res.)	
η(m)	ρ_s(m)	θ_s(°)	χ^n_z	z(m)	χ^n_η
3825	279	309.3	.0	183	30.2
3875	242	301.8	-.0	233	323.9
3925	211	291.9	126.4	283	447.0
3975	188	279.1	312.1	333	198.8
4025	176	263.7	386.8	383	.0
4075	179	247.6	83.2		
4125	195	233.0	78.4		
4175	221	221.1	13.1		
4225	254	212.1	.0		
4275	292	205.3	.0		

Period 8-83, θ_L =172.3° (fine)

CONDORS '83 AVERAGED OIL FOG PROFILES — Period # 8
Release Rate: 23.5 g/s — Azimuth 172.3
Release Height: 266.1 m

Horizontal Profile (25.0 m res.)				Vertical Profile (25.0 m res.)	
η(m)	ρ_s(m)	θ_s(°)	χ^n_z	z(m)	χ^n_η
3213	925	323.1	.0	-30	.0
3238	903	322.3	.0	-5	.0
3263	882	321.5	.0	20	.0
3288	861	320.7	.0	45	.0
3313	839	319.8	.2	70	.2
3338	818	318.8	.3	95	.6
3363	798	317.8	.3	120	6.8
3388	777	316.8	.2	145	37.4
3413	757	315.7	.2	170	68.9
3438	737	314.5	.2	195	98.6
3463	717	313.3	.2	220	136.2
3488	698	312.0	.3	245	189.8
3513	679	310.6	.3	270	113.2
3538	661	309.2	.4	295	239.1
3563	643	307.7	.4	320	243.7
3588	625	306.1	.3	345	64.4
3613	608	304.4	.6	370	89.6
3638	592	302.6	.4	395	267.7
3663	576	300.7	.6	420	263.5
3688	561	298.7	.8	445	112.9
3713	546	296.6	4.3	470	18.8
3738	533	294.3	28.4	495	25.8
3763	520	292.0	69.7	520	17.2
3788	508	289.5	129.5	545	4.1
3813	497	287.0	116.4	570	.4

η(m)	ρ_s(m)	θ_s(°)	χ^n_z	z(m)	χ^n_η
3838	487	284.3	146.5	595	.6
3863	478	281.5	141.2	620	.3
3888	471	278.7	91.9	645	.0
3913	464	275.7	288.8	670	.0
3938	459	272.7	214.2	695	.0
3963	455	269.6	265.1		
3988	453	266.4	186.2		
4013	452	263.3	66.6		
4038	452	260.1	34.8		
4063	454	256.9	40.1		
4088	457	253.8	43.4		
4113	461	250.7	23.6		
4138	467	247.7	26.7		
4163	474	244.8	22.8		
4188	482	242.0	28.5		
4213	491	239.2	17.2		
4238	501	236.6	6.5		
4263	513	234.1	1.7		
4288	525	231.7	.3		
4313	538	229.4	.0		
4338	552	227.2	.0		
4363	567	225.1	.0		
4388	582	223.2	.0		
4413	598	221.3	.0		
4438	615	219.6	.0		

Table A.1 (8-83/168.4° to 172.3°/fine)

Period 8-83, θ_L =172.3° (normal)

CONDORS '83 AVERAGED OIL FOG PROFILES — Period # 8
Release Rate: 23.5 g/s — Azimuth 172.3
Release Height: 266.1 m

Horizontal Profile (50.0 m res.)				Vertical Profile (50.0 m res.)	
η(m)	ρ_s(m)	θ_s(°)	X^n_z	z(m)	X^n_η
3225	914	322.7	.0	-17	.0
3275	871	321.1	.0	33	.0
3325	829	319.3	.2	83	.4
3375	787	317.3	.3	133	22.1
3425	747	315.1	.2	183	83.7
3475	708	312.7	.2	233	163.0
3525	670	309.9	.3	283	176.2
3575	634	306.9	.4	333	154.0
3625	600	303.5	.5	383	178.6
3675	568	299.7	.7	433	188.2
3725	539	295.5	16.3	483	22.3
3775	514	290.8	99.6	533	10.7
3825	492	285.7	131.5	583	.5
3875	474	280.1	116.5	633	.2
3925	462	274.2	251.5	683	.0
3975	454	268.0	225.6		
4025	452	261.7	50.7		
4075	455	255.4	41.8		
4125	464	249.2	25.1		
4175	478	243.4	25.7		
4225	496	237.9	11.8		
4275	519	232.9	1.0		
4325	545	228.3	.0		
4375	575	224.1	.0		
4425	607	220.4	.0		

Period 8-83, θ_L =176.1° (fine)

CONDORS '83 AVERAGED OIL FOG PROFILES — Period # 8
Release Rate: 23.5 g/s — Azimuth 176.1
Release Height: 266.1 m

Horizontal Profile (25.0 m res.)				Vertical Profile (25.0 m res.)	
η(m)	ρ_s(m)	θ_s(°)	X^n_z	z(m)	X^n_η
3213	1051	313.1	.0	-30	.0
3238	1033	312.2	.0	-5	.0
3263	1015	311.2	-.0	20	.0
3288	997	310.2	.0	45	1.3
3313	980	309.1	-.0	70	12.9
3338	963	308.0	.1	95	25.6
3363	947	306.9	.1	120	11.1
3388	931	305.7	.2	145	7.6
3413	915	304.5	.2	170	16.6
3438	900	303.3	.1	195	69.5
3463	885	302.0	-.0	220	140.8
3488	870	300.7	.0	245	142.1
3513	856	299.3	.1	270	183.4
3538	843	297.9	1.5	295	128.0
3563	830	296.4	4.1	320	100.0
3588	818	294.9	6.8	345	127.0
3613	806	293.3	8.4	370	154.2
3638	795	291.7	13.7	395	205.0
3663	784	290.1	28.2	420	209.5
3688	774	288.4	56.4	445	140.8
3713	765	286.7	105.3	470	61.4
3738	757	284.9	104.4	495	53.6
3763	749	283.1	95.7	520	60.7
3788	742	281.2	88.4	545	53.3
3813	736	279.4	80.2	570	40.2
3838	731	277.4	122.0	595	21.2
3863	726	275.5	187.7	620	16.0
3888	723	273.6	223.1	645	15.0
3913	720	271.6	162.4	670	3.2
3938	718	269.6	156.6	695	.1
3963	717	267.6	134.8		
3988	717	265.6	92.4		
4013	717	263.6	78.0		
4038	719	261.6	57.4		
4063	721	259.6	47.6		
4088	724	257.7	35.3		
4113	729	255.7	25.3		
4138	733	253.8	20.7		
4163	739	251.9	29.3		
4188	746	250.0	25.3		
4213	753	248.2	6.3		
4238	761	246.4	1.5		
4263	770	244.7	.3		
4288	779	243.0	.1		
4313	789	241.3	.0		
4338	800	239.7	.0		
4363	812	238.1	.0		
4388	824	236.6	.0		
4413	836	235.1	.0		
4438	850	233.6	.0		

Period 8-83, θ_L =176.1° (normal)

CONDORS '83 AVERAGED OIL FOG PROFILES — Period # 8
Release Rate: 23.5 g/s — Azimuth 176.1
Release Height: 266.1 m

Horizontal Profile (50.0 m res.)				Vertical Profile (50.0 m res.)	
η(m)	ρ_s(m)	θ_s(°)	X^n_z	z(m)	X^n_η
3225	1042	312.6	.0	-17	.0
3275	1006	310.7	-.0	33	.7
3325	972	308.6	.0	83	19.2
3375	939	306.3	.2	133	9.3
3425	907	303.9	.2	183	43.1
3475	877	301.3	.0	233	141.4
3525	850	298.6	.8	283	155.7
3575	824	295.7	5.5	333	113.5
3625	800	292.5	11.0	383	179.6
3675	779	289.2	42.3	433	175.2
3725	761	285.8	104.8	483	57.5
3775	746	282.2	92.1	533	57.0
3825	733	278.4	101.1	583	30.7
3875	724	274.5	205.4	633	15.5
3925	719	270.6	159.5	683	1.6
3975	717	266.6	113.6		
4025	718	262.6	67.7		
4075	723	258.7	41.5		
4125	731	254.8	23.0		
4175	742	251.0	27.3		
4225	757	247.3	3.9		
4275	774	243.8	.2		
4325	795	240.5	.0		
4375	818	237.3	.0		
4425	843	234.3	.0		

Table A.1 (8-83/172.3°/normal to 176.1°)

Period 8-83, θ_L =178.9° (normal)

CONDORS .'83 AVERAGED OIL FOG PROFILES — Period # 8
Release Rate: 23.5 g/s — Azimuth 178.9
Release Height: 266.1 m

Horizontal Profile (50.0 m res.)				Vertical Profile (50.0 m res.)	
η(m)	ρ_s(m)	θ_s(°)	χ^n_z	z(m)	χ^n_η
3025	1292	314.1	.0	-17	.0
3075	1257	312.5	.0	33	13.7
3125	1223	310.8	.1	83	24.5
3175	1190	309.0	.3	133	40.3
3225	1159	307.1	.4	183	51.6
3275	1129	305.1	.6	233	80.9
3325	1100	303.0	.6	283	124.1
3375	1073	300.8	1.0	333	134.7
3425	1047	298.5	1.5	383	115.2
3475	1023	296.0	2.9	433	144.5
3525	1001	293.5	7.4	483	138.7
3575	982	290.8	13.8	533	59.9
3625	964	288.1	33.4	583	36.8
3675	949	285.2	86.1	633	24.5
3725	936	282.2	79.6	683	9.0
3775	926	279.3	111.8	733	1.4
3825	918	276.2	176.3	783	.2
3875	913	273.1	158.6	833	.0
3925	911	269.9	105.5	883	.0
3975	911	266.8	70.9	933	.0
4025	915	263.7	53.4		
4075	920	260.6	52.2		
4125	929	257.5	22.9		
4175	940	254.5	9.6		
4225	954	251.6	8.2		
4275	970	248.8	1.5		
4325	988	246.1	.1		
4375	1009	243.5	.0		
4425	1031	240.9	.1		
4475	1056	238.5	.1		
4525	1082	236.3	.4		
4575	1109	234.1	.4		
4625	1139	232.0	.3		
4675	1169	230.1	.0		
4725	1201	228.2	.0		

Period 8-83, θ_L =183.1° (normal)

CONDORS .'83 AVERAGED OIL FOG PROFILES — Period # 8
Release Rate: 23.5 g/s — Azimuth 183.1
Release Height: 266.1 m

Horizontal Profile (50.0 m res.)				Vertical Profile (50.0 m res.)	
η(m)	ρ_s(m)	θ_s(°)	χ^n_z	z(m)	χ^n_η
2775	1619	315.4	.0	-17	1.6
2825	1585	314.1	.0	33	64.1
2875	1553	312.7	.1	83	63.6
2925	1522	311.2	.2	133	55.8
2975	1491	309.7	.1	183	41.4
3025	1462	308.1	.3	233	79.2
3075	1434	306.5	.3	283	106.0
3125	1407	304.8	.4	333	113.6
3175	1381	303.0	.5	383	93.6
3225	1357	301.2	.2	433	67.1
3275	1334	299.3	.3	483	65.6
3325	1313	297.4	2.2	533	98.6
3375	1293	295.3	5.2	583	82.0
3425	1275	293.3	4.5	633	45.4
3475	1259	291.1	11.7	683	18.6
3525	1244	288.9	35.2	733	4.1
3575	1232	286.7	43.9	783	-.3
3625	1221	284.4	40.1	833	.0
3675	1212	282.1	54.7	883	.0
3725	1205	279.7	93.3	933	.0
3775	1201	277.4	90.5		
3825	1198	275.0	70.8		
3875	1197	272.6	80.8		
3925	1199	270.2	93.5		
3975	1203	267.8	93.1		
4025	1208	265.5	94.8		
4075	1216	263.1	73.2		
4125	1226	260.8	35.4		
4175	1237	258.6	34.9		
4225	1251	256.3	19.3		
4275	1266	254.2	7.7		
4325	1283	252.1	4.8		
4375	1302	250.0	7.4		
4425	1322	248.0	.7		
4475	1344	246.1	.0		

Period 8-83, θ_L =188.0° (normal)

CONDORS .'83 AVERAGED OIL FOG PROFILES — Period # 8
Release Rate: 23.5 g/s — Azimuth 188.0
Release Height: 266.1 m

Horizontal Profile (50.0 m res.)				Vertical Profile (50.0 m res.)	
η(m)	ρ_s(m)	θ_s(°)	χ^n_z	z(m)	χ^n_η
2975	1707	304.9	.0	-17	.7
3025	1685	303.4	.0	33	52.7
3075	1664	301.9	-.0	83	52.2
3125	1644	300.3	.1	133	65.1
3175	1626	298.6	.0	183	78.3
3225	1609	297.0	.5	233	92.9
3275	1594	295.3	3.6	283	110.6
3325	1579	293.5	6.9	333	102.3
3375	1567	291.8	5.6	383	110.5
3425	1556	290.0	18.7	433	92.4
3475	1546	288.2	29.6	483	84.1
3525	1538	286.3	40.3	533	72.1
3575	1531	284.5	51.1	583	45.2
3625	1527	282.6	55.2	633	28.4
3675	1523	280.7	70.7	683	9.2
3725	1522	278.9	74.1	733	2.9
3775	1522	277.0	86.3	783	.5
3825	1524	275.1	90.4	833	.0
3875	1527	273.2	80.0	883	.0
3925	1532	271.4	72.5	933	.0
3975	1538	269.5	57.7		
4025	1547	267.7	38.9		
4075	1556	265.9	32.7		
4125	1568	264.1	25.2		

η(m)	ρ_s(m)	θ_s(°)	χ^n_z	z(m)	χ^n_η
4175	1580	262.3	23.5		
4225	1595	260.6	23.7		
4275	1610	258.9	24.3		
4325	1627	257.2	28.5		
4375	1646	255.6	19.1		
4425	1665	254.0	5.5		
4475	1686	252.5	3.9		
4525	1709	251.0	6.1		
4575	1732	249.5	10.1		
4625	1756	248.0	8.1		
4675	1782	246.7	2.3		
4725	1808	245.3	-.0		
4775	1836	244.0	-.2		
4825	1864	242.7	-.2		
4875	1893	241.5	-.1		
4925	1924	240.3	-.2		
4975	1955	239.1	.4		
5025	1986	238.0	.6		
5075	2019	236.9	.0		
5125	2052	235.9	.0		
5175	2086	234.8	.0		

Table A.1 (8-83/178.9° to 188°)

Period 9-83, θ_L =168.4° (fine)

CONDORS '83 AVERAGED OIL FOG PROFILES — Period # 9
Release Rate: 24.9 g/s — Azimuth 168.4
Release Height: 266.1 m

Horizontal Profile (12.5 m res.)				Vertical Profile (12.5 m res.)	
η(m)	ρ_s(m)	θ_s(°)	χ^n_z	z(m)	χ^n_η
3856	254	305.1	.0	164	.0
3869	245	303.1	.0	176	.0
3881	237	301.0	.0	189	.0
3894	229	298.7	.0	201	.0
3906	221	296.2	.0	214	.6
3919	213	293.5	-.1	226	5.1
3931	206	290.7	.2	239	99.5
3944	200	287.6	4.1	251	308.9
3956	194	284.4	127.1	264	414.1
3969	189	281.0	666.7	276	1350.9
3981	184	277.4	476.0	289	546.3
3994	181	273.7	559.5	301	343.8
4006	178	269.8	495.9	314	619.4
4019	176	265.8	388.2	326	272.2
4031	175	261.7	325.0	339	38.0
4044	174	257.6	165.1	351	1.0
4056	175	253.5	225.6	364	.0
4069	176	249.5	292.9	376	.0
4081	179	245.5	182.7	389	.0
4094	182	241.7	60.8	401	.0
4106	186	238.0	16.3		
4119	191	234.5	7.0		
4131	196	231.1	4.3		
4144	202	228.0	2.3		
4156	209	225.0	.0		
4169	216	222.2	.0		
4181	223	219.7	.0		
4194	231	217.2	.0		
4206	240	215.0	.0		
4219	249	212.9	.0		

Period 9-83, θ_L =168.4° (normal)

CONDORS '83 AVERAGED OIL FOG PROFILES — Period # 9
Release Rate: 24.9 g/s — Azimuth 168.4
Release Height: 266.1 m

Horizontal Profile (50.0 m res.)				Vertical Profile (50.0 m res.)	
η(m)	ρ_s(m)	θ_s(°)	χ^n_z	z(m)	χ^n_η
3875	241	302.1	.0	183	.0
3925	210	292.1	1.0	233	103.5
3975	187	279.2	457.3	283	663.8
4025	175	263.8	343.6	333	232.6
4075	178	247.5	190.5	383	.0
4125	193	232.8	7.5		
4175	220	220.9	.0		

Period 9-83, θ_L =172.3° (fine)

CONDORS '83 AVERAGED OIL FOG PROFILES — Period # 9
Release Rate: 26.8 g/s — Azimuth 172.3
Release Height: 266.1 m

Horizontal Profile (25.0 m res.)				Vertical Profile (25.0 m res.)	
η(m)	ρ_s(m)	θ_s(°)	χ^n_z	z(m)	χ^n_η
3563	642	307.8	.0	-30	.0
3588	624	306.2	.0	-5	.0
3613	607	304.5	.0	20	.0
3638	591	302.7	.0	45	.0
3663	575	300.8	.0	70	.2
3688	560	298.8	.1	95	15.1
3713	545	296.6	2.9	120	63.9
3738	531	294.4	7.9	145	97.2
3763	519	292.1	4.9	170	148.1
3788	507	289.6	10.8	195	37.6
3813	496	287.1	26.7	220	90.0
3838	486	284.4	28.4	245	165.5
3863	477	281.6	67.1	270	238.0
3888	469	278.7	71.6	295	223.9
3913	46	275.7	85.4	320	134.1
3938	458	272.7	184.5	345	62.7
3963	4 4	269.6	351.8	370	122.3
3988	451	266.4	408.2	395	191.1
4013	450	263.3	388.8	420	205.4
4038	450	260.1	194.1	445	133.8
4063	452	256.9	84.2	470	27.2
4088	455	253.8	45.6	495	33.5
4113	459	250.7	22.9	520	10.4
4138	465	247.7	8.2	545	.0
4163	472	244.7	3.8	570	.0
4188	480	241.9	1.4	595	.0
4213	489	239.1	.4	620	.0
4238	500	236.5	.0	645	.0
4263	511	234.0	.0	670	.0
4288	523	231.6	.0	695	.0

Period 9-83, θ_L =172.3° (normal)

CONDORS '83 AVERAGED OIL FOG PROFILES — Period # 9
Release Rate: 26.8 g/s — Azimuth 172.3
Release Height: 266.1 m

Horizontal Profile (50.0 m res.)				Vertical Profile (50.0 m res.)	
η(m)	ρ_s(m)	θ_s(°)	χ^n_z	z(m)	χ^n_η
3575	633	307.0	.0	-17	.0
3625	599	303.6	.0	33	.0
3675	567	299.8	.1	83	7.6
3725	538	295.5	5.4	133	80.5
3775	512	290.9	7.8	183	92.9
3825	490	285.7	27.6	233	127.8
3875	473	280.2	69.3	283	230.9
3925	460	274.2	135.0	333	98.4
3975	452	268.0	380.0	383	156.7
4025	450	261.7	291.5	433	169.6
4075	453	255.3	64.9	483	30.3
4125	462	249.2	15.6	533	5.2
4175	476	243.3	2.6	583	.0
4225	494	237.8	.2	633	.0
4275	517	232.8	.0	683	.0

Table A.1 (9-83/168.4° to 172.3°)

Period 9-83, θ_L =176.1° (normal)

CONDORS '83 AVERAGED OIL FOG PROFILES — Period # 9
Release Rate: 26.8 g/s — Azimuth 176.1
Release Height: 266.1 m

Horizontal Profile (50.0 m res.)				Vertical Profile (50.0 m res.)	
η(m)	ρ_s(m)	θ_s(°)	χ^n_z	z(m)	χ^n_η
3375	939	306.3	.0	-17	.0
3425	908	303.9	.0	33	30.1
3475	878	301.3	1.6	83	28.4
3525	850	298.6	4.2	133	48.0
3575	825	295.6	6.6	183	59.8
3625	801	292.5	4.6	233	122.1
3675	780	289.2	6.7	283	152.8
3725	762	285.8	26.7	333	110.3
3775	747	282.1	61.5	383	41.1
3825	735	278.4	93.0	433	71.7
3875	726	274.5	106.8	483	122.1
3925	720	270.6	118.4	533	100.5
3975	718	266.6	169.7	583	67.3
4025	719	262.6	144.5	633	26.1
4075	724	258.7	71.8	683	18.0
4125	732	254.8	29.7	733	1.5
4175	743	251.0	25.7	783	-.0
4225	758	247.3	36.6	833	.0
4275	776	243.9	46.4	883	.0
4325	796	240.5	27.4	933	.0
4375	819	237.4	8.7		
4425	844	234.4	7.3		
4475	871	231.6	1.8		
4525	901	229.0	.0		
4575	932	226.5	.0		

Period 9-83, θ_L =178.9° (normal)

CONDORS '83 AVERAGED OIL FOG PROFILES — Period # 9
Release Rate: 26.8 g/s — Azimuth 178.9
Release Height: 266.1 m

Horizontal Profile (50.0 m res.)				Vertical Profile (50.0 m res.)	
η(m)	ρ_s(m)	θ_s(°)	χ^n_z	z(m)	χ^n_η
3225	1159	307.1	.0	-17	.0
3275	1129	305.1	.0	33	40.7
3325	1100	303.0	.1	83	48.5
3375	1073	300.8	4.8	133	37.4
3425	1047	298.5	9.0	183	62.7
3475	1023	296.0	5.8	233	81.6
3525	1002	293.5	4.6	283	118.1
3575	982	290.8	8.3	333	151.7
3625	964	288.1	12.8	383	151.3
3675	949	285.2	31.4	433	80.1
3725	936	282.3	44.2	483	60.3
3775	926	279.3	51.8	533	48.6
3825	918	276.2	137.5	583	52.9
3875	913	273.1	178.6	633	38.1
3925	911	269.9	139.9	683	18.3
3975	912	266.8	108.9	733	6.1
4025	915	263.7	103.2	783	3.3
4075	921	260.6	36.8	833	.3
4125	929	257.5	12.3	883	.0
4175	940	254.5	14.2	933	.0
4225	954	251.6	17.2		
4275	970	248.8	18.3		
4325	988	246.1	20.7		
4375	1009	243.5	18.3		
4425	1031	240.9	7.5		
4475	1056	238.6	5.3		
4525	1082	236.3	7.8		
4575	1110	234.1	.8		
4625	1139	232.0	.0		
4675	1170	230.1	.0		

Period 9-83, θ_L =183.1° (normal)

CONDORS '83 AVERAGED OIL FOG PROFILES — Period # 9
Release Rate: 26.8 g/s — Azimuth 183.1
Release Height: 266.1 m

Horizontal Profile (50.0 m res.)				Vertical Profile (50.0 m res.)	
η(m)	ρ_s(m)	θ_s(°)	χ^n_z	z(m)	χ^n_η
3125	1406	304.8	.0	-17	2.9
3175	1381	303.0	.5	33	142.3
3225	1357	301.2	.6	83	92.5
3275	1334	299.3	6.2	133	90.5
3325	1312	297.4	40.3	183	70.9
3375	1293	295.3	41.4	233	121.8
3425	1275	293.3	37.8	283	109.2
3475	1258	291.1	23.9	333	57.7
3525	1244	288.9	15.8	383	40.2
3575	1231	286.7	20.5	433	43.2
3625	1220	284.4	20.1	483	52.7
3675	1211	282.1	31.2	533	34.7
3725	1205	279.7	48.7	583	17.0
3775	1200	277.4	62.3	633	19.5
3825	1197	275.0	107.0	683	23.8
3875	1197	272.6	112.0	733	35.1
3925	1198	270.2	93.3	783	37.4
3975	1202	267.8	65.2	833	8.4
4025	1207	265.5	54.9	883	.0
4075	1215	263.1	49.2	933	.0
4125	1225	260.8	26.5		
4175	1236	258.5	40.3		
4225	1250	256.3	46.2		
4275	1265	254.2	11.9		
4325	1282	252.0	9.5		
4375	1301	250.0	12.0		
4425	1321	248.0	17.1		
4475	1343	246.1	5.3		
4525	1367	244.2	.5		
4575	1392	242.4	.0		

Period 9-83, θ_L =188.0° (normal)

CONDORS '83 AVERAGED OIL FOG PROFILES — Period # 9
Release Rate: 26.8 g/s — Azimuth 188.0
Release Height: 266.1 m

Horizontal Profile (50.0 m res.)				Vertical Profile (50.0 m res.)	
η(m)	ρ_s(m)	θ_s(°)	χ^n_z	z(m)	χ^n_η
2975	1707	304.9	.0	-17	1.1
3025	1685	303.4	.2	33	45.1
3075	1664	301.9	.2	83	66.0
3125	1645	300.3	.8	133	101.3
3175	1627	298.6	2.4	183	90.1
3225	1610	297.0	4.3	233	98.5
3275	1594	295.3	7.2	283	96.8
3325	1580	293.5	11.9	333	81.7
3375	1567	291.8	19.5	383	62.3
3425	1556	290.0	19.4	433	52.4
3475	1547	288.2	14.5	483	60.3
3525	1539	286.3	15.4	533	49.5
3575	1532	284.5	22.3	583	64.5
3625	1527	282.6	39.4	633	40.6
3675	1524	280.7	45.4	683	34.4
3725	1523	278.9	61.0	733	31.0
3775	1523	277.0	88.7	783	15.9
3825	1524	275.1	86.0	833	8.0
3875	1528	273.2	88.9	883	.4
3925	1533	271.4	79.8	933	.0
3975	1539	269.5	81.4		
4025	1547	267.7	73.7		
4075	1557	265.9	71.2		
4125	1568	264.1	70.4		
4175	1581	262.3	53.0		
4225	1595	260.6	27.4		
4275	1611	258.9	13.1		
4325	1628	257.2	2.6		
4375	1647	255.6	.2		
4425	1666	254.0	-.1		

Table A.1 (9-83/176.1° to 188°)

Period 9-83, θ_L =195.0° (normal)

CONDORS '83 AVERAGED OIL FOG PROFILES — Period # 9
Release Rate: 26.8 g/s — Azimuth 195.0
Release Height: 266.1 m

Horizontal Profile (50.0 m res.)				Vertical Profile (50.0 m res.)	
η(m)	ρ_s(m)	θ_s(°)	X_z^n	z(m)	X_η^n
2825	2092	304.8	.0	-17	4.1
2875	2076	303.5	.1	33	53.7
2925	2060	302.2	.4	83	64.9
2975	2046	300.9	2.8	133	70.9
3025	2033	299.5	4.5	183	68.4
3075	2021	298.1	3.9	233	66.8
3125	2010	296.8	3.4	283	66.4
3175	2001	295.4	4.2	333	68.5
3225	1992	293.9	9.1	383	82.9
3275	1985	292.5	20.3	433	85.7
3325	1979	291.1	26.6	483	64.4
3375	1974	289.6	22.9	533	44.5
3425	1971	288.2	20.4	583	43.6
3475	1969	286.7	30.1	633	54.5
3525	1968	285.3	35.0	683	54.6
3575	1968	283.8	33.1	733	45.2
3625	1970	282.4	36.1	783	33.8
3675	1973	280.9	47.3	833	20.7
3725	1977	279.5	49.6	883	6.1
3775	1983	278.0	55.7	933	.1
3825	1989	276.6	62.5		
3875	1997	275.2	52.2		
3925	2006	273.8	43.3		
3975	2017	272.4	39.0		
4025	2028	271.0	48.4		
4075	2041	269.6	56.1		
4125	2055	268.3	58.2		
4175	2070	267.0	47.9		
4225	2086	265.7	35.0		
4275	2103	264.4	42.8		
4325	2121	263.1	39.8		
4375	2140	261.9	24.9		
4425	2160	260.7	15.2		
4475	2181	259.5	10.8		
4525	2203	258.3	5.8		
4575	2226	257.1	5.4		
4625	2250	256.0	4.8		
4675	2275	254.9	2.3		
4725	2300	253.8	.0		
4775	2326	252.8	.0		

Period 10-83, θ_L =172.3° (normal)

CONDORS '83 AVERAGED OIL FOG PROFILES — Period #10
Release Rate: 71.8 g/s — Azimuth 172.3
Release Height: Surface

Horizontal Profile (50.0 m res.)				Vertical Profile (50.0 m res.)	
η(m)	ρ_s(m)	θ_s(°)	X_z^n	z(m)	X_η^n
2525	1472	339.3	.0	-17	.0
2575	1423	338.8	.0	33	142.2
2625	1374	338.4	.0	83	167.6
2675	1326	337.8	.0	133	159.6
2725	1277	337.3	.0	183	140.1
2775	1229	336.7	.3	233	89.8
2825	1181	336.0	.6	283	37.5
2875	1133	335.3	9.9	333	37.8
2925	1086	334.6	11.1	383	49.2
2975	1038	333.7	6.1	433	43.0
3025	991	332.8	4.3	483	29.5
3075	944	331.8	4.8	533	16.9
3125	897	330.7	5.5	583	8.6
3175	851	329.4	5.9	633	8.6
3225	805	328.0	13.3	683	7.9
3275	760	326.5	16.8	733	10.6
3325	715	324.7	16.4	783	15.7
3375	671	322.8	19.1	833	25.3
3425	628	320.5	24.6	883	9.6
3475	586	318.0	50.4	933	.5
3525	545	315.0	41.5	983	.0
3575	507	311.6	22.4	1033	.0
3625	470	307.6	38.4	1083	.0
3675	436	303.0	52.6	1133	.0
3725	405	297.6	62.1	1183	.0
3775	378	291.4	187.9		
3825	357	284.4	159.0		
3875	341	276.5	56.8		
3925	332	268.2	52.8		
3975	331	259.5	46.7		
4025	337	251.0	9.7		
4075	350	242.9	9.0		
4125	370	235.6	14.1		
4175	395	229.1	21.8		
4225	424	223.4	17.0		
4275	457	218.5	8.4		
4325	493	214.3	6.0		
4375	531	210.7	3.9		
4425	571	207.6	.9		
4475	613	204.9	.0		
4525	655	202.5	.0		
4575	699	200.5	-.0		
4625	743	198.7	.0		
4675	789	197.0	.0		
4725	834	195.6	-.0		
4775	880	194.3	.0		
4825	927	193.2	.0		
4875	974	192.1	.0		
4925	1021	191.2	.0		
4975	1068	190.3	.0		

Table A.1 (9-83/195° to 10-83/172.3°)

Period 10-83, θ_L =175.0° (normal)

CONDORS '83 AVERAGED OIL FOG PROFILES — Period #10
Release Rate: 71.8 g/s — Azimuth 175.0
Release Height: Surface

Horizontal Profile (50.0 m res.)				Vertical Profile (50.0 m res.)	
η(m)	ρ_s(m)	θ_s(°)	χ^n_z	z(m)	χ^n_η
1925	2080	340.6	.0	-17	.2
1975	2031	340.2	.0	33	61.4
2025	1983	339.8	.0	83	100.7
2075	1935	339.5	.1	133	108.1
2125	1886	339.0	.1	183	131.6
2175	1838	338.6	.2	233	107.4
2225	1791	338.2	.2	283	64.6
2275	1743	337.7	.2	333	49.0
2325	1695	337.2	.2	383	56.5
2375	1648	336.7	.1	433	54.3
2425	1600	336.1	.2	483	29.5
2475	1553	335.5	.1	533	27.3
2525	1506	334.9	.2	583	35.6
2575	1459	334.2	.3	633	36.8
2625	1412	333.5	.6	683	28.6
2675	1366	332.7	.9	733	32.3
2725	1320	331.9	1.2	783	30.5
2775	1274	331.0	1.0	833	30.3
2825	1229	330.0	4.7	883	13.5
2875	1183	329.0	10.5	933	1.8
2925	1139	327.9	17.1	983	.1
2975	1094	326.7	14.9	1033	-.0
3025	1051	325.4	18.6	1083	.0
3075	1008	324.0	23.0	1133	.0
3125	965	322.5	33.8	1183	.0
3175	923	320.8	36.5		
3225	882	319.0	28.3		
3275	842	317.0	25.9		
3325	804	314.8	25.8		
3375	766	312.4	21.6		
3425	730	309.7	22.3		
3475	696	306.8	22.1		
3525	663	303.6	27.6		
3575	634	300.0	50.8		
3625	606	296.2	33.6		
3675	582	292.0	36.6		
3725	561	287.4	56.9		
3775	544	282.5	95.4		
3825	531	277.4	80.2		
3875	523	272.0	51.7		
3925	519	266.5	52.2		
3975	520	261.0	41.1		
4025	526	255.6	27.5		
4075	536	250.3	22.6		
4125	551	245.3	19.3		
4175	570	240.5	15 4		
4225	592	236.1	15.2		
4275	618	232.0	12.6		
4325	647	228.3	9.6		
4375	678	224.9	9.2		
4425	711	221.9	11.7		
4475	746	219.0	10.4		
4525	783	216.5	3.8		
4575	821	214.2	1.5		
4625	860	212.1	1.1		
4675	901	210.2	1.3		
4725	942	208.4	1.0		
4775	984	206.8	.9		
4825	1027	205.3	.2		
4875	1070	204.0	-.0		

Period 10-83, θ_L =178.9° (normal)

CONDORS '83 AVERAGED OIL FOG PROFILES — Period #10
Release Rate: 71.8 g/s — Azimuth 178.9
Release Height: Surface

Horizontal Profile (50.0 m res.)				Vertical Profile (50.0 m res.)	
η(m)	ρ_s(m)	θ_s(°)	χ^n_z	z(m)	χ^n_η
2025	2028	336.1	.0	-17	.2
2075	1982	335.5	.0	33	44.8
2125	1936	335.0	.0	83	94.0
2175	1890	334.3	-.0	133	102.1
2225	1845	333.7	.0	183	74.8
2275	1800	333.0	.1	233	64.9
2325	1755	332.3	.1	283	47.8
2375	1711	331.6	.2	333	41.6
2425	1666	330.8	.2	383	42.1
2475	1622	329.9	.3	433	49.6
2525	1579	329.1	.4	483	51.3
2575	1536	328.1	1.3	533	52.2
2625	1493	327.1	2.2	583	46.1
2675	1451	326.1	1.9	633	42.7
2725	1409	325.0	2.5	683	37.2
2775	1368	323.8	5.0	733	43.6
2825	1327	322.6	10.3	783	55.9
2875	1287	321.3	19.3	833	57.7
2925	1248	319.9	26.2	883	37.2
2975	1210	318.4	27.4	933	10.8
3025	1172	316.8	17.5	983	2.6
3075	1135	315.1	29.1	1033	.5
3125	1100	313.3	29.1	1083	-.0
3175	1066	311.4	28.3	1133	.0
3225	1032	309.3	33.4	1183	.0
3275	1001	307.1	32.6		
3325	971	304.8	22.4		
3375	942	302.4	16.8		
3425	916	299.7	16.6		
3475	891	297.0	21.2		
3525	869	294.1	24.7		
3575	848	291.0	26.5		
3625	831	287.8	41.1		
3675	816	284.5	54.1		
3725	804	281.1	69.9		
3775	795	277.5	54.0		
3825	789	273.9	28.9		
3875	786	270.3	27.0		
3925	787	266.7	26.3		
3975	790	263.0	32.6		
4025	797	259.5	43.3		
4075	807	256.0	45.7		
4125	819	252.6	44.8		
4175	835	249.3	34.7		
4225	853	246.1	25.1		
4275	873	243.1	20.0		
4325	896	240.2	15.2		
4375	921	237.5	12.1		
4425	949	234.9	8.3		
4475	977	232.5	6.2		
4525	1008	230.2	6.0		
4575	1040	228.0	3.6		
4625	1073	226.0	1.9		
4675	1108	224.1	1.8		
4725	1144	222.3	1.1		
4775	1181	220.7	.4		
4825	1218	219.1	.2		
4875	1257	217.6	-.0		
4925	1296	216.2	.0		
4975	1336	214.9	.0		

Table A.1 (10-83/175° to 178.9°)

Period 10-83, θ_L =183.1° (normal)

CONDORS '83 AVERAGED OIL FOG PROFILES — Period #10
Release Rate: 71.8 g/s — Azimuth 183.1
Release Height: Surface

Horizontal Profile (50.0 m res.)				Vertical Profile (50.0 m res.)	
η(m)	ρ_s(m)	θ_s(°)	χ^n_z	z(m)	χ^n_η
1725	2358	336.1	.0	-17	.4
1775	2313	335.6	.0	33	26.7
1825	2269	335.0	.1	83	37.5
1875	2225	334.4	.1	133	53.2
1925	2181	333.8	.1	183	61.0
1975	2138	333.1	.1	233	65.2
2025	2095	332.4	.2	283	79.0
2075	2052	331.7	.3	333	81.5
2125	2009	331.0	.4	383	61.3
2175	1967	330.2	.2	433	52.4
2225	1925	329.4	.3	483	55.2
2275	1884	328.5	.4	533	58.9
2325	1843	327.7	.5	583	42.1
2375	1803	326.7	.7	633	39.4
2425	1763	325.8	.9	683	48.1
2475	1723	324.8	1.2	733	53.1
2525	1684	323.7	1.8	783	58.8
2575	1646	322.6	2.8	833	63.7
2625	1608	321.4	4.6	883	47.7
2675	1571	320.2	7.6	933	11.2
2725	1535	319.0	6.8	983	3.2
2775	1499	317.6	8.2	1033	.3
2825	1465	316.2	10.8	1083	-.0
2875	1431	314.8	16.0	1133	.0
2925	1398	313.2	14.5	1183	.0
2975	1367	311.6	13.2		
3025	1336	310.0	17.4		
3075	1307	308.2	22.2		
3125	1279	306.4	24.2		
3175	1252	304.5	26.7		
3225	1227	302.5	30.7		
3275	1203	300.4	34.7		
3325	1181	298.2	34.3		
3375	1160	296.0	32.3		
3425	1142	293.7	23.3		
3475	1125	291.3	21.5		
3525	1111	288.8	25.4		
3575	1098	286.3	31.6		
3625	1088	283.8	36.4		
3675	1080	281.2	41.6		
3725	1074	278.5	50.1		
3775	1070	275.9	66.4		
3825	1069	273.2	69.7		
3875	1070	270.5	57.3		
3925	1074	267.8	32.3		
3975	1079	265.2	21.8		
4025	1088	262.6	20.5		
4075	1098	260.0	20.2		
4125	1110	257.5	20.1		
4175	1125	255.0	21.8		
4225	1141	252.7	18.9		
4275	1160	250.3	19.1		
4325	1180	248.1	16.0		
4375	1202	245.9	13.2		
4425	1225	243.9	12.5		
4475	1251	241.9	13.1		
4525	1277	239.9	12.5		
4575	1305	238.1	8.7		
4625	1337	236.3	4.6		
4675	1365	234.7	2.6		
4725	1397	233.1	1.6		
4775	1429	231.5	1.2		
4825	1463	230.1	1.0		
4875	1498	228.7	.3		
4925	1533	227.3	.1		
4975	1569	226.1	.2		
5025	1606	224.8	.2		
5075	1644	223.7	.0		
5125	1682	222.6	.0		
5175	1721	221.5	.0		

Period 10-83, θ_L =190.0° (normal)

CONDORS '83 AVERAGED OIL FOG PROFILES — Period #10
Release Rate: 71.8 g/s — Azimuth 190.0
Release Height: Surface

Horizontal Profile (50.0 m res.)				Vertical Profile (50.0 m res.)	
η(m)	ρ_s(m)	θ_s(°)	χ^n_z	z(m)	χ^n_η
1925	2315	328.9	.0	-17	.8
1975	2278	328.1	-.0	33	25.6
2025	2241	327.2	.2	83	31.2
2075	2204	326.4	.4	133	35.3
2125	2168	325.5	.8	183	39.2
2175	2133	324.5	1.2	233	45.5
2225	2098	323.5	1.2	283	54.7
2275	2064	322.5	1.3	333	61.1
2325	2031	321.5	.8	383	60.0
2375	1998	320.4	.9	433	55.7
2425	1966	319.3	1.0	483	55.4
2475	1935	318.2	.8	533	56.2
2525	1904	317.0	.9	583	59.7
2575	1875	315.8	1.3	633	66.4
2625	1846	314.5	2.0	683	63.7
2675	1818	313.2	2.2	733	65.1
2725	1791	311.9	2.3	783	71.0
2775	1765	310.5	3.8	833	69.0
2825	1740	309.1	6.3	883	56.4
2875	1717	307.6	10.3	933	27.3
2925	1694	306.1	11.8	983	.7
2975	1673	304.6	10.2	1033	.0
3025	1653	303.0	12.9	1083	.0
3075	1634	301.4	16.6	1133	.0
3125	1616	299.7	20.7	1183	.0
3175	1600	298.0	21.0		
3225	1585	296.3	19.3		
3275	1572	294.6	20.6		
3325	1560	292.8	22.0		
3375	1550	291.0	26.4		
3425	1541	289.2	29.0		
3475	1534	287.3	32.7		
3525	1529	285.5	31.8		
3575	1525	283.6	33.7		
3625	1522	281.7	31.4		
3675	1522	279.8	32.4		
3725	1523	277.9	32.8		
3775	1525	276.1	35.6		
3825	1530	274.2	39.6		
3875	1535	272.3	41.2		
3925	1543	270.5	38.0		
3975	1552	268.7	37.8		
4025	1563	266.9	40.2		
4075	1575	265.1	44.6		
4125	1588	263.4	40.0		
4175	1603	261.7	38.2		
4225	1620	260.0	35.0		
4275	1638	258.3	30.2		
4325	1657	256.7	27.2		
4375	1677	255.2	22.7		
4425	1699	253.6	18.5		
4475	1722	252.1	14.5		
4525	1745	250.7	10.8		
4575	1771	249.3	8.4		
4625	1797	247.9	6.8		
4675	1824	246.6	5.9		
4725	1852	245.3	5.1		
4775	1881	244.0	3.7		
4825	1910	242.8	3.2		
4875	1941	241.6	3.2		
4925	1973	240.5	2.2		
4975	2005	239.4	1.0		
5025	2038	238.3	.8		
5075	2071	237.3	.8		
5125	2105	236.3	1.1		
5175	2140	235.3	.9		
5225	2176	234.4	.1		
5275	2212	233.5	.0		
5325	2248	232.6	.0		
5375	2285	231.8	.0		

Table A.1 (10-83/183.1° to 190°)

Period 10-83, θ_L = 205.0° (normal)

CONDORS '83 AVERAGED OIL FOG PROFILES — Period #10
Release Rate: 71.8 g/s — Azimuth 205.0
Release Height: Surface

Horizontal Profile (50.0 m res.)				Vertical Profile (50.0 m res.)	
η(m)	ρ_s(m)	θ_s(°)	χ^n_z	z(m)	χ^n_η
2525	2499	309.5	.0	-17	.7
2575	2487	308.4	.0	33	34.0
2625	2475	307.3	.0	83	64.1
2675	2465	306.2	.1	133	68.6
2725	2456	305.0	.6	183	73.8
2775	2448	303.9	1.8	233	68.2
2825	2441	302.7	2.5	283	66.3
2875	2435	301.5	6.4	333	65.0
2925	2429	300.4	8.6	383	61.1
2975	2425	299.2	8.4	433	57.5
3025	2422	298.0	5.5	483	50.5
3075	2420	296.8	4.5	533	51.7
3125	2419	295.6	5.3	583	54.4
3175	2419	294.5	7.0	633	47.5
3225	2420	293.3	8.0	683	48.4
3275	2422	292.1	9.0	733	52.6
3325	2425	290.9	10.2	783	49.0
3375	2429	289.7	10.7	833	42.6
3425	2434	288.6	16.9	883	35.1
3475	2440	287.4	23.1	933	9.7
3525	2447	286.2	21.9	983	-.9
3575	2456	285.1	20.9	1033	.0
3625	2465	283.9	23.5	1083	.0
3675	2475	282.8	26.0	1133	.0
3725	2486	281.7	25.5	1183	.0
3775	2498	280.6	28.1		
3825	2511	279.4	33.2		
3875	2525	278.4	36.4		
3925	2539	277.3	40.8		
3975	2555	276.2	42.0		
4025	2572	275.2	44.0		
4075	2589	274.1	43.8		
4125	2607	273.1	41.2		
4175	2626	272.1	38.8		
4225	2646	271.1	37.7		
4275	2667	270.1	36.5		
4325	2688	269.1	34.8		
4375	2711	268.2	31.5		
4425	2733	267.2	27.4		
4475	2757	266.3	27.7		
4525	2781	265.4	27.1		
4575	2806	264.5	24.2		
4625	2832	263.7	21.9		
4675	2858	262.8	23.0		
4725	2885	262.0	17.9		
4775	2913	261.1	11.1		
4825	2941	260.3	6.4		
4875	2970	259.5	6.0		
4925	2999	258.8	5.7		
4975	3029	258.0	6.3		
5025	3059	257.2	6.6		
5075	3090	256.5	6.5		
5125	3122	255.8	5.5		
5175	3153	255.1	5.8		
5225	3186	254.4	5.2		
5275	3219	253.7	5.4		
5325	3252	253.1	5.0		
5375	3285	252.4	4.6		
5425	3319	251.8	3.7		
5475	3354	251.2	3.6		
5525	3389	250.5	3.0		
5575	3424	249.9	2.6		
5625	3459	249.4	1.8		
5675	3495	248.8	1.0		
5725	3532	248.2	.0		

Period 11-83, θ_L = 172.3° (normal)

CONDORS '83 AVERAGED OIL FOG PROFILES — Period #11
Release Rate: 69.2 g/s — Azimuth 172.3
Release Height: Surface

Horizontal Profile (50.0 m res.)				Vertical Profile (50.0 m res.)	
η(m)	ρ_s(m)	θ_s(°)	χ^n_z	z(m)	χ^n_η
3325	715	324.8	.0	-17	.0
3375	671	322.8	.0	33	178.2
3425	628	320.5	.0	83	248.7
3475	586	318.0	.0	133	208.1
3525	545	315.0	.6	183	129.5
3575	506	311.6	1.3	233	87.5
3625	470	307.6	2.0	283	37.7
3675	436	303.0	3.7	333	27.4
3725	405	297.6	10.7	383	18.4
3775	378	291.4	21.2	433	11.3
3825	356	284.4	29.0	483	9.9
3875	341	276.6	51.6	533	11.8
3925	332	268.2	152.0	583	10.2
3975	331	259.5	235.9	633	4.9
4025	337	251.0	184.7	683	4.3
4075	350	242.9	112.1	733	6.2
4125	369	235.6	83.3	783	5.2
4175	394	229.1	42.3	833	.7
4225	424	223.4	20.1	883	.0
4275	457	218.5	12.7	933	.0
4325	493	214.3	7.5		
4375	531	210.7	4.5		
4425	571	207.6	4.5		
4475	613	204.9	3.6		
4525	655	202.5	3.3		
4575	699	200.5	4.1		
4625	743	198.6	3.7		
4675	788	197.0	2.2		
4725	834	195.6	.8		
4775	880	194.3	.7		
4825	927	193.1	.5		
4875	974	192.1	.4		
4925	1021	191.1	.1		
4975	1068	190.3	.2		
5025	1116	189.5	.4		
5075	1164	188.7	.0		
5125	1212	188.1	.0		
5175	1260	187.5	.0		
5225	1308	186.9	.0		
5275	1357	186.3	.0		

Table A.1 (10-83/205° to 11-83/172.3°)

Period 11-83, θ_L =175.0° (normal)

CONDORS '83 AVERAGED OIL FOG PROFILES — Period #11
Release Rate: 69.2 g/s — Azimuth 175.0
Release Height: Surface

Horizontal Profile (50.0 m res.)				Vertical Profile (50.0 m res.)	
η(m)	ρ_s(m)	θ_s(°)	χ^n_z	z(m)	χ^n_η
3225	883	319.0	.0	-17	.0
3275	843	317.0	.0	33	62.6
3325	804	314.8	.0	83	108.9
3375	767	312.3	.0	133	117.4
3425	731	309.7	.2	183	86.2
3475	696	306.8	.2	233	97.6
3525	664	303.5	.5	283	80.7
3575	634	300.0	1.7	333	68.3
3625	607	296.1	4.4	383	73.6
3675	583	291.9	7.3	433	51.8
3725	562	287.4	14.8	483	49.3
3775	545	282.5	33.4	533	68.5
3825	532	277.4	54.8	583	48.0
3875	524	272.0	75.6	633	29.0
3925	520	266.5	95.2	683	22.4
3975	521	261.0	99.9	733	16.6
4025	527	255.6	111.2	783	12.9
4075	537	250.3	113.0	833	4.8
4125	552	245.3	97.0	883	1.5
4175	571	240.6	70.1	933	-.1
4225	593	236.2	50.6		
4275	619	232.1	36.2		
4325	648	228.4	28.6		
4375	679	225.0	24.0		
4425	712	221.9	17.0		
4475	747	219.1	11.1		
4525	784	216.6	7.7		
4575	822	214.3	10.1		
4625	861	212.2	9.9		
4675	901	210.2	8.0		
4725	943	208.5	6.1		
4775	985	206.9	3.7		
4825	1027	205.4	1.9		
4875	1071	204.1	1.2		
4925	1115	202.8	1.6		
4975	1159	201.7	2.3		
5025	1204	200.6	.6		
5075	1250	199.6	.0		
5125	1295	198.7	.0		
5175	1341	197.8	.0		

Period 11-83, θ_L =178.9° (normal)

CONDORS '83 AVERAGED OIL FOG PROFILES — Period #11
Release Rate: 69.2 g/s — Azimuth 178.9
Release Height: Surface

Horizontal Profile (50.0 m res.)				Vertical Profile (50.0 m res.)	
η(m)	ρ_s(m)	θ_s(°)	χ^n_z	z(m)	χ^n_η
3125	1100	313.3	.0	-17	.0
3175	1066	311.4	-.0	33	43.1
3225	1033	309.3	-.0	83	85.0
3275	1001	307.1	.0	133	122.5
3325	971	304.8	.1	183	125.8
3375	943	302.3	.5	233	90.4
3425	916	299.7	2.0	283	79.3
3475	891	297.0	3.0	333	66.4
3525	869	294.1	2.9	383	59.6
3575	849	291.0	3.7	433	38.7
3625	831	287.8	4.8	483	34.7
3675	817	284.5	6.1	533	43.5
3725	805	281.1	8.7	583	39.6
3775	796	277.5	21.0	633	34.7
3825	790	273.9	41.2	683	33.7
3875	787	270.3	64.3	733	34.3
3925	787	266.7	102.3	783	28.4
3975	791	263.1	112.5	833	23.2
4025	797	259.5	91.6	883	13.6
4075	807	256.0	94.9	933	3.4
4125	820	252.6	93.8	983	.0
4175	835	249.3	79.1	1033	.0
4225	853	246.1	68.0	1083	.0
4275	874	243.1	46.9	1133	.0
4325	897	240.2	37.8	1183	.0
4375	922	237.5	28.0		
4425	949	234.9	23.8		
4475	978	232.5	18.8		
4525	1008	230.2	11.1		
4575	1040	228.0	6.9		
4625	1074	226.0	4.9		
4675	1108	224.1	3.7		
4725	1144	222.4	4.1		
4775	1181	220.7	4.3		
4825	1219	219.1	3.4		
4875	1257	217.7	2.6		
4925	1297	216.3	2.1		
4975	1337	215.0	.9		
5025	1378	213.7	.3		
5075	1419	212.6	.0		

Table A.1 (11-83/175° to 178.9°)

Period 11-83, θ_L =183.1° (normal)

CONDORS '83 AVERAGED OIL FOG PROFILES — Period #11
Release Rate: 69.2 g/s — Azimuth 183.1
Release Height: Surface

Horizontal Profile (50.0 m res.)				Vertical Profile (50.0 m res.)	
η(m)	ρ_s(m)	θ_s(°)	χ^n_z	z(m)	χ^n_η
2925	1399	313.2	.0	-17	.0
2975	1367	311.6	.0	33	39.2
3025	1336	309.9	.0	83	50.4
3075	1307	308.2	.0	133	56.6
3125	1279	306.4	.1	183	67.0
3175	1252	304.4	.2	233	73.6
3225	1227	302.5	.3	283	67.8
3275	1203	300.4	.3	333	59.8
3325	1181	298.2	.8	383	61.6
3375	1161	296.0	2.4	433	63.0
3425	1142	293.7	3.8	483	63.5
3475	1126	291.3	4.6	533	65.8
3525	1111	288.8	6.6	583	60.4
3575	1099	286.3	8.4	633	53.3
3625	1088	283.8	10.2	683	49.0
3675	1080	281.2	14.1	733	48.8
3725	1074	278.5	19.0	783	45.4
3775	1071	275.9	25.4	833	40.8
3825	1070	273.2	33.6	883	25.3
3875	1071	270.5	41.3	933	8.6
3925	1074	267.8	47.0	983	.0
3975	1080	265.2	46.7	1033	.0
4025	1088	262.6	45.8	1083	.0
4075	1098	260.0	55.9	1133	.0
4125	1111	257.5	61.9	1183	.0
4175	1125	255.1	68.9		
4225	1142	252.7	79.6		
4275	1160	250.4	70.2		
4325	1180	248.1	58.7		
4375	1202	246.0	48.5		
4425	1226	243.9	39.9		
4475	1251	241.9	34.7		
4525	1278	240.0	34.5		
4575	1306	238.1	31.0		
4625	1335	236.4	24.9		
4675	1366	234.7	20.0		
4725	1397	233.1	15.5		
4775	1430	231.5	11.3		
4825	1464	230.1	8.0		
4875	1498	228.7	6.4		
4925	1534	227.3	4.6		
4975	1570	226.1	3.8		
5025	1607	224.9	3.0		
5075	1644	223.7	2.9		
5125	1683	222.6	2.4		
5175	1722	221.5	1.1		
5225	1761	220.5	.5		
5275	1801	219.6	.6		
5325	1841	218.6	.4		
5375	1882	217.8	.2		
5425	1924	216.9	.0		
5475	1966	216.1	.0		
5525	2008	215.3	.0		
5575	2050	214.6	.0		
5625	2093	213.9	.0		

Period 11-83, θ_L =190.0° (normal)

CONDORS '83 AVERAGED OIL FOG PROFILES — Period #11
Release Rate: 69.2 g/s — Azimuth 190.0
Release Height: Surface

Horizontal Profile (50.0 m res.)				Vertical Profile (50.0 m res.)	
η(m)	ρ_s(m)	θ_s(°)	χ^n_z	z(m)	χ^n_η
2925	1694	306.1	-.0	-17	.0
2975	1672	304.6	.0	33	15.1
3025	1652	303.0	.2	83	35.0
3075	1633	301.4	.5	133	41.0
3125	1616	299.7	.6	183	46.7
3175	1600	298.0	.9	233	52.4
3225	1585	296.3	1.3	283	53.6
3275	1572	294.6	1.5	333	54.6
3325	1560	292.8	2.0	383	59.2
3375	1550	291.0	3.5	433	67.7
3425	1541	289.2	5.3	483	74.6
3475	1534	287.3	7.5	533	79.9
3525	1528	285.5	10.5	583	79.6
3575	1524	283.6	13.4	633	82.3
3625	1522	281.7	14.4	683	78.2
3675	1521	279.8	16.6	733	67.0
3725	1522	277.9	18.0	783	50.1
3775	1525	276.1	19.7	833	33.0
3825	1529	274.2	20.8	883	20.5
3875	1535	272.3	23.8	933	8.6
3925	1542	270.5	26.1	983	.9
3975	1551	268.7	26.9	1033	-.0
4025	1562	266.9	28.9	1083	.0
4075	1574	265.1	32.4	1133	.0
4125	1588	263.4	35.0	1183	.0
4175	1603	261.6	37.2		
4225	1619	260.0	35.9		
4275	1637	258.3	32.2		
4325	1656	256.7	29.0		
4375	1677	255.1	30.1		
4425	1698	253.6	30.8		
4475	1721	252.1	32.7		
4525	1745	250.7	33.4		
4575	1770	249.3	32.8		
4625	1796	247.9	33.7		
4675	1823	246.6	34.4		
4725	1851	245.3	31.8		
4775	1880	244.0	32.1		
4825	1910	242.8	31.9		
4875	1941	241.6	28.8		
4925	1972	240.5	27.5		
4975	2004	239.4	25.8		
5025	2037	238.3	23.4		
5075	2071	237.3	19.4		
5125	2105	236.2	17.8		
5175	2140	235.3	14.9		
5225	2175	234.4	13.3		
5275	2211	233.5	12.2		
5325	2248	232.6	9.6		
5375	2285	231.8	6.6		
5425	2323	230.9	6.0		
5475	2361	230.1	6.0		
5525	2399	229.4	5.2		
5575	2438	228.6	3.2		
5625	2477	227.9	1.7		
5675	2517	227.2	1.9		
5725	2557	226.5	1.9		
5775	2597	225.9	1.8		
5825	2638	225.2	1.6		
5875	2679	224.6	1.3		
5925	2720	224.0	1.1		
5975	2762	223.4	.3		
6025	2804	222.9	.2		
6075	2846	222.3	.2		
6125	2888	221.8	.2		
6175	2931	221.3	.1		
6225	2974	220.8	.1		
6275	3017	220.3	.1		
6325	3060	219.8	-.0		
6375	3103	219.4	.0		

Table A.1 (11-83/183.1° to 190°)

Period 11-83, θ_L =205.0° (normal)

CONDORS '83 AVERAGED OIL FOG PROFILES Period 811
Release Rate: 49.2 g/s Azimuth 205.0
Release Height: Surface

Horizontal Profile (50.0 m res.)				Vertical Profile (50.0 m res.)	
η(m)	ρ_s(m)	θ_s(°)	χ^n_z	z(m)	χ^n_η
3225	2420	293.3	-.0	-17	.1
3275	2422	292.1	.0	33	25.4
3325	2425	290.9	.1	83	43.4
3375	2429	289.7	.2	133	43.5
3425	2434	288.6	.6	183	49.1
3475	2440	287.4	1.3	233	53.2
3525	2448	286.2	2.8	283	59.8
3575	2456	285.1	4.2	333	63.9
3625	2465	283.9	6.1	383	64.7
3675	2475	282.8	7.5	433	67.8
3725	2486	281.7	11.3	483	72.9
3775	2498	280.6	12.5	533	71.7
3825	2511	279.4	13.8	583	71.1
3875	2525	278.4	15.2	633	69.9
3925	2540	277.3	17.6	683	67.0
3975	2555	276.2	20.5	733	63.8
4025	2572	275.2	22.9	783	59.2
4075	2589	274.1	24.9	833	39.2
4125	2607	273.1	27.2	883	12.4
4175	2627	272.1	26.9	933	2.3
4225	2646	271.1	26.6	983	-.4
4275	2667	270.1	26.6	1033	.0
4325	2689	269.1	27.5	1083	.0
4375	2711	268.2	27.4	1133	.0
4425	2734	267.2	27.6	1183	.0
4475	2757	266.3	30.6		
4525	2782	265.4	30.0		
4575	2807	264.5	29.8		
4625	2832	263.7	29.8		
4675	2859	262.8	25.1		
4725	2886	262.0	24.4		
4775	2913	261.1	23.8		
4825	2941	260.3	23.3		
4875	2970	259.5	22.3		
4925	2999	258.8	21.3		
4975	3029	258.0	21.8		
5025	3060	257.2	21.4		
5075	3090	256.5	21.4		
5125	3122	255.8	21.2		
5175	3154	255.1	20.7		
5225	3186	254.4	20.8		
5275	3219	253.7	18.1		
5325	3252	253.1	17.9		
5375	3286	252.4	17.7		
5425	3320	251.8	17.9		
5475	3354	251.2	17.0		
5525	3389	250.6	15.7		
5575	3424	250.0	11.8		
5625	3460	249.4	10.0		
5675	3496	248.8	10.1		
5725	3532	248.2	10.0		
5775	3568	247.7	10.8		
5825	3605	247.1	11.2		
5875	3643	246.6	10.9		
5925	3680	246.1	11.1		
5975	3718	245.6	10.2		
6025	3756	245.1	8.7		
6075	3794	244.6	7.6		
6125	3833	244.1	7.1		
6175	3872	243.7	5.9		
6225	3911	243.2	4.8		
6275	3951	242.8	4.1		
6325	3990	242.3	3.9		
6375	4030	241.9	3.2		
6425	4070	241.5	2.1		
6475	4111	241.1	2.1		
6525	4151	240.6	2.2		
6575	4192	240.3	1.8		
6625	4233	239.9	1.8		
6675	4274	239.5	1.6		
6725	4315	239.1	1.6		
6775	4357	238.7	1.2		
6825	4398	238.4	.6		
6875	4440	238.0	.2		
6925	4482	237.7	.0		

Table A.1 (11-83/205°)

Fig. A.1. Plots of lidar scans showing concentration profiles listed in Table A.1. See caption of Fig. 3.7 for parameters presented in the plots. Shown chronologically by period, within periods by increasing lidar azimuth. Subfigures referenced by (period number/azimuth).

1-82

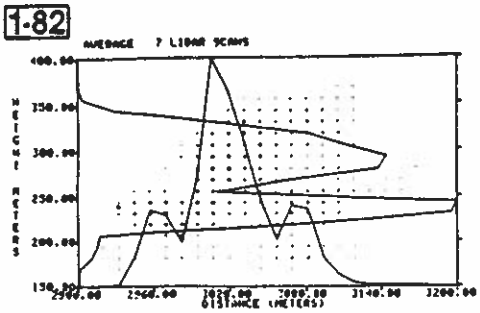

Period 1-82, θ_L =150.0° (fine)

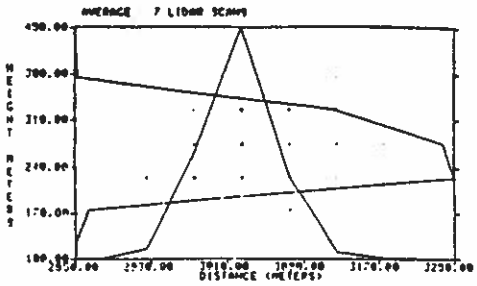

Period 1-82, θ_L =150.0° (normal)

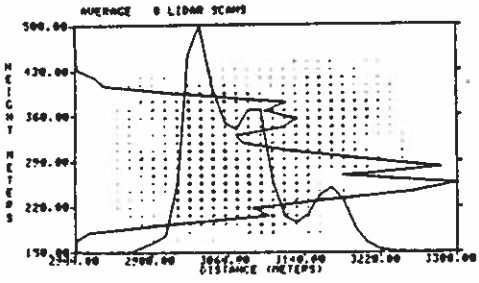

Period 1-82, θ_L =154.9° (fine)

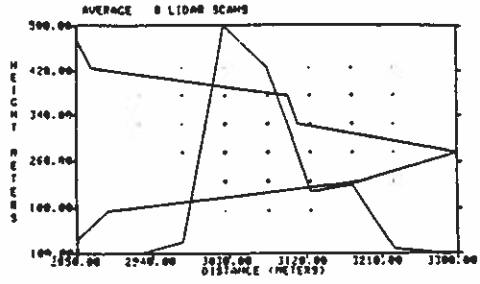

Period 1-82, θ_L =154.9° (normal)

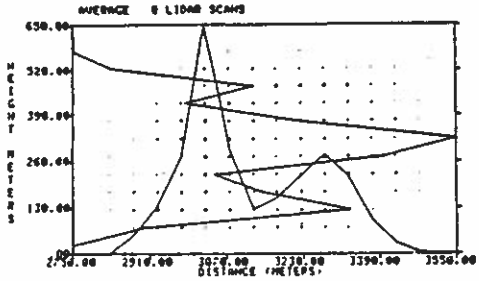

Period 1-82, θ_L =162.5° (normal)

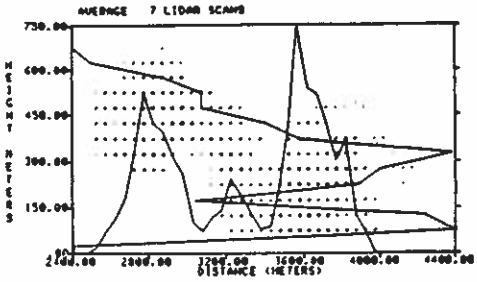

Period 1-82, θ_L =176.6° (normal)

2-82

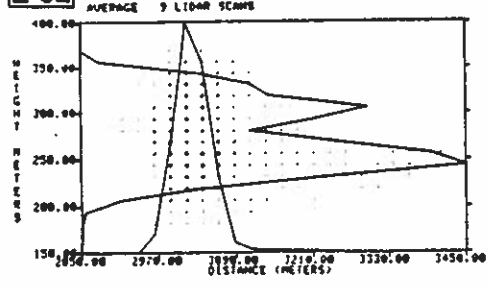

Period 2-82, θ_L =150.0° (fine)

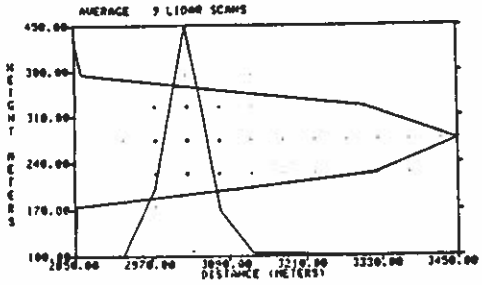

Period 2-82, θ_L =150.0° (normal)

Fig. A.1 (1-82/150° to 2-82/150°)

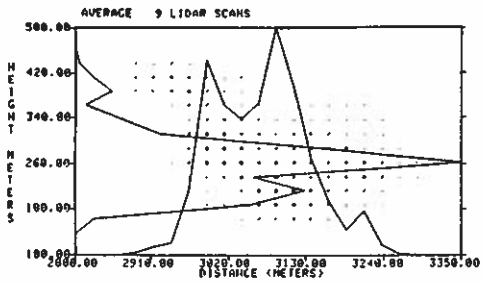

Period 2-82, θ_L =154.9° (fine)

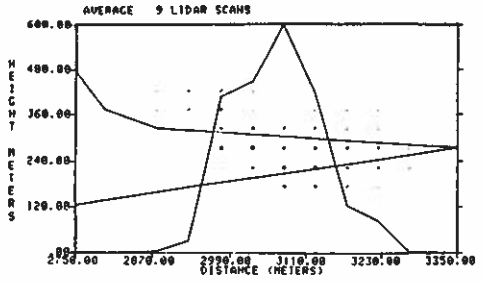

Period 2-82, θ_L =154.9° (normal)

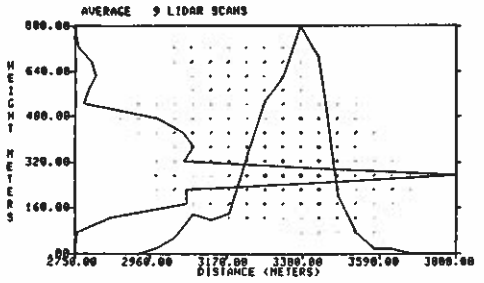

Period 2-82, θ_L =162.5° (normal)

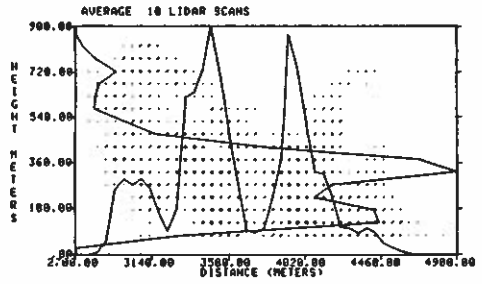

Period 2-82, θ_L =176.6° (normal)

3-82

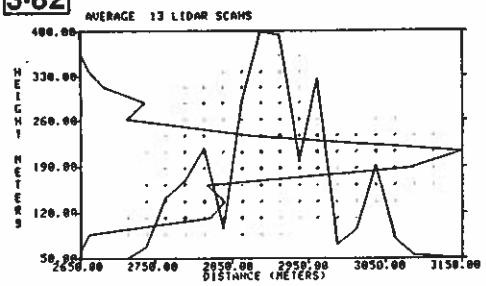

Period 3-82, θ_L =147.8° (fine)

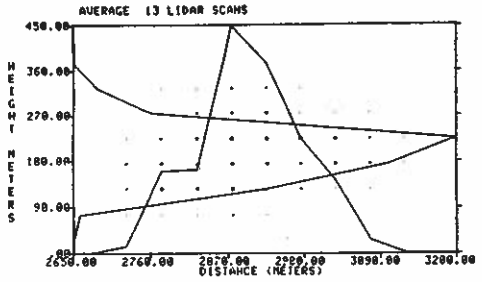

Period 3-82, θ_L =147.8° (normal)

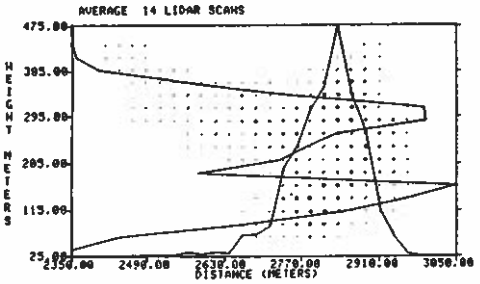

Period 3-82, θ_L =150.0° (fine)

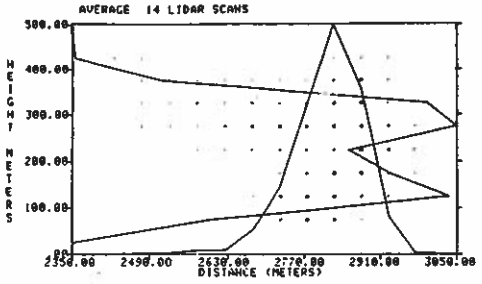

Period 3-82, θ_L =150.0° (normal)

Fig. A.1 (2-82/154.9° to 3-82/150°)

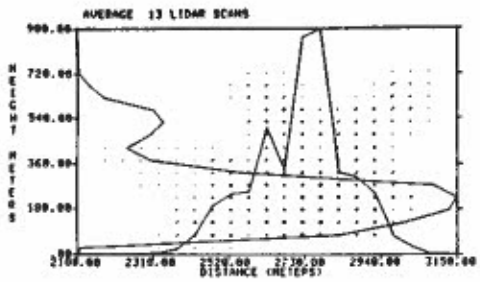

Period 3-82, θ_L =154.9° (normal)

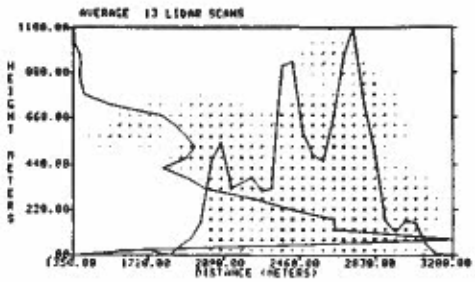

Period 3-82, θ_L =165.0° (normal)

4-82

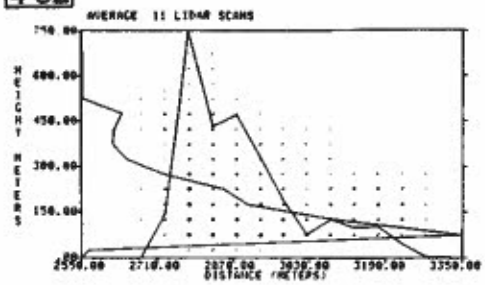

Period 4-82, θ_L =150.0° (normal)

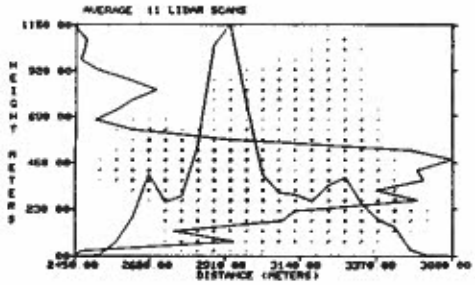

Period 4-82, θ_L =154.9° (normal)

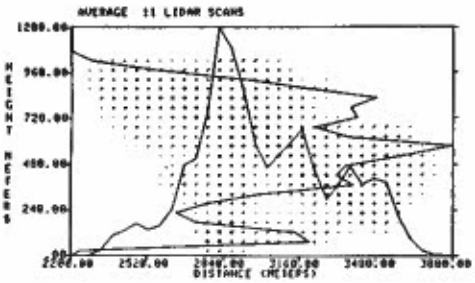

Period 4-82, θ_L =159.7° (normal)

5-82

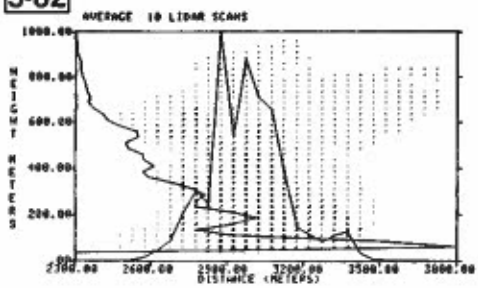

Period 5-82, θ_L =150.0° (fine)

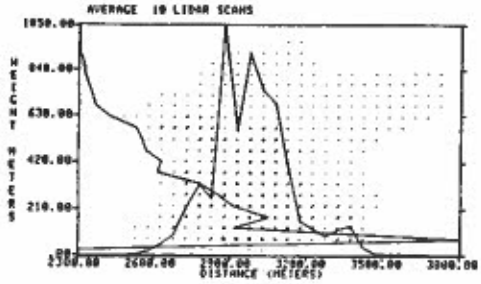

Period 5-82, θ_L =150.0° (normal)

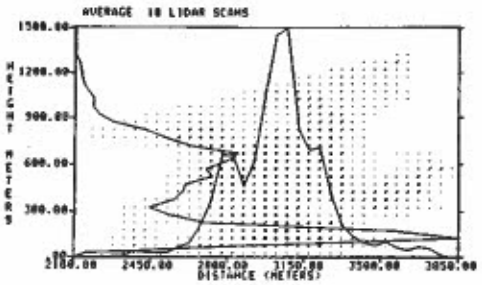

Period 5-82, θ_L =154.9° (normal)

Fig. A.1 (3-82/154.9° to 5-82/154.9°)

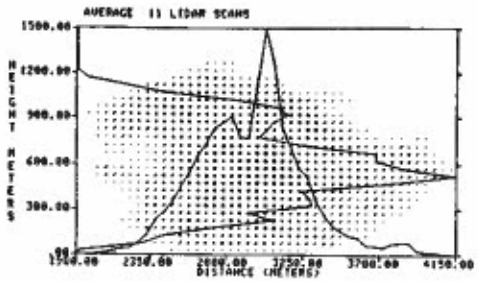

Period 5-82, θ_L =159.7° (normal)

1-83

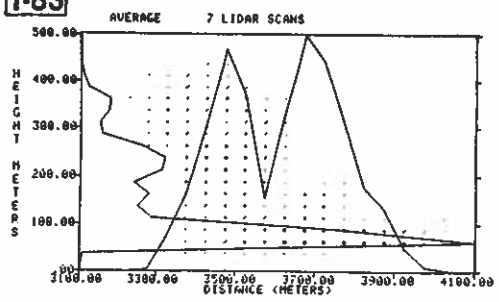

Period 1-83, θ_L =169.9° (fine)

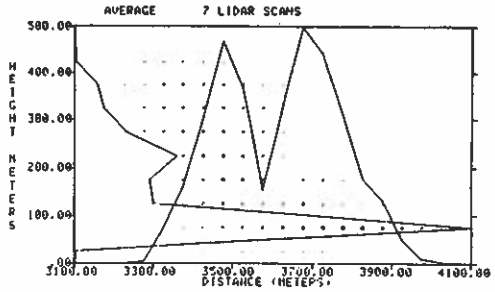

Period 1-83, θ_L =169.9° (normal)

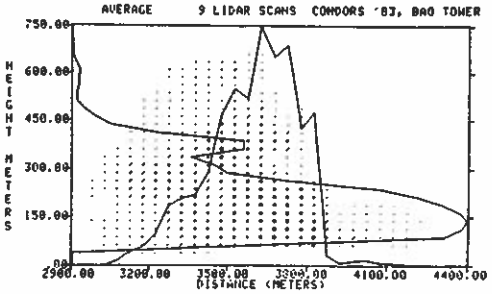

Period 1-83, θ_L =174.0° (fine)

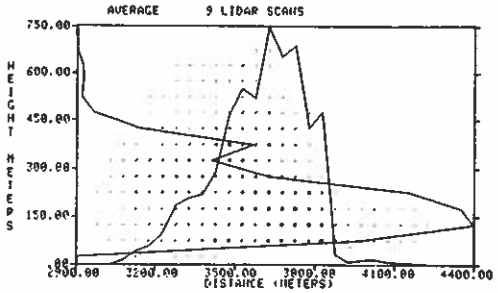

Period 1-83, θ_L =174.0° (normal)

Fig. A.1 (5-82/159.7° to 1-83/174°)

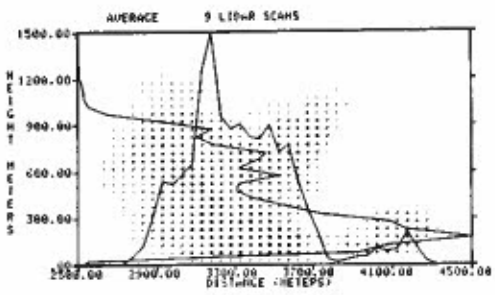

Period 1-83, θ_L =181.1° (normal)

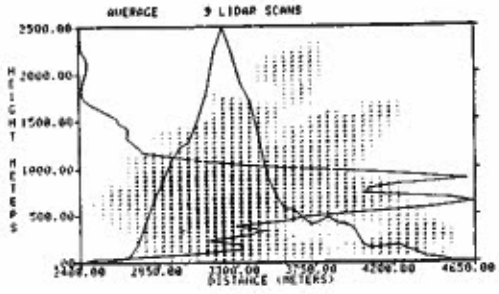

Period 1-83, θ_L =190.0° (normal)

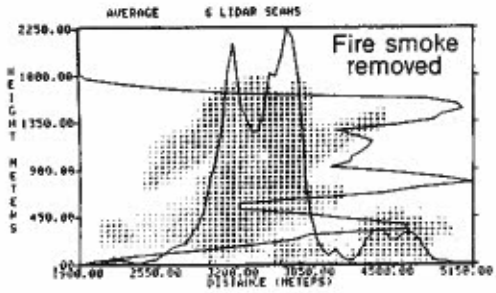

Period 1-83, θ_L =200.1° (normal)

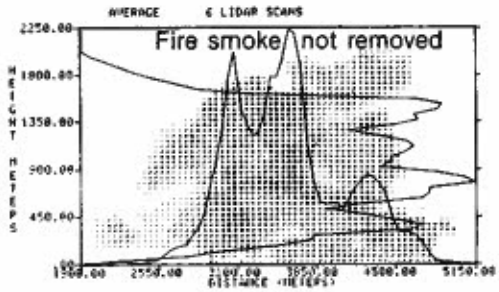

Period 1-83, θ_L =200.1° (normal)

2-83

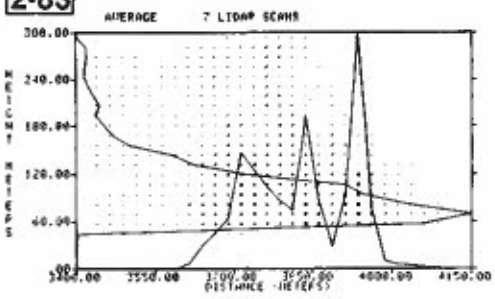

Period 2-83, θ_L =169.9° (fine)

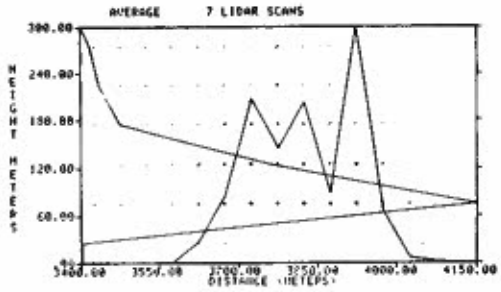

Period 2-83, θ_L =169.9° (normal)

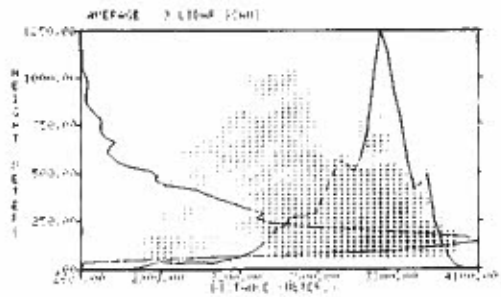

Period 2-83, θ_L =174.0° (fine)

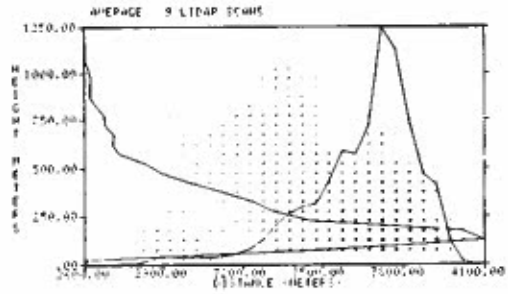

Period 2-83, θ_L =174.0° (normal)

Fig. A.1 (1-83/181.1° to 2-83/174°)

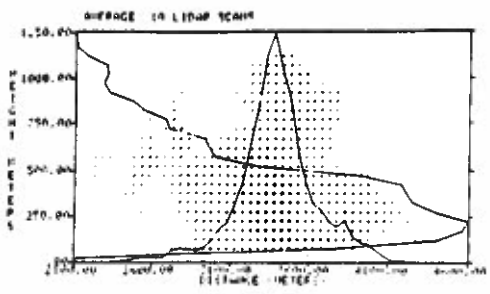

Period 2-83, θ_L =181.1° (normal)

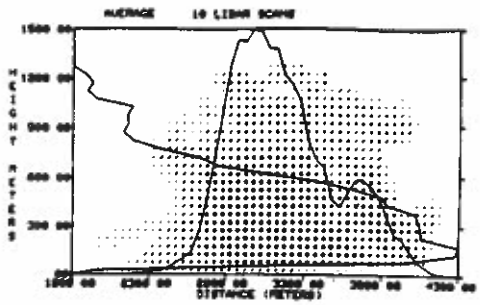

Period 2-83, θ_L =190.0° (normal)

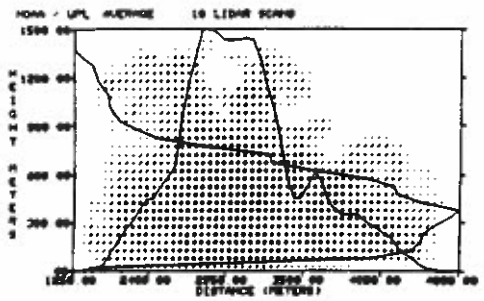

Period 2-83, θ_L =200.1° (normal)

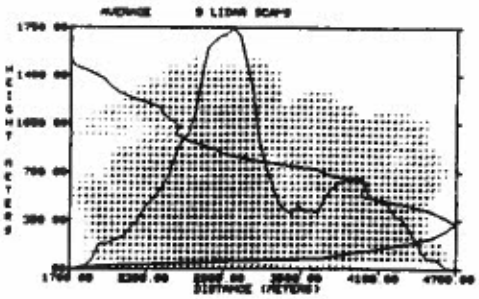

Period 2-83, θ_L =210.0° (normal)

3-83

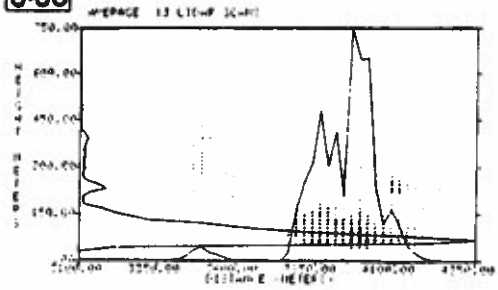

Period 3-83, θ_L =169.9° (fine)

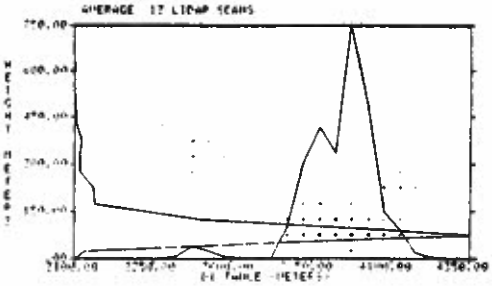

Period 3-83, θ_L =169.9° (normal)

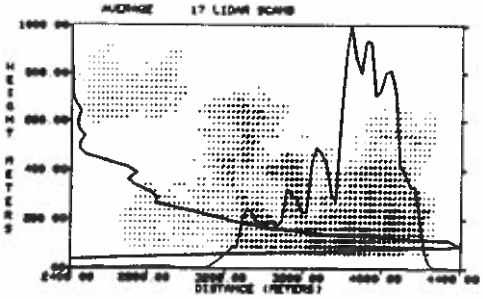

Period 3-83, θ_L =174.0° (fine)

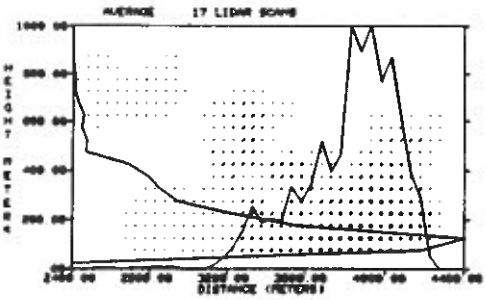

Period 3-83, θ_L =174.0° (normal)

Fig. A.1 (2-83/181.1° to 3-83/174°)

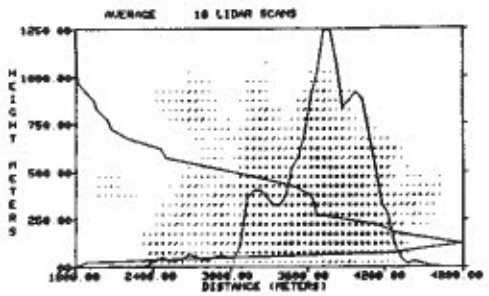

Period 3-83, θ_L =181.1° (normal)

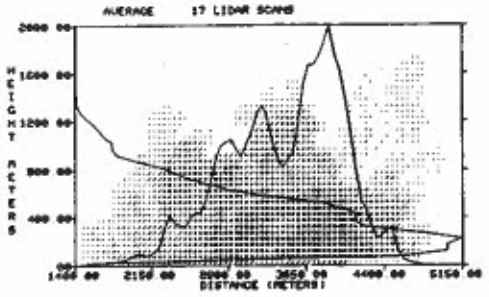

Period 3-83, θ_L =190.0° (normal)

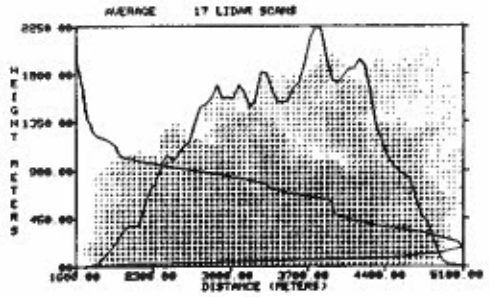

Period 3-83, θ_L =200.1° (normal)

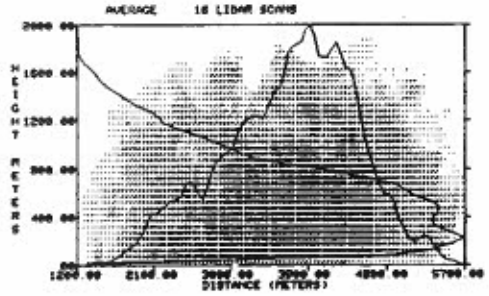

Period 3-83, θ_L =210.0° (normal)

4-83

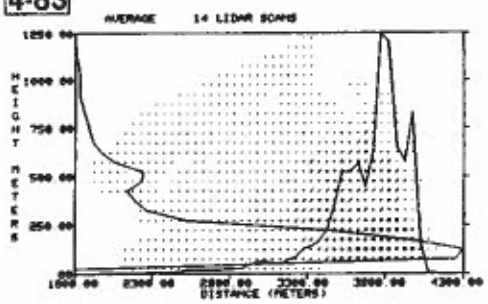

Period 4-83, θ_L =169.9° (normal)

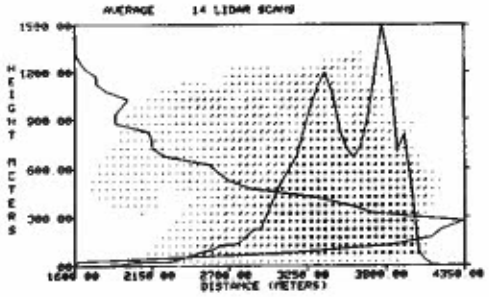

Period 4-83, θ_L =173.0° (normal)

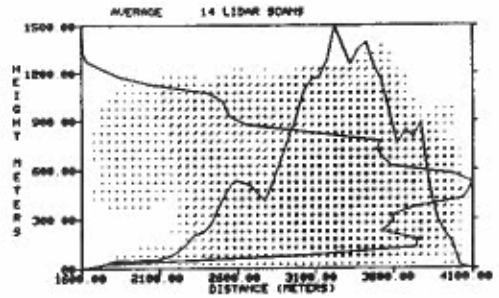

Period 4-83, θ_L =177.5° (normal)

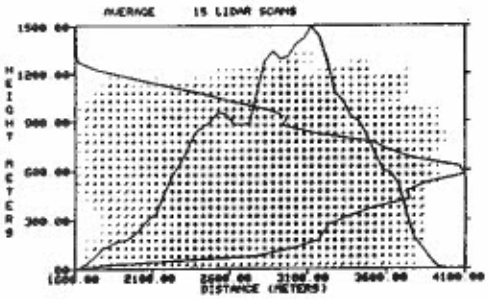

Period 4-83, θ_L =183.1° (normal)

Fig. A.1 (3-83/181.1° to 4-83/183.1°)

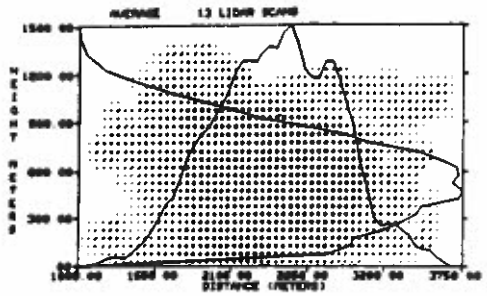

Period 4-83, θ_L =195.0° (normal)

5-83

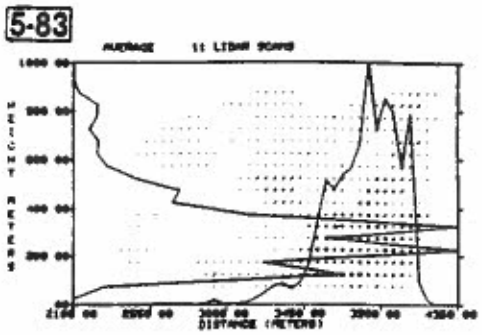

Period 5-83, θ_L =169.9° (normal)

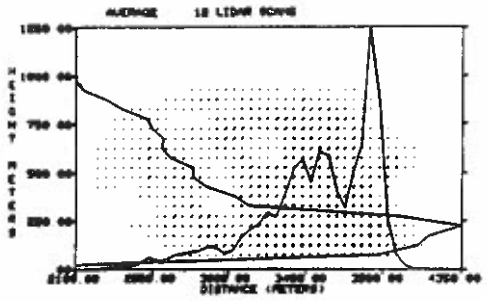

Period 5-83, θ_L =174.0° (normal)

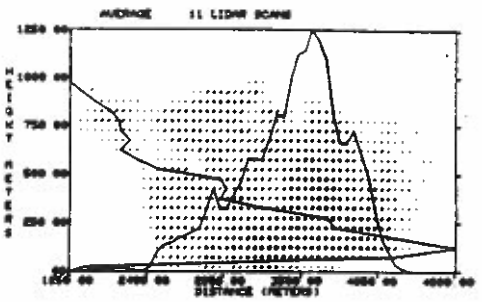

Period 5-83, θ_L =178.9° (normal)

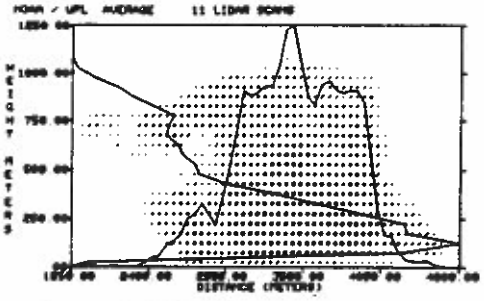

Period 5-83, θ_L =183.1° (normal)

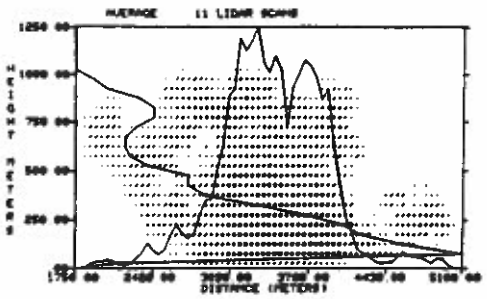

Period 5-83, θ_L =188.0° (normal)

6-83

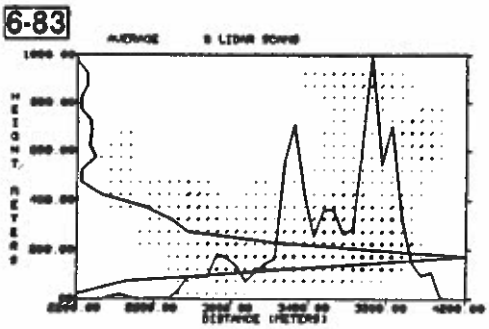

Period 6-83, θ_L =169.9° (normal)

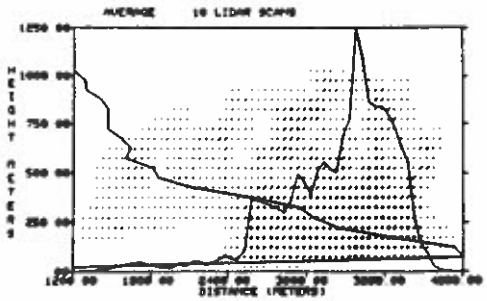

Period 6-83, θ_L =174.0° (normal)

Fig. A.1 (4-83/195° to 6-83/174°)

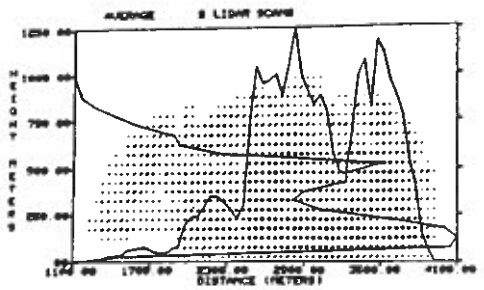

Period 6-83, θ_L =178.9° (normal)

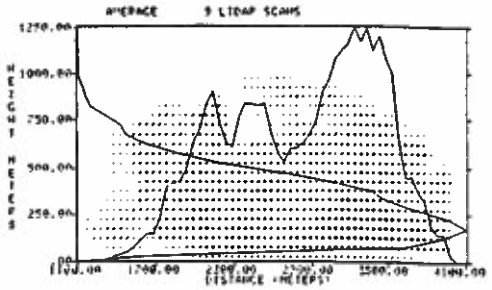

Period 6-83, θ_L =183.1° (normal)

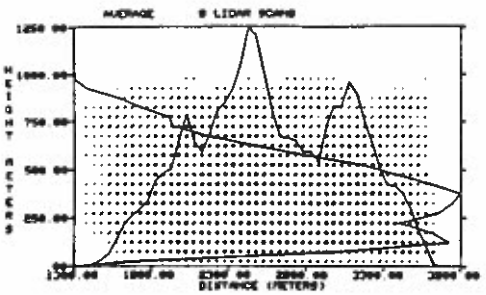

Period 6-83, θ_L =188.0° (normal)

7-83

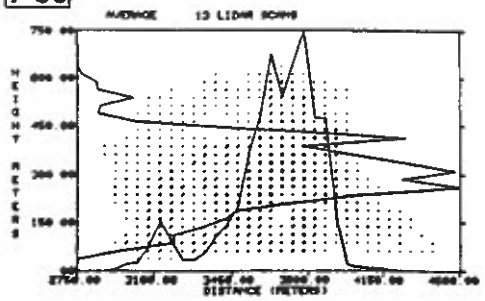

Period 7-83, θ_L =169.9° (fine)

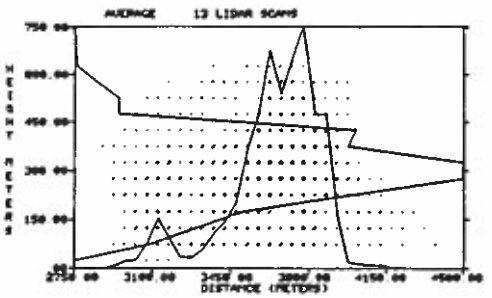

Period 7-83, θ_L =169.9° (normal)

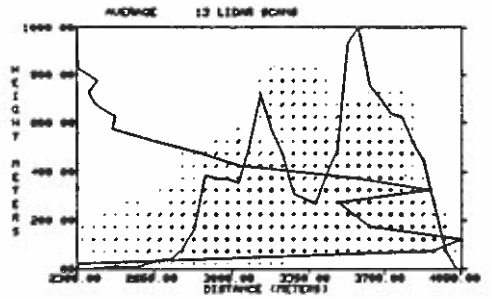

Period 7-83, θ_L =174.0° (normal)

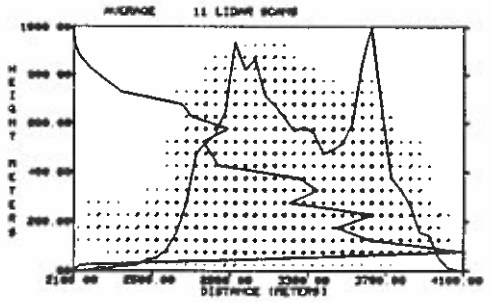

Period 7-83, θ_L =178.9° (normal)

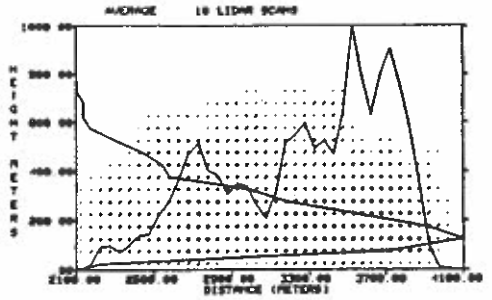

Period 7-83, θ_L =183.1° (normal)

Fig. A.1 (6-83/178.9° to 7-83/183.1°)

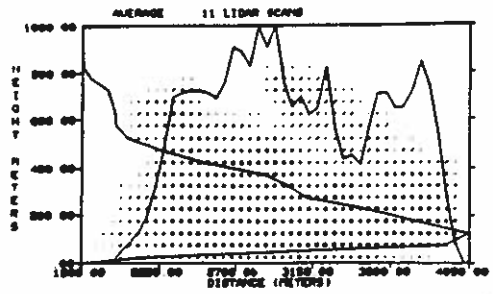

Period 7-83, θ_L =188.0° (normal)

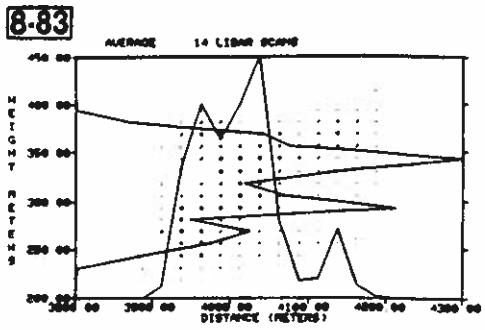

Period 8-83, θ_L =168.4° (fine)

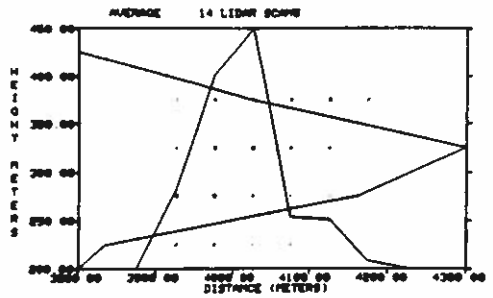

Period 8-83, θ_L =168.4° (normal)

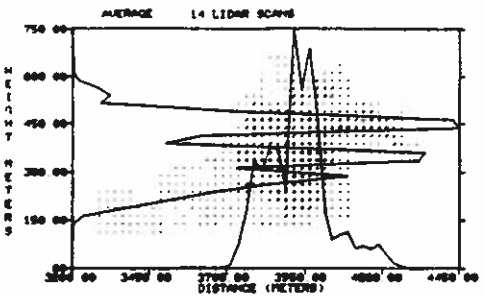

Period 8-83, θ_L =172.3° (fine)

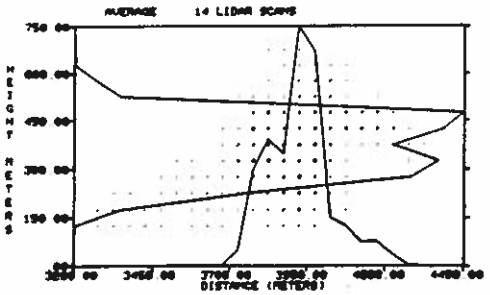

Period 8-83, θ_L =172.3° (normal)

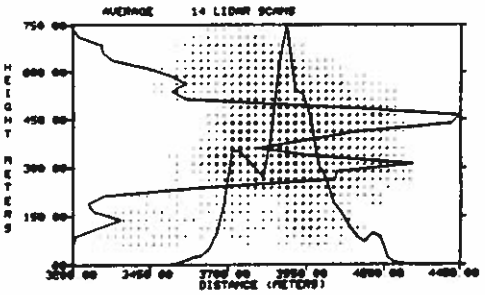

Period 8-83, θ_L =176.1° (fine)

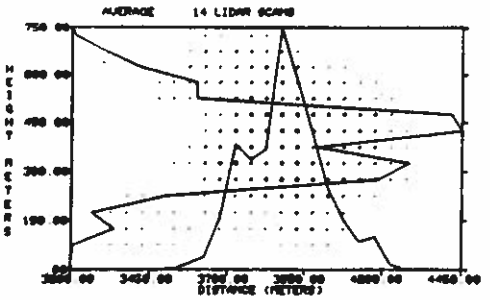

Period 8-83, θ_L =176.1° (normal)

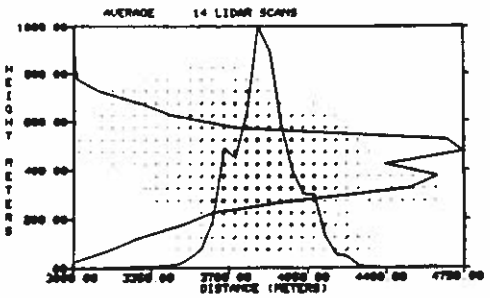

Period 8-83, θ_L =178.9° (normal)

Fig. A.1 (7-83/188° to 8-83/178.9°)

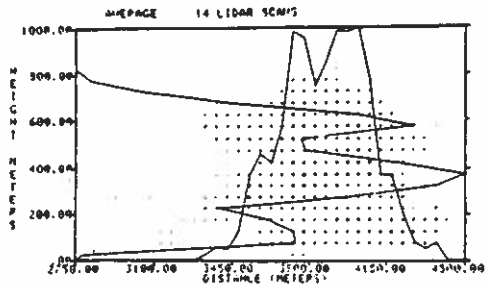

Period 8-83, θ_L =183.1° (normal)

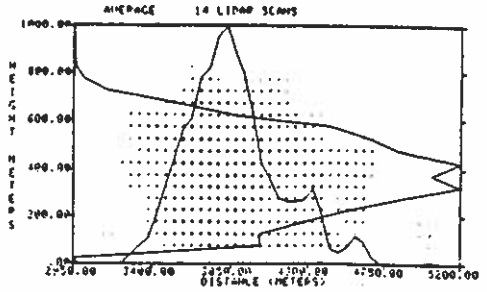

Period 8-83, θ_L =188.0° (normal)

9-83

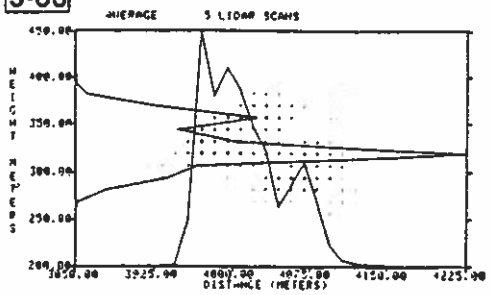

Period 9-83, θ_L =168.4° (fine)

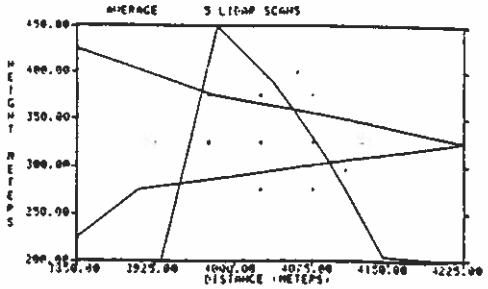

Period 9-83, θ_L =168.4° (normal)

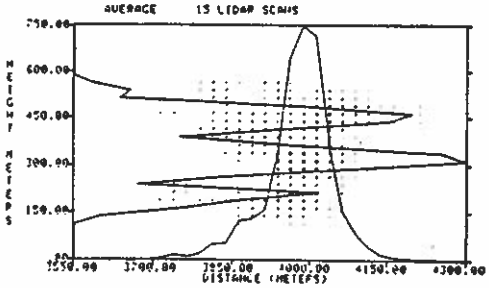

Period 9-83, θ_L =172.3° (fine)

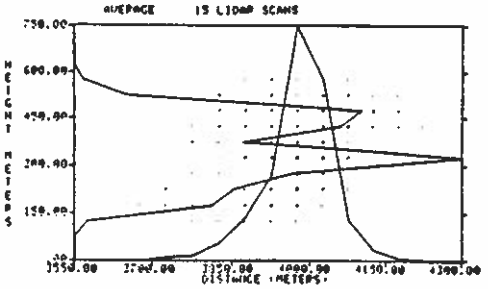

Period 9-83, θ_L =172.3° (normal)

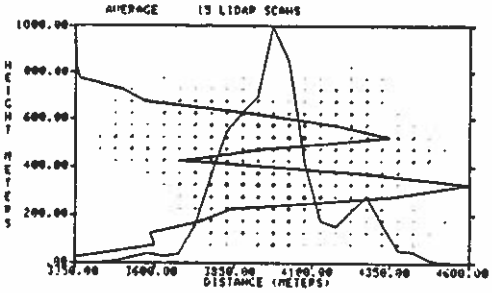

Period 9-83, θ_L =176.1° (normal)

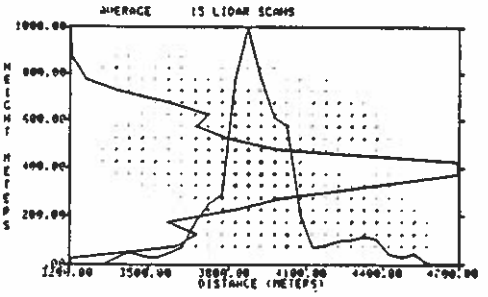

Period 9-83, θ_L =178.9° (normal)

Fig. A.1 (8-83/183.1° to 9-83/176.1°)

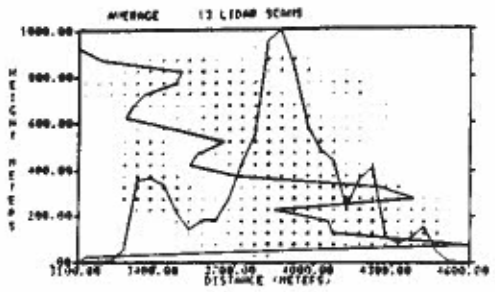

Period 9-83, θ_L =183.1° (normal)

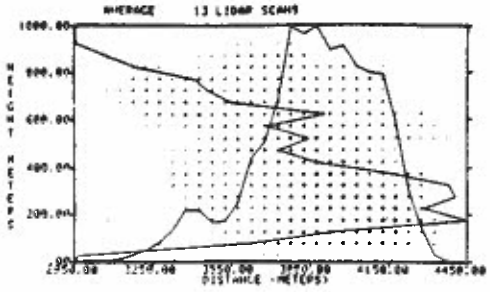

Period 9-83, θ_L =188.0° (normal)

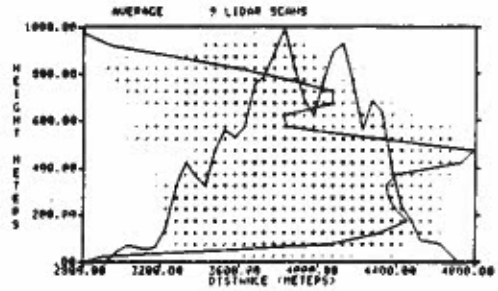

Period 9-83, θ_L =195.0° (normal)

10-83

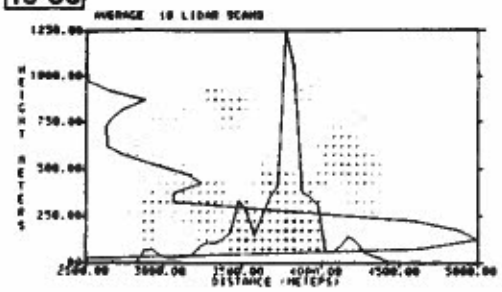

Period 10-83, θ_L =172.3° (normal)

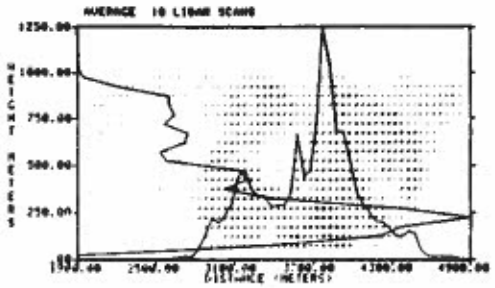

Period 10-83, θ_L =175.0° (normal)

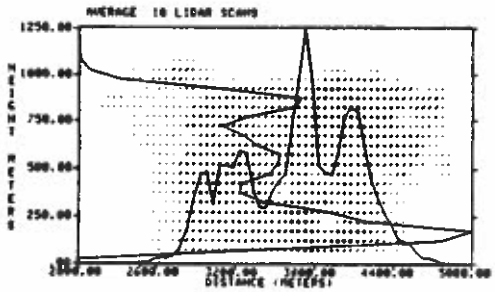

Period 10-83, θ_L =178.9° (normal)

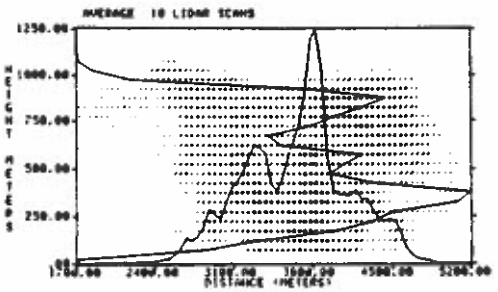

Period 10-83, θ_L =183.1° (normal)

Fig. A.1 (9-83/183.1° to 10-83/183.1°)

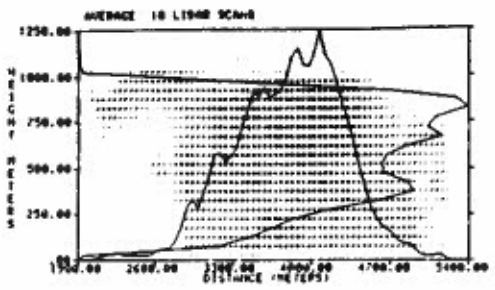

Period 10-83, θ_L =190.0° (normal)

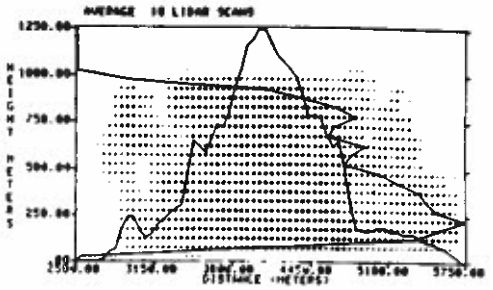

Period 10-83, θ_L =205.0° (normal)

11-83

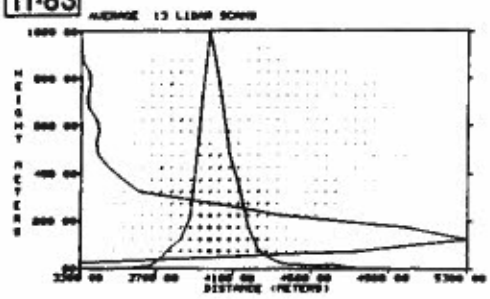

Period 11-83, θ_L =172.3° (normal)

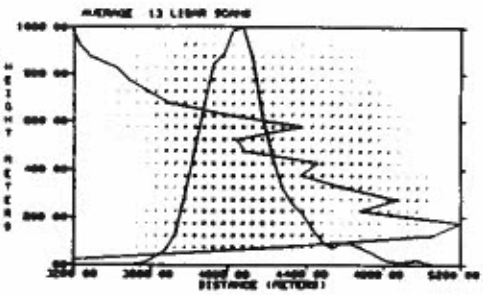

Period 11-83, θ_L =175.0° (normal)

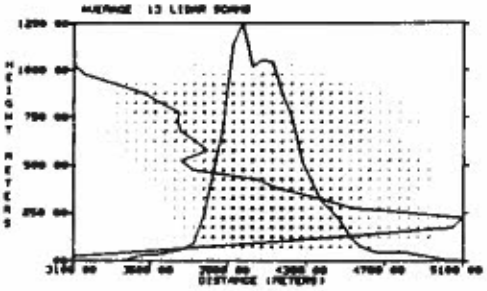

Period 11-83, θ_L =178.9° (normal)

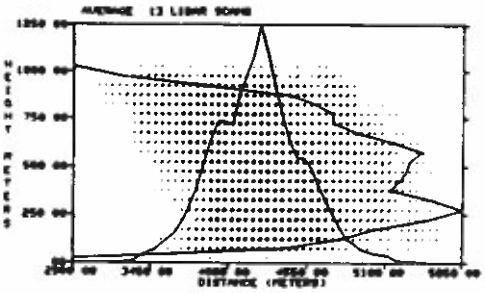

Period 11-83, θ_L =183.1° (normal)

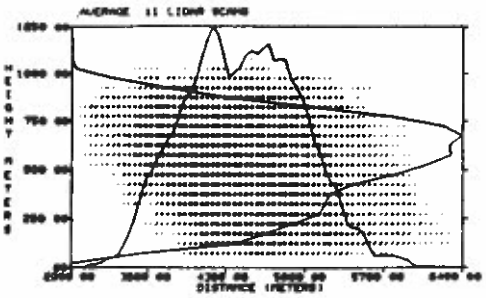

Period 11-83, θ_L =190.0° (normal)

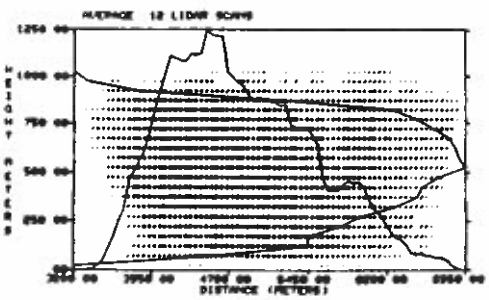

Period 11-83, θ_L =205.0° (normal)

Fig. A.1 (10-83/190° to 11-83/205°)

Table A.2 Adjustments to vertical profile of oil fog near-surface X_η^η for CONDORS 82 and CONDORS 83

Period	Azimuth (°)	Height (m)	Additional Value
1-82	176.6	38	62.7
2-82	176.6	38	34.4
3-82	150.0	26	7.2
3-82	150.0	38	3.6
3-82	154.9	38	5.3
4-82	150.0	38	13.7
4-82	154.9	38	1.4
4-82	159.7	38	0.5
5-82	150.0	26	17.1
5-82	150.0	38	8.6
5-82	154.9	38	3.3
5-82	159.7	38	0.7
1-83	169.9	20	263.9
1-83	169.9	33	132.0
1-83	174.0	20	49.2
1-83	174.0	33	24.6
1-83	181.1	33	7.9
2-83	169.9	14	416.8
2-83	169.9	33	104.2
2-83	174.0	20	38.7
2-83	174.0	33	19.3
2-83	181.1	33	12.0
3-83	169.9	14	260.4
3-83	169.9	33	65.1
3-83	174.0	20	123.0
3-83	174.0	33	61.5
3-83	181.1	33	12.6
4-83	169.9	33	49.5
4-83	173.0	33	14.9
5-83	174.0	33	35.7
5-83	178.9	33	10.1
5-83	183.1	33	9.9
5-83	188.0	33	10.8
6-83	169.9	33	11.4
6-83	174.0	33	27.0
6-83	178.9	33	7.0

Table A.2 Adjustments to vertical profile of oil fog near-surface x_η^n for CONDORS 82 and CONDORS 83 (continued)

Period	Azimuth (°)	Height (m)	Additional Value
7-83	169.9	20	13.6
7-83	169.9	33	6.8
7-83	174.0	33	26.1
7-83	178.9	33	14.0
8-83	178.9	33	3.9
8-83	183.1	33	4.9
8-83	188.0	33	3.2
9-83	176.1	33	12.1
9-83	178.9	33	11.3
9-83	183.1	33	9.4
9-83	188.0	33	3.5
9-83	195.0	33	1.3
10-83	172.3	33	67.5
10-83	175.0	33	19.6
10-83	178.9	33	10.4
10-83	183.1	33	5.4
10-83	190.0	33	6.0
10-83	205.0	33	10.1
11-83	172.3	33	59.4
11-83	175.0	33	40.7
11-83	178.9	33	20.3
11-83	183.1	33	9.3
11-83	190.0	33	15.2
11-83	205.0	33	10.6

Table A.3 Near-surface profiles of the dilution factor (i.e., inferred X/Q) for the oil fog. Distance and azimuth from the source are ρ_s and θ_s, respectively. Profiles tabulated chronologically by period, within periods by increasing lidar azimuth. Azimuths containing no resolvable oil fog concentrations near the surface are omitted.

Period 1-82, θ_L =150.0°

1982 NEAR-SURFACE OIL FOG PROFILE
Min El. = 13.2 m Period # 1
Max El. = 38.2 m Azimuth 150.0

Horizontal Profile (50.0 m res.)

ρ_s(m)	θ_s (°)	χ/Q (s m^{-3})
278	252.3	.000
272	242.0	.000
275	231.5	.000
286	221.5	.000

Period 1-82, θ_L =154.9°

1982 NEAR-SURFACE OIL FOG PROFILE
Min El. = 13.2 m Period # 1
Max El. = 38.2 m Azimuth 154.9

Horizontal Profile (50.0 m res.)

ρ_s(m)	θ_s (°)	χ/Q (s m^{-3})
527	242.2	.000
532	236.8	.000
541	231.6	.000
555	226.5	.000

Period 1-82, θ_L =162.5°

1982 NEAR-SURFACE OIL FOG PROFILE
Min El. = 13.2 m Period # 1
Max El. = 38.2 m Azimuth 162.5

Horizontal Profile (50.0 m res.)

ρ_s(m)	θ_s (°)	χ/Q (s m^{-3})
915	257.5	.000
912	254.4	.105E-09
912	251.2	.681E-09
915	248.1	.223E-09
920	245.0	.538E-08
928	241.9	.563E-09
938	238.9	.000
951	236.0	.148E-07
967	233.2	.419E-06
984	230.4	.337E-06
1004	227.8	.943E-07
1026	225.2	.545E-07
1050	222.8	.181E-07
1076	220.5	.000

Period 1-82, θ_L =176.6°

1982 NEAR-SURFACE OIL FOG PROFILE
Min El. = 35.2 m Period # 1
Max El. = 60.2 m Azimuth 176.6

Horizontal Profile (50.0 m res.)

ρ_s(m)	θ_s (°)	χ/Q (s m^{-3})
1699	244.9	.130E-07
1719	243.4	.193E-06
1739	241.8	.283E-06
1760	240.4	.351E-06
1783	238.9	.373E-06
1807	237.5	.342E-06
1832	236.2	.650E-06
1858	234.8	.159E-05
1884	233.5	.226E-05
1912	232.3	.218E-05
1941	231.1	.256E-05
1970	229.9	.222E-05
2001	228.7	.515E-06
2032	227.6	.727E-06
2063	226.5	.705E-06
2096	225.5	.644E-06
2129	224.5	.107E-06
2163	223.5	.153E-07
2197	222.5	.000

Period 2-82, θ_L =150.0°

1982 NEAR-SURFACE OIL FOG PROFILE
Min El. = 13.2 m Period # 2
Max El. = 38.2 m Azimuth 150.0

Horizontal Profile (50.0 m res.)

ρ_s(m)	θ_s (°)	χ/Q (s m^{-3})
279	252.3	.000
272	242.0	.000
275	231.5	.000
287	221.6	.000

Period 2-82, θ_L =154.9°

1982 NEAR-SURFACE OIL FOG PROFILE
Min El. = 13.2 m Period # 2
Max El. = 38.2 m Azimuth 154.9

Horizontal Profile (50.0 m res.)

ρ_s(m)	θ_s (°)	χ/Q (s m^{-3})
526	242.2	.000
531	236.8	.000
540	231.5	.000
554	226.5	.000

Period 2-82, θ_L =162.5°

1982 NEAR-SURFACE OIL FOG PROFILE
Min El. = 13.2 m Period # 2
Max El. = 38.2 m Azimuth 162.5

Horizontal Profile (50.0 m res.)

ρ_s(m)	θ_s (°)	χ/Q (s m^{-3})
1026	225.2	.000
1050	222.8	.000
1075	220.5	.000
1103	218.3	.000

Period 2-82, θ_L =176.6°

1982 NEAR-SURFACE OIL FOG PROFILE
Min El. = 48.2 m Period # 2
Max El. = 68.2 m Azimuth 176.6

Horizontal Profile (50.0 m res.)

ρ_s(m)	θ_s (°)	χ/Q (s m^{-3})
1651	249.8	.309E-09
1666	248.1	.173E-07
1682	246.5	.154E-07
1700	244.9	-.624E-08
1719	243.4	-.773E-09
1740	241.9	-.178E-07
1761	240.4	.167E-07
1784	238.9	.191E-06
1808	237.5	.711E-06
1832	236.2	.813E-06
1858	234.8	.122E-06
1885	233.5	.358E-06
1913	232.3	.167E-06
1941	231.1	.286E-07
1971	229.9	.838E-08
2001	228.7	.295E-07
2032	227.6	.118E-06
2064	226.5	.617E-07
2097	225.5	.287E-07
2130	224.5	.364E-06
2164	223.5	.989E-06
2198	222.6	.506E-06
2233	221.6	.464E-06
2269	220.7	.275E-06
2305	219.9	.185E-06
2342	219.0	.311E-06
2379	218.2	.358E-06
2416	217.4	.249E-06
2455	216.7	.120E-06
2493	215.9	.136E-06
2532	215.2	.213E-06
2571	214.5	.115E-06
2611	213.8	.509E-07
2651	213.2	.661E-08
2691	212.6	.494E-08
2732	211.9	-.216E-09
2773	211.3	.958E-09
2814	210.8	.000

Period 3-82, θ_L =147.8°

1982 NEAR-SURFACE OIL FOG PROFILE
Min El. = 13.2 m Period # 3
Max El. = 38.2 m Azimuth 147.8

Horizontal Profile (50.0 m res.)

ρ_s(m)	θ_s (°)	χ/Q (s m^{-3})
269	292.0	.000
230	284.7	.000
196	274.6	.000
171	261.1	.000

Period 3-82, θ_L =150.0°

1982 NEAR-SURFACE OIL FOG PROFILE
Min El. = 17.2 m Period # 3
Max El. = 37.2 m Azimuth 150.0

Horizontal Profile (50.0 m res.)

ρ_s(m)	θ_s (°)	χ/Q (s m^{-3})
451	292.9	.000
412	288.7	.925E-08
376	283.7	.357E-06
343	277.6	.435E-05
315	270.4	.119E-05
293	262.0	.000

Table A.3 (1-82/150° to 3-82/150°)

Period 3-82, θ_L =154.9°

1982 NEAR-SURFACE OIL FOG PROFILE
Min El. = 21.2 m Period # 3
Max El. = 51.2 m Azimuth 154.9

Horizontal Profile (50.0 m res.)

ρ_s(m)	θ_s (°)	χ/Q (s m^{-3})
856	297.0	.000
817	294.9	.771E-07
779	292.5	.230E-06
743	289.9	.959E-06
709	287.0	.110E-05
676	283.9	.754E-06
646	280.4	.168E-06
618	276.7	.337E-06
593	272.6	.711E-06
572	268.1	.617E-05
554	263.4	.424E-05
540	258.3	.125E-05
531	253.1	.150E-05
526	247.7	.574E-06
526	242.2	.363E-07

Period 3-82, θ_L =165.0°

1982 NEAR-SURFACE OIL FOG PROFILE
Min El. = 14.2 m Period # 3
Max El. = 44.2 m Azimuth 165.0

Horizontal Profile (50.0 m res.)

ρ_s(m)	θ_s (°)	χ/Q (s m^{-3})
1331	294.0	-.218E-08
1300	292.3	.307E-06
1271	290.5	.151E-05
1242	288.6	.727E-06
1215	286.6	.849E-06
1190	284.6	.324E-06
1166	282.5	.220E-06
1144	280.2	.186E-06
1124	277.9	.169E-05
1105	275.5	.109E-05
1089	273.1	.343E-06
1074	270.5	.202E-06
1062	267.9	.487E-06
1052	265.3	.144E-05
1044	262.6	.536E-05
1039	259.8	.396E-05
1036	257.1	.244E-05
1035	254.3	.300E-05
1037	251.5	.125E-05
1041	248.8	.678E-06
1048	246.1	.952E-06
1056	243.4	.366E-06
1068	240.8	.253E-07
1081	238.2	.000
1096	235.7	.000

Period 4-82, θ_L =159.7°

1982 NEAR-SURFACE OIL FOG PROFILE
Min El. = 20.2 m Period # 4
Max El. = 60.2 m Azimuth 159.7

Horizontal Profile (50.0 m res.)

ρ_s(m)	θ_s (°)	χ/Q (s m^{-3})
677	261.1	.000
669	256.9	.523E-08
665	252.7	.263E-05
664	248.3	.349E-05
667	244.1	.548E-06
674	239.8	.878E-07
684	235.7	.147E-06
698	231.7	.305E-06
715	227.9	.741E-06
735	224.3	.813E-06
758	220.9	.548E-06
783	217.7	.242E-06
811	214.7	.503E-07
841	211.9	.000

Period 5-82, θ_L =150.0°

1982 NEAR-SURFACE OIL FOG PROFILE
Min El. = 21.2 m Period # 5
Max El. = 41.2 m Azimuth 150.0

Horizontal Profile (50.0 m res.)

ρ_s(m)	θ_s (°)	χ/Q (s m^{-3})
445	305.9	.495E-08
400	303.0	.114E-06
356	299.4	.259E-06
314	294.7	.110E-06
274	288.7	.227E-06
239	280.7	.473E-06
210	270.3	.339E-06
190	257.2	.161E-05
181	241.9	.396E-04
187	226.4	.786E-05
204	212.6	.159E-04
232	201.6	.619E-05
266	193.1	.569E-05
304	186.6	.271E-05
345	181.7	.437E-06
389	177.8	.421E-06
434	174.7	.267E-06
480	172.2	.765E-06
526	170.2	.114E-05
573	168.4	.334E-07
621	167.0	.000

Period 4-82, θ_L =150.0°

1982 NEAR-SURFACE OIL FOG PROFILE
Min El. = 23.2 m Period # 4
Max El. = 43.2 m Azimuth 150.0

Horizontal Profile (50.0 m res.)

ρ_s(m)	θ_s (°)	χ/Q (s m^{-3})
314	294.7	.000
274	288.6	.968E-08
239	280.7	.162E-06
210	270.3	.773E-05
190	257.2	.953E-05
181	241.9	.129E-04
187	226.4	.929E-05
204	212.6	.529E-05
232	201.6	.132E-05
266	193.1	.266E-05
304	186.6	.961E-06
345	181.7	.593E-06
389	177.8	.815E-07
434	174.7	.000
480	172.2	.000

Period 4-82, θ_L =154.9°

1982 NEAR-SURFACE OIL FOG PROFILE
Min El. = 20.2 m Period # 4
Max El. = 50.2 m Azimuth 154.9

Horizontal Profile (50.0 m res.)

ρ_s(m)	θ_s (°)	χ/Q (s m^{-3})
463	267.8	.000
446	261.8	.207E-09
434	255.5	.497E-06
428	248.9	.203E-05
427	242.2	.332E-05
433	235.6	.414E-06
443	229.2	.849E-07
459	223.2	.297E-06
480	217.6	.735E-06
505	212.6	.581E-06
533	208.0	.207E-08
565	204.0	.231E-06
599	200.4	.257E-06
635	197.1	.980E-07
673	194.3	.000
712	191.7	.000

Period 5-82, θ_L =154.9°

1982 NEAR-SURFACE OIL FOG PROFILE
Min El. = 18.2 m Period # 5
Max El. = 48.2 m Azimuth 154.9

Horizontal Profile (50.0 m res.)

ρ_s(m)	θ_s (°)	χ/Q (s m^{-3})
761	300.8	.000
720	298.5	.114E-08
681	296.0	.764E-07
643	293.2	.307E-06
606	290.1	.663E-07
572	286.6	.638E-08
540	282.6	.117E-07
511	278.1	.585E-08
485	273.2	.452E-07
464	267.8	.539E-06
447	261.8	.788E-06
435	255.5	.280E-05
428	248.9	.218E-05
428	242.2	.775E-06

ρ_s(m)	θ_s (°)	χ/Q (s m^{-3})
433	235.6	.199E-05
444	229.2	.206E-05
460	223.2	.515E-06
481	217.7	.543E-06
505	212.6	.960E-06
534	208.1	.882E-06
565	204.0	.733E-06
599	200.4	.363E-07
635	197.2	.143E-06
673	194.3	.279E-06
712	191.8	.922E-07
753	189.5	.805E-07
795	187.4	.217E-07
837	185.6	.000

Table A.3 (3-83/154.9° to 5-82/154.9°)

Period 5-82, θ_L =159.7°

1982 NEAR-SURFACE OIL FOG PROFILE		
Min El. = 23.2 m		Period # 5
Max El. = 63.2 m		Azimuth 159.7
Horizontal Profile (50.0 m res.)		
ρ_s(m)	θ_s (°)	χ/Q (s m^{-3})
822	285.8	.000
794	282.9	.484E-09
768	279.7	.793E-08
744	276.4	.245E-07
723	272.9	.754E-07
705	269.1	.120E-06
690	265.2	.102E-06
678	261.1	.187E-06
670	256.9	.646E-06
666	252.7	.447E-06
665	248.3	.282E-06
668	244.1	.484E-06
675	239.8	.419E-06
685	235.7	.370E-06
699	231.7	.382E-06
716	227.9	.250E-06
736	224.3	.123E-06
759	220.9	.114E-06
784	217.7	.163E-06
812	214.7	.110E-06
841	211.9	.112E-06
873	209.3	.156E-06
906	206.9	.891E-07
941	204.7	.112E-07
977	202.6	-.113E-08

Period 1-83, θ_L =169.9°

1983 NEAR-SURFACE OIL FOG PROFILE		
Min El. = 22.6 m		Period # 1
Max El. = 32.6 m		Azimuth 169.9
Horizontal Profile (50.0 m res.)		
ρ_s(m)	θ_s (°)	χ/Q (s m^{-3})
665	335.6	.000
617	334.4	.678E-07
569	333.1	.534E-06
521	331.5	.205E-05
474	329.6	.574E-05
427	327.2	.939E-05
382	324.4	.238E-04
337	320.7	.274E-04
295	315.9	.440E-04
255	309.7	.723E-04
219	301.2	.293E-04
190	289.7	.620E-05
170	275.0	.664E-05
164	257.9	.796E-06
174	241.2	.436E-06
195	227.2	.000

Period 1-83, θ_L =174.0°

1983 NEAR-SURFACE OIL FOG PROFILE		
Min El. = 17.6 m		Period # 1
Max El. = 47.6 m		Azimuth 174.0
Horizontal Profile (50.0 m res.)		
ρ_s(m)	θ_s (°)	χ/Q (s m^{-3})
1072	329.1	.000
1027	327.9	.311E-08
982	326.6	.127E-07
938	325.2	.334E-07
894	323.7	.135E-06
852	322.0	.100E-06
810	320.1	.171E-06
769	318.0	.370E-06
729	315.7	.138E-05
690	313.2	.237E-05
653	310.3	.226E-05
618	307.1	.795E-06
585	303.5	.699E-06
555	299.5	.354E-05
527	295.1	.433E-05
503	290.2	.120E-05
483	284.9	.714E-06
468	279.1	.764E-05
457	273.1	.466E-06
452	266.8	.122E-06
453	260.5	.273E-06
458	254.2	.203E-06
469	248.2	.743E-07
485	242.5	.408E-07
506	237.2	.191E-08
530	232.4	.000

Period 1-83, θ_L =181.1°

1983 NEAR-SURFACE OIL FOG PROFILE		
Min El. = 22.6 m		Period # 1
Max El. = 72.6 m		Azimuth 181.1
Horizontal Profile (50.0 m res.)		
ρ_s(m)	θ_s (°)	χ/Q (s m^{-3})
1433	320.4	.000
1395	319.1	.647E-10
1359	317.7	.382E-08
1323	316.2	.278E-07
1288	314.6	.381E-07
1254	312.9	.113E-06
1221	311.2	.183E-06
1190	309.3	.491E-06
1159	307.4	.815E-06
1130	305.4	.108E-05
1103	303.2	.859E-06
1077	301.0	.561E-06
1053	298.6	.374E-06
1031	296.1	.482E-06
1011	293.6	.108E-05
993	290.9	.134E-05

ρ_s(m)	θ_s (°)	χ/Q (s m^{-3})
977	288.1	.207E-05
964	285.3	.593E-06
953	282.4	.352E-07
944	279.4	.289E-07
938	276.4	.115E-07
935	273.3	.397E-07
934	270.3	.233E-06
936	267.2	.385E-06
941	264.2	.419E-06
948	261.2	.498E-06
958	258.2	.441E-06
971	255.3	.140E-06
985	252.5	.136E-06
1002	249.8	.258E-07
1022	247.2	.000

Table A.3 (5-82/159.7° to 1-83/181.1°)

Period 1-83, θ_L = 190.0°

1983 NEAR-SURFACE OIL FOG PROFILE
Min El. = 7.6 m — Period # 1
Max El. = 57.6 m — Azimuth 190.0

Horizontal Profile (50.0 m res.)

ρ_s(m)	θ_s (°)	χ/Q (s m^{-3})
1818	313.2	.000
1791	311.9	.159E-08
1765	310.5	.146E-07
1741	309.1	.181E-07
1717	307.6	.135E-07
1694	306.1	.116E-07
1673	304.6	.781E-08
1653	303.0	.718E-08
1634	301.4	.272E-07
1616	299.7	.475E-07
1600	298.0	.292E-06
1585	296.3	.386E-06
1572	294.6	.363E-06
1560	292.8	.398E-06
1550	291.0	.258E-06
1541	289.2	.635E-07
1534	287.3	.154E-07
1529	285.5	.127E-07
1525	283.6	.312E-07
1522	281.7	.363E-07
1522	279.8	.405E-07
1523	277.9	.320E-07
1525	276.1	.103E-07
1530	274.2	.983E-09
1536	272.3	-.299E-09
1543	270.5	-.834E-09
1552	268.7	.864E-08
1563	266.9	.835E-08
1575	265.1	.156E-07
1588	263.4	.253E-07
1603	261.7	.516E-07
1620	260.0	.646E-07
1638	258.3	.231E-07
1657	256.7	.114E-07
1677	255.2	.119E-08
1699	253.6	-.192E-08
1722	252.1	.122E-08
1746	250.7	.000

Period 1-83, θ_L = 200.1°

1983 NEAR-SURFACE OIL FOG PROFILE
Min El. = -7.4 m — Period # 1
Max El. = 42.6 m — Azimuth 200.1

Horizontal Profile (50.0 m res.)

ρ_s(m)	θ_s (°)	χ/Q (s m^{-3})
2203	303.8	.000
2192	302.5	-.517E-08
2182	301.3	-.279E-08
2172	300.0	.432E-07
2164	298.7	.102E-07
2158	297.3	.183E-07
2152	296.0	.153E-08
2147	294.7	.000
2144	293.4	.000
2142	292.0	.000
2141	290.7	.000
2141	289.3	.000
2142	288.0	-.116E-08
2144	286.7	.869E-08
2148	285.3	.456E-07
2153	284.0	.490E-07
2158	282.7	.463E-07
2165	281.4	.332E-07
2174	280.1	.613E-08
2183	278.8	.204E-07
2193	277.5	.126E-07
2205	276.2	.190E-07
2217	275.0	.106E-07
2231	273.7	.112E-07
2245	272.5	.511E-08
2261	271.3	.360E-08
2277	270.1	.576E-08
2295	268.9	.193E-07
2314	267.8	.222E-07
2333	266.7	.190E-07
2353	265.5	.219E-07
2375	264.4	.369E-07
2397	263.4	.384E-07
2419	262.3	.206E-07
2443	261.3	.183E-07
2468	260.3	.456E-07
2493	259.3	.220E-07
2519	258.3	.789E-08
2546	257.3	.385E-07
2573	256.4	.252E-07
2601	255.5	-.613E-11
2630	254.6	.000

Period 2-83, θ_L = 169.9°

1983 NEAR-SURFACE OIL FOG PROFILE
Min El. = 17.6 m — Period # 2
Max El. = 27.6 m — Azimuth 169.9

Horizontal Profile (50.0 m res.)

ρ_s(m)	θ_s (°)	χ/Q (s m^{-3})
474	329.4	-.518E-07
428	327.0	.518E-07
382	324.1	.406E-05
338	320.4	.851E-05
296	315.6	.228E-04
256	309.3	.111E-04
220	300.8	.485E-04
191	289.5	.218E-04
172	274.8	.753E-04
166	257.9	.254E-04
175	241.4	.206E-05
197	227.5	.141E-05
228	216.8	.000

Period 2-83, θ_L = 174.0°

1983 NEAR-SURFACE OIL FOG PROFILE
Min El. = 27.6 m — Period # 2
Max El. = 52.6 m — Azimuth 174.0

Horizontal Profile (50.0 m res.)

ρ_s(m)	θ_s (°)	χ/Q (s m^{-3})
1397	335.2	.000
1350	334.5	.101E-08
1303	333.8	.365E-07
1256	333.0	.589E-07
1209	332.1	.172E-06
1163	331.2	.375E-06
1117	330.2	.277E-06
1072	329.1	.100E-06
1027	327.9	.884E-07
982	326.7	.295E-07
938	325.3	.160E-07
894	323.7	.928E-08
851	322.0	.341E-07
810	320.1	.154E-07
769	318.1	.143E-06
729	315.8	.799E-06
690	313.2	.873E-06
653	310.3	.753E-06
618	307.1	.340E-05
585	303.5	.505E-05
554	299.5	.320E-05
527	295.1	.287E-05
503	290.2	.533E-05
483	284.9	.540E-05
467	279.2	.207E-05
457	273.1	.200E-05
452	266.8	.111E-05
452	260.5	.118E-05
458	254.2	.115E-06
469	248.2	.000

Table A.3 (1-83/190° to 2-83/174°)

Period 2-83, θ_L = 181.1°

1983 NEAR-SURFACE OIL FOG PROFILE
Min El. = 22.6 m — Period # 2
Max El. = 72.6 m — Azimuth 181.1

Horizontal Profile (50.0 m res.)

ρ_s(m)	θ_s (°)	χ/Q (s m^{-3})
1714	328.0	.000
1672	327.1	.000
1631	326.1	.388E-09
1590	325.1	.520E-08
1550	324.0	.979E-08
1511	322.9	.777E-08
1472	321.7	.126E-07
1433	320.4	.371E-07
1396	319.0	.655E-07
1359	317.6	.142E-06
1323	316.1	.164E-06
1289	314.6	.295E-06
1255	312.9	.513E-06
1222	311.2	.419E-06
1190	309.3	.477E-06
1160	307.4	.534E-06
1131	305.3	.617E-06
1104	303.2	.598E-06
1078	300.9	.122E-05
1054	298.6	.184E-05
1032	296.1	.168E-05
1012	293.5	.249E-05
994	290.9	.213E-05
978	288.1	.186E-05
965	285.3	.117E-05
954	282.4	.114E-05
945	279.4	.102E-05
939	276.4	.422E-06
936	273.3	.123E-06
936	270.3	.172E-06
938	267.2	.527E-07
942	264.2	.318E-08
950	261.2	-.707E-08
960	258.2	-.520E-08
972	255.4	-.497E-08
987	252.6	-.854E-09
1004	249.9	.137E-07
1023	247.3	.126E-07
1044	244.7	-.112E-07
1067	242.3	-.202E-08

Period 2-83, θ_L = 190.0°

1983 NEAR-SURFACE OIL FOG PROFILE
Min El. = 17.6 m — Period # 2
Max El. = 67.6 m — Azimuth 190.0

Horizontal Profile (50.0 m res.)

ρ_s(m)	θ_s (°)	χ/Q (s m^{-3})
2204	326.4	.000
2168	325.5	.104E-08
2133	324.5	.188E-07
2098	323.5	.457E-07
2064	322.5	.556E-07
2030	321.5	.880E-07
1998	320.4	.577E-07
1966	319.3	.754E-07
1934	318.2	.620E-07
1904	317.0	.903E-07
1874	315.8	.171E-06
1845	314.5	.272E-06
1818	313.2	.310E-06
1791	311.9	.370E-06
1765	310.5	.471E-06
1740	309.1	.777E-06
1716	307.6	.905E-06
1694	306.1	.837E-06
1672	304.6	.906E-06
1652	303.0	.105E-05
1633	301.4	.110E-05
1616	299.7	.110E-05
1600	298.0	.903E-06
1585	296.3	.103E-05
1571	294.6	.836E-06
1560	292.8	.781E-06
1549	291.0	.646E-06
1541	289.2	.777E-06
1533	287.3	.532E-06
1528	285.5	.364E-06
1524	283.6	.195E-06
1522	281.7	.240E-06
1521	279.8	.346E-06
1522	277.9	.257E-06
1525	276.1	.269E-06
1529	274.2	.224E-06
1535	272.3	.218E-06
1542	270.5	.242E-06
1551	268.7	.151E-06
1562	266.9	.427E-07
1574	265.1	.241E-07
1588	263.4	.897E-09
1603	261.6	.000

Period 2-83, θ_L = 200.1°

1983 NEAR-SURFACE OIL FOG PROFILE
Min El. = 22.6 m — Period # 2
Max El. = 72.6 m — Azimuth 200.1

Horizontal Profile (50.0 m res.)

ρ_s(m)	θ_s (°)	χ/Q (s m^{-3})
2570	323.7	.000
2543	322.8	.132E-07
2516	321.8	.240E-07
2490	320.8	.195E-07
2465	319.8	.347E-07
2441	318.8	.792E-07
2417	317.8	.105E-06
2394	316.7	.139E-06
2372	315.6	.156E-06
2351	314.5	.166E-06
2331	313.4	.198E-06
2312	312.3	.389E-06
2293	311.1	.344E-06
2276	309.9	.243E-06
2260	308.7	.486E-06
2244	307.5	.492E-06
2230	306.3	.488E-06
2216	305.1	.536E-06
2204	303.8	.588E-06
2193	302.5	.585E-06
2182	301.2	.655E-06
2173	300.0	.597E-06
2165	298.6	.708E-06
2158	297.3	.601E-06
2153	296.0	.473E-06
2148	294.7	.464E-06
2145	293.4	.463E-06
2142	292.0	.498E-06
2141	290.7	.478E-06
2141	289.3	.318E-06
2143	288.0	.246E-06
2145	286.7	.255E-06
2149	285.3	.334E-06
2153	284.0	.250E-06
2159	282.7	.161E-06
2166	281.4	.221E-06
2175	280.1	.208E-06
2184	278.8	.262E-06
2194	277.5	.179E-06
2206	276.2	.178E-06
2218	275.0	.206E-06
2232	273.8	.194E-06
2246	272.5	.147E-06
2262	271.3	.101E-06
2278	270.1	.863E-07
2296	269.0	.639E-07
2315	267.8	.612E-07
2334	266.7	.669E-07
2354	265.6	.210E-07
2376	264.5	.518E-08
2398	263.4	.000
2421	262.3	.000

Period 2-83, θ_L = 210.0°

1983 NEAR-SURFACE OIL FOG PROFILE
Min El. = 22.6 m — Period # 2
Max El. = 72.6 m — Azimuth 210.0

Horizontal Profile (50.0 m res.)

ρ_s(m)	θ_s (°)	χ/Q (s m^{-3})
2922	323.3	.000
2903	322.4	.115E-08
2884	321.4	.549E-08
2867	320.5	.270E-07
2849	319.6	.261E-07
2833	318.6	.249E-07
2818	317.6	.372E-07
2803	316.7	.411E-07
2789	315.7	.527E-07
2776	314.7	.589E-07
2764	313.7	.805E-07
2752	312.7	.616E-07
2742	311.7	.718E-07
2732	310.6	.797E-07
2723	309.6	.983E-07
2715	308.6	.157E-06
2708	307.5	.277E-06
2702	306.5	.282E-06
2697	305.4	.291E-06
2693	304.3	.306E-06
2690	303.3	.366E-06
2687	302.2	.419E-06
2686	301.2	.412E-06
2685	300.1	.409E-06
2686	299.0	.372E-06
2687	298.0	.309E-06
2689	296.9	.285E-06
2693	295.8	.211E-06
2697	294.8	.198E-06
2702	293.7	.213E-06
2708	292.7	.245E-06
2715	291.6	.185E-06
2722	290.6	.128E-06
2731	289.5	.195E-06
2741	288.5	.164E-06
2751	287.5	.170E-06
2762	286.5	.156E-06
2774	285.5	.121E-06
2787	284.5	.177E-06
2801	283.5	.236E-06
2816	282.5	.249E-06
2831	281.6	.224E-06
2848	280.6	.209E-06
2865	279.7	.227E-06
2882	278.7	.206E-06
2901	277.8	.184E-06
2920	276.9	.210E-06
2940	276.0	.220E-06
2961	275.1	.216E-06
2982	274.2	.208E-06
3004	273.4	.152E-06
3027	272.5	.870E-07
3051	271.7	.837E-07
3075	270.9	.106E-06
3099	270.1	.116E-06
3125	269.3	.126E-06
3150	268.5	.138E-06
3177	267.7	.137E-07
3204	267.0	.000

Table A.3 (2-83/181.1° to 210°)

Period 3-83, θ_L =169.9°

1983 NEAR-SURFACE OIL FOG PROFILE
Min El. = 15.6 m Period # 3
Max El. = 25.6 m Azimuth 169.9

Horizontal Profile (50.0 m res.)

ρ_s(m)	θ_s (°)	χ/Q (s m^{-3})
617	334.4	.000
569	333.1	.000
521	331.5	.000
474	329.6	.000
427	327.2	.000
382	324.3	.000
337	320.7	.164E-07
295	315.9	.274E-08
255	309.6	.567E-06
219	301.1	.892E-05
190	289.7	.231E-04
170	275.0	.854E-05
165	257.9	.318E-04
174	241.2	.438E-04
195	227.2	.872E-05
226	216.5	.351E-05
263	208.5	.489E-06
304	202.6	.452E-07

Period 3-83, θ_L =174.0°

1983 NEAR-SURFACE OIL FOG PROFILE
Min El. = 25.6 m Period # 3
Max El. = 55.6 m Azimuth 174.0

Horizontal Profile (50.0 m res.)

ρ_s(m)	θ_s (°)	χ/Q (s m^{-3})
1350	334.5	.000
1303	333.8	.692E-08
1256	333.0	.889E-08
1209	332.1	.642E-08
1163	331.2	.185E-07
1117	330.2	.185E-07
1071	329.1	.148E-08
1026	328.0	.494E-09
982	326.7	.988E-09
938	325.3	-.247E-09
894	323.7	.321E-08
851	322.1	.284E-07
809	320.2	.278E-06
768	318.1	.179E-05
728	315.8	.126E-05
690	313.2	.412E-06
653	310.4	.606E-06
617	307.1	.118E-05
584	303.6	.521E-06
554	299.6	.327E-05
526	295.1	.518E-05
502	290.3	.317E-05
482	284.9	.347E-05
467	279.2	.791E-05
456	273.1	.572E-05
451	266.8	.539E-05
451	260.5	.328E-05
457	254.2	.261E-05
468	248.2	.141E-05
484	242.5	.144E-05
505	237.2	.945E-06
529	232.4	.113E-06
557	228.0	.198E-08
588	224.0	.000

Period 3-83, θ_L =181.1°

1983 NEAR-SURFACE OIL FOG PROFILE
Min El. = 22.6 m Period # 3
Max El. = 72.6 m Azimuth 181.1

Horizontal Profile (50.0 m res.)

ρ_s(m)	θ_s (°)	χ/Q (s m^{-3})
1884	331.4	.000
1841	330.6	-.469E-09
1798	329.8	.182E-08
1756	328.9	.703E-07
1714	328.1	.201E-06
1672	327.1	.224E-06
1631	326.1	.826E-07
1590	325.1	.702E-07
1550	324.0	.423E-07
1510	322.9	.128E-07
1471	321.7	.241E-08
1433	320.4	.323E-08
1396	319.1	.136E-07
1359	317.6	.388E-07
1323	316.2	.269E-07
1288	314.6	.202E-07
1254	312.9	.212E-07
1221	311.2	.370E-07
1190	309.3	.119E-06
1160	307.4	.236E-06
1131	305.4	.282E-06
1103	303.2	.290E-06
1078	301.0	.269E-06
1054	298.6	.401E-06
1032	296.1	.575E-06
1011	293.6	.657E-06
993	290.9	.376E-06
978	288.1	.343E-06
964	285.3	.462E-06
953	282.4	.871E-06
945	279.4	.131E-05
939	276.4	.146E-05
935	273.3	.182E-05
935	270.3	.188E-05
937	267.2	.165E-05
942	264.2	.150E-05
949	261.2	.150E-05
959	258.2	.134E-05
971	255.4	.851E-06
986	252.6	.576E-06
1003	249.8	.413E-06
1022	247.2	.310E-06
1043	244.7	.813E-07
1067	242.3	.113E-07
1092	240.0	-.469E-09

Period 3-83, θ_L =190.0°

1983 NEAR-SURFACE OIL FOG PROFILE
Min El. = 22.6 m Period # 3
Max El. = 72.6 m Azimuth 190.0

Horizontal Profile (50.0 m res.)

ρ_s(m)	θ_s (°)	χ/Q (s m^{-3})
2712	335.9	.000
2671	335.3	.130E-09
2630	334.7	.241E-08
2589	334.0	.149E-07
2549	333.4	.955E-08
2509	332.7	.110E-07
2469	332.0	.100E-07
2430	331.3	.323E-07
2391	330.5	.273E-07
2353	329.7	.146E-07
2315	328.9	.124E-07
2277	328.1	.396E-07
2241	327.3	.465E-07
2204	326.4	.434E-07
2168	325.5	.444E-07
2133	324.5	.430E-07
2098	323.5	.474E-07
2064	322.5	.482E-07
2030	321.5	.521E-07
1998	320.4	.459E-07
1966	319.3	.370E-07
1934	318.2	.437E-07
1904	317.0	.953E-07
1874	315.8	.721E-07
1845	314.5	.647E-07
1818	313.2	.944E-07
1791	311.9	.108E-06
1765	310.5	.136E-06
1740	309.1	.213E-06
1716	307.6	.258E-06
1694	306.1	.260E-06
1672	304.6	.254E-06
1652	303.0	.216E-06
1633	301.4	.188E-06
1616	299.7	.123E-06
1600	298.0	.165E-06
1585	296.3	.170E-06
1572	294.6	.119E-06
1560	292.8	.155E-06
1549	291.0	.219E-06
1541	289.2	.210E-06
1534	287.3	.207E-06
1528	285.5	.323E-06
1524	283.6	.625E-06
1522	281.7	.714E-06
1521	279.8	.589E-06
1522	277.9	.599E-06
1525	276.1	.718E-06
1529	274.2	.724E-06
1535	272.3	.830E-06
1542	270.5	.655E-06
1551	268.7	.540E-06
1562	266.9	.528E-06
1574	265.1	.530E-06

Table A.3 (3-83/169.9° to 190°)

Period 3-83, $\theta_L = 190.0°$

1983 NEAR-SURFACE OIL FOG PROFILE
Min El. = 22.6 m Period # 3
Max El. = 72.6 m Azimuth 190.0

Horizontal Profile (50.0 m res.)

ρ_s(m)	θ_s (°)	X/Q (s m^{-3})
1588	263.4	.432E-06
1603	261.6	.286E-06
1619	260.0	.315E-06
1637	258.3	.259E-06
1656	256.7	.115E-06
1676	255.1	.119E-06
1698	253.6	.652E-07
1721	252.1	.818E-07
1745	250.7	.594E-07
1770	249.3	.197E-07
1796	247.9	.119E-07
1823	246.6	.496E-08
1851	245.3	.110E-07
1880	244.0	-.215E-08
1910	242.8	-.260E-09
1940	241.6	.000

Period 3-83, $\theta_L = 200.1°$

1983 NEAR-SURFACE OIL FOG PROFILE
Min El. = 22.6 m Period # 3
Max El. = 72.6 m Azimuth 200.1

Horizontal Profile (50.0 m res.)

ρ_s(m)	θ_s (°)	X/Q (s m^{-3})
2748	328.9	.000
2717	328.1	.201E-09
2686	327.2	.154E-08
2656	326.4	.732E-08
2627	325.5	.191E-07
2598	324.6	.323E-07
2570	323.7	.455E-07
2543	322.7	.524E-07
2516	321.8	.711E-07
2491	320.8	.662E-07
2465	319.8	.552E-07
2441	318.8	.497E-07
2417	317.8	.652E-07
2395	316.7	.606E-07
2373	315.6	.540E-07
2352	314.5	.721E-07
2331	313.4	.124E-06
2312	312.3	.117E-06
2294	311.1	.128E-06
2276	309.9	.131E-06
2260	308.7	.128E-06
2244	307.5	.164E-06
2230	306.3	.179E-06
2217	305.1	.216E-06
2204	303.8	.209E-06
2193	302.5	.214E-06
2183	301.2	.216E-06
2174	300.0	.210E-06
2166	298.6	.208E-06
2159	297.3	.211E-06
2153	296.0	.322E-06
2149	294.7	.262E-06
2145	293.4	.191E-06
2143	292.0	.214E-06
2142	290.7	.255E-06
2142	289.3	.233E-06
2143	288.0	.166E-06
2146	286.7	.196E-06
2149	285.3	.210E-06
2154	284.0	.166E-06
2160	282.7	.115E-06
2167	281.4	.145E-06
2175	280.1	.148E-06
2184	278.8	.184E-06
2195	277.5	.258E-06
2206	276.3	.251E-06
2219	275.0	.233E-06
2232	273.8	.237E-06
2247	272.5	.301E-06
2262	271.3	.278E-06
2279	270.1	.233E-06
2297	269.0	.281E-06
2315	267.8	.314E-06
2335	266.7	.288E-06
2355	265.6	.265E-06
2376	264.5	.259E-06
2398	263.4	.207E-06
2421	262.3	.197E-06
2445	261.3	.184E-06
2469	260.3	.171E-06
2495	259.3	.149E-06
2521	258.3	.899E-07
2547	257.3	.719E-07
2575	256.4	.614E-07
2603	255.5	.453E-07
2632	254.6	.124E-07
2661	253.7	-.241E-09
2691	252.9	.000

Period 3-83, $\theta_L = 210.0°$

1983 NEAR-SURFACE OIL FOG PROFILE
Min El. = 32.6 m Period # 3
Max El. = 82.6 m Azimuth 210.0

Horizontal Profile (50.0 m res.)

ρ_s(m)	θ_s (°)	X/Q (s m^{-3})
3153	331.6	.000
3127	330.9	.140E-09
3102	330.1	.219E-08
3077	329.3	.169E-07
3053	328.4	.115E-07
3030	327.6	.346E-08
3007	326.8	.480E-08
2985	325.9	.745E-08
2963	325.0	.161E-07
2942	324.2	.249E-07
2922	323.3	.327E-07
2903	322.4	.286E-07
2884	321.4	.279E-07
2866	320.5	.429E-07
2849	319.6	.611E-07
2833	318.6	.774E-07
2817	317.6	.909E-07
2803	316.7	.813E-07
2789	315.7	.739E-07
2776	314.7	.734E-07
2763	313.7	.844E-07
2752	312.7	.841E-07
2741	311.7	.881E-07
2732	310.6	.896E-07
2723	309.6	.893E-07
2715	308.6	.100E-06
2708	307.5	.973E-07
2702	306.5	.101E-06
2697	305.4	.998E-07
2693	304.3	.107E-06
2689	303.3	.114E-06
2687	302.2	.120E-06
2686	301.2	.121E-06
2685	300.1	.109E-06
2686	299.0	.901E-07
2687	298.0	.797E-07
2689	296.9	.914E-07
2692	295.8	.973E-07
2696	294.8	.105E-06
2701	293.7	.969E-07
2707	292.7	.110E-06
2714	291.6	.117E-06
2722	290.6	.128E-06
2731	289.5	.128E-06
2740	288.5	.150E-06
2751	287.5	.157E-06
2762	286.5	.160E-06
2774	285.5	.164E-06
2787	284.5	.185E-06
2801	283.5	.196E-06
2816	282.5	.206E-06
2831	281.5	.199E-06
2847	280.6	.189E-06
2864	279.7	.182E-06
2882	278.7	.173E-06
2901	277.8	.179E-06
2920	276.9	.195E-06
2940	276.0	.197E-06
2961	275.1	.194E-06
2982	274.2	.211E-06
3004	273.4	.207E-06
3027	272.5	.201E-06
3050	271.7	.195E-06
3074	270.9	.209E-06
3099	270.1	.225E-06
3124	269.3	.189E-06
3150	268.5	.156E-06
3176	267.7	.137E-06
3203	267.0	.103E-06
3231	266.2	.776E-07
3259	265.5	.753E-07
3288	264.8	.704E-07
3317	264.1	.625E-07
3346	263.4	.527E-07
3376	262.7	.388E-07
3407	262.0	.332E-07
3438	261.4	.270E-07
3469	260.7	.219E-07
3501	260.1	.282E-07
3534	259.5	.243E-07
3566	258.9	.285E-07
3599	258.3	.314E-07
3633	257.7	.142E-07
3667	257.1	.332E-08
3701	256.5	.340E-08
3735	256.0	.123E-08
3770	255.4	.000

Table A.3 (3-83/190° cont. to 210°)

Period 4-83, θ_L =169.9°

1983 NEAR-SURFACE OIL FOG PROFILE
Min El. = 32.6 m Period # 4
Max El. = 57.6 m Azimuth 169.9

Horizontal Profile (50.0 m res.)

ρ_s(m)	θ_s (°)	χ/Q (s m^{-3})
1902	344.9	.000
1852	344.8	.136E-08
1802	344.6	.273E-07
1752	344.5	.273E-07
1702	344.3	.170E-07
1653	344.2	.681E-08
1603	344.0	.116E-07
1553	343.8	.307E-07
1503	343.6	.184E-07
1454	343.4	.409E-07
1404	343.1	.634E-07
1354	342.9	.600E-07
1305	342.6	.872E-07
1255	342.3	.940E-07
1206	342.0	.995E-07
1156	341.7	.114E-06
1107	341.3	.886E-07
1057	340.9	.118E-06
1008	340.5	.168E-06
959	340.0	.253E-06
909	339.4	.214E-06
860	338.8	.216E-06
811	338.2	.315E-06
762	337.4	.183E-06
714	336.5	.223E-06
665	335.5	.292E-06
617	334.4	.192E-06
569	333.0	.528E-06
521	331.4	.279E-05
474	329.5	.558E-05
427	327.2	.583E-05
382	324.3	.108E-04
337	320.6	.379E-05
295	315.9	.227E-05
255	309.6	.199E-04
219	301.1	.203E-04
190	289.7	.411E-05
171	274.9	.506E-05
165	257.9	.218E-04
174	241.2	.514E-05
196	227.2	.277E-06
227	216.5	.221E-06
264	208.6	.375E-07
304	202.7	.000

Period 4-83, θ_L =173.0°

1983 NEAR-SURFACE OIL FOG PROFILE
Min El. = 22.6 m Period # 4
Max El. = 52.6 m Azimuth 173.0

Horizontal Profile (50.0 m res.)

ρ_s(m)	θ_s (°)	χ/Q (s m^{-3})
1869	341.2	.000
1820	340.9	.934E-08
1771	340.6	.210E-07
1722	340.2	.199E-07
1673	339.8	.294E-07
1625	339.4	.620E-07
1576	339.0	.755E-07
1528	338.6	.126E-06
1479	338.1	.174E-06
1431	337.6	.136E-06
1383	337.0	.133E-06
1335	336.4	.136E-06
1287	335.8	.988E-07
1240	335.1	.766E-07
1192	334.4	.784E-07
1145	333.6	.951E-07
1098	332.7	.128E-06
1051	331.7	.102E-06
1005	330.7	.202E-06
959	329.6	.674E-06
913	328.3	.806E-06
868	326.9	.788E-06
823	325.4	.638E-06
779	323.7	.119E-05
736	321.8	.135E-05
694	319.7	.184E-05
652	317.2	.112E-05
613	314.5	.507E-06
574	311.4	.616E-06
538	307.9	.698E-06
504	303.8	.149E-05
473	299.2	.112E-05
445	294.0	.108E-05
421	288.2	.161E-05
403	281.8	.388E-05
389	274.8	.499E-06
382	267.4	.982E-06
382	259.9	.156E-05
388	252.5	.176E-06
400	245.5	.141E-07
418	238.9	.000

Period 4-83, θ_L =177.4°

1983 NEAR-SURFACE OIL FOG PROFILE
Min El. = 7.6 m Period # 4
Max El. = 57.6 m Azimuth 177.4

Horizontal Profile (50.0 m res.)

ρ_s(m)	θ_s (°)	χ/Q (s m^{-3})
2245	339.7	.000
2198	339.3	.839E-09
2150	338.9	.382E-08
2103	338.4	.308E-08
2056	338.0	.619E-08
2009	337.5	.103E-07
1962	337.0	.149E-07
1915	336.5	.212E-07
1868	335.9	.205E-07
1822	335.3	.314E-07
1776	334.7	.378E-07
1730	334.1	.438E-07
1684	333.4	.757E-07
1638	332.7	.125E-06
1593	332.0	.156E-06
1548	331.2	.240E-06
1503	330.3	.289E-06
1459	329.4	.236E-06
1415	328.5	.171E-06
1372	327.5	.172E-06
1328	326.4	.170E-06
1286	325.2	.219E-06
1244	324.0	.189E-06
1202	322.7	.306E-06
1162	321.3	.374E-06
1122	319.8	.467E-06
1082	318.2	.427E-06
1044	316.4	.524E-06
1007	314.6	.615E-06
971	312.6	.914E-06
936	310.4	.995E-06
903	308.1	.613E-06
871	305.6	.947E-06
841	302.9	.984E-06
813	300.1	.757E-06
787	297.0	.324E-06
764	293.7	.131E-06
743	290.3	.136E-06
725	286.6	.655E-07
710	282.8	.563E-07
699	278.8	.750E-07
690	274.8	.454E-07
686	270.6	.304E-07
685	266.4	.665E-08
688	262.3	.892E-08
694	258.2	.106E-08
704	254.1	.000

Period 4-83, θ_L =183.1°

1983 NEAR-SURFACE OIL FOG PROFILE
Min El. = 2.6 m Period # 4
Max El. = 52.6 m Azimuth 183.1

Horizontal Profile (50.0 m res.)

ρ_s(m)	θ_s (°)	χ/Q (s m^{-3})
2447	337.2	.000
2402	336.7	.151E-07
2358	336.1	.315E-07
2313	335.6	.402E-07
2269	335.0	.574E-07
2225	334.4	.633E-07
2181	333.8	.694E-07
2138	333.1	.599E-07
2095	332.4	.833E-07
2052	331.7	.115E-06
2009	331.0	.105E-06
1967	330.2	.163E-06
1925	329.4	.231E-06
1884	328.5	.255E-06
1843	327.7	.245E-06
1803	326.7	.253E-06
1763	325.8	.269E-06
1723	324.8	.229E-06
1684	323.7	.220E-06
1646	322.6	.238E-06
1608	321.4	.210E-06
1571	320.2	.239E-06
1535	319.0	.221E-06
1499	317.6	.178E-06
1465	316.2	.164E-06
1431	314.8	.256E-06
1398	313.2	.370E-06
1367	311.6	.416E-06
1336	310.0	.263E-06
1307	308.2	.255E-06
1279	306.4	.254E-06
1252	304.5	.201E-06
1227	302.5	.153E-06
1203	300.4	.188E-06
1181	298.2	.354E-06
1161	296.0	.404E-06
1142	293.7	.512E-06
1125	291.3	.331E-06
1111	288.8	.267E-06
1098	286.3	.165E-06
1088	283.8	.139E-06
1080	281.2	.679E-07
1074	278.5	.410E-07
1070	275.9	.144E-07
1069	273.2	-.492E-08
1070	270.5	.000

Table A.3 (4-83/169.9° to 183.1°)

Period 4-83, θ_L =195.0°

1983 NEAR-SURFACE OIL FOG PROFILE
Min El. = -2.4 m Period # 4
Max El. = 47.6 m Azimuth 195.0

Horizontal Profile (50.0 m res.)

ρ_s(m)	θ_s (°)	χ/Q (s m^{-3})
3060	338.2	.000
3020	337.6	.115E-08
2981	337.0	.940E-08
2941	336.4	.111E-07
2902	335.8	.119E-07
2864	335.2	.205E-07
2826	334.5	.386E-07
2788	333.8	.551E-07
2750	333.2	.729E-07
2713	332.4	.452E-07
2677	331.7	.802E-07
2641	331.0	.130E-06
2605	330.2	.172E-06
2570	329.4	.300E-06
2535	328.6	.342E-06
2501	327.8	.283E-06
2467	326.9	.294E-06
2434	326.1	.319E-06
2401	325.2	.353E-06
2369	324.2	.359E-06
2338	323.3	.429E-06
2308	322.3	.501E-06
2278	321.3	.577E-06
2248	320.3	.612E-06
2220	319.2	.593E-06
2192	318.2	.570E-06
2165	317.0	.408E-06
2139	315.9	.339E-06
2114	314.7	.308E-06
2090	313.6	.352E-06
2066	312.3	.326E-06
2044	311.1	.219E-06
2022	309.8	.259E-06
2002	308.5	.273E-06
1982	307.2	.174E-06
1964	305.8	.888E-07
1947	304.5	.570E-07
1931	303.1	.242E-07
1916	301.7	.528E-07
1902	300.2	.180E-06
1890	298.7	.400E-07
1878	297.3	.455E-07
1868	295.8	.461E-07
1860	294.2	.384E-07
1852	292.7	.522E-07
1846	291.2	.679E-07
1842	289.6	.405E-07
1838	288.1	.589E-08
1836	286.5	.000

Period 5-83, θ_L =169.9°

1983 NEAR-SURFACE OIL FOG PROFILE
Min El. = 12.6 m Period # 5
Max El. = 22.6 m Azimuth 169.9

Horizontal Profile (50.0 m res.)

ρ_s(m)	θ_s (°)	χ/Q (s m^{-3})
1833	341.1	.000
1783	340.8	.789E-08
1734	340.6	.671E-08
1684	340.3	.829E-08
1635	340.0	.750E-08
1586	339.7	.237E-08
1537	339.4	.276E-08
1488	339.0	.118E-08
1439	338.6	-.118E-08
1390	338.2	-.315E-08
1341	337.8	-.394E-09
1292	337.3	.118E-08
1243	336.8	.237E-08
1194	336.3	.394E-09
1146	335.7	.000
1097	335.1	.000
1049	334.4	.000
1001	333.6	.000
953	332.8	.000
906	331.8	.000
858	330.8	.000
811	329.6	.000
764	328.3	.000
718	326.9	.000
672	325.2	.000
627	323.3	.000
583	321.1	.000
540	318.5	.000
498	315.6	.789E-09
457	312.0	.150E-07
419	307.8	.134E-06
383	302.8	.158E-07
351	296.8	.711E-08
323	289.7	.182E-07
302	281.5	.158E-08
287	272.1	-.394E-09
281	262.1	.000
283	252.0	.000
294	242.3	.000

Period 5-83, θ_L =174.0°

1983 NEAR-SURFACE OIL FOG PROFILE
Min El. = 22.6 m Period # 5
Max El. = 52.6 m Azimuth 174.0

Horizontal Profile (50.0 m res.)

ρ_s(m)	θ_s (°)	χ/Q (s m^{-3})
1586	332.9	.000
1540	332.3	-.374E-08
1494	331.5	-.149E-08
1447	330.8	.867E-08
1402	330.0	.332E-07
1356	329.1	.160E-06
1311	328.2	.324E-07
1266	327.2	.867E-08
1222	326.2	.248E-07
1178	325.0	.308E-07
1134	323.8	.239E-07
1091	322.5	.720E-07
1049	321.1	.132E-06
1007	319.5	.332E-06
967	317.8	.900E-06
927	316.0	.135E-05
888	314.0	.173E-05
850	311.9	.232E-05
814	309.5	.240E-05
779	306.9	.208E-05
746	304.1	.177E-05
715	301.0	.944E-06
686	297.7	.978E-06
659	294.1	.959E-06
636	290.2	.478E-05
615	286.0	.272E-05
598	281.5	.240E-05
585	276.9	.135E-05
576	272.0	.106E-05
571	267.0	.572E-07
571	262.0	.793E-07
575	257.0	.562E-07
583	252.2	.236E-07
595	247.4	.256E-07
611	242.9	.941E-08
631	238.7	.000

Period 5-83, θ_L =178.9°

1983 NEAR-SURFACE OIL FOG PROFILE
Min El. = 22.6 m Period # 5
Max El. = 52.6 m Azimuth 178.9

Horizontal Profile (50.0 m res.)

ρ_s(m)	θ_s (°)	χ/Q (s m^{-3})
1770	327.9	.000
1727	327.1	.000
1685	326.2	.202E-07
1643	325.2	.132E-06
1601	324.2	.134E-06
1561	323.2	.913E-07
1520	322.1	.734E-07
1481	320.9	.782E-07
1442	319.7	.518E-06
1403	318.4	.756E-06
1366	317.0	.338E-06
1329	315.6	.245E-06
1293	314.1	.290E-06
1258	312.5	.279E-06
1224	310.8	.629E-06
1191	309.0	.616E-06
1160	307.1	.820E-06
1129	305.1	.175E-05
1101	303.0	.227E-05
1073	300.8	.138E-05
1048	298.5	.123E-05
1024	296.0	.104E-05
1002	293.5	.761E-06
983	290.8	.136E-05
965	288.1	.117E-05
950	285.2	.799E-06
937	282.3	.821E-06
927	279.3	.894E-06
919	276.2	.132E-05
914	273.1	.151E-05
912	270.0	.123E-05
912	266.8	.680E-06
915	263.7	.427E-06
921	260.6	.205E-06
930	257.6	.186E-06
941	254.6	.545E-07
955	251.7	.231E-07
971	248.8	.000
989	246.1	-.249E-08
1009	243.5	.426E-09
1032	241.0	.000

Table A.3 (4-83/195° to 5-83/178.9°)

Period 5-83, θ_L = 183.1°

1983 NEAR-SURFACE OIL FOG PROFILE
Min El. = 22.6 m Period # 5
Max El. = 72.6 m Azimuth 183.1

Horizontal Profile (50.0 m res.)

ρ_s(m)	θ_s (°)	χ/Q (s m^{-3})
1796	321.3	.000
1759	320.2	.751E-08
1723	319.1	.675E-07
1688	317.9	.144E-06
1653	316.7	.138E-06
1619	315.4	.509E-06
1585	314.1	.339E-06
1553	312.7	.146E-06
1522	311.2	.145E-06
1491	309.7	.155E-06
1462	308.2	.245E-06
1434	306.5	.478E-06
1407	304.8	.493E-06
1381	303.1	.653E-06
1357	301.2	.678E-06
1334	299.3	.886E-06
1313	297.4	.809E-06
1293	295.4	.670E-06
1275	293.3	.824E-06
1259	291.1	.832E-06
1244	288.9	.761E-06
1231	286.7	.847E-06
1221	284.4	.993E-06
1212	282.1	.144E-05
1205	279.8	.155E-05
1200	277.4	.121E-05
1198	275.0	.926E-06
1197	272.6	.865E-06
1198	270.2	.731E-06
1202	267.8	.465E-06
1208	265.5	.246E-06
1215	263.1	.262E-06
1225	260.8	.375E-06
1237	258.6	.228E-06
1250	256.4	.197E-07
1265	254.2	.129E-07
1282	252.1	.142E-07
1301	250.0	.781E-07
1322	248.0	.864E-07
1344	246.1	.126E-07
1367	244.2	.000
1392	242.4	.000

Period 5-83, θ_L = 188.1°

1983 NEAR-SURFACE OIL FOG PROFILE
Min El. = 17.6 m Period # 5
Max El. = 67.6 m Azimuth 188.1

Horizontal Profile (50.0 m res.)

ρ_s(m)	θ_s (°)	χ/Q (s m^{-3})
1955	316.7	.000
1924	315.6	.117E-08
1894	314.4	.166E-07
1865	313.1	.255E-08
1836	311.9	.384E-07
1809	310.6	.114E-06
1783	309.2	.171E-06
1757	307.8	.331E-06
1733	306.4	.216E-06
1710	304.9	.160E-06
1688	303.4	.290E-06
1667	301.8	.446E-06
1648	300.2	.563E-06
1629	298.6	.140E-05
1612	296.9	.137E-05
1597	295.2	.102E-05
1583	293.5	.111E-05
1570	291.8	.138E-05
1559	290.0	.146E-05
1550	288.2	.163E-05
1542	286.3	.132E-05
1535	284.5	.635E-06
1531	282.6	.107E-05
1527	280.8	.103E-05
1526	278.9	.112E-05
1526	277.0	.952E-06
1528	275.1	.940E-06
1531	273.3	.700E-06
1536	271.4	.110E-05
1543	269.6	.806E-06
1551	267.7	.498E-06
1561	265.9	.244E-06
1572	264.1	.176E-06
1585	262.4	.252E-06
1599	260.7	.163E-06
1614	259.0	.164E-06
1631	257.3	.195E-06
1650	255.7	.148E-06
1670	254.1	.112E-06
1690	252.5	.976E-07
1713	251.0	-.316E-08
1736	249.6	-.178E-08
1760	248.1	-.186E-07
1786	246.7	-.225E-07
1812	245.4	-.375E-07
1840	244.1	-.799E-08
1868	242.8	.000

Period 6-83, θ_L = 169.9°

1983 NEAR-SURFACE OIL FOG PROFILE
Min El. = 17.6 m Period # 6
Max El. = 37.6 m Azimuth 169.9

Horizontal Profile (50.0 m res.)

ρ_s(m)	θ_s (°)	χ/Q (s m^{-3})
1635	340.0	.000
1586	339.7	.000
1537	339.4	.000
1488	339.0	.000
1439	338.6	.000
1390	338.2	-.175E-08
1341	337.8	.141E-07
1292	337.3	.496E-07
1243	336.8	.230E-07
1194	336.3	.105E-06
1146	335.7	.952E-06
1097	335.1	.514E-06
1049	334.4	-.177E-07
1001	333.6	.620E-07
953	332.8	.147E-06
905	331.8	.494E-06
858	330.8	.595E-06
811	329.6	.615E-06
764	328.3	.743E-06
718	326.9	.764E-06
672	325.2	.711E-06
627	323.3	.193E-05
583	321.1	.408E-06
540	318.6	.120E-05
498	315.6	.307E-06
457	312.0	.152E-06
419	307.8	.673E-07
383	302.8	-.349E-08
351	296.8	.000
323	289.7	.000
302	281.5	.000

Period 6-83, θ_L = 174.0°

1983 NEAR-SURFACE OIL FOG PROFILE
Min El. = 22.6 m Period # 6
Max El. = 57.6 m Azimuth 174.0

Horizontal Profile (50.0 m res.)

ρ_s(m)	θ_s (°)	χ/Q (s m^{-3})
1822	335.8	.000
1775	335.2	.203E-07
1727	334.7	.998E-07
1680	334.2	.735E-07
1633	333.6	.373E-07
1586	332.9	.154E-06
1540	332.3	.610E-06
1494	331.5	.779E-06
1448	330.8	.126E-05
1402	330.0	.744E-06
1356	329.1	.469E-06
1311	328.2	.388E-06
1266	327.2	.581E-06
1222	326.2	.445E-06
1178	325.0	.440E-06
1134	323.8	.452E-06
1091	322.5	.121E-05
1049	321.1	.159E-05
1007	319.5	.128E-05
967	317.8	.745E-06
927	316.0	.185E-05
888	314.0	.360E-05
850	311.8	.956E-05
814	309.5	.550E-05
779	306.9	.152E-05
746	304.1	.597E-06
715	301.0	.769E-06
686	297.7	.169E-05
659	294.1	.291E-05
636	290.2	.240E-05
615	286.0	.186E-05
599	281.5	.131E-05
585	276.9	.812E-06
576	272.0	.118E-06
572	267.0	.167E-07
571	262.0	.344E-07
575	257.0	-.227E-07
583	252.2	-.657E-08
595	247.4	-.149E-08
612	243.0	.000

Table A.3 (5-83/183.1° to 6-83/174°)

Period 6-83, θ_L =178.9°

1983 NEAR-SURFACE OIL FOG PROFILE
Min El. = 7.6 m Period # 6
Max El. = 57.6 m Azimuth 178.9

Horizontal Profile (50.0 m res.)

ρ_s(m)	θ_s (°)	χ/Q (s m^{-3})
2259	335.1	.000
2213	334.6	.237E-07
2167	334.1	.838E-07
2122	333.5	.469E-07
2077	332.9	.252E-07
2032	332.3	.106E-06
1988	331.6	.114E-06
1943	331.0	.997E-07
1899	330.3	.155E-06
1856	329.5	.159E-06
1812	328.8	.909E-07
1769	327.9	.983E-07
1726	327.1	.307E-06
1684	326.2	.497E-06
1642	325.2	.298E-06
1601	324.3	.432E-06
1560	323.2	.311E-06
1520	322.1	.464E-06
1480	321.0	.548E-06
1441	319.7	.100E-05
1402	318.4	.113E-05
1365	317.1	.136E-05
1328	315.6	.129E-05
1292	314.1	.205E-05
1257	312.5	.167E-05
1223	310.8	.809E-06
1190	309.0	.604E-06
1159	307.1	.801E-06
1128	305.1	.674E-06
1100	303.0	.583E-06
1072	300.8	.806E-06
1047	298.5	.100E-05
1023	296.1	.731E-06
1001	293.5	.503E-06
981	290.9	.546E-06
964	288.1	.122E-05
948	285.3	.113E-05
936	282.3	.515E-06
925	279.3	.104E-05
918	276.2	.677E-06
913	273.1	.138E-06
910	270.0	.513E-08
911	266.8	.000

Period 6-83, θ_L =183.1°

1983 NEAR-SURFACE OIL FOG PROFILE
Min El. = 12.6 m Period # 6
Max El. = 62.6 m Azimuth 183.2

Horizontal Profile (50.0 m res.)

ρ_s(m)	θ_s (°)	χ/Q (s m^{-3})
2899	338.7	.000
2853	338.3	.593E-09
2808	337.8	.444E-08
2763	337.4	.225E-07
2718	336.9	.183E-07
2673	336.5	.113E-07
2629	336.0	.556E-08
2584	335.5	.111E-09
2540	335.0	.333E-09
2496	334.4	.889E-09
2452	333.8	.155E-07
2409	333.3	.241E-07
2366	332.7	.286E-07
2323	332.0	.389E-07
2280	331.4	.591E-07
2238	330.7	.983E-07
2196	330.0	.190E-06
2154	329.3	.526E-06
2113	328.5	.109E-05
2072	327.7	.349E-06
2031	326.9	.426E-06
1991	326.1	.531E-06
1952	325.2	.580E-06
1912	324.3	.546E-06
1874	323.3	.382E-06
1836	322.3	.334E-06
1798	321.3	.246E-06
1761	320.2	.187E-06
1725	319.0	.172E-06
1689	317.9	.258E-06
1655	316.6	.517E-06
1621	315.4	.634E-06
1588	314.0	.688E-06
1555	312.6	.506E-06
1524	311.2	.591E-06
1494	309.7	.771E-06
1465	308.1	.119E-05
1436	306.5	.102E-05
1410	304.8	.904E-06
1384	303.0	.838E-06
1360	301.2	.836E-06
1337	299.3	.481E-06
1316	297.3	.352E-06
1296	295.3	.432E-06
1278	293.2	.528E-06
1262	291.1	.739E-06
1248	288.9	.950E-06
1235	286.7	.503E-06
1224	284.4	.249E-06
1216	282.1	.278E-06
1209	279.7	.322E-06
1204	277.4	.278E-06
1201	275.0	.209E-06
1201	272.6	.179E-06
1202	270.2	.111E-06
1206	267.9	.896E-08
1212	265.5	.000

Period 6-83, θ_L =188.0°

1983 NEAR-SURFACE OIL FOG PROFILE
Min El. = 7.6 m Period # 6
Max El. = 57.6 m Azimuth 188.0

Horizontal Profile (50.0 m res.)

ρ_s(m)	θ_s (°)	χ/Q (s m^{-3})
2695	333.6	.000
2654	333.0	.461E-08
2613	332.4	.318E-07
2573	331.7	.715E-07
2532	331.0	.778E-07
2493	330.3	.115E-06
2453	329.6	.179E-06
2414	328.9	.180E-06
2376	328.1	.142E-06
2338	327.3	.258E-06
2300	326.5	.874E-06
2263	325.7	.557E-06
2226	324.8	.529E-06
2190	323.9	.449E-06
2154	323.0	.398E-06
2119	322.1	.316E-06
2085	321.1	.380E-06
2051	320.0	.338E-06
2018	319.0	.332E-06
1985	317.9	.455E-06
1954	316.8	.460E-06
1923	315.6	.265E-06
1893	314.4	.284E-06
1863	313.2	.356E-06
1835	311.9	.233E-06
1808	310.6	.241E-06
1781	309.2	.330E-06
1756	307.8	.352E-06
1732	306.4	.275E-06
1708	304.9	.257E-06
1686	303.4	.198E-06
1666	301.9	.280E-06
1646	300.3	.195E-06
1628	298.6	.176E-06
1611	297.0	.237E-06
1595	295.3	.290E-06
1581	293.5	.229E-06
1568	291.8	.340E-06
1557	290.0	.345E-06
1548	288.2	.263E-06
1540	286.3	.174E-06
1533	284.5	.176E-06
1528	282.6	.372E-07
1525	280.8	.000

Period 7-83, θ_L =169.9°

1983 NEAR-SURFACE OIL FOG PROFILE
Min El. = 22.6 m Period # 7
Max El. = 42.6 m Azimuth 169.9

Horizontal Profile (50.0 m res.)

ρ_s(m)	θ_s (°)	χ/Q (s m^{-3})
1146	335.6	.000
1098	335.0	.193E-06
1050	334.3	.145E-06
1002	333.5	.281E-06
954	332.7	.673E-06
906	331.7	.234E-06
859	330.7	.212E-06
812	329.5	.668E-06
765	328.2	.303E-06
719	326.7	.178E-06
673	325.1	.178E-06
628	323.2	.135E-06
584	320.9	.252E-06
541	318.4	.621E-06
499	315.4	.466E-06
458	311.8	.434E-06
420	307.6	.133E-05
385	302.6	.212E-05
353	296.6	.199E-06
325	289.5	.835E-07
304	281.3	-.111E-07
289	272.0	-.229E-07
283	262.1	-.315E-07
285	252.0	.278E-07
296	242.4	.649E-07
315	233.7	-.988E-08
340	226.1	.179E-08
370	219.7	.597E-09
404	214.3	.491E-08
442	209.7	.365E-08
481	205.9	.000

Table A.3 (6-83/178.9° to 7-83/169.9°)

Period 7-83, θ_L =174.0°

1983 NEAR-SURFACE OIL FOG PROFILE		
Min El. = 22.6 m		Period # 7
Max El. = 72.6 m		Azimuth 174.0
Horizontal Profile (50.0 m res.)		
ρ_s(m)	θ_s (°)	χ/Q (s m^{-3})
1822	335.8	.000
1774	335.3	-.352E-09
1727	334.7	.313E-07
1680	334.2	.278E-07
1633	333.6	.618E-07
1586	332.9	.640E-07
1540	332.3	.701E-07
1493	331.6	.900E-07
1447	330.8	.992E-07
1402	330.0	.773E-07
1356	329.1	.272E-06
1311	328.2	.439E-06
1266	327.2	.145E-05
1222	326.2	.152E-05
1178	325.0	.153E-05
1134	323.8	.945E-06
1091	322.5	.940E-06
1049	321.1	.135E-05
1007	319.5	.142E-05
967	317.8	.140E-05
927	316.0	.894E-06
888	314.0	.629E-06
850	311.9	.542E-06
814	309.5	.565E-06
779	306.9	.482E-06
746	304.1	.521E-06
714	301.0	.546E-06
685	297.7	.482E-06
659	294.1	.919E-06
635	290.2	.600E-06
615	286.0	.138E-05
598	281.5	.282E-05
585	276.9	.375E-05
576	272.0	.220E-05
571	267.0	.755E-06
571	262.0	.281E-07
575	257.0	.000

Period 7-83, θ_L =178.9°

1983 NEAR-SURFACE OIL FOG PROFILE		
Min El. = 22.6 m		Period # 7
Max El. = 57.6 m		Azimuth 178.9
Horizontal Profile (50.0 m res.)		
ρ_s(m)	θ_s (°)	χ/Q (s m^{-3})
1988	331.6	.000
1943	331.0	.000
1899	330.3	.135E-07
1856	329.5	.518E-07
1812	328.8	.784E-07
1769	327.9	.781E-07
1726	327.1	.862E-07
1684	326.2	.836E-07
1642	325.2	.104E-06
1601	324.3	.139E-06
1560	323.2	.186E-06
1520	322.1	.185E-06
1480	321.0	.259E-06
1441	319.7	.294E-06
1402	318.4	.832E-06
1365	317.1	.184E-05
1328	315.6	.424E-06
1292	314.1	.218E-06
1257	312.5	.414E-06
1223	310.8	.280E-06
1190	309.0	.283E-06
1159	307.1	.533E-06
1128	305.1	.803E-06
1100	303.0	.111E-05
1072	300.8	.822E-06
1047	298.5	.629E-06
1023	296.1	.650E-06
1001	293.5	.145E-05
981	290.9	.148E-05
964	288.1	.220E-05
948	285.3	.173E-05
936	282.3	.135E-05
925	279.3	.143E-05
918	276.2	.946E-06
913	273.1	.581E-06
910	270.0	.711E-06
911	266.8	.250E-06
914	263.7	.967E-07
920	260.6	.178E-08

Period 7-83, θ_L =183.1°

1983 NEAR-SURFACE OIL FOG PROFILE		
Min El. = 12.6 m		Period # 7
Max El. = 62.6 m		Azimuth 183.1
Horizontal Profile (50.0 m res.)		
ρ_s(m)	θ_s (°)	χ/Q (s m^{-3})
2153	329.3	.000
2112	328.6	.847E-08
2071	327.8	.561E-07
2030	327.0	.140E-06
1990	326.1	.149E-06
1950	325.2	.132E-06
1911	324.3	.138E-06
1872	323.4	.114E-06
1834	322.4	.241E-06
1797	321.3	.378E-06
1760	320.2	.427E-06
1723	319.1	.402E-06
1688	317.9	.534E-06
1653	316.7	.642E-06
1619	315.4	.503E-06
1586	314.1	.349E-06
1553	312.7	.218E-06
1522	311.2	.213E-06
1492	309.7	.184E-06
1462	308.1	.219E-06
1434	306.5	.151E-06
1407	304.8	.412E-06
1382	303.0	.625E-06
1357	301.2	.594E-06
1335	299.3	.712E-06
1313	297.4	.891E-06
1294	295.3	.102E-05
1275	293.3	.814E-06
1259	291.1	.115E-05
1245	288.9	.131E-05
1232	286.7	.127E-05
1221	284.4	.847E-06
1212	282.1	.957E-06
1205	279.8	.151E-05
1201	277.4	.146E-05
1198	275.0	.138E-05
1197	272.6	.108E-05
1199	270.2	.259E-06
1202	267.8	.435E-08
1208	265.5	-.473E-10
1216	263.1	.000

Period 7-83, θ_L =188.0°

1983 NEAR-SURFACE OIL FOG PROFILE		
Min El. = 12.6 m		Period # 7
Max El. = 62.6 m		Azimuth 188.0
Horizontal Profile (50.0 m res.)		
ρ_s(m)	θ_s (°)	χ/Q (s m^{-3})
2414	328.9	.000
2375	328.1	.948E-09
2337	327.4	.155E-07
2299	326.5	.723E-07
2262	325.7	.600E-07
2226	324.8	.720E-07
2189	323.9	.115E-06
2154	323.0	.207E-06
2119	322.1	.317E-06
2084	321.1	.318E-06
2050	320.1	.266E-06
2017	319.0	.397E-06
1985	317.9	.589E-06
1953	316.8	.776E-06
1922	315.6	.629E-06
1892	314.4	.420E-06
1863	313.2	.662E-06
1834	311.9	.723E-06
1807	310.6	.527E-06
1781	309.2	.532E-06
1755	307.8	.676E-06
1731	306.4	.635E-06
1708	304.9	.352E-06
1685	303.4	.224E-06
1665	301.9	.444E-06
1645	300.3	.557E-06
1627	298.6	.829E-06
1610	297.0	.117E-05
1594	295.3	.626E-06
1580	293.5	.377E-06
1567	291.8	.403E-06
1556	290.0	.282E-06
1547	288.2	.737E-06
1539	286.4	.612E-06
1532	284.5	.603E-06
1527	282.6	.782E-06
1524	280.8	.965E-06
1523	278.9	.100E-05
1523	277.0	.993E-06
1524	275.1	.634E-06
1528	273.2	.340E-06
1533	271.4	.153E-06
1539	269.5	.999E-08
1547	267.7	.000

Table A.3 (7-83/174° to 188°)

Period 8-83, θ_L =168.4°

1983 NEAR-SURFACE OIL FOG PROFILE
Min El. = 7.6 m Period # 8
Max El. = 32.6 m Azimuth 168.4

Horizontal Profile (50.0 m res.)

ρ_s(m)	θ_s (°)	χ/Q (s m^{-3})
211	291.9	.000
188	279.1	.000
176	263.7	.000
179	247.6	.000

Period 8-83, θ_L =172.3°

1983 NEAR-SURFACE OIL FOG PROFILE
Min El. = 7.6 m Period # 8
Max El. = 32.6 m Azimuth 172.3

Horizontal Profile (50.0 m res.)

ρ_s(m)	θ_s (°)	χ/Q (s m^{-3})
492	285.7	.000
474	280.1	.000
462	274.2	.000
454	268.0	.000

Period 8-83, θ_L =176.1°

1983 NEAR-SURFACE OIL FOG PROFILE
Min El. = 22.6 m Period # 8
Max El. = 57.6 m Azimuth 176.1

Horizontal Profile (50.0 m res.)

ρ_s(m)	θ_s (°)	χ/Q (s m^{-3})
1006	310.7	-.657E-09
972	308.6	.263E-08
939	306.3	.493E-08
907	303.9	.329E-08
877	301.3	.395E-08
850	298.6	.362E-08
824	295.7	-.657E-09
800	292.5	-.164E-08
779	289.2	-.230E-08
761	285.8	-.657E-09
746	282.2	.000
733	278.4	-.263E-08
724	274.5	.362E-08
719	270.6	.247E-07
717	266.6	.474E-07
718	262.6	.657E-09
723	258.7	-.164E-08
731	254.8	-.657E-09
742	251.0	.000
757	247.3	.000

Period 8-83, θ_L =178.9°

1983 NEAR-SURFACE OIL FOG PROFILE
Min El. = 22.6 m Period # 8
Max El. = 57.6 m Azimuth 178.9

Horizontal Profile (50.0 m res.)

ρ_s(m)	θ_s (°)	χ/Q (s m^{-3})
1047	298.5	.000
1023	296.0	.452E-08
1001	293.5	.864E-08
982	290.8	.851E-08
964	288.1	.275E-08
949	285.2	.824E-08
936	282.3	.754E-07
926	279.3	.144E-06
918	276.2	.241E-06
913	273.1	.720E-06
911	269.9	.192E-06
911	266.8	.491E-07
915	263.7	.124E-07
920	260.6	.506E-08
929	257.5	.522E-08
940	254.5	.178E-08
954	251.6	.112E-06
970	248.8	.504E-07
988	246.1	.122E-08
1009	243.5	.000

Period 8-83, θ_L =183.1°

1983 NEAR-SURFACE OIL FOG PROFILE
Min El. = 19.6 m Period # 8
Max El. = 69.6 m Azimuth 183.1

Horizontal Profile (50.0 m res.)

ρ_s(m)	θ_s (°)	χ/Q (s m^{-3})
1491	309.7	.000
1462	308.1	.121E-07
1434	306.5	.143E-07
1407	304.8	.250E-07
1381	303.0	.248E-07
1357	301.2	.749E-08
1334	299.3	.302E-08
1313	297.4	.949E-08
1293	295.3	.375E-08
1275	293.3	.807E-08
1259	291.1	.979E-08
1244	288.9	.825E-08
1232	286.7	.176E-06
1221	284.4	.380E-06
1212	282.1	.723E-06
1205	279.7	.967E-06
1201	277.4	.725E-06
1198	275.0	.428E-06
1197	272.6	.329E-06
1199	270.2	.218E-06
1203	267.8	.141E-06
1208	265.5	.262E-06
1216	263.1	.371E-06
1226	260.8	.289E-06
1237	258.6	.413E-06
1251	256.3	.533E-06
1266	254.2	.252E-06
1283	252.1	.137E-06
1302	250.0	.198E-06
1322	248.0	.116E-07
1344	246.1	.000

Period 8-83, θ_L =188.0°

1983 NEAR-SURFACE OIL FOG PROFILE
Min El. = 20.6 m Period # 8
Max El. = 70.6 m Azimuth 188.0

Horizontal Profile (50.0 m res.)

ρ_s(m)	θ_s (°)	χ/Q (s m^{-3})
1685	303.4	.000
1664	301.9	-.557E-10
1644	300.3	.202E-08
1626	298.6	.437E-08
1609	297.0	.316E-08
1594	295.3	.284E-08
1579	293.5	.245E-08
1567	291.8	.248E-08
1556	290.0	.159E-07
1546	288.2	.338E-07
1538	286.3	.102E-06
1531	284.5	.146E-06
1527	282.6	.166E-06
1523	280.7	.427E-06
1522	278.9	.400E-06
1522	277.0	.445E-06
1524	275.1	.437E-06
1527	273.2	.363E-06
1532	271.4	.348E-06
1538	269.5	.224E-06
1547	267.7	.134E-06
1556	265.9	.107E-06
1568	264.1	.345E-06
1580	262.3	.312E-06
1595	260.6	.173E-06
1610	258.9	.765E-07
1627	257.2	.672E-07
1646	255.6	.270E-06
1665	254.0	.237E-06
1686	252.5	.141E-06
1709	251.0	.173E-07
1732	249.5	.574E-08
1756	248.0	.330E-08
1782	246.7	-.358E-08
1808	245.3	-.748E-08
1836	244.0	-.672E-08
1864	242.7	-.103E-07
1893	241.5	-.106E-07
1924	240.3	-.111E-07
1955	239.1	-.149E-08
1986	238.0	.189E-07
2019	236.9	.603E-08
2052	235.9	.418E-10
2086	234.8	.000

Table A.3 (8-83/168.4° to 188°)

Period 9-83, θ_L =168.4°

1983 NEAR-SURFACE OIL FOG PROFILE
Min El. = 7.6 m Period # 9
Max El. = 32.6 m Azimuth 168.4

Horizontal Profile (50.0 m res.)

ρ_s(m)	θ_s (°)	χ/Q (s m^{-3})
210	292.1	.000
187	279.2	.000
175	263.8	.000
178	247.5	.000

Period 9-83, θ_L =172.3°

1983 NEAR-SURFACE OIL FOG PROFILE
Min El. = 7.6 m Period # 9
Max El. = 32.6 m Azimuth 172.3

Horizontal Profile (50.0 m res.)

ρ_s(m)	θ_s (°)	χ/Q (s m^{-3})
490	285.7	.000
473	280.2	.000
460	274.2	.000
452	268.0	.000

Period 9-83, θ_L =176.1°

1983 NEAR-SURFACE OIL FOG PROFILE
Min El. = 22.6 m Period # 9
Max El. = 52.6 m Azimuth 176.1

Horizontal Profile (50.0 m res.)

ρ_s(m)	θ_s (°)	χ/Q (s m^{-3})
762	285.8	.000
747	282.1	.432E-07
735	278.4	.134E-07
726	274.5	-.416E-08
720	270.6	.130E-06
718	266.6	.177E-05
719	262.6	.861E-06
724	258.7	.312E-07
732	254.8	.715E-08
743	251.0	.197E-07
758	247.3	.263E-07
776	243.9	.222E-07
796	240.5	.743E-07
819	237.4	.513E-07
844	234.4	.219E-07
871	231.6	-.111E-09
901	229.0	.000

Period 9-83, θ_L =178.9°

1983 NEAR-SURFACE OIL FOG PROFILE
Min El. = 22.6 m Period # 9
Max El. = 57.6 m Azimuth 178.9

Horizontal Profile (50.0 m res.)

ρ_s(m)	θ_s (°)	χ/Q (s m^{-3})
1002	293.5	.000
982	290.8	.258E-07
964	288.1	.114E-07
949	285.2	.468E-07
936	282.3	.219E-07
926	279.3	.103E-06
918	276.2	.259E-06
913	273.1	.237E-06
911	269.9	.110E-06
912	266.8	.320E-06
915	263.7	.158E-05
921	260.6	.782E-06
929	257.5	.251E-08
940	254.5	.286E-08
954	251.6	.197E-08
970	248.8	.743E-07
988	246.1	.413E-07
1009	243.5	.130E-06
1031	240.9	.112E-06
1056	238.6	.127E-06
1082	236.3	.170E-06
1110	234.1	.107E-07
1139	232.0	.000

Period 9-83, θ_L =183.1°

1983 NEAR-SURFACE OIL FOG PROFILE
Min El. = 12.6 m Period # 9
Max El. = 62.6 m Azimuth 183.1

Horizontal Profile (50.0 m res.)

ρ_s(m)	θ_s (°)	χ/Q (s m^{-3})
1275	293.3	.000
1258	291.1	.154E-08
1244	288.9	.671E-08
1231	286.7	.530E-07
1220	284.4	.594E-07
1211	282.1	.188E-07
1205	279.7	.327E-06
1200	277.4	.111E-05
1197	275.0	.259E-05
1197	272.6	.240E-05
1198	270.2	.135E-05
1202	267.8	.146E-05
1207	265.5	.119E-05
1215	263.1	.543E-06
1225	260.8	.635E-07
1236	258.5	.772E-07
1250	256.3	.162E-06
1265	254.2	.894E-07
1282	252.0	.121E-06
1301	250.0	.123E-06
1321	248.0	.493E-06
1343	246.1	.256E-06
1367	244.2	.759E-08
1392	242.4	.000

Period 9-83, θ_L =188.0°

1983 NEAR-SURFACE OIL FOG PROFILE
Min El. = 17.6 m Period # 9
Max El. = 67.6 m Azimuth 188.0

Horizontal Profile (50.0 m res.)

ρ_s(m)	θ_s (°)	χ/Q (s m^{-3})
1707	304.9	.000
1685	303.4	-.548E-10
1664	301.9	.310E-09
1645	300.3	.113E-08
1627	298.6	.420E-09
1610	297.0	.595E-08
1594	295.3	.769E-08
1580	293.5	.661E-08
1567	291.8	.648E-08
1556	290.0	.407E-08
1547	288.2	.732E-08
1539	286.3	.948E-08
1532	284.5	.401E-07
1527	282.6	.936E-07
1524	280.7	.198E-06
1523	278.9	.378E-06
1523	277.0	.385E-06
1524	275.1	.348E-06
1528	273.2	.322E-06
1533	271.4	.312E-06
1539	269.5	.584E-06
1547	267.7	.404E-06
1557	265.9	.378E-06
1568	264.1	.546E-06
1581	262.3	.253E-06
1595	260.6	.744E-07
1611	258.9	.223E-07
1628	257.2	.332E-07
1647	255.6	.000

Table A.3 (9-83/168.4° to 188°)

Period 9-83, θ_L =195.0°

1983 NEAR-SURFACE OIL FOG PROFILE
Min El. = 17.6 m Period # 9
Max El. = 67.6 m Azimuth 195.0

Horizontal Profile (50.0 m res.)

ρ_s(m)	θ_s (°)	χ/Q (s m^{-3})
2010	296.8	.000
2001	295.4	-.127E-08
1992	293.9	.130E-07
1985	292.5	.572E-07
1979	291.1	.123E-06
1974	289.6	.853E-07
1971	288.2	.426E-07
1969	286.7	.522E-07
1968	285.3	.366E-07
1968	283.8	.553E-07
1970	282.4	.897E-07
1973	280.9	.188E-06
1977	279.5	.278E-06
1983	278.0	.340E-06
1989	276.6	.247E-06
1997	275.2	.199E-06
2006	273.8	.196E-06
2017	272.4	.272E-06
2028	271.0	.357E-06
2041	269.6	.322E-06
2055	268.3	.291E-06
2070	267.0	.271E-06
2086	265.7	.323E-06
2103	264.4	.346E-06
2121	263.1	.455E-06
2140	261.9	.364E-06
2160	260.7	.949E-07
2181	259.5	.134E-07
2203	258.3	.108E-08
2226	257.1	.000

Period 10-83, θ_L =172.3°

1983 NEAR-SURFACE OIL FOG PROFILE
Min El. = 29.6 m Period #10
Max El. = 44.6 m Azimuth 172.3

Horizontal Profile (50.0 m res.)

ρ_s(m)	θ_s (°)	χ/Q (s m^{-3})
1277	337.3	.000
1229	336.7	.000
1181	336.0	.133E-08
1133	335.3	.776E-07
1086	334.6	.216E-06
1038	333.7	.105E-06
991	332.8	.717E-08
944	331.8	.611E-08
897	330.7	.425E-08
851	329.4	.587E-07
805	328.0	.704E-07
760	326.5	.608E-07
715	324.7	.385E-07
671	322.8	.834E-07
628	320.5	.244E-05
586	318.0	.499E-05
545	315.0	.127E-05
507	311.6	.134E-05
470	307.6	.487E-05
436	303.0	.565E-05
405	297.6	.271E-05
378	291.4	.850E-05
357	284.4	.466E-05
341	276.5	.111E-05
332	268.2	.438E-05
331	259.5	.774E-05
337	251.0	.000
350	242.9	.000
370	235.6	.000
395	229.1	.000

Period 10-83, θ_L =175.0°

1983 NEAR-SURFACE OIL FOG PROFILE
Min El. = 28.6 m Period #10
Max El. = 48.6 m Azimuth 175.0

Horizontal Profile (50.0 m res.)

ρ_s(m)	θ_s (°)	χ/Q (s m^{-3})
1506	334.9	.000
1459	334.2	-.153E-08
1412	333.5	-.306E-09
1366	332.7	.725E-08
1320	331.9	.267E-07
1274	331.0	.233E-07
1229	330.0	.979E-07
1183	329.0	.130E-06
1139	327.9	.915E-07
1094	326.7	.580E-07
1051	325.4	.992E-07
1008	324.0	.143E-06
965	322.5	.251E-06
923	320.8	.444E-06
882	319.0	.293E-06
842	317.0	.176E-06
804	314.8	.136E-06
766	312.4	.286E-06
730	309.7	.636E-06
696	306.8	.431E-06
663	303.6	.765E-06
634	300.0	.327E-05
606	296.2	.126E-05
582	292.0	.329E-06
561	287.4	.625E-06
544	282.5	.129E-05
531	277.4	.694E-06
523	272.0	.214E-05
519	266.5	.279E-05
520	261.0	.323E-06
526	255.6	.541E-07
536	250.3	-.163E-08
551	245.3	.204E-07
570	240.5	.919E-07
592	236.1	.104E-06
618	232.0	.346E-07
647	228.3	.204E-09
678	224.9	.000
711	221.9	.000
746	219.0	.000

Table A.3 (9-83/195° to 10-83/175°)

Period 10-83, θ_L =178.9°

1983 NEAR-SURFACE OIL FOG PROFILE
Min El. = 30.6 m Period #10
Max El. = 50.6 m Azimuth 178.9

Horizontal Profile (50.0 m res.)

ρ_s(m)	θ_s (°)	χ/Q (s m^{-3})
1666	330.8	.000
1622	329.9	.000
1579	329.1	-.184E-09
1536	328.1	.985E-08
1493	327.1	.203E-07
1451	326.1	.190E-07
1409	325.0	.195E-07
1368	323.8	.494E-07
1327	322.6	.675E-07
1287	321.3	.114E-06
1248	319.9	.122E-06
1210	318.4	.168E-07
1172	316.8	.240E-07
1135	315.1	.825E-07
1100	313.3	.231E-06
1066	311.4	.292E-06
1032	309.3	.367E-06
1001	307.1	.408E-06
971	304.8	.102E-06
942	302.4	.843E-07
916	299.7	.153E-06
891	297.0	.812E-07
869	294.1	.575E-07
848	291.0	.233E-06
831	287.8	.308E-06
816	284.5	.994E-06
804	281.1	.295E-05
795	277.5	.227E-05
789	273.9	.867E-06
786	270.3	.411E-06
787	266.7	.419E-06
790	263.0	.385E-06
797	259.5	.362E-06
807	256.0	.551E-07
819	252.6	.991E-07
835	249.3	.954E-07
853	246.1	.172E-07
873	243.1	.435E-07
896	240.2	.536E-07
921	237.5	.218E-07
949	234.9	.414E-08
977	232.5	-.552E-09
1008	230.2	-.184E-09
1040	228.0	.000
1073	226.0	.000

Period 10-83, θ_L =183.1°

1983 NEAR-SURFACE OIL FOG PROFILE
Min El. = 31.6 m Period #10
Max El. = 81.6 m Azimuth 183.1

Horizontal Profile (50.0 m res.)

ρ_s(m)	θ_s (°)	χ/Q (s m^{-3})
1763	325.8	.000
1723	324.8	.000
1684	323.7	.264E-08
1646	322.6	.514E-08
1608	321.4	.106E-07
1571	320.2	.117E-08
1535	319.0	.290E-08
1499	317.6	.865E-08
1465	316.2	.215E-07
1431	314.8	.172E-07
1398	313.2	.181E-07
1367	311.6	.113E-07
1336	310.0	.223E-09
1307	308.2	.260E-09
1279	306.4	-.128E-08
1252	304.5	.315E-07
1227	302.5	.347E-06
1203	300.4	.307E-06
1181	298.2	.398E-06
1160	296.0	.323E-06
1142	293.7	.212E-06
1125	291.3	.238E-06
1111	288.8	.190E-06
1098	286.3	.207E-06
1088	283.8	.286E-06
1080	281.2	.594E-06
1074	278.5	.330E-06
1070	275.9	.329E-06
1069	273.2	.536E-06
1070	270.5	.431E-06
1074	267.8	.488E-06
1079	265.2	.292E-06
1088	262.6	.215E-06
1098	260.0	.156E-06
1110	257.5	.669E-07
1125	255.0	.958E-07
1141	252.7	.376E-07
1160	250.3	.953E-08
1180	248.1	.734E-08
1202	245.9	.152E-07
1225	243.9	.244E-07
1251	241.9	.407E-07
1277	239.9	.455E-07
1305	238.1	.307E-07
1335	236.3	-.184E-08
1365	234.7	.000

Period 10-83, θ_L =190.0°

1983 NEAR-SURFACE OIL FOG PROFILE
Min El. = 35.6 m Period #10
Max El. = 85.6 m Azimuth 190.0

Horizontal Profile (50.0 m res.)

ρ_s(m)	θ_s (°)	χ/Q (s m^{-3})
1740	309.1	-.139E-08
1717	307.6	.364E-07
1694	306.1	.662E-07
1673	304.6	.476E-07
1653	303.0	.388E-07
1634	301.4	.261E-07
1616	299.7	.398E-07
1600	298.0	.851E-07
1585	296.3	.105E-06
1572	294.6	.103E-06
1560	292.8	.759E-07
1550	291.0	.176E-06
1541	289.2	.235E-06
1534	287.3	.247E-06
1529	285.5	.216E-06
1525	283.6	.186E-06
1522	281.7	.262E-06
1522	279.8	.278E-06
1523	277.9	.469E-06
1525	276.1	.375E-06
1530	274.2	.371E-06
1535	272.3	.270E-06
1543	270.5	.193E-06
1552	268.7	.150E-06
1563	266.9	.146E-06
1575	265.1	.168E-06
1588	263.4	.151E-06
1603	261.7	.152E-06
1620	260.0	.111E-06
1638	258.3	.150E-06
1657	256.7	.168E-06
1677	255.2	.149E-06
1699	253.6	.146E-06
1722	252.1	.115E-06
1745	250.7	.940E-07
1771	249.3	.778E-07
1797	247.9	.691E-07
1824	246.6	.709E-07
1852	245.3	.843E-07
1881	244.0	.729E-07
1910	242.8	.489E-07
1941	241.6	.538E-07
1973	240.5	.592E-07
2005	239.4	.198E-07
2038	238.3	.142E-07
2071	237.3	.114E-07
2105	236.3	.115E-07
2140	235.3	.873E-08
2176	234.4	.343E-08
2212	233.5	.000

Period 10-83, θ_L =205.0°

1983 NEAR-SURFACE OIL FOG PROFILE
Min El. = 52.6 m Period #10
Max El. = 82.6 m Azimuth 205.0

Horizontal Profile (50.0 m res.)

ρ_s(m)	θ_s (°)	χ/Q (s m^{-3})
2448	303.9	.000
2441	302.7	.909E-10
2435	301.5	.273E-09
2429	300.4	.403E-07
2425	299.2	.565E-07
2422	298.0	.422E-07
2420	296.8	.298E-07
2419	295.6	.361E-07
2419	294.5	.835E-07
2420	293.3	.108E-06
2422	292.1	.137E-06
2425	290.9	.145E-06
2429	289.7	.174E-06
2434	288.6	.264E-06
2440	287.4	.224E-06
2447	286.2	.229E-06
2456	285.1	.159E-06
2465	283.9	.164E-06
2475	282.8	.152E-06
2486	281.7	.138E-06
2498	280.6	.209E-06
2511	279.4	.276E-06
2525	278.4	.356E-06
2539	277.3	.355E-06
2555	276.2	.394E-06
2572	275.2	.373E-06
2589	274.1	.302E-06
2607	273.1	.364E-06
2626	272.1	.474E-06
2646	271.1	.582E-06
2667	270.1	.517E-06
2688	269.1	.386E-06
2711	268.2	.322E-06
2733	267.2	.429E-06
2757	266.3	.371E-06
2781	265.4	.329E-06
2806	264.5	.270E-06
2832	263.7	.368E-06
2858	262.8	.516E-06
2885	262.0	.442E-06
2913	261.1	.217E-06
2941	260.3	.157E-06
2970	259.5	.107E-06
2999	258.8	.127E-06
3029	258.0	.214E-06
3059	257.2	.212E-06
3090	256.5	.185E-06
3122	255.8	.207E-06
3153	255.1	.115E-06
3186	254.4	.618E-07
3219	253.7	.132E-06
3252	253.1	.135E-06
3285	252.4	.129E-06
3319	251.8	.131E-06
3354	251.2	.129E-06
3389	250.5	.123E-06
3424	249.9	.123E-06
3459	249.4	.624E-07
3495	248.8	.310E-07
3532	248.2	.000

Table A.3 (10-83/178.9° to 205°)

Period 11-83, θ_L =172.3°

1983 NEAR-SURFACE OIL FOG PROFILE
Min El. = 26.6 m Period #11
Max El. = 51.6 m Azimuth 172.3

Horizontal Profile (50.0 m res.)

ρ_s(m)	θ_s (°)	χ/Q (s m^{-3})
628	320.5	.000
586	318.0	.134E-07
545	315.0	.294E-07
506	311.6	.345E-07
470	307.6	.123E-06
436	303.0	.141E-06
405	297.6	.130E-06
378	291.4	.301E-06
356	284.4	.931E-06
341	276.6	.187E-05
332	268.2	.924E-05
331	259.5	.204E-04
337	251.0	.186E-04
350	242.9	.508E-05
369	235.6	.267E-05
394	229.1	.226E-05
424	223.4	.873E-06
457	218.5	.498E-06
493	214.3	.385E-06
531	210.7	.212E-06
571	207.6	.760E-07
613	204.9	.639E-08
655	202.5	-.128E-08
699	200.5	.000
743	198.6	.000

Period 11-83, θ_L =175.0°

1983 NEAR-SURFACE OIL FOG PROFILE
Min El. = 34.6 m Period #11
Max El. = 59.6 m Azimuth 175.0

Horizontal Profile (50.0 m res.)

ρ_s(m)	θ_s (°)	χ/Q (s m^{-3})
767	312.3	.000
731	309.7	.000
696	306.8	-.111E-08
664	303.5	.611E-08
634	300.0	.606E-07
607	296.1	.262E-07
583	291.9	.250E-07
562	287.4	.917E-07
545	282.5	.286E-06
532	277.4	.489E-06
524	272.0	.873E-06
520	266.5	.226E-05
521	261.0	.302E-05
527	255.6	.356E-05
537	250.3	.331E-05
552	245.3	.269E-05
571	240.6	.230E-05
593	236.2	.254E-05
619	232.1	.160E-05
648	228.4	.106E-05
679	225.0	.607E-06
712	221.9	.361E-06
747	219.1	.917E-07
784	216.6	.708E-07
822	214.3	.657E-07
861	212.2	.482E-07
901	210.2	.563E-07
943	208.5	.327E-07
985	206.9	.222E-08
1027	205.4	.244E-08
1071	204.1	-.133E-08
1115	202.8	-.111E-08
1159	201.7	.189E-08
1204	200.6	.778E-09
1250	199.6	.000

Period 11-83, θ_L =178.9°

1983 NEAR-SURFACE OIL FOG PROFILE
Min El. = 39.6 m Period #11
Max El. = 64.6 m Azimuth 178.9

Horizontal Profile (50.0 m res.)

ρ_s(m)	θ_s (°)	χ/Q (s m^{-3})
916	299.7	.000
891	297.0	.000
869	294.1	.000
849	291.0	.000
831	287.8	-.503E-09
817	284.5	-.122E-08
805	281.1	.338E-07
796	277.5	.538E-06
790	273.9	.857E-06
787	270.3	.925E-06
787	266.7	.229E-05
791	263.1	.230E-05
797	259.5	.185E-05
807	256.0	.122E-05
820	252.6	.123E-05
835	249.3	.103E-05
853	246.1	.116E-05
874	243.1	.117E-05
897	240.2	.933E-06
922	237.5	.686E-06
949	234.9	.591E-06
978	232.5	.591E-06
1008	230.2	.292E-06
1040	228.0	.131E-06
1074	226.0	.825E-07
1108	224.1	.801E-07
1144	222.4	.103E-06
1181	220.7	.799E-07
1219	219.1	.846E-07
1257	217.7	.104E-06
1297	216.3	.921E-07
1337	215.0	.610E-08
1378	213.7	.000
1419	212.6	.000
1461	211.5	.000

Period 11-83, θ_L =183.1°

1983 NEAR-SURFACE OIL FOG PROFILE
Min El. = 27.6 m Period #11
Max El. = 77.6 m Azimuth 183.1

Horizontal Profile (50.0 m res.)

ρ_s(m)	θ_s (°)	χ/Q (s m^{-3})
1142	293.7	-.112E-09
1126	291.3	.258E-08
1111	288.8	.100E-07
1099	286.3	.108E-07
1088	283.8	.129E-07
1080	281.2	.291E-07
1074	278.5	.136E-06
1071	275.9	.204E-06
1070	273.2	.236E-06
1071	270.5	.160E-06
1074	267.8	.353E-06
1080	265.2	.660E-06
1088	262.6	.766E-06
1098	260.0	.105E-05
1111	257.5	.120E-05
1125	255.1	.115E-05
1142	252.7	.113E-05
1160	250.4	.102E-05
1180	248.1	.920E-06
1202	246.0	.943E-06
1226	243.9	.739E-06
1251	241.9	.626E-06
1278	240.0	.525E-06
1306	238.1	.376E-06
1335	236.4	.342E-06
1366	234.7	.264E-06
1397	233.1	.150E-06
1430	231.5	.476E-07
1464	230.1	.261E-07
1498	228.7	.136E-07
1534	227.3	.775E-08
1570	226.1	.102E-07
1607	224.9	-.974E-09
1644	223.7	.494E-08
1683	222.6	.607E-08
1722	221.5	.479E-08
1761	220.5	.103E-07
1801	219.6	.981E-08
1841	218.6	.981E-08
1882	217.8	.742E-08
1924	216.9	.614E-08
1966	216.1	.393E-08
2008	215.3	.670E-08
2050	214.6	.330E-08
2093	213.9	.000

Table A.3 (11-83/172.3° to 183.1°)

Period 11-83, $\theta_L = 190.0°$

1983 NEAR-SURFACE OIL FOG PROFILE		
Min El. = 52.6 m		Period #11
Max El. = 102.6 m		Azimuth 190.0
Horizontal Profile (50.0 m res.)		
ρ_s(m)	θ_s (°)	χ/Q (s m^{-3})
1522	277.9	.000
1525	276.1	.000
1529	274.2	.716E-09
1535	272.3	.188E-07
1542	270.5	.360E-07
1551	268.7	.464E-07
1562	266.9	.821E-07
1574	265.1	.215E-06
1588	263.4	.401E-06
1603	261.6	.367E-06
1619	260.0	.282E-06
1637	258.3	.242E-06
1656	256.7	.289E-06
1677	255.1	.381E-06
1698	253.6	.374E-06
1721	252.1	.358E-06
1745	250.7	.407E-06
1770	249.3	.490E-06
1796	247.9	.402E-06
1823	246.6	.432E-06
1851	245.3	.573E-06
1880	244.0	.524E-06
1910	242.8	.430E-06
1941	241.6	.418E-06
1972	240.5	.421E-06
2004	239.4	.312E-06
2037	238.3	.252E-06
2071	237.3	.214E-06
2105	236.3	.222E-06
2140	235.3	.256E-06
2175	234.4	.247E-06
2211	233.5	.211E-06
2248	232.6	.141E-06
2285	231.8	.799E-07
2323	230.9	.604E-07
2361	230.1	.731E-07
2399	229.4	.669E-07
2438	228.6	.432E-07
2477	227.9	.271E-07
2517	227.2	.306E-07
2557	226.5	.452E-07
2597	225.9	.304E-07
2638	225.2	.263E-07
2679	224.6	.348E-07
2720	224.0	.394E-07
2762	223.4	.121E-07
2804	222.9	.100E-07
2846	222.3	.115E-07
2888	221.8	.782E-08
2931	221.3	.643E-08
2974	220.8	.125E-07
3017	220.3	.110E-07
3060	219.8	.184E-08
3103	219.4	.394E-09
3147	218.9	.000

Period 11-83, $\theta_L = 205.0°$

1983 NEAR-SURFACE OIL FOG PROFILE		
Min El. = 46.6 m		Period #11
Max El. = 106.6 m		Azimuth 205.0
Horizontal Profile (50.0 m res.)		
ρ_s(m)	θ_s (°)	χ/Q (s m^{-3})
2465	283.9	.000
2475	282.8	.362E-10
2486	281.7	.105E-07
2498	280.6	.708E-07
2511	279.4	.962E-07
2525	278.4	.121E-06
2540	277.3	.169E-06
2555	276.2	.191E-06
2572	275.2	.180E-06
2589	274.1	.174E-06
2607	273.1	.129E-06
2627	272.1	.146E-06
2646	271.1	.234E-06
2667	270.1	.217E-06
2689	269.1	.253E-06
2711	268.2	.279E-06
2734	267.2	.272E-06
2757	266.3	.420E-06
2782	265.4	.420E-06
2807	264.5	.465E-06
2832	263.7	.579E-06
2859	262.8	.436E-06
2886	262.0	.365E-06
2913	261.1	.351E-06
2941	260.3	.334E-06
2970	259.5	.382E-06
2999	258.8	.383E-06
3029	258.0	.335E-06
3060	257.2	.281E-06
3090	256.5	.436E-06
3122	255.8	.428E-06
3154	255.1	.379E-06
3186	254.4	.421E-06
3219	253.7	.388E-06
3252	253.1	.426E-06
3286	252.4	.503E-06
3320	251.8	.421E-06
3354	251.2	.358E-06
3389	250.6	.309E-06
3424	250.0	.228E-06
3460	249.4	.236E-06
3496	248.8	.199E-06
3532	248.2	.186E-06
3568	247.7	.173E-06
3605	247.1	.179E-06
3643	246.6	.130E-06
3680	246.1	.105E-06
3718	245.6	.137E-06
3756	245.1	.773E-07
3794	244.6	.645E-07
3833	244.1	.448E-07
3872	243.7	.153E-07
3911	243.2	.330E-07
3951	242.8	-.199E-07
3990	242.3	-.250E-07
4030	241.9	-.289E-08
4070	241.5	-.280E-07
4111	241.1	.859E-08
4151	240.6	.542E-08
4192	240.3	.127E-09

Table A.3 (11-83/190° to 205°)

APPENDIX B

HORIZONTAL AND VERTICAL PROFILES OF CHAFF CONCENTRATION, AND PLOTS OF OTHER CHAFF PLUME PARAMETERS

Here we present profiles of crosswind integrated and vertically integrated chaff concentration and plots of chaff plume parameters as functions of distance from the source, x. A full definition of these quantities can be found in Sec. 4.6.

Figures B.1 and B.2 show tabular data for crosswind integrated and vertically integrated chaff concentrations, respectively. With few exceptions, the data are normalized concentrations (indicated by superscript n), each column being normalized to total 1000. In Fig. B.1, data are presented for various downwind distances and for every 50 m step in altitude (beginning at z = 35 m above the tower base). For ease of reading, alternate columns were offset slightly in the vertical. The true location for each data point can be obtained by shifting columns down or up by 12.5 m, as appropriate, so that the numbers line up in the horizontal. Periods 0-82 and 1-82 were processed in 50 m increments of x, while subsequent periods were smoothed by averaging over larger increments of x: 300 m for Period 3-82 and 250 m for the remainder of the periods. The values listed in Figs. B.1 and B.2, which really resemble tables, are placed so that $\bar{x}$ for each average lies near the right edge of the numbers.

Figures B.3 through B.9 show plots of the parameters listed in Tables 9.1 to 9.12 in Chapter 9. Because our data processing techniques evolved during the course of CONDORS, plots are either not available or are only available in altered form for some of the 1982 data presented in Chapter 9. Table B.1 shows which parameters are missing (M) or altered (A).

Table B.1 List of missing (M) and altered chaff (A) parameters in plots of Figs. B.3 to B.9

Period	x_y	x_z	$\bar{y}$	σ_y	y of $(x_z)_{max}$	$\bar{z}$	σ_z	z of $(x_y)_{max}$	$(x_y)_{max}$	x_{yz}
0-82	M	M	M	M	M	-	M	M	-	-
1-82	A	M	M	-	M	-	M	-	-	-
2-82	-	A	M	-	M	-	-	-	-	-
3-82	-	M	M	-	M	-	-	-	-	-
4-82	-	M	M	-	M	-	-	-	-	-
5-82	-	A	M	-	M	-	-	-	-	-
2-83	-	-	M	-	-	-	-	-	-	-
4-83	-	-	M	-	-	-	-	-	-	-
5,6-83	-	-	M	-	-	-	-	-	-	-
7-83	-	-	M	-	-	-	-	-	-	-
8-83	-	-	M	-	-	-	-	-	-	-
9-83	-	-	M	-	-	-	-	-	-	-

Figure B.10 shows horizontal contours of vertically integrated chaff concentration for each individual volume scan included in the 1983 averaging periods. (These figures are not available for 1982.) The single contour shown encloses those areas over which the vertically integrated chaff density exceeded 100 filaments per 50 meter square column. This figure is included to give the reader some idea of the temporal stationarity (or lack of it) during each averaging period for 1983.

Fig. B.1. Crosswind integrated chaff concentrations along the xz plane. Numbers shown are normalized values, except for Periods 0-82 and 1-82 for which only the unnormalized values are available. Shown chronologically by period. Subfigures referenced by (period number).

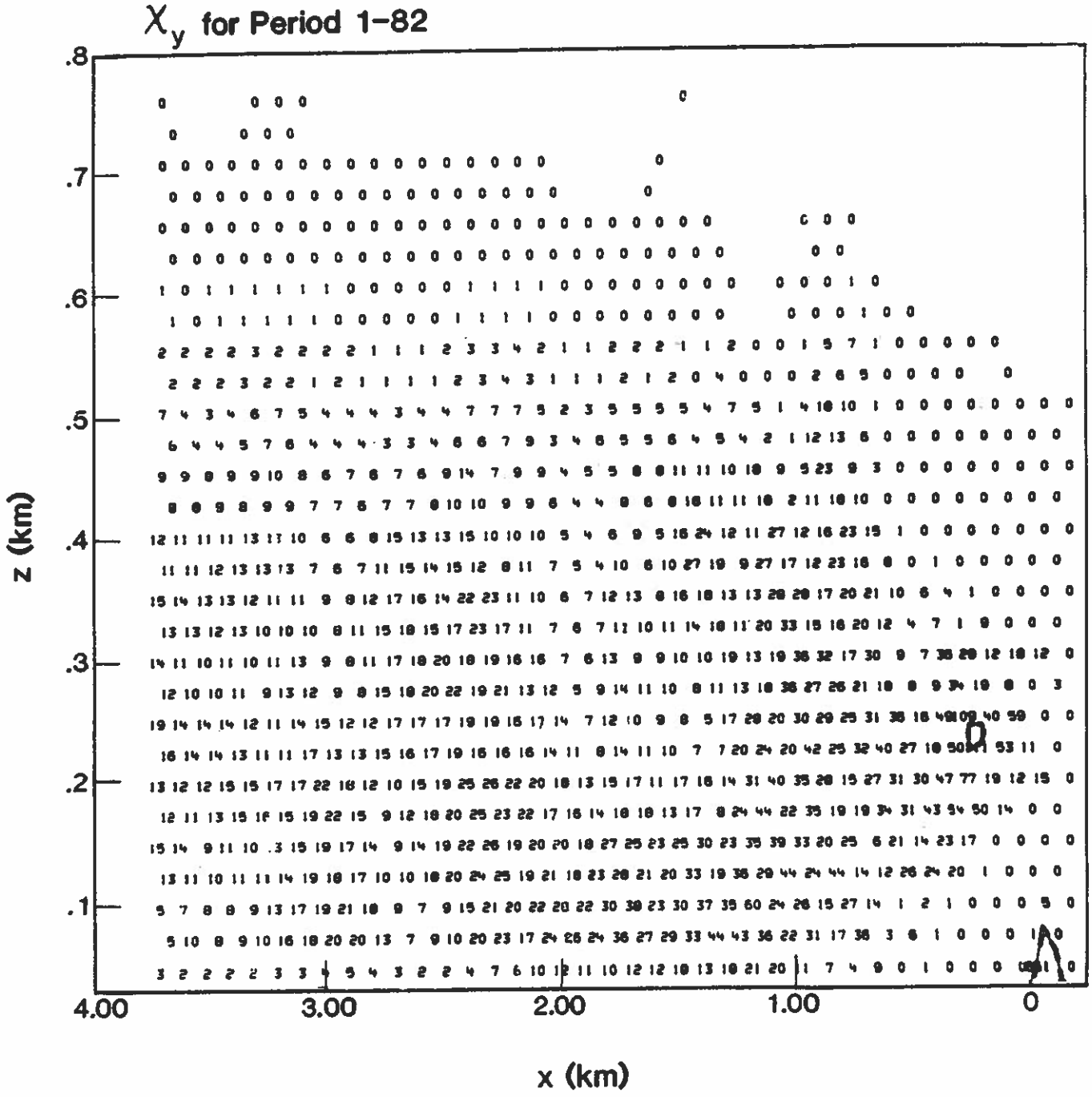

Fig. 8.1 (1-82)

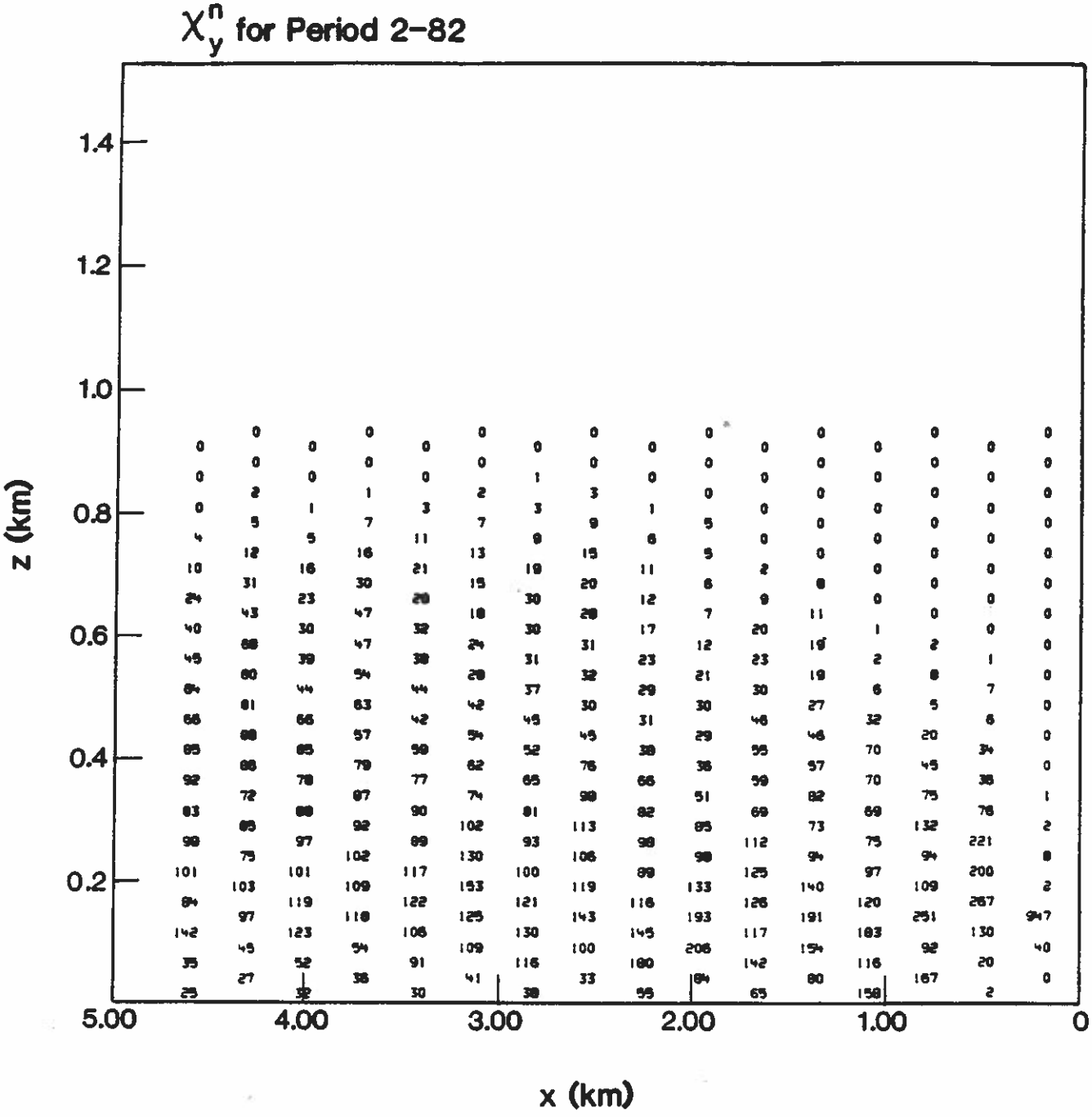
χ^n_y for Period 2-82
z (km)
1.4
1.2
1.0
0.8
0.6
0.4
0.2
5.00
4.00
3.00
2.00
1.00
0
x (km)

Fig. B.1 (2-82)

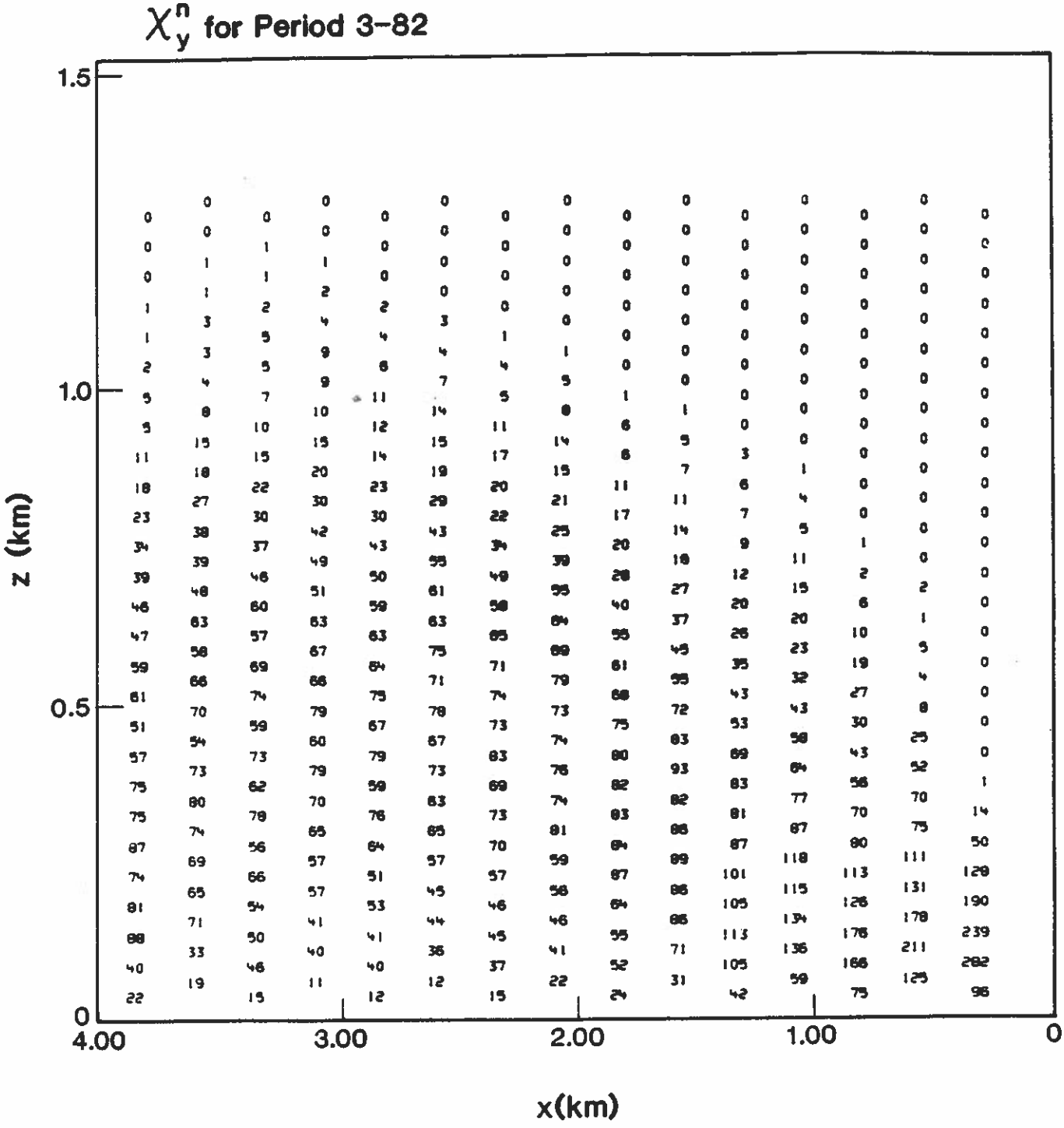

Fig. B.1 (3-82)

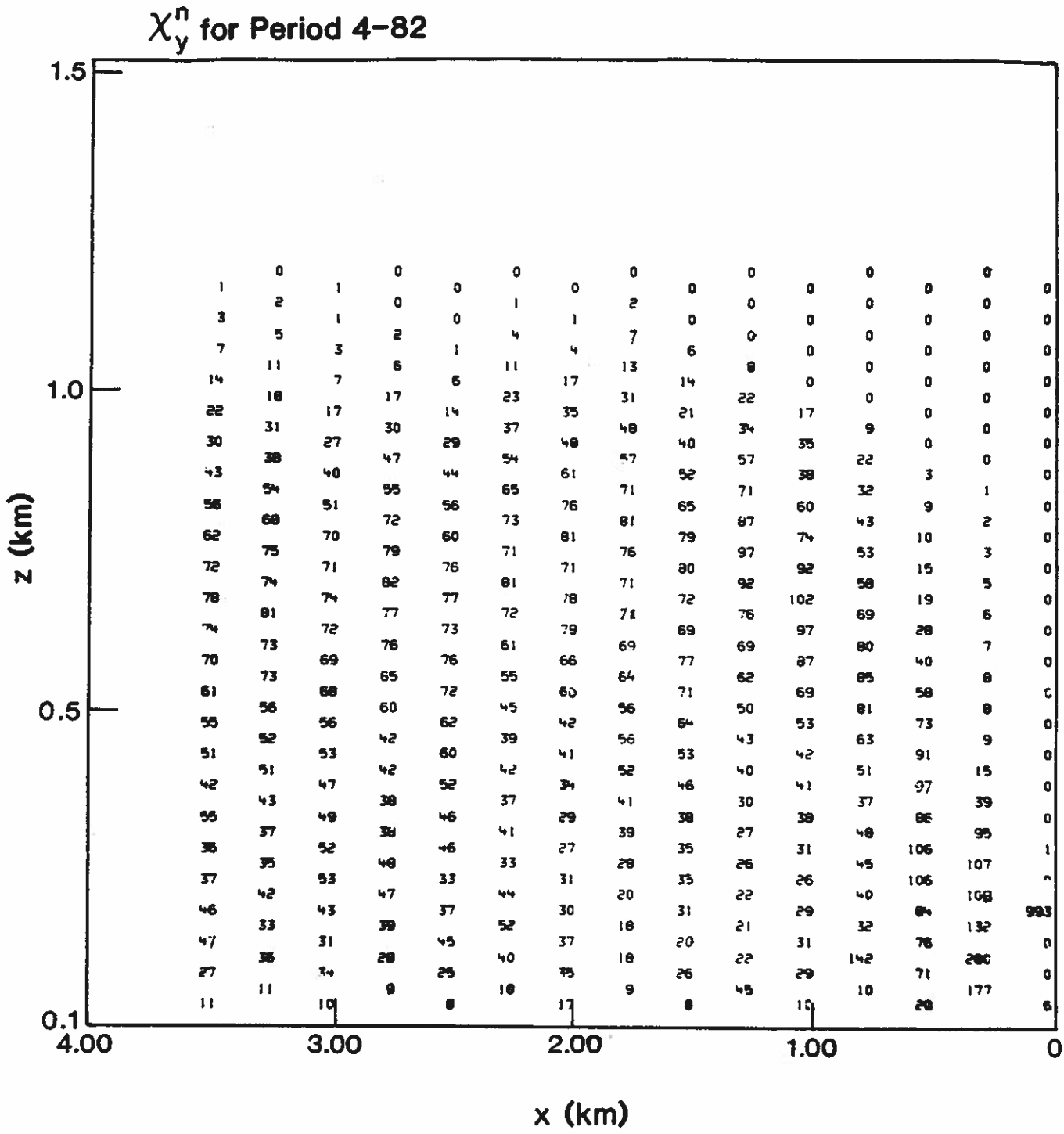

Fig. B.1 (4-82)

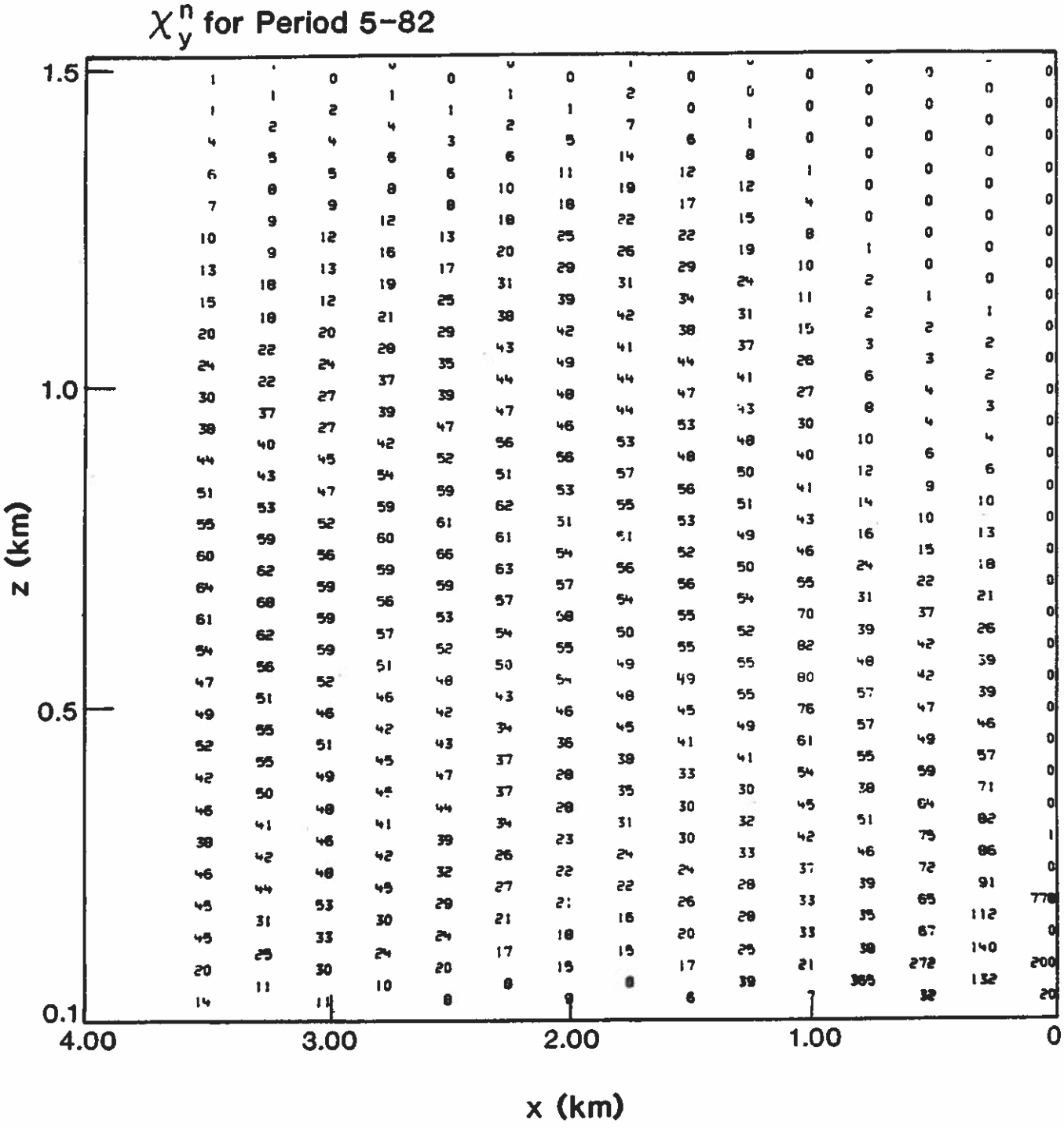

Fig. B.1 (5-82)

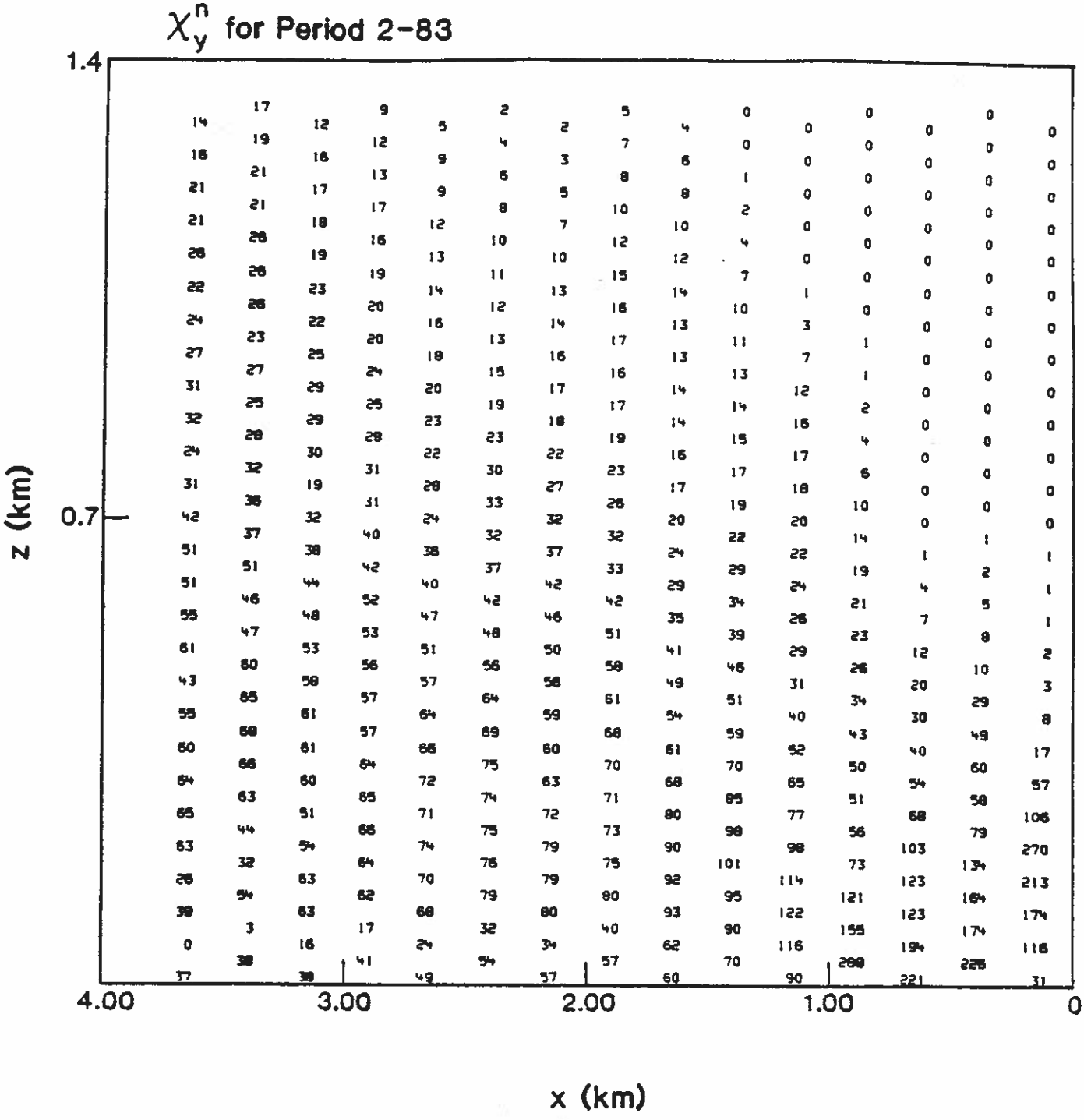

Fig. B.1 (2-83)

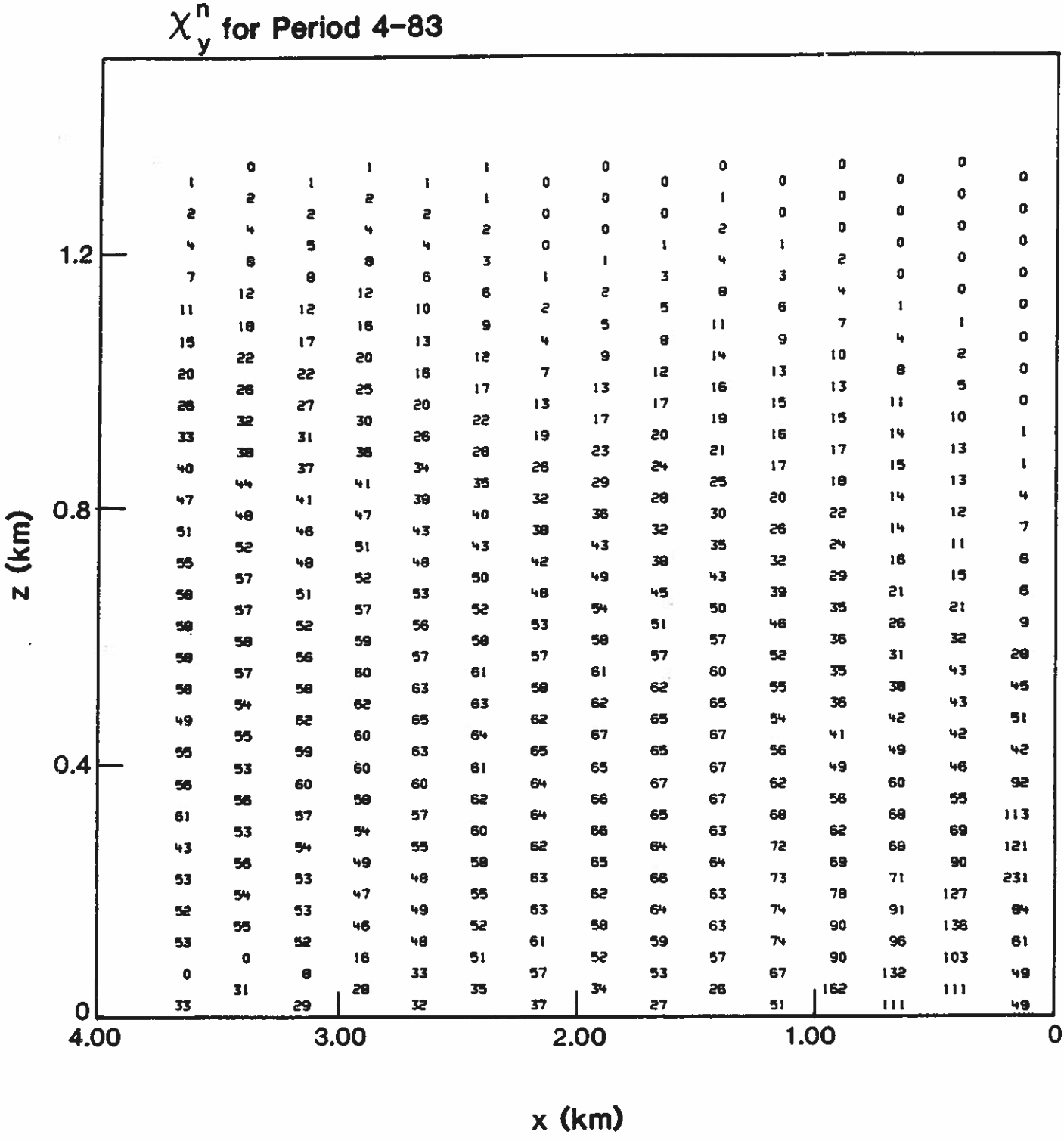

Fig. B.1 (4-83)

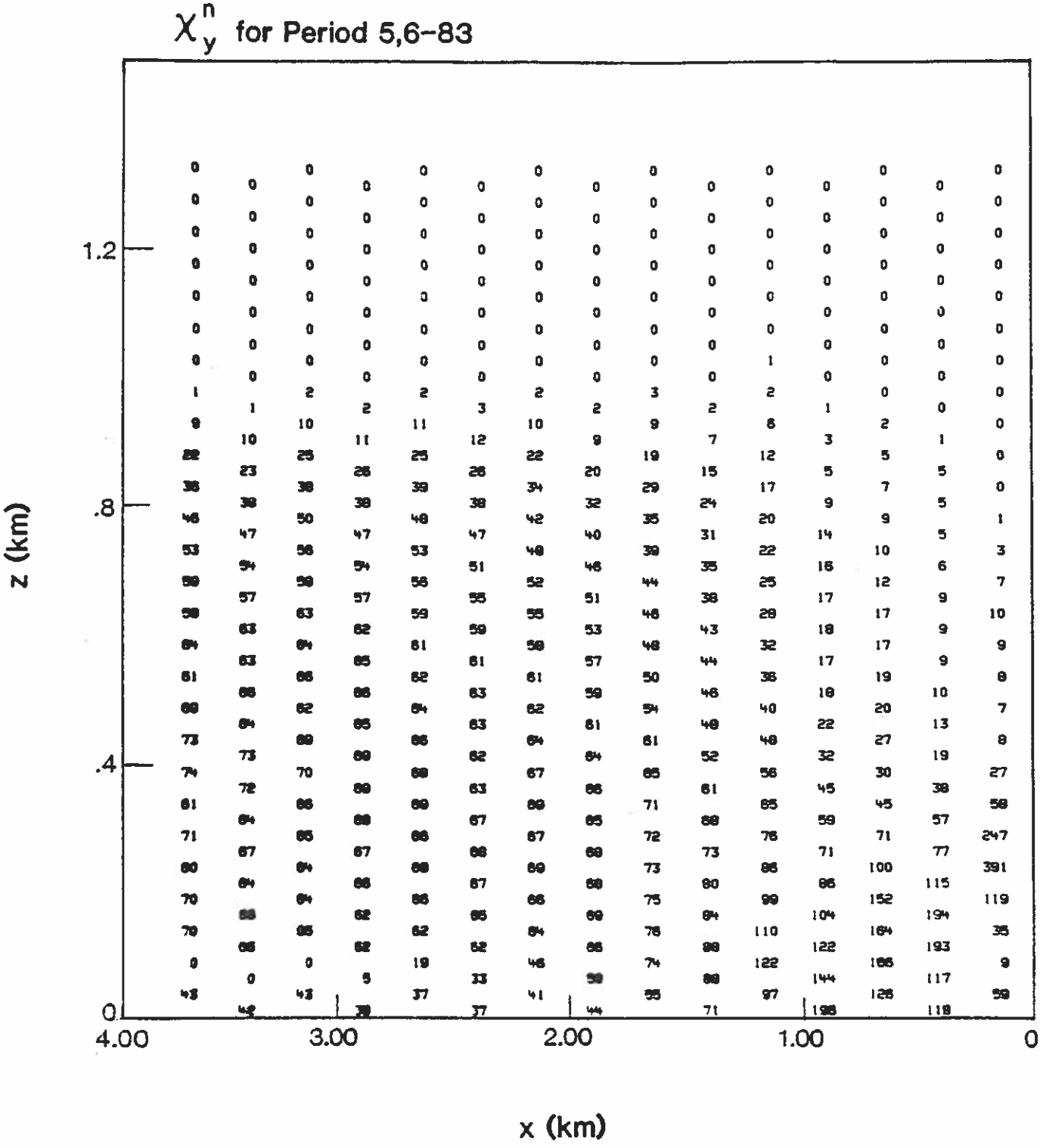

Fig. B.1 (5,6-83)

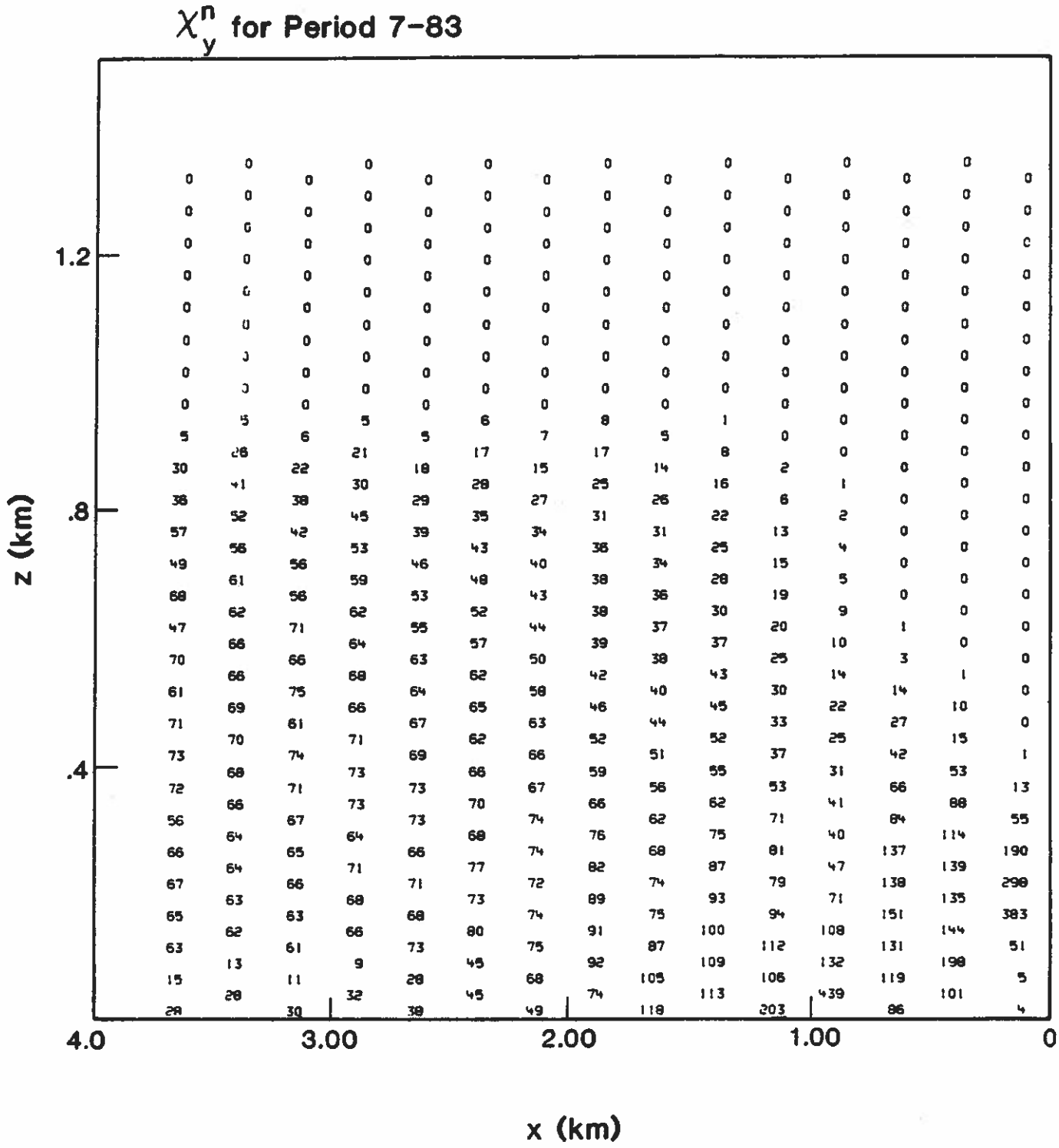

Fig. B.1 (7-83)

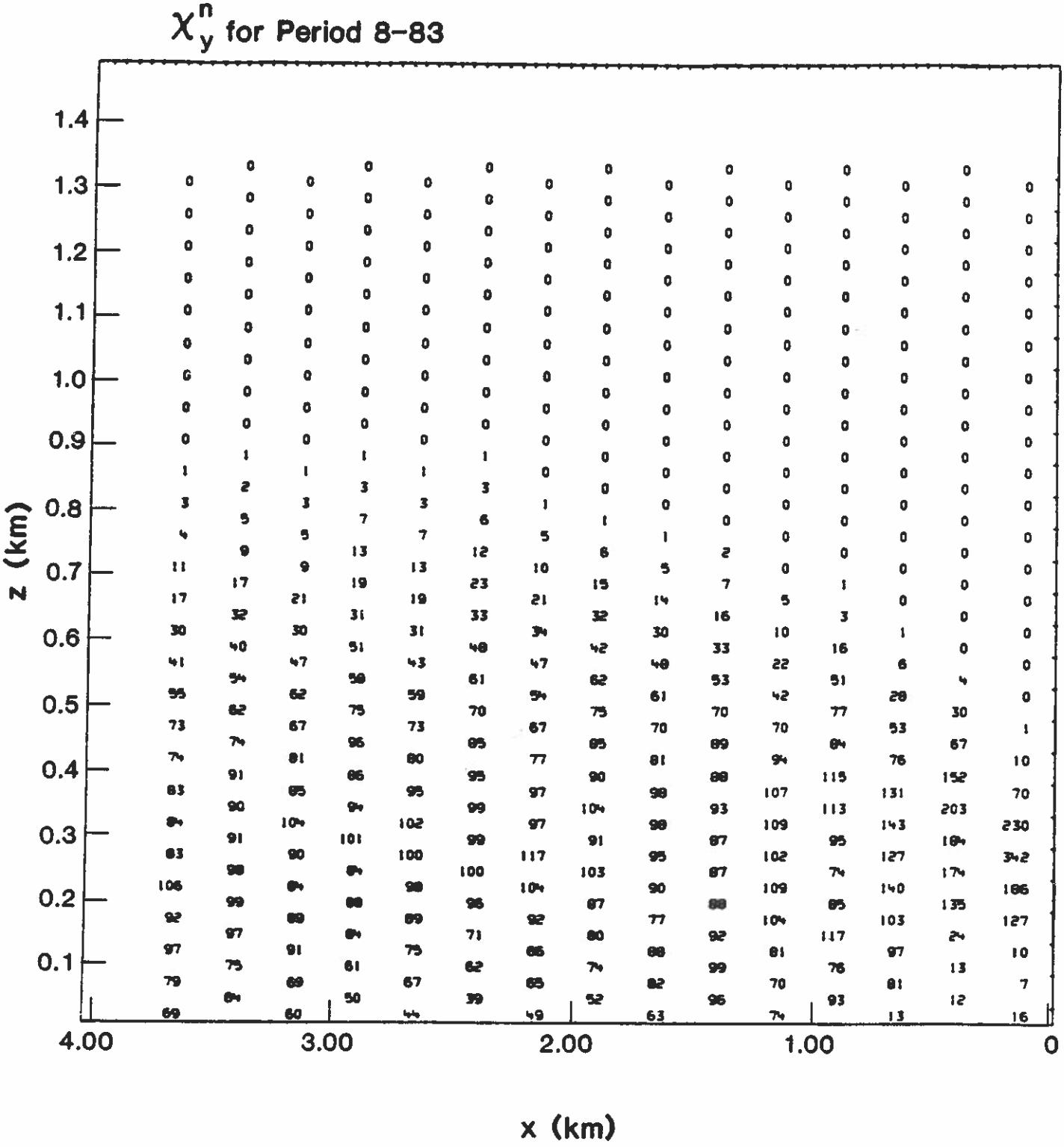
χ^n_y for Period 8-83
z (km)
x (km)
1.4
1.3
1.2
1.1
1.0
0.9
0.8
0.7
0.6
0.5
0.4
0.3
0.2
0.1
4.00
3.00
2.00
1.00
0

Fig. 8.1 (8-83)

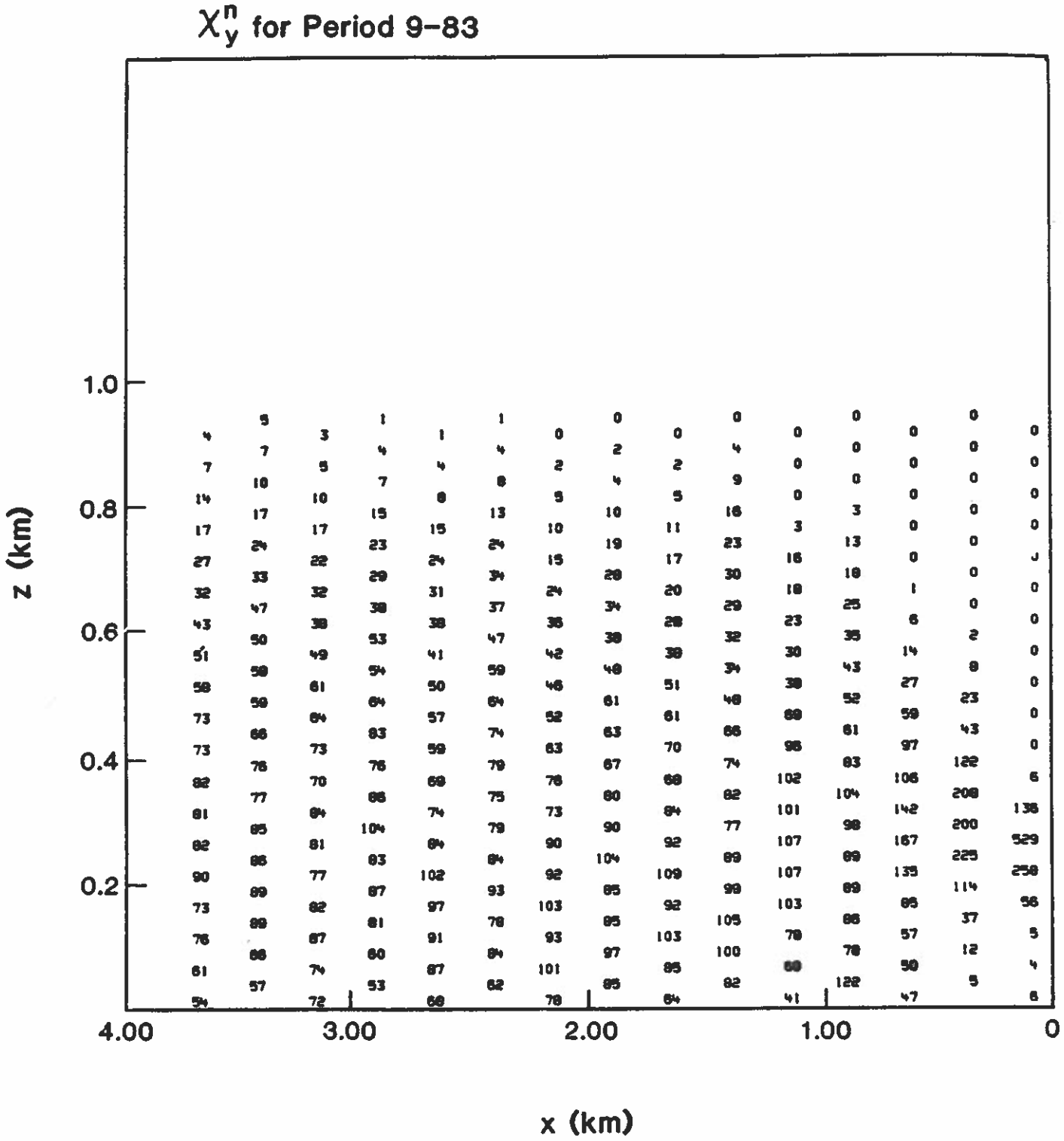

Fig. B.1 (9-83)

Fig. B.2. Vertically integrated chaff concentrations along the xy plane. Numbers shown are normalized values except for Periods 2-82 and 5-82 for which only the unnormalized values are available. Shown chronologically by period. Subfigures referenced by (period number).

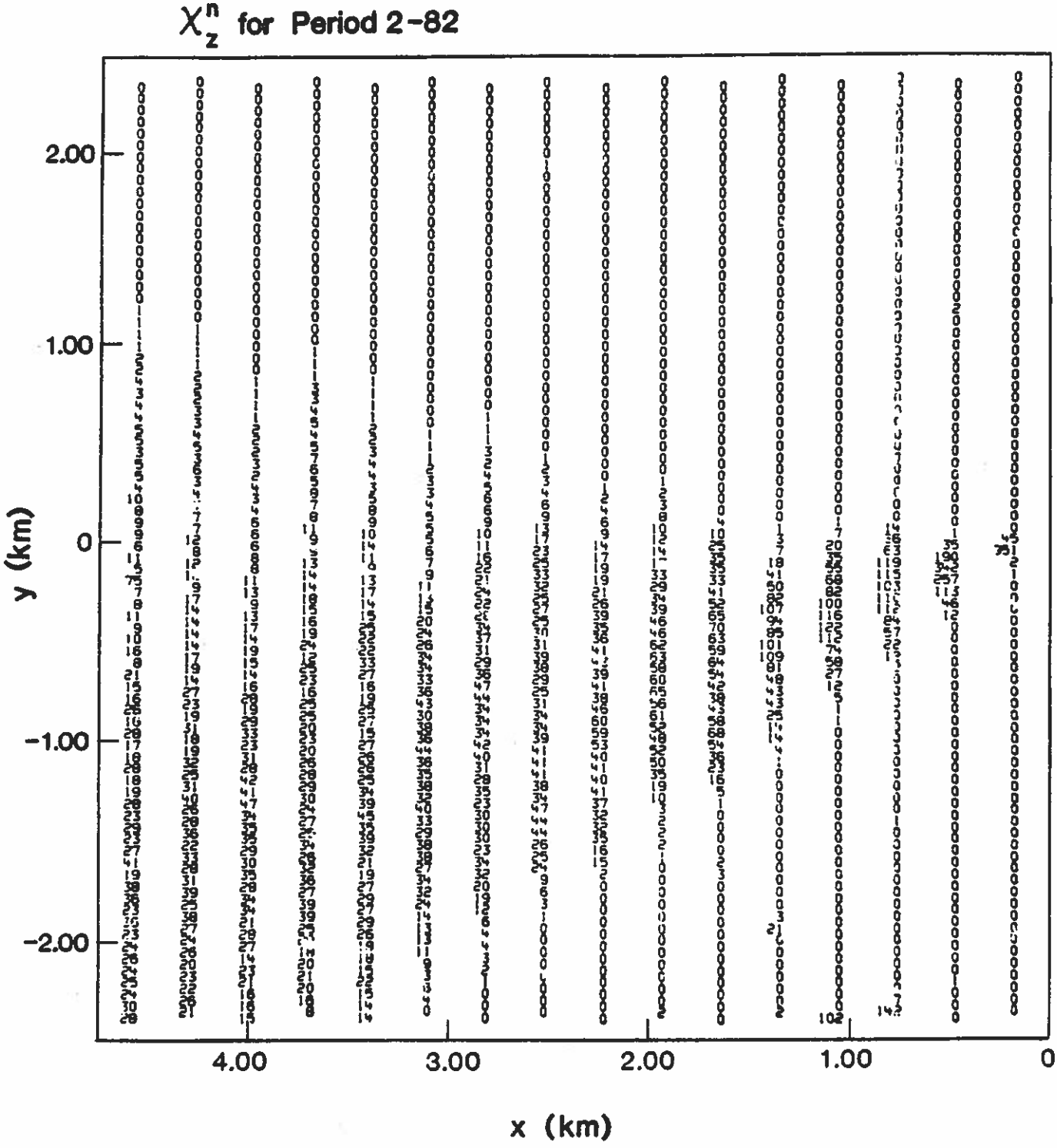

Fig. B.2 (2-82)

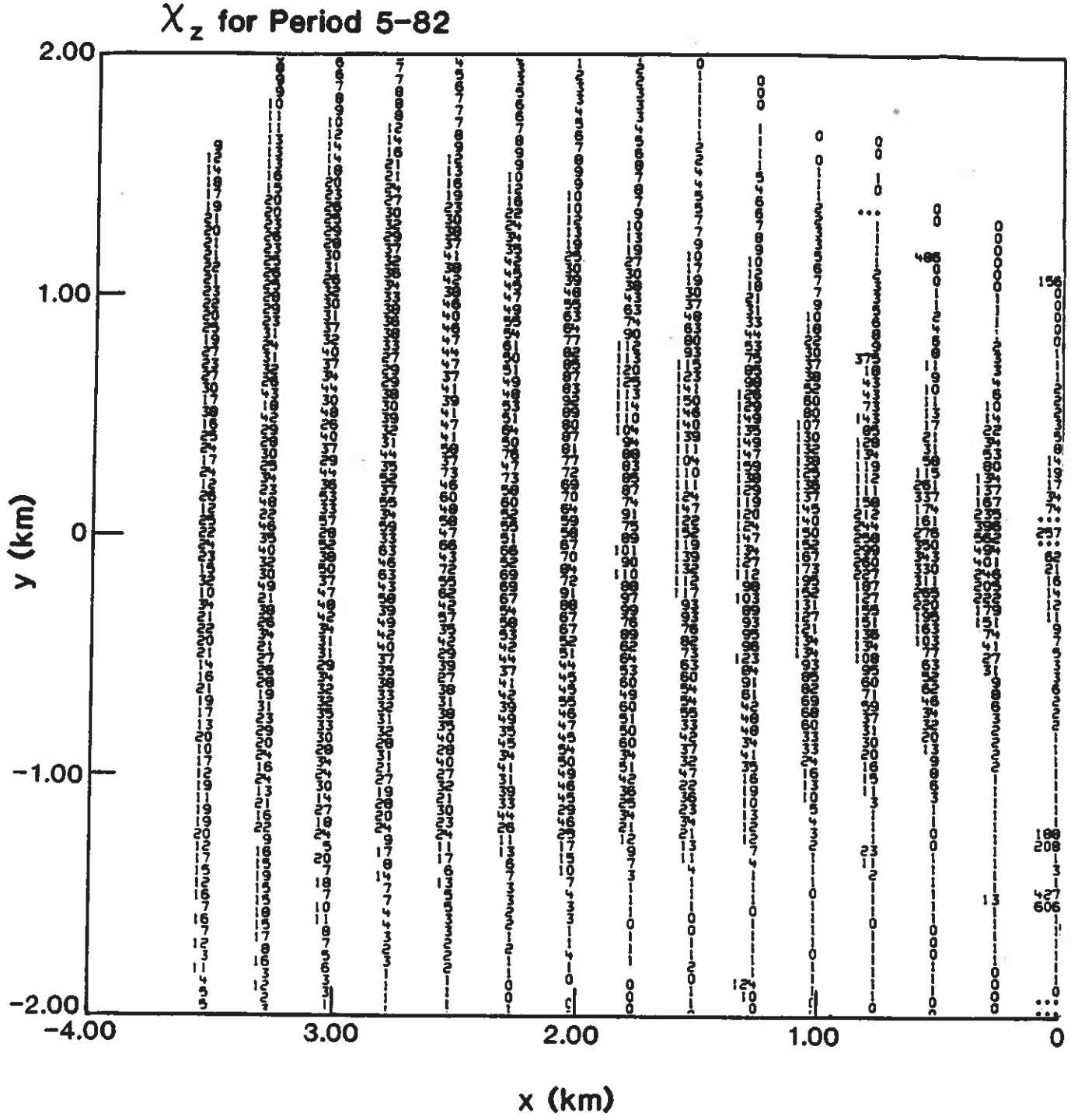

Fig. B.2 (5-82)

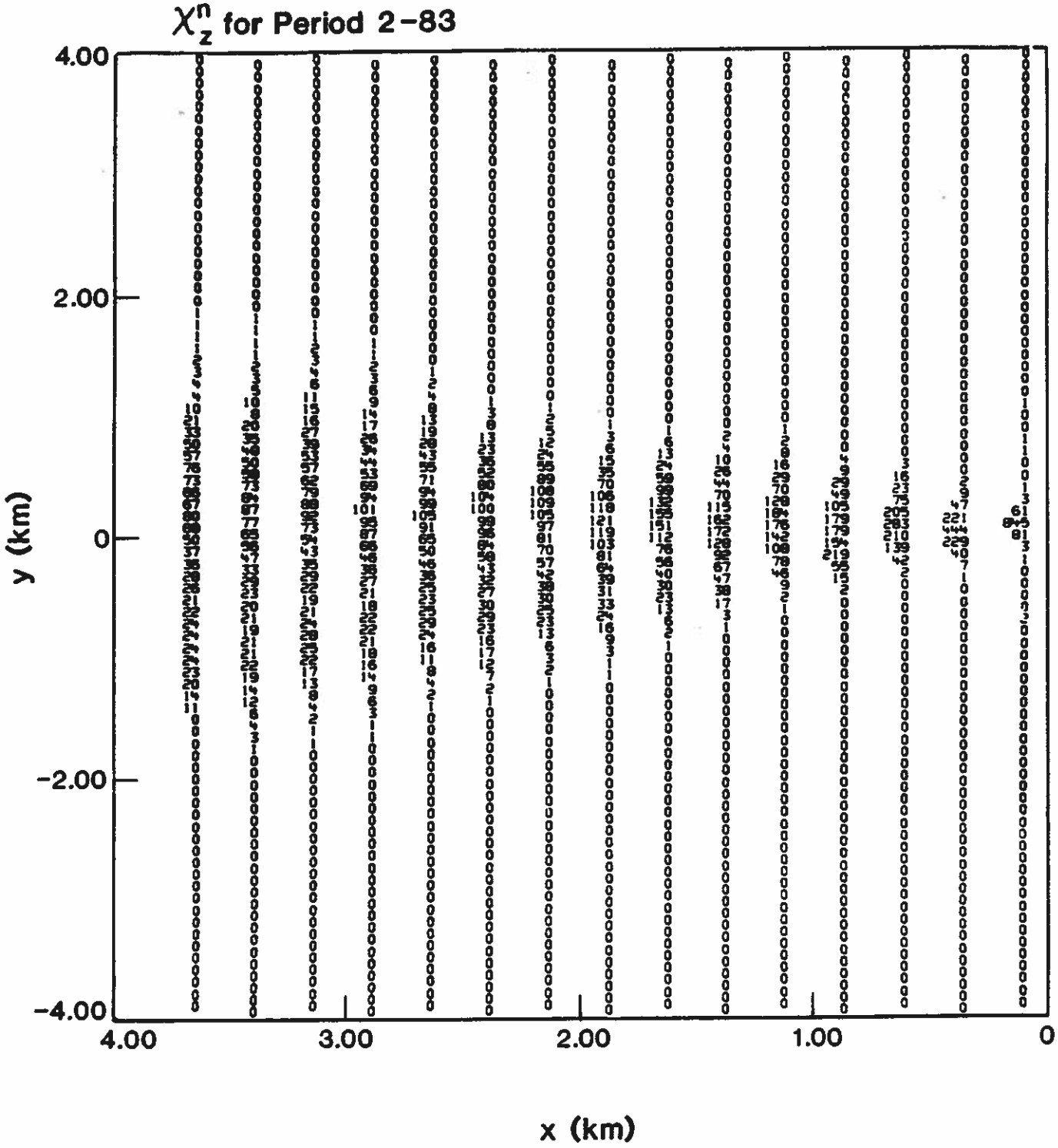

Fig. B.2 (2-83)

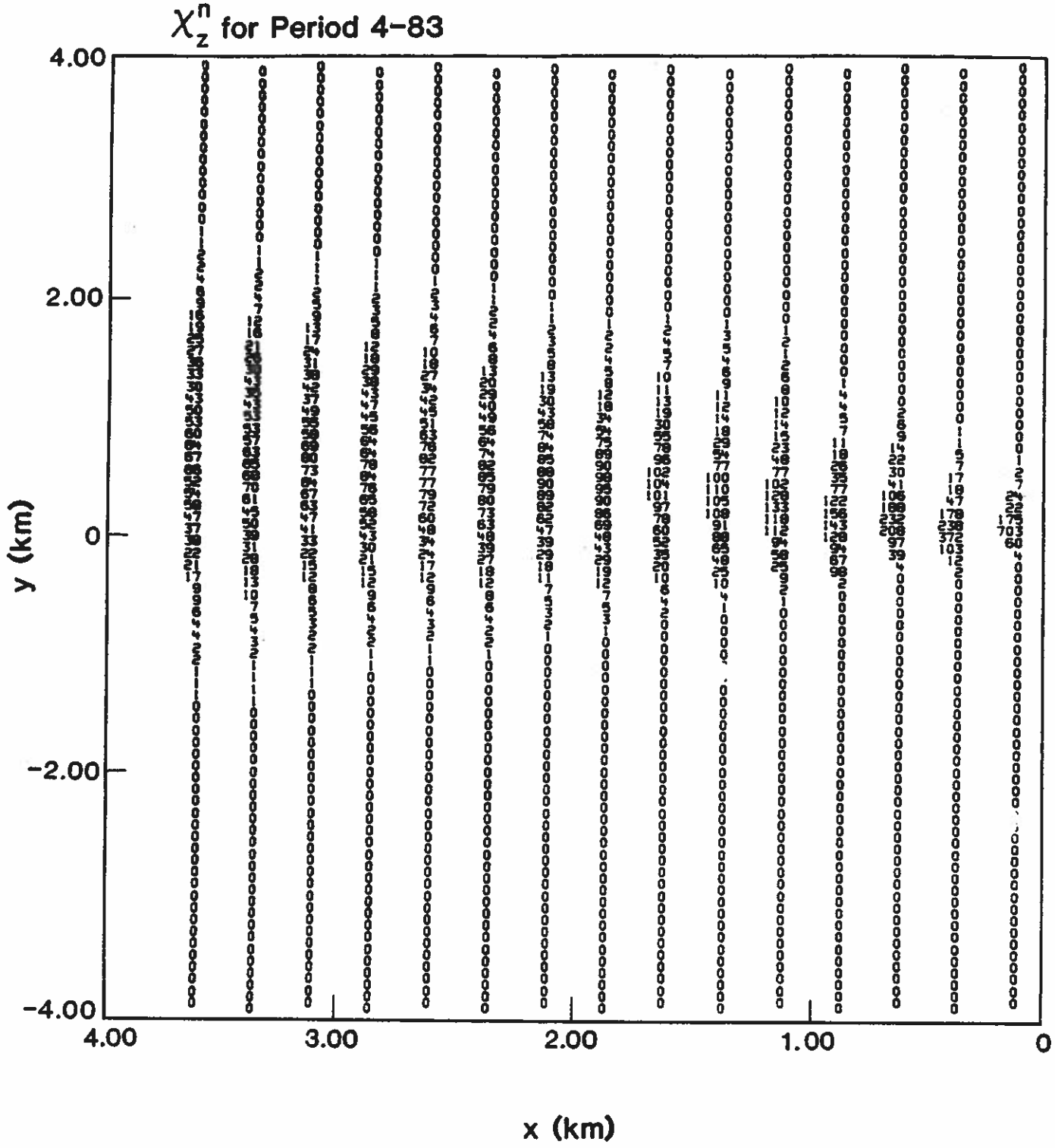

Fig. B.2 (4-83)

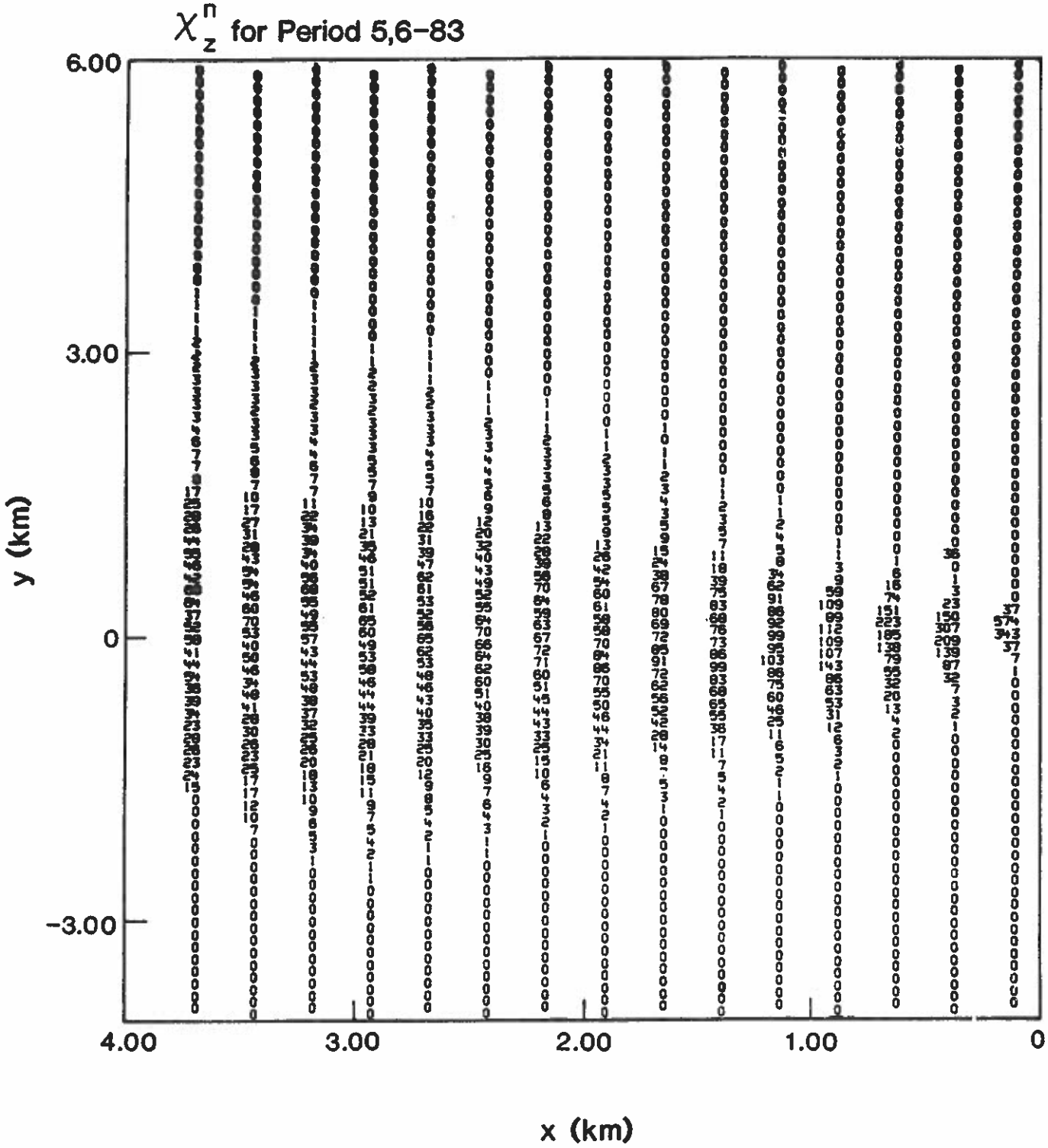

Fig. B.2 (5,6-83)

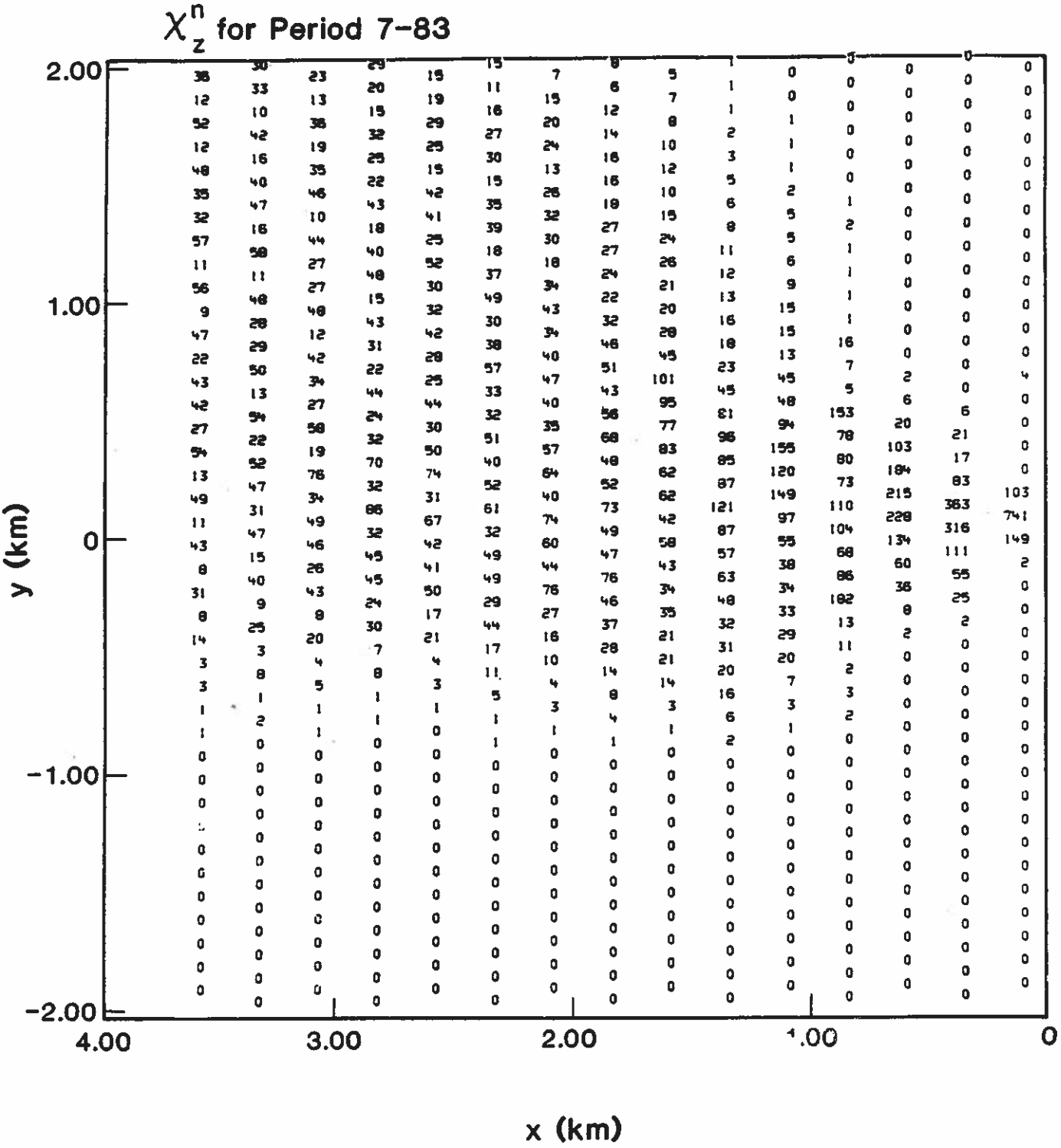

Fig. B.2 (7-83)

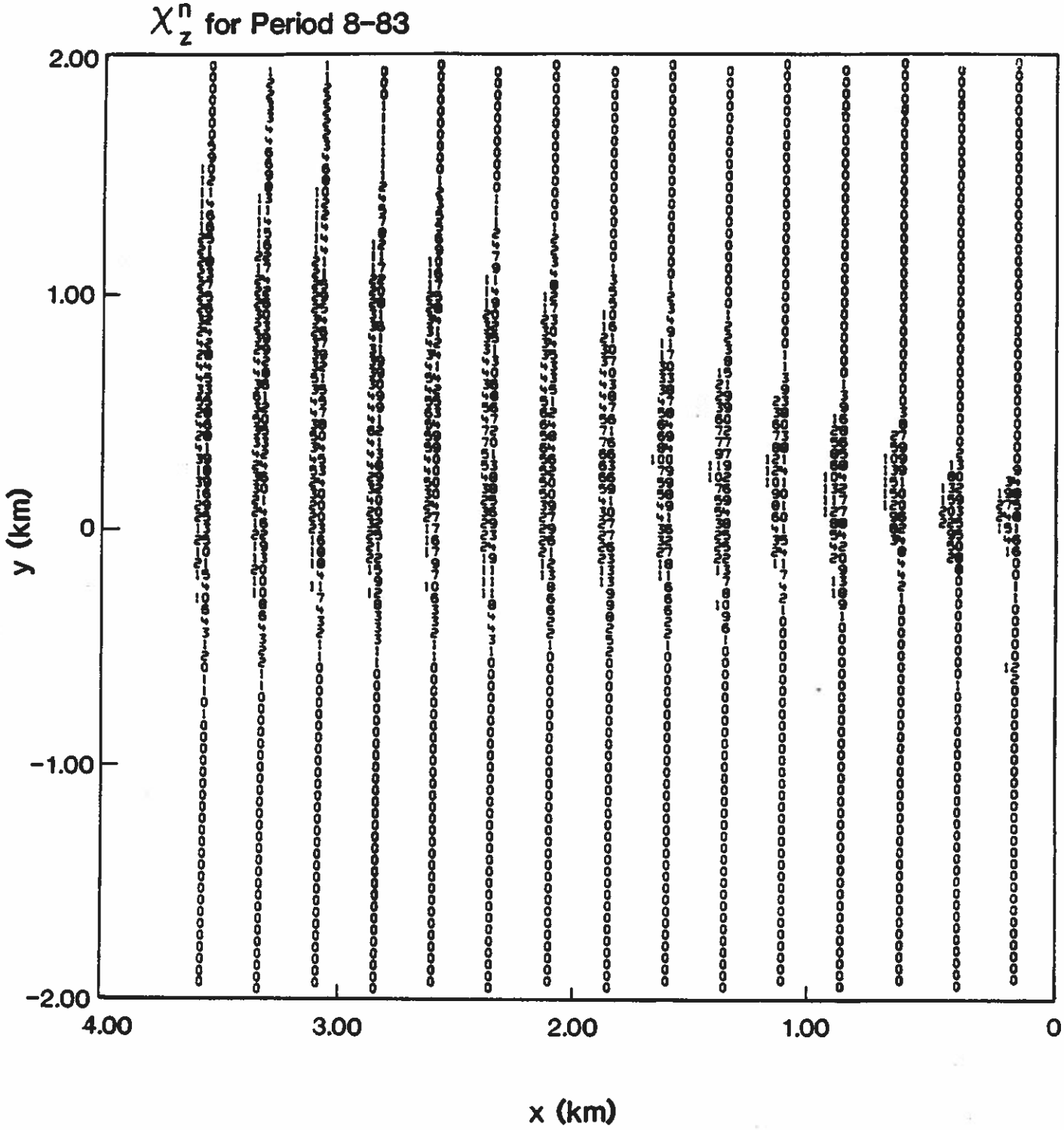

Fig. B.2 (8-83)

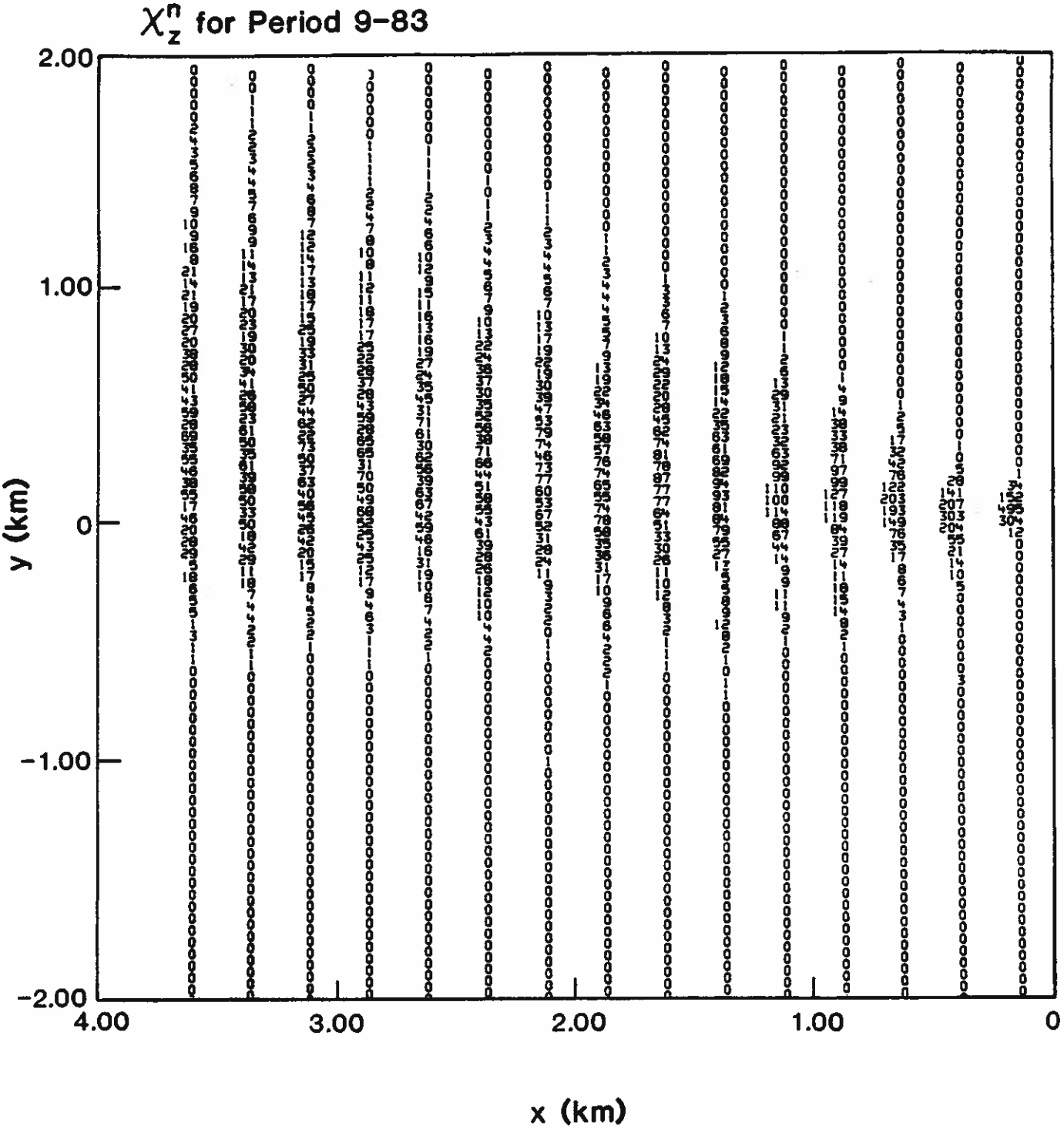

Fig. B.2 (9-83)

Fig. B.3. Chaff σ_y plotted as a function of x.

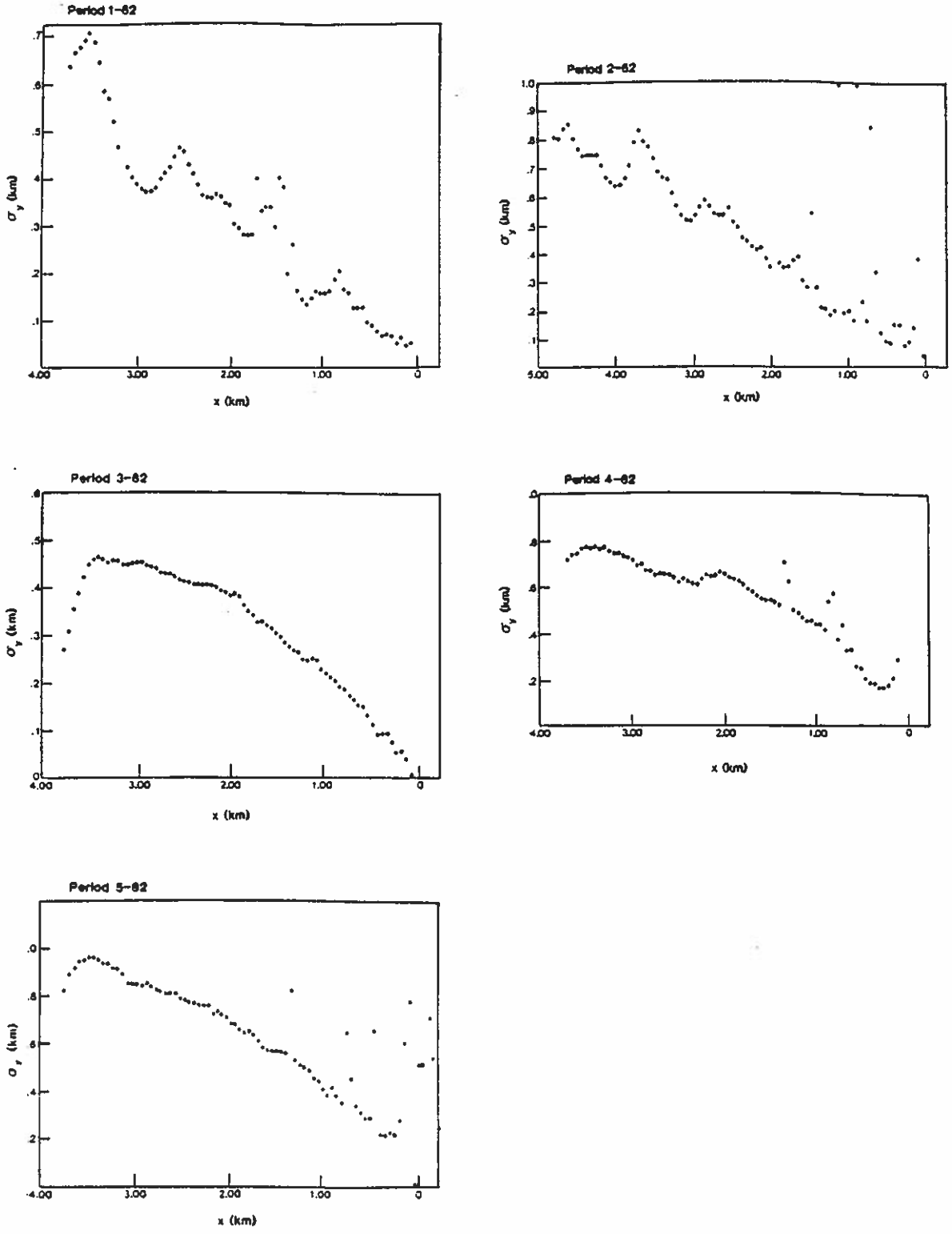

Fig. B.3 (1-82 to 5-82)

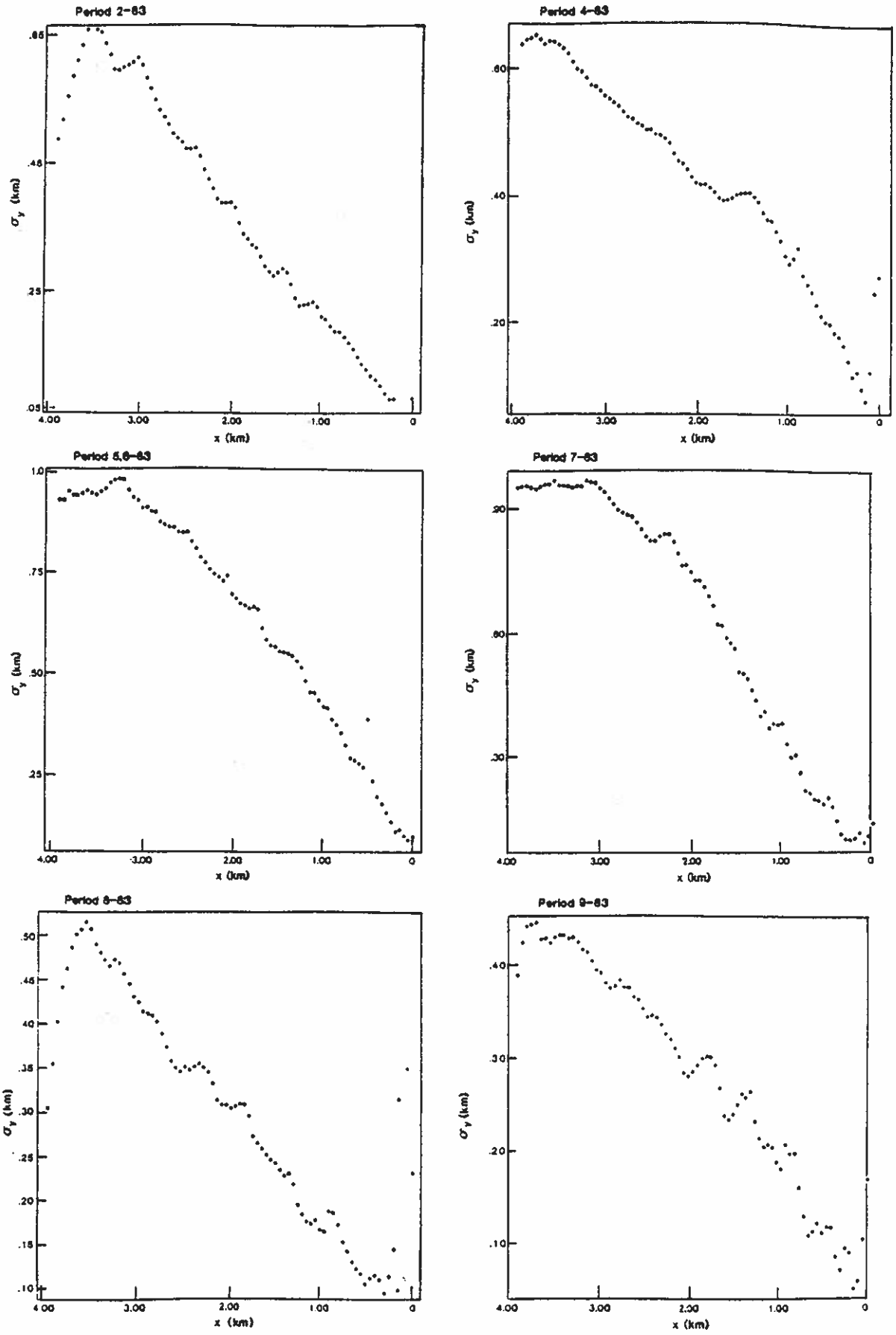

Fig. B.3 (2-83 to 9-83)

Fig. B.4. Chaff y of $(x_z)_{max}$ plotted as a function of x.

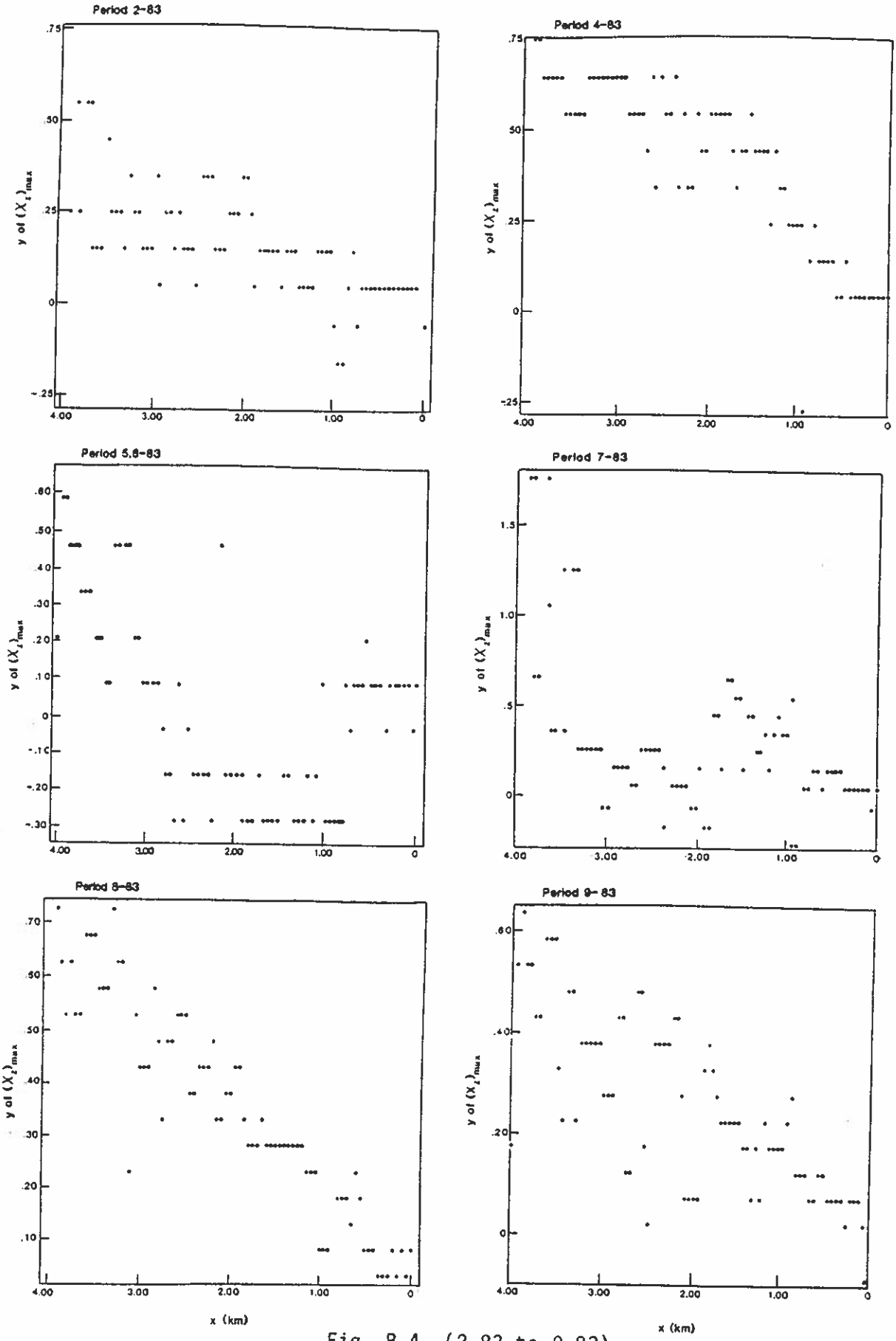

Fig. B.4 (2-83 to 9-83)

Fig. B.5. Chaff $\overline{z}$ plotted as a function of x.

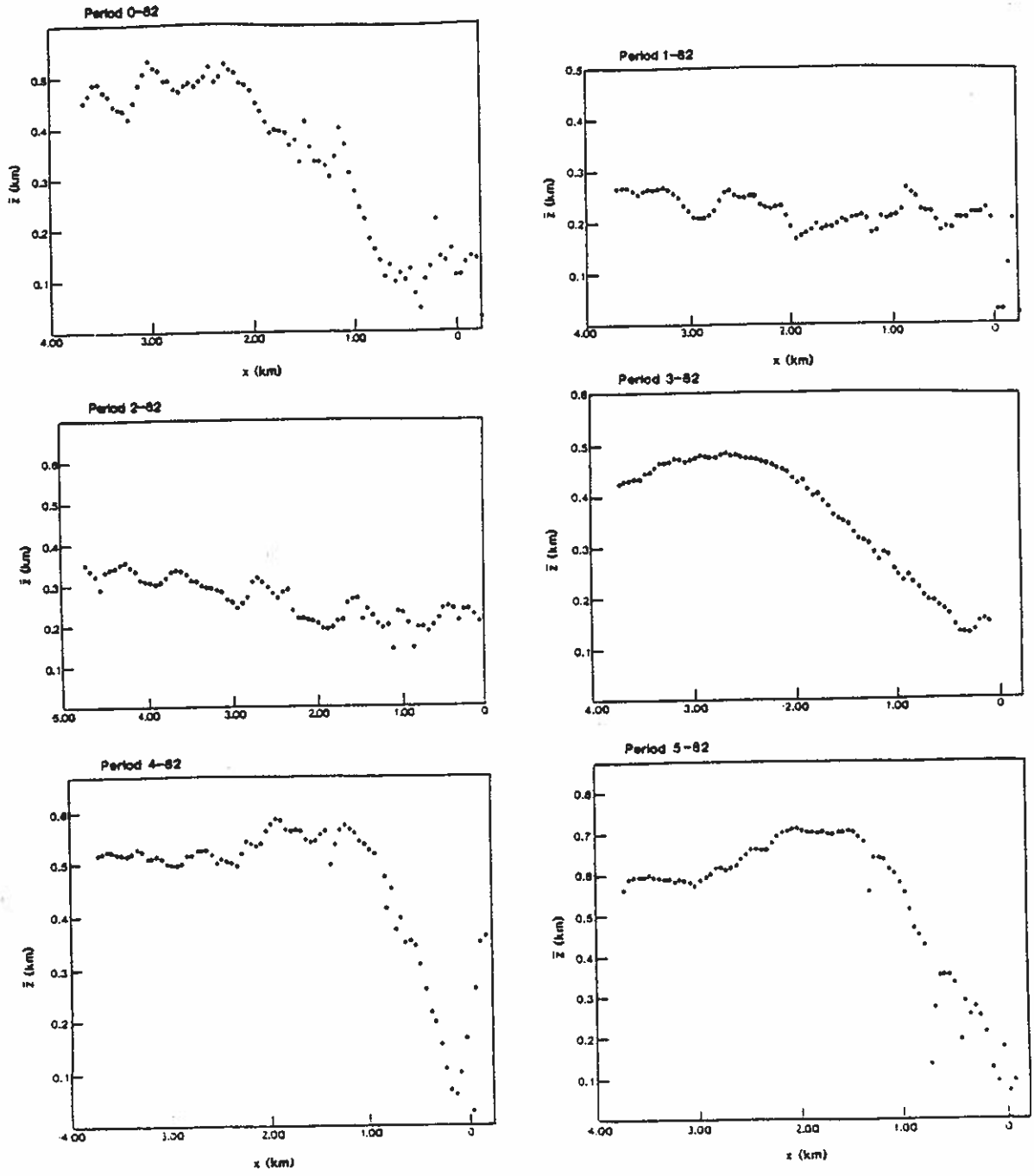

Fig. B.5 (0-82 to 5-82)

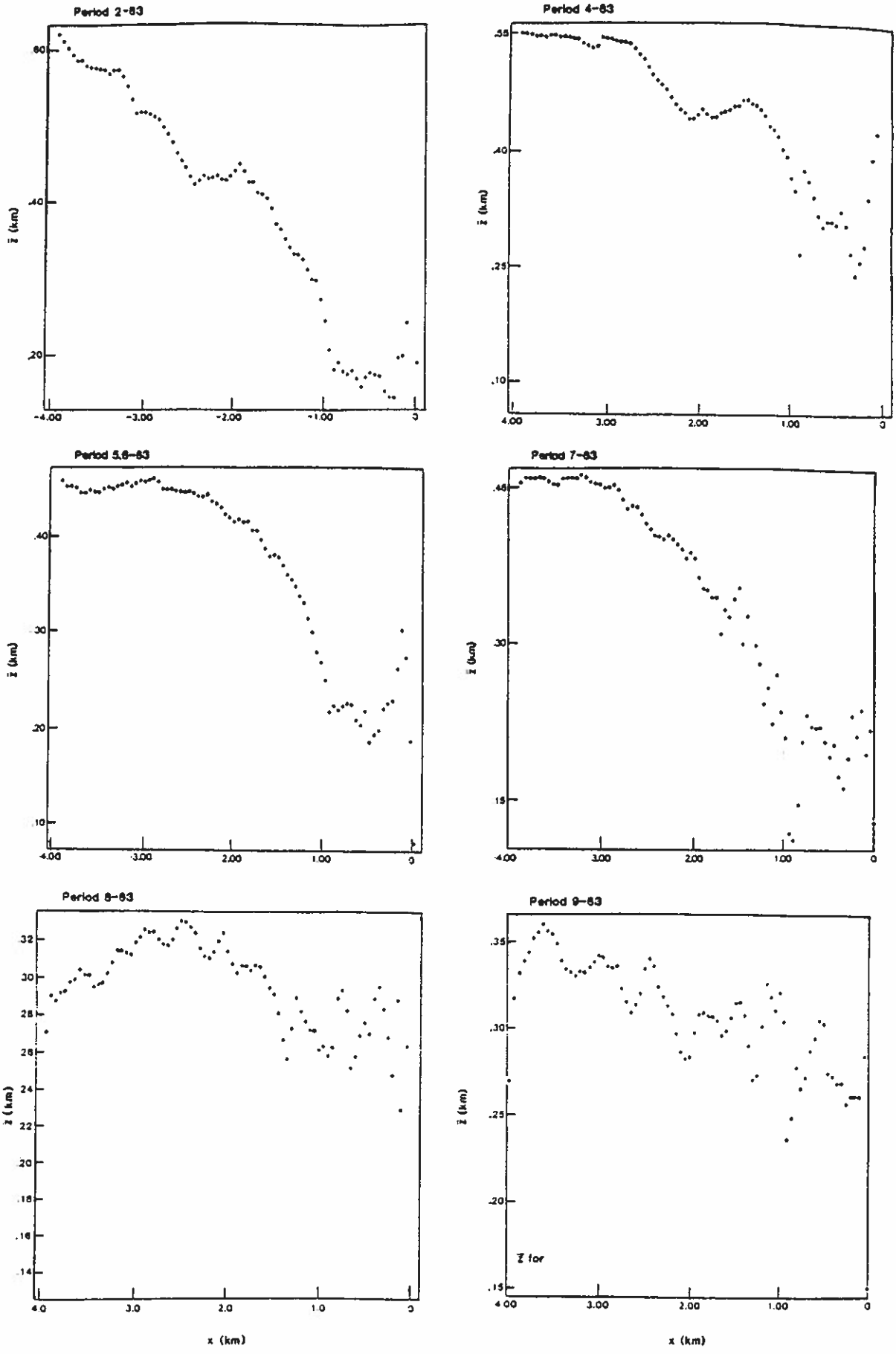

Fig. B.5 (2-83 to 9-83)

Fig. B.6. Chaff σ_z plotted as a function of x.

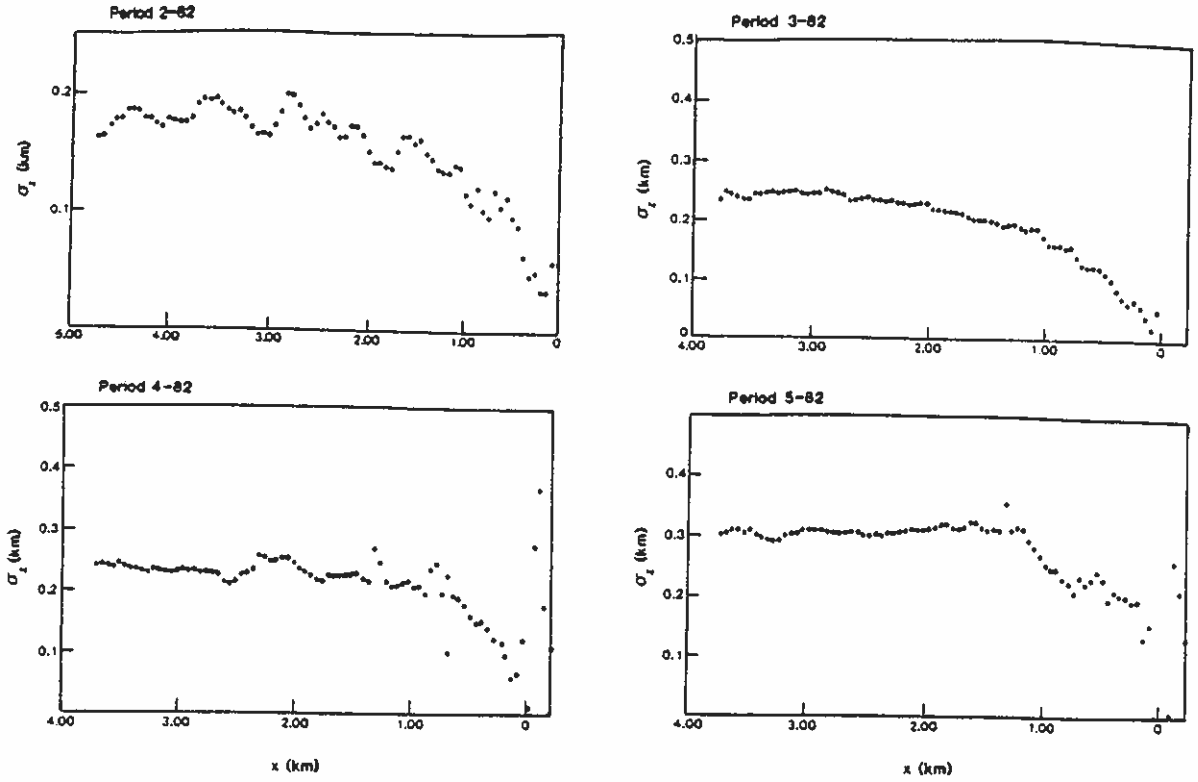

Fig. B.6 (2-82 to 5-82)

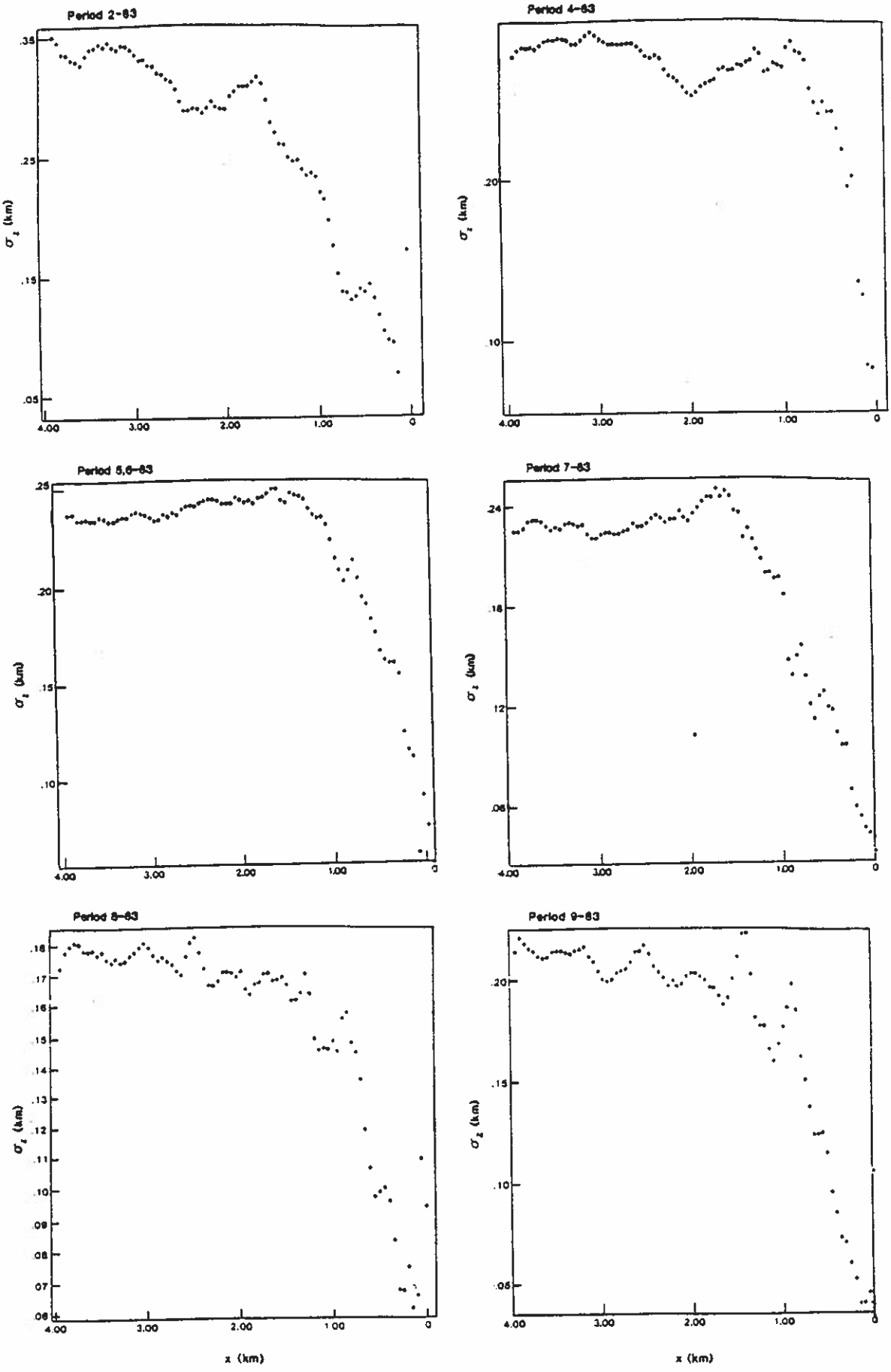

Fig. B.6 (2-83 to 9-83)

Fig. B.7. Chaff z of $(x_y)_{max}$ plotted as a function of x.

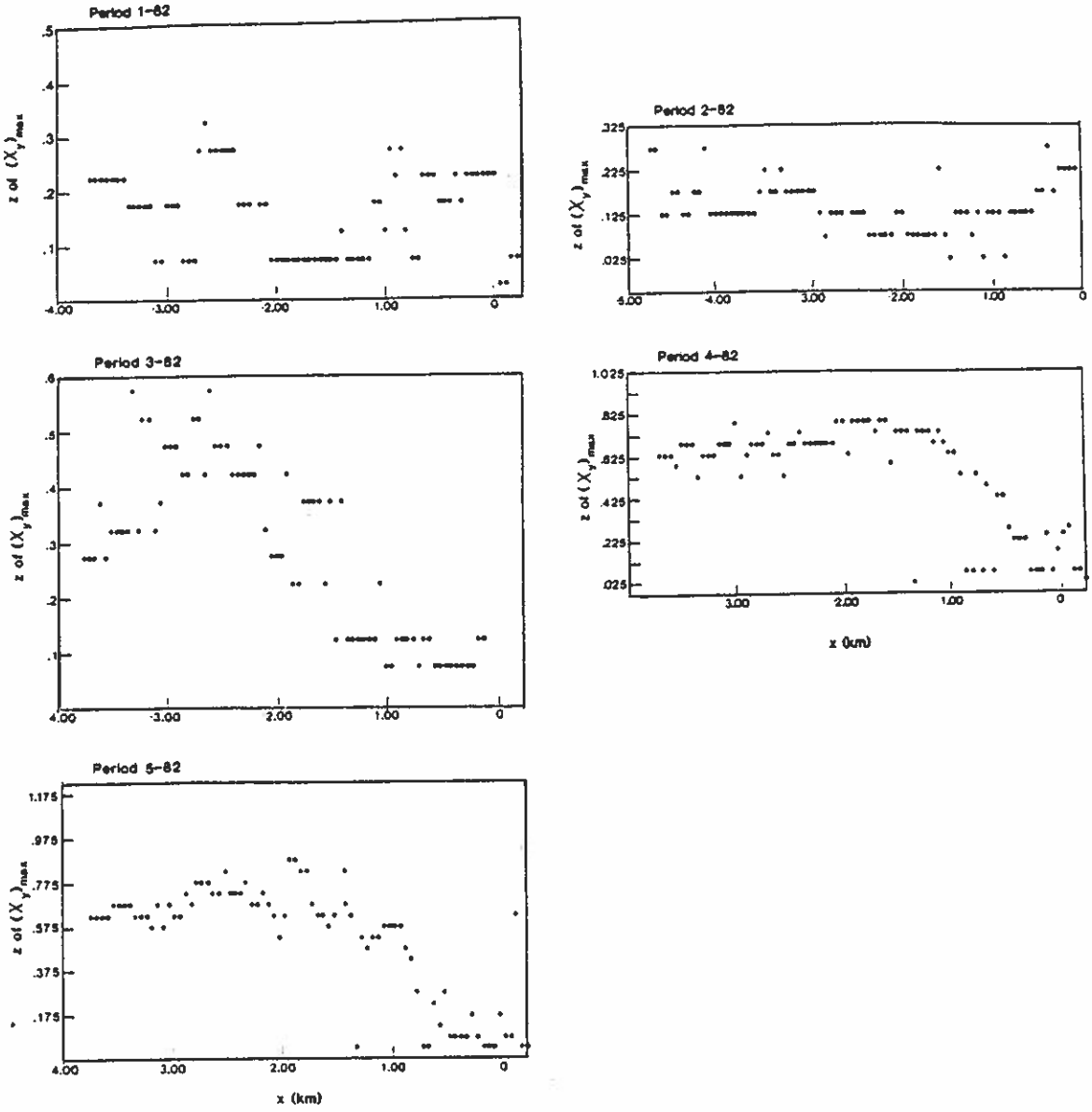

Fig. B.7 (1-82 to 5-82)

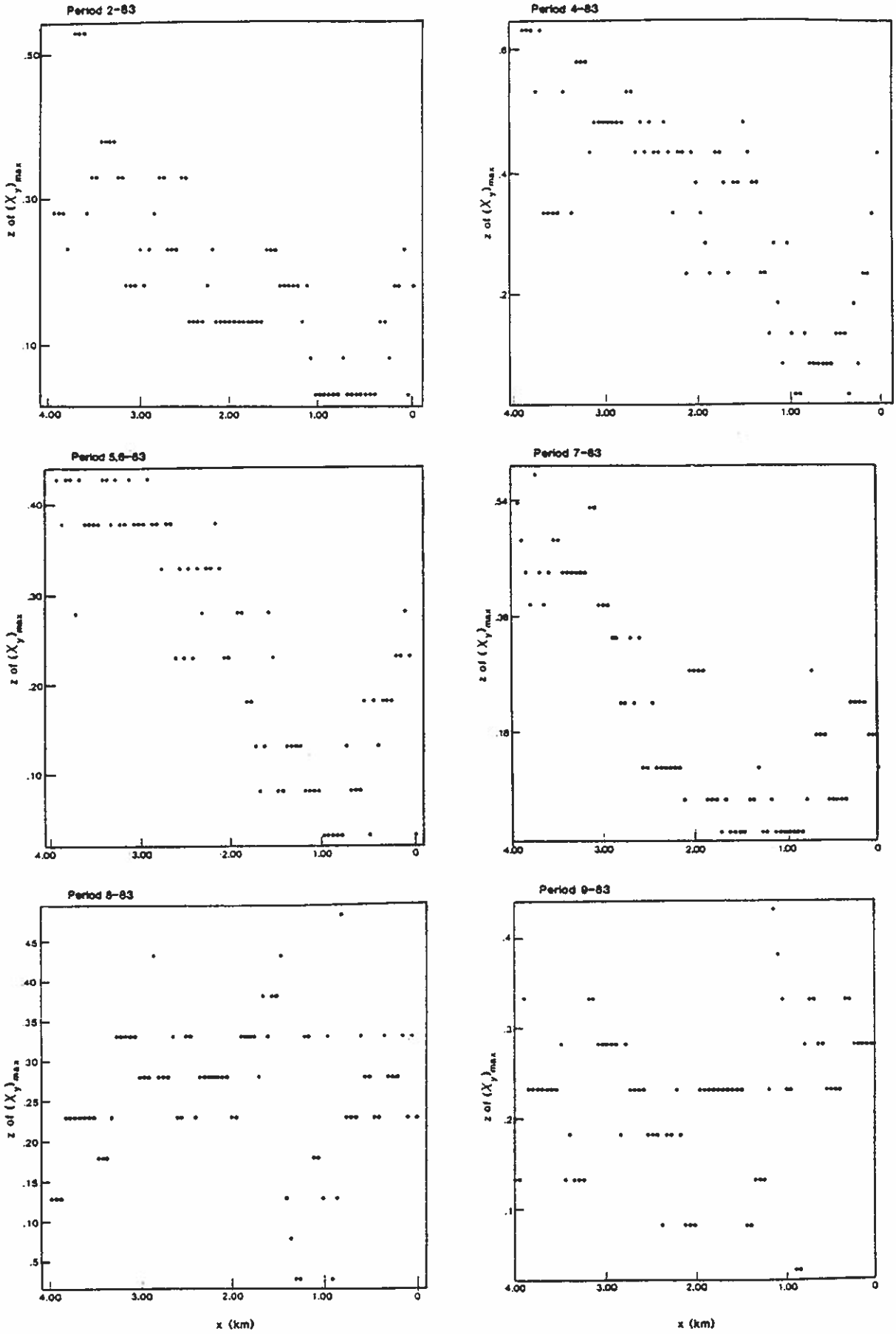

Fig. B.7 (2-83 to 9-83)

Fig. B.8. Chaff x_{yz} plotted as a function of x.

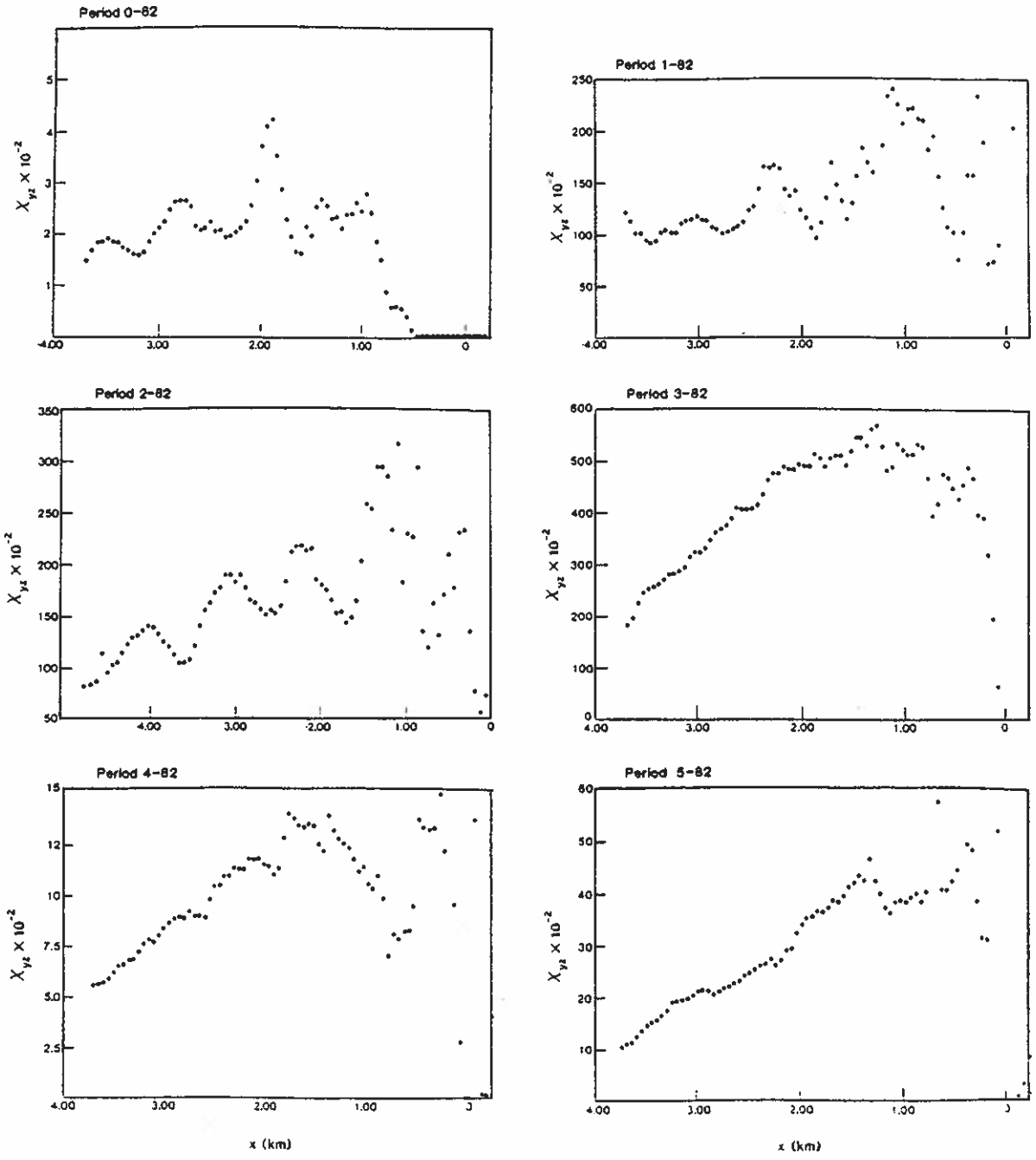

Fig. B.8 (0-82 to 5-82)

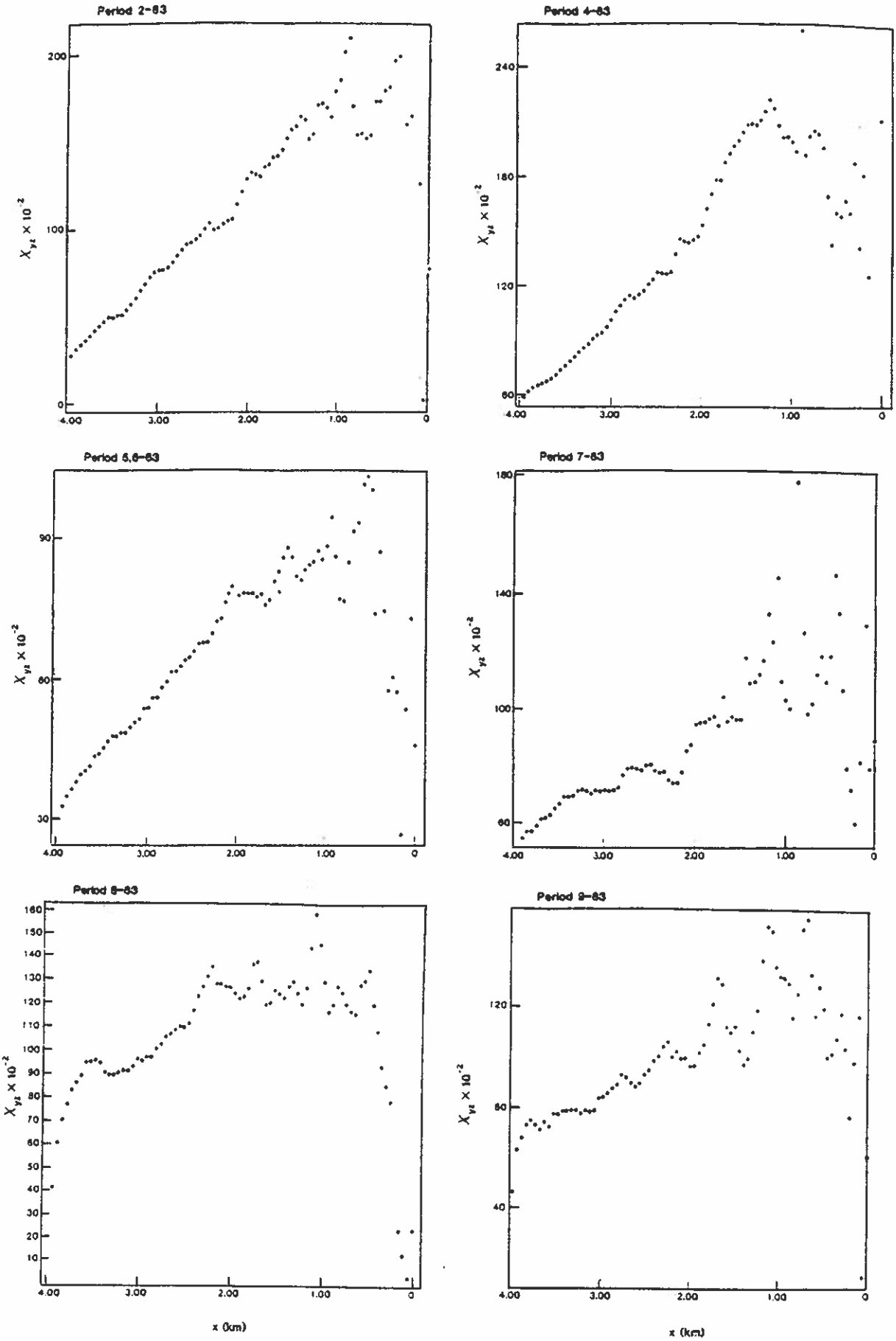

Fig. B.8 (2-83 to 9-83)

Fig. B.9 Chaff $(x_y)_{max}$ plotted as a function of x.

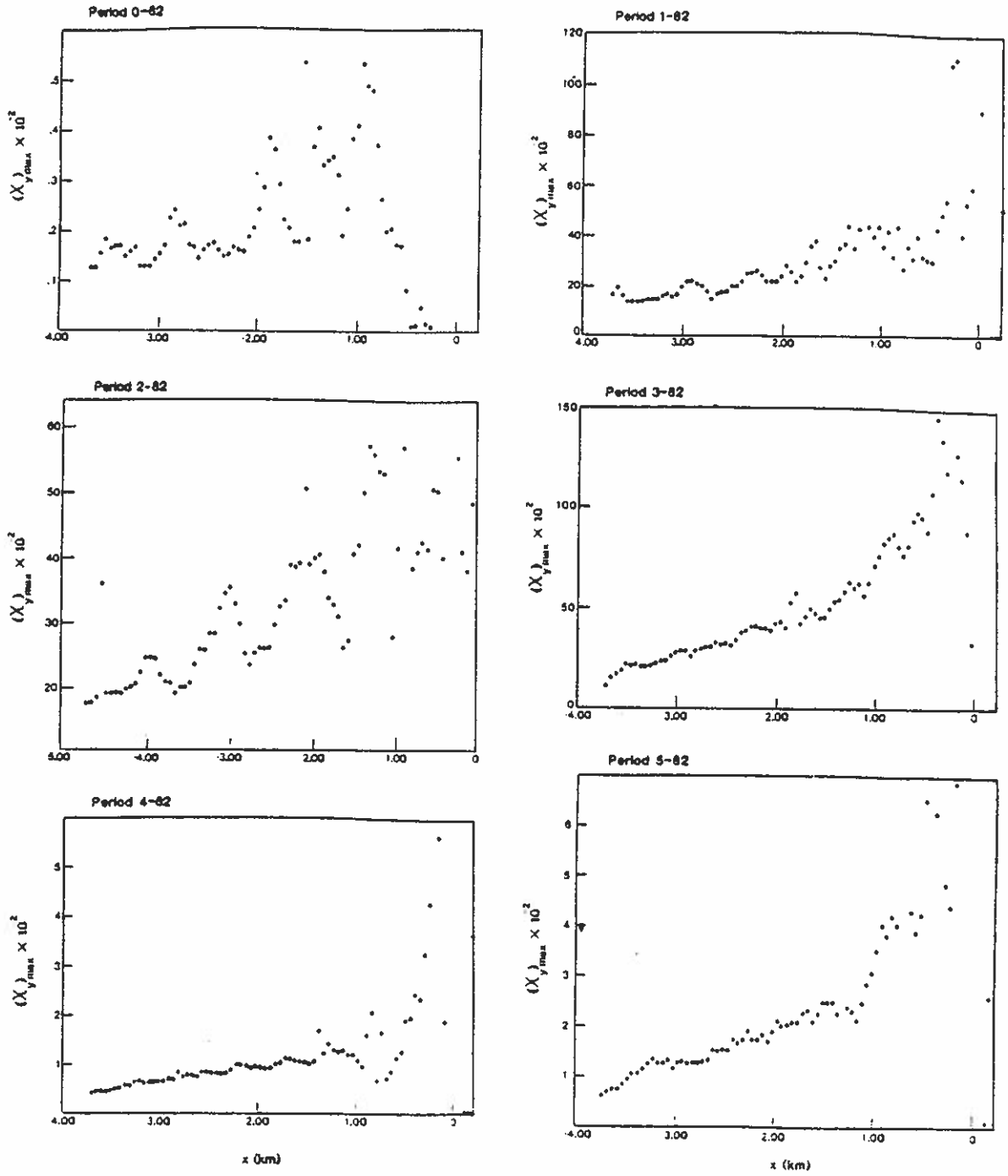

Fig. B.9 (0-82 to 5-82)

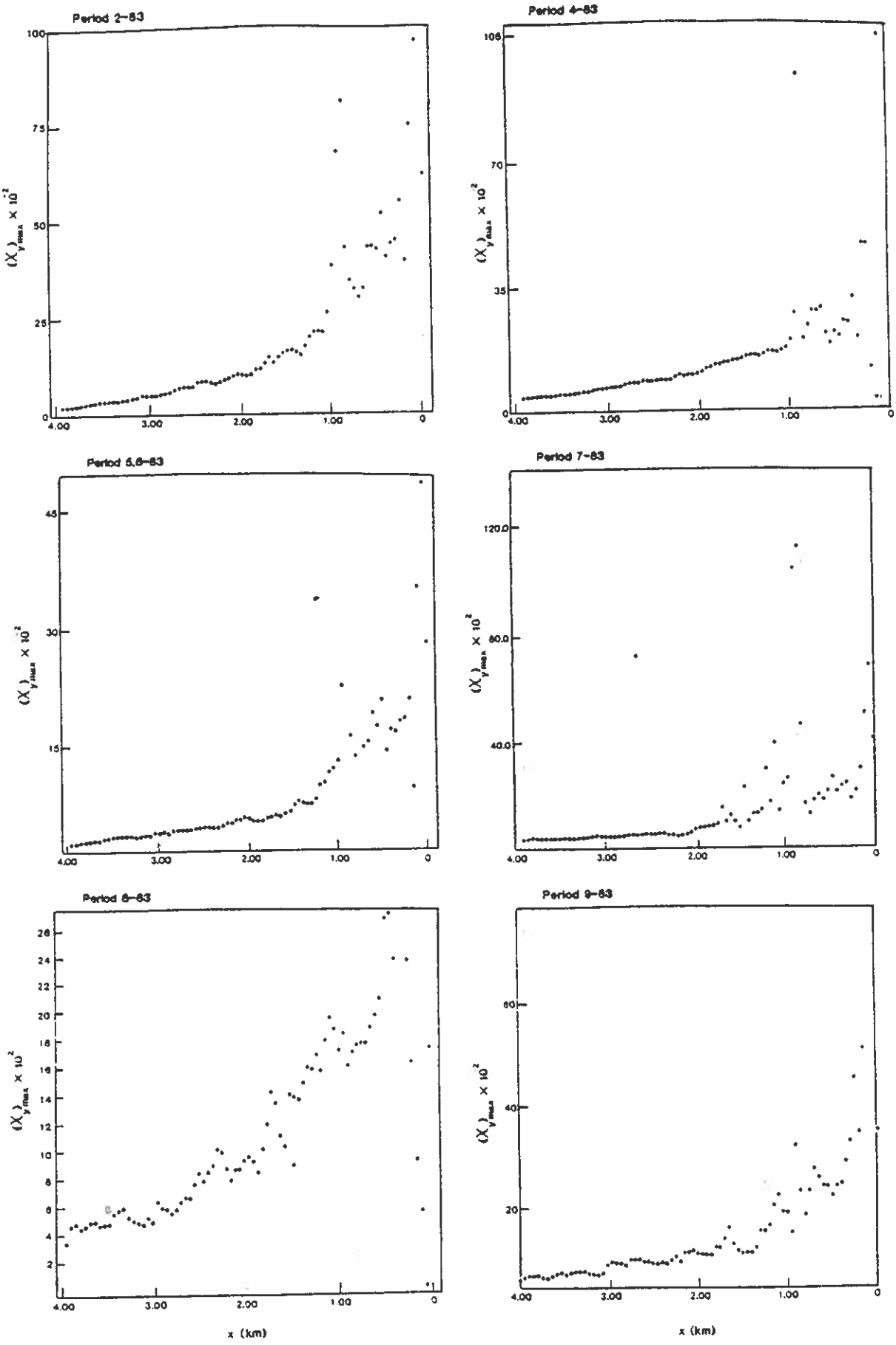

Fig. B.9 (2-83 to 9-83)

Fig. B.10. Evolution of the χ_7 = 100 filaments/(50 m)^2 column contour on the xy plane shown at different time steps during periods analyzed for CONDORS 83. For periods 7-83, 8-83 and 9-83, some of the apparent jaggedness of the contour is an artifact of the high scan rates needed to scan the entire plume.

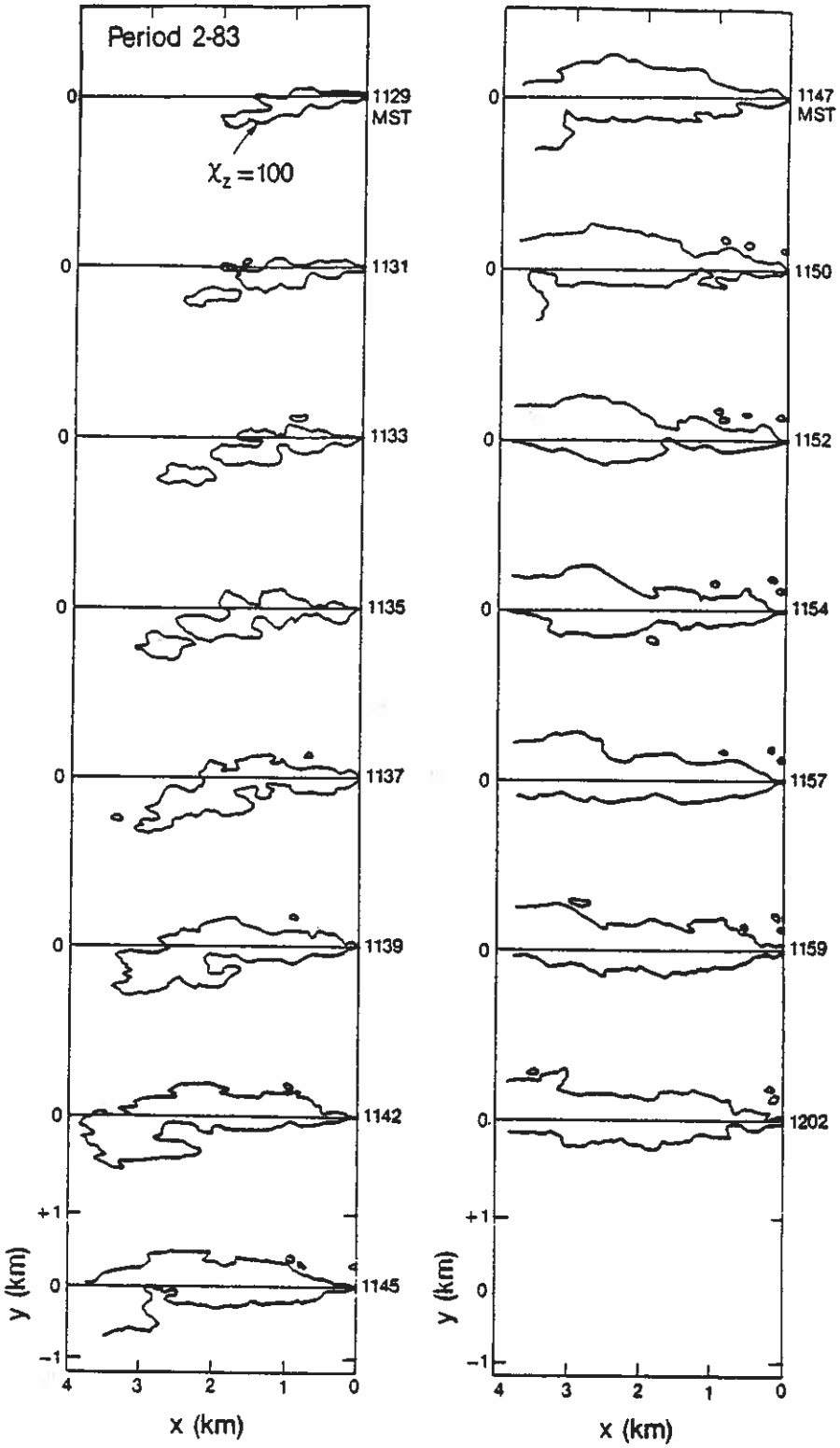
Period 2-83
1129 MST
$\chi_z = 100$
1131
1133
1135
1137
1139
1142
1145
1147 MST
1150
1152
1154
1157
1159
1202
y (km)
x (km)

Fig. B.10 (2-83)

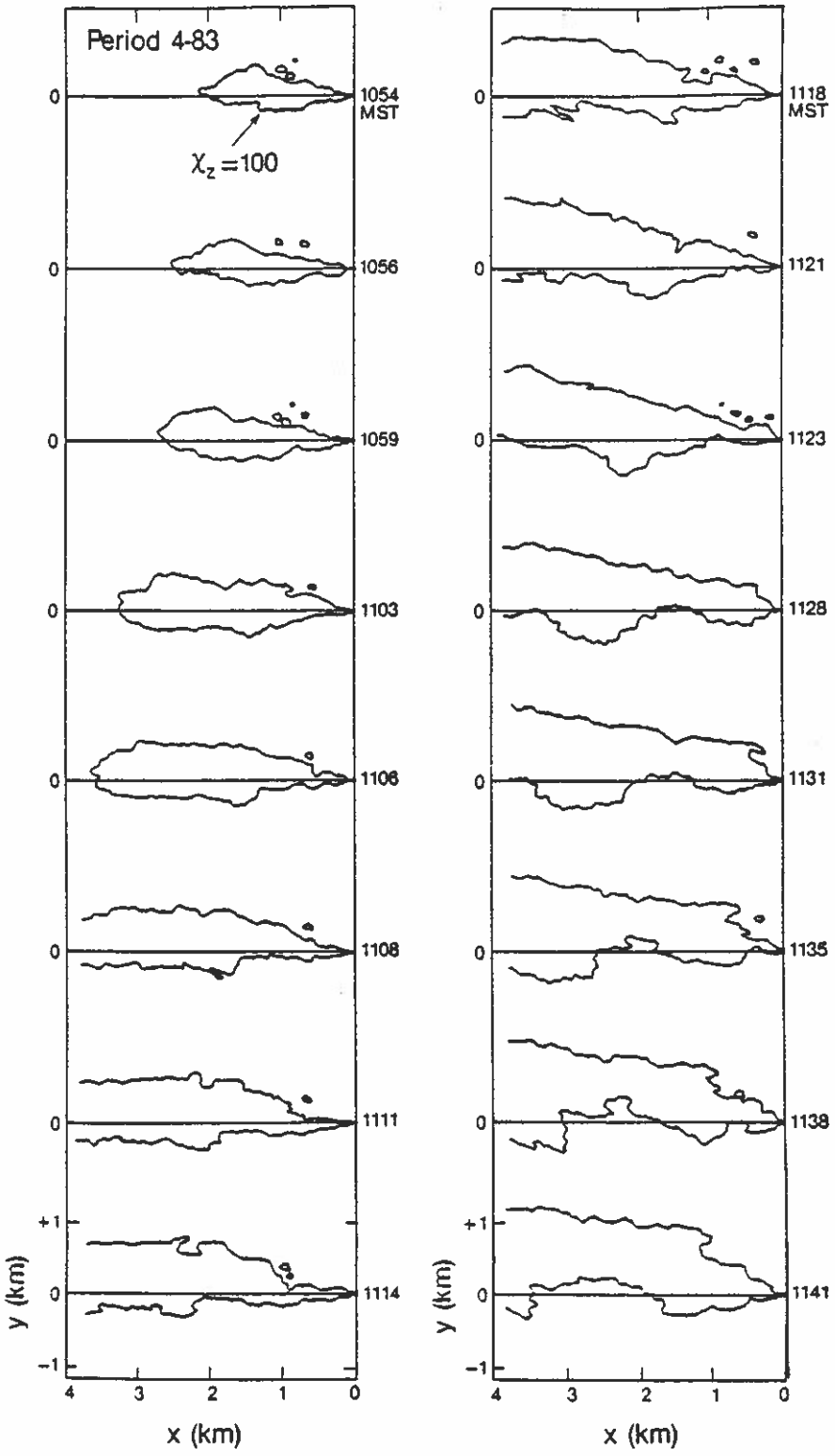
Period 4-83
χ_z =100
1054 MST
1056
1059
1103
1106
1108
1111
1114
1118 MST
1121
1123
1128
1131
1135
1138
1141
0
+1
-1
4
3
2
1
0
y (km)
x (km)

Fig. B.10 (4-83)

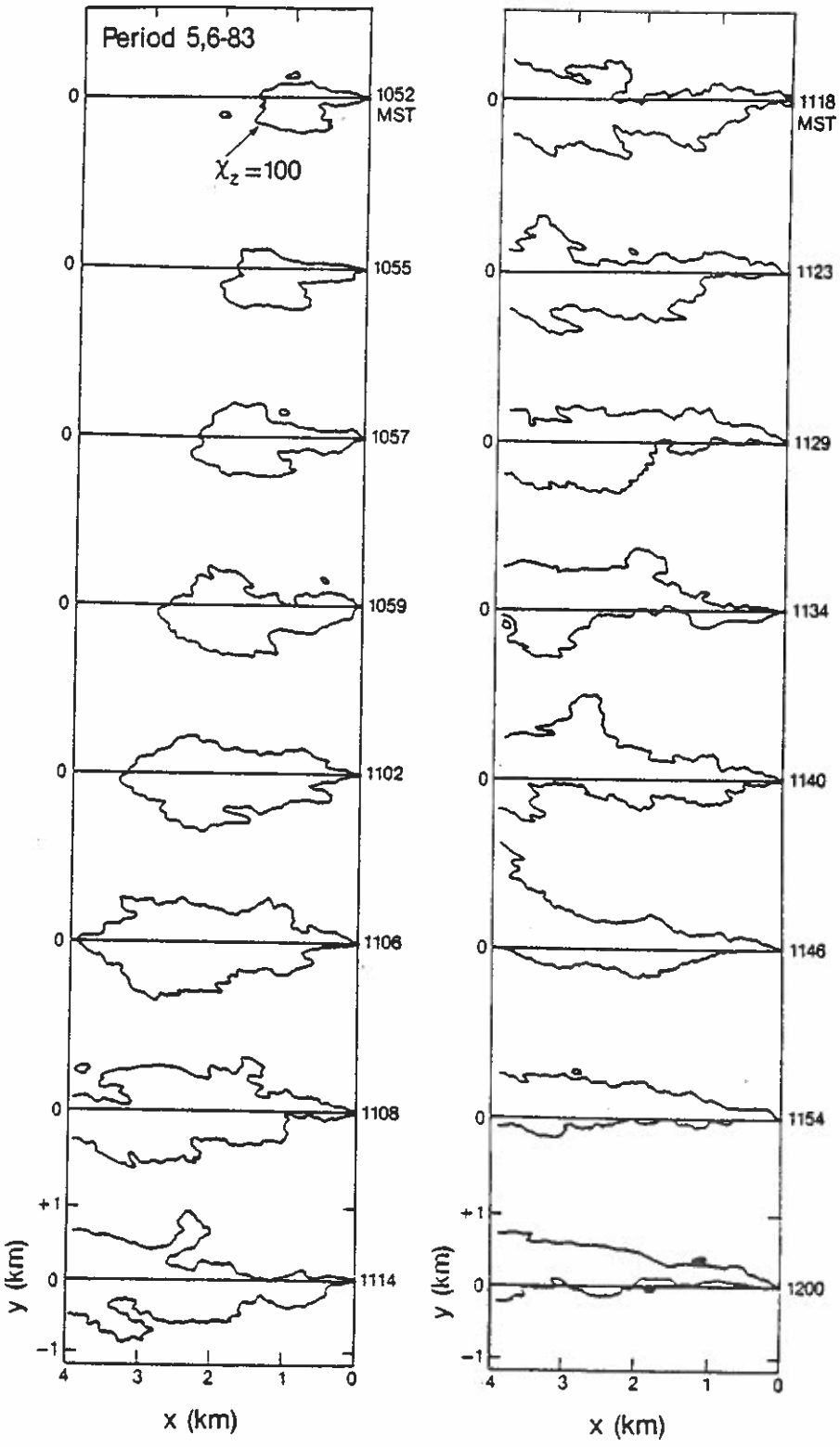
Period 5,6-83
1052 MST
$\chi_z = 100$
1055
1057
1059
1102
1106
1108
1114
1118 MST
1123
1129
1134
1140
1146
1154
1200
y (km)
x (km)

Fig. B.10 (5,6-83)

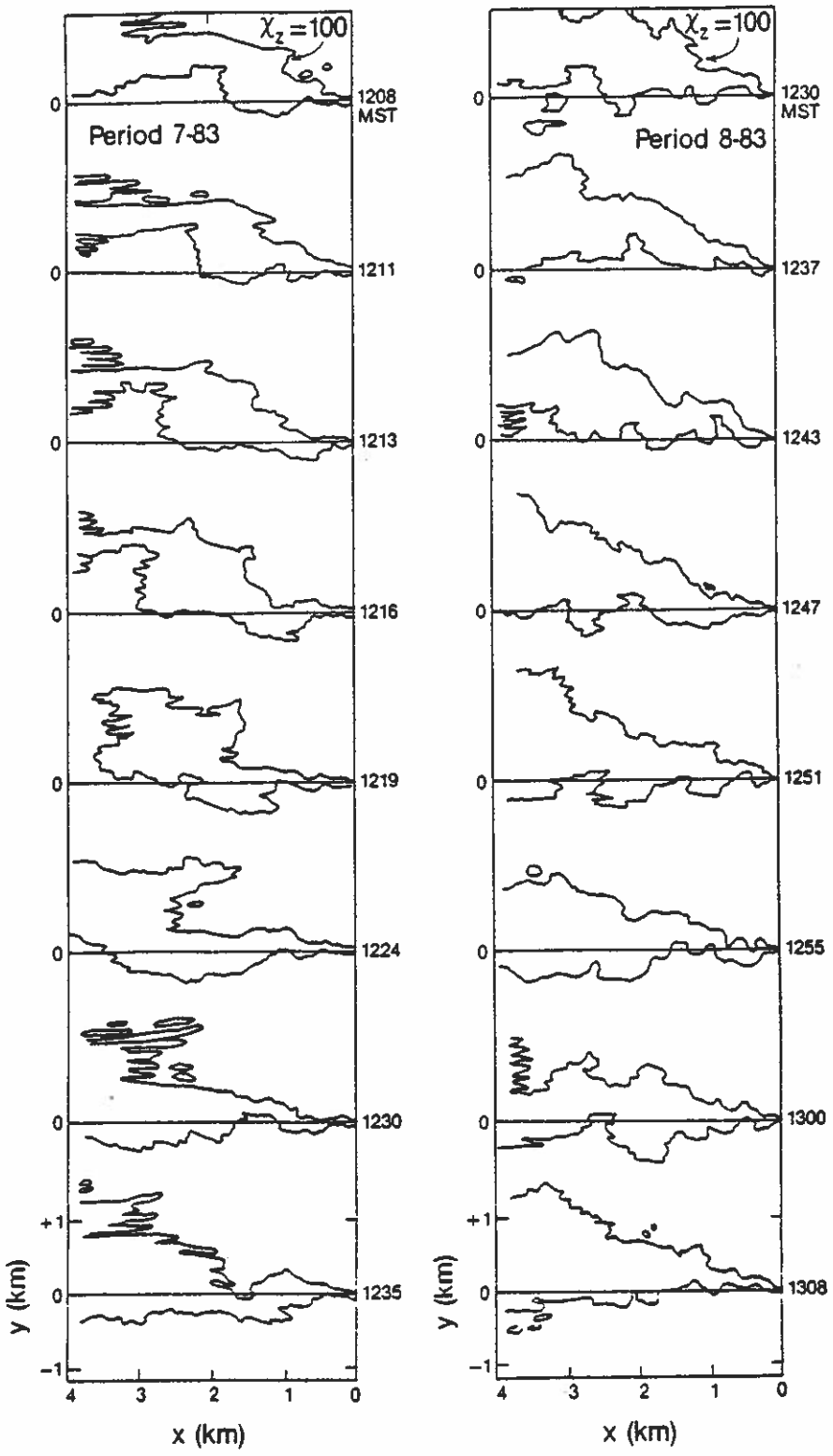
$\chi_z = 100$
Period 7-83
1208 MST
1211
1213
1216
1219
1224
1230
1235
$\chi_z = 100$
Period 8-83
1230 MST
1237
1243
1247
1251
1255
1300
1308
y (km)
x (km)
+1
0
−1
4
3
2
1
0

Fig. B.10 (7-83)

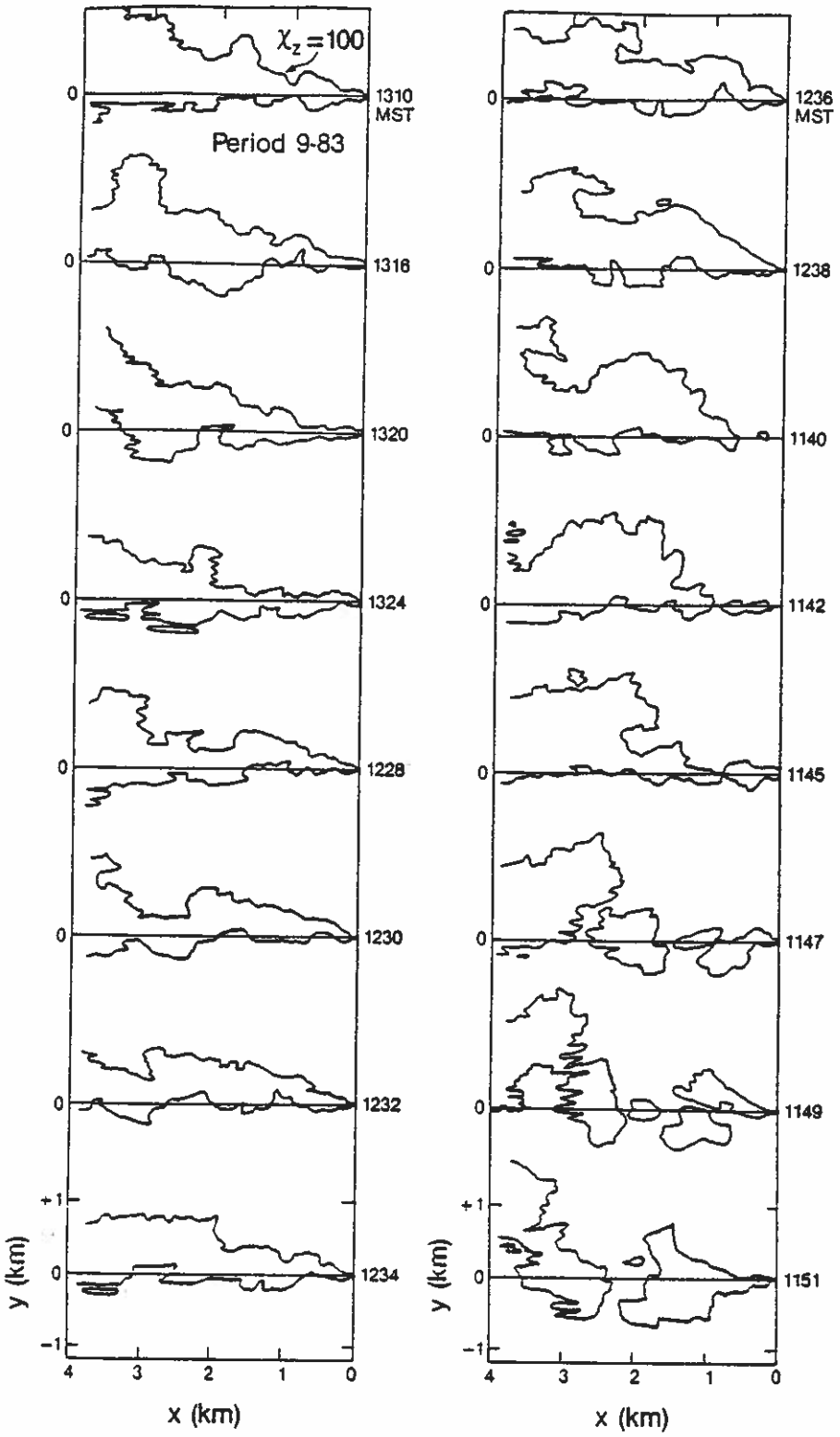
$\chi_z = 100$
Period 9-83
1310 MST
1316
1320
1324
1228
1230
1232
1234
1236 MST
1238
1140
1142
1145
1147
1149
1151
y (km)
x (km)
+1
0
-1
4
3
2
1
0

Fig. B.10 (9-83)

APPENDIX C

QUALITY CONTROL EVALUATION REPORT

C.1. Oil Fog Measurements

The lidar crew and processing staff adhered to our standard procedures for quality control during CONDORS. Chapter 3 discusses the methodology in detail, and Chapters 3 and 11 describe the limitations of the processed data. Except for these minor restrictions, we consider the lidar data to be a correct and dependable measure of plume concentrations. Summarized below are the important challenges and problems that we faced and our responses to them.

Tracer: Because atmospheric haze sets a threshold for the minimum detectable amount of oil fog, the magnitude of oil release rate was a matter of concern. Tests were performed during the spring of 1982 to determine the appropriate rate. During CONDORS 82 the lidar could not adequately measure the plume quite as far downwind as desired, so a second oil fogger was acquired to double the maximum release rate during CONDORS 83. This step plus the use of a heavier, less volatile oil in 1983 extended the range of usable scans for ground source plumes to $x \sim 2.5$ km, compared with 0.7 km in 1982. Because the second oil fogger could not be used on the tower carriage for the elevated releases, there was only a modest improvement in maximum plume scan range in 1983 for these cases; the smallest maximum scan range was $x \approx 1.5$ km, compared with 1.1 km in 1982; the largest usable range for elevated sources was $x \approx 2$ km in both years.

The constancy of oil fog release rates and of oil droplet size distribution, which affects the backscatter coefficient, is harder to assess. Checks of oil

levels during runs showed that the oil consumption rate did not vary more than 10% within a run. Rates of consumption per fogger ranged from 21 to 36 g/s, except on 6 September 1983, when the consumption rate, Q, fell to only 9 g/s. The K_o values for the day, which are already normalized with Q, were at least a factor of two lower than those on other elevated plume days (see Tables 8.1 to 8.3 and 8.10 to 8.14); this suggests a less efficient droplet size distribution for producing backscatter. Qualitatively, the oil foggers appeared to produce smoke at nearly constant rates within each run. We feel that problems associated with uncertainty about the constancy of Q and backscatter quality during runs are largely avoided by the use of local downwind flux measured in each scan in place of Q as a normalizing quantity (this, in essence, is the function of K_o).

Imperfect conservation of tracer: Data from plume dispersion experiments before CONDORS indicated that scan-integrated optical backscatter of the oil fog decreases with distance. The degree of decrease was quantified during CONDORS 82. A more viscous oil with lower vapor pressure was used during CONDORS 83, which reduced the rate of loss considerably. This is shown by the empirical calibration factors, K_o, in the tables in Chapter 8 (K_o is the measured downwind flux of backscatter for each scan, divided by Q, assuming constant wind throughout the scan). Especially for elevated source periods, there is much less decrease in K_o with distance in 1983 than in 1982, which suggests less evaporation. The multiplication of Q by K_o provides a means to compensate for loss of tracer by using the local downwind flux of oil fog as a concentration normalizer. The results will be equivalent to those from a conservative tracer if the relative vaporization rate is constant across the plume cross section, a condition that we can only assume.

Site change: The lidar site was moved for CONDORS 83 so that the scans could intercept the plume axis more orthogonally for the anticipated range of wind directions. The site was also moved farther from the BAO tower to allow adequate cross sections at greater distances downwind of the source. Experience showed that these were both wise choices, as the anticipated dominance of southeasterly winds during CONDORS 83 runs did occur.

Quality assurance during data acquisition: As is standard practice, calibrations were performed on a regular basis during both experimental periods. The system passed a check for accurate elevation and azimuth alignment before every run. An electronic test signal, which was substituted for the detector output before each run, verified proper performance of the data acquisition system. Integrity of lidar operation was assured through real-time displays of the raw signal and system parameters. Crew assignments were organized such that all operator actions could be observed by at least one other member of the crew. All unusual occurrences were noted in the logbook or on audio cassette for later disposition.

Quality assurance during processing: Standard practice was followed during data reduction. Accordingly, all processing decisions and actions were reviewed in detail by at least two staff members. All pertinent processing options and an extensive amount of intermediate data were printed or graphed (on hardcopy) by the computer to aid in this review.

Sensitivity tests for attenuation correction: As stated in Chapter 3, the largest source of error in scans close to the plume's release point was inaccurate correction for the attenuation that was caused by the plume. Sensitivity

tests showed that varying the degree of attenuation correction over a reasonable range did not significantly change the shape of the normalized vertical profiles. The criteria for significance was whether the attenuation-dependent change in relative profile values exceeded the apparently random deviations about a smooth profile in the averaged scans.

Editing of "foreign" signals: In the judgment of WPL scientists, signals from foreign material, such as clouds and power lines, were edited from the data to an adequate degree. Several problem areas, which are discussed in the data report, seemed to have only minor effects on the averaged profiles.

Blockage: Oil fog could not be measured in the first few tens of meters above the surface because the scan was limited to ensure eye-safe laser operation. The data report marks those values in the vertical profile that were affected by the lower scan limit.

C.2 Aluminized Chaff Measurements

Discussed below are the major potential areas of concern regarding the quality of the radar data. We believe that in all cases, we have successfully addressed these areas of concern, so that the radar data presented in this report are trustworthy when they are used within the scope of the provisos mentioned in Chapter 4.

Tracer: The high sensitivity of the radar to reflections from the chaff, with detection of concentrations as low as one filament per 700,000 m^3, assured more than adequate plume detection in the ranges of interest for this experiment. The chaff cutter released chaff steadily at the rate of 38,000

filaments/s. However, in spite of the dispersal effect of the air jet, the majority of these filaments tended to clump together and fall quickly to the ground, with high settling speed. Evidence of this can be found in the behavior of chaff $\bar{z}$ near elevated release points (see tables in Chapter 9). In CONDORS 83 the apparent mean chaff speed at $\bar{x} \approx 80$ m, $\overline{\frac{d}{dz}(\bar{z} - z_s)}$, ranged from -3.87 to +0.28 m/s, while the mean vertical velocity, $\bar{w}$, measured at z = 250 m on the tower ranged from -0.45 to +0.28 m/s during elevated releases. The apparent chaff settling velocity, $[\overline{\frac{d}{dz}(\bar{z} - z_s)} - \bar{w}]$, ranged from -3.68 to +0.37 m/s at this distance, while at $\bar{x} \approx 330$ m it ranged only from -0.76 to +0.01 m/s (the time-weighted mean at the latter distance is -0.20 m/s, somewhat less than the expected settling speed of 0.3 m/s). This suggests wide variations in the degree of clumping and the mean fall speed within the first 200 m of the release point. The range of fall speeds appears to be much less beyond x = 200 m, but we suspect that the range of surviving downwind chaff flux can be large (in 1983, the maximum $\bar{u}x_{yz}$ ranged from 500 to 1320 filaments/s during periods with elevated plumes). As was the case concerning oil fog droplet evaporation, we believe that normalizing chaff concentrations with the local downwind flux of concentration, instead of with the source release rate, largely overcomes interpretational difficulties due to uncertain <u>effective</u> source strengths.

Chaff terminal velocity: Because of the approximately 0.3 m/s terminal velocity of the chaff, the chaff plume was expected to settle somewhat with respect to the oil fog plume. A major purpose of CONDORS 82 was to assess this effect. The CONDORS 82 results indicate that, in the convectively active conditions studied, the settling is slight compared with the statistical variations of the plumes, is of the expected magnitude, and is correctable near elevated release points up to distances near maximum surface impact.

Deposition: After substantial chaff concentrations reach the ground, it is more difficult to adequately correct the vertical concentration distribution for settling effects, because they are then affected by surface reflection, deposition, and resuspension (deposition is probably the most dominant of these three effects); this is the main reason chaff was used only as an elevated-source tracer in 1983. Because we normalized with local downwind flux, we only need to be concerned about the effects on the shape, not the magnitude, of the χ_z profile. At distances where full mixing between the surface and z_i is obtained, deposition loss may not strongly alter the shape of the χ_z profile, because in the time it would take for all the chaff to settle out of still air--about $z_i/(0.3\ m/s)$--the convective boundary layer air "turns over" about three times (a typical time for air to traverse the mixing layer in a thermal or downdraft is $2\ z_i/w_*$ and w_* typically was 1.8 m/s during CONDORS). Deposition may cause a (relatively) lower χ_z near the surface compared with that from a non-depositing tracer, due to less material reflected. However, this effect may be counterbalanced somewhat by a general slumping of the profile because of gravitational settling. Further exploration of these questions, using both theory and oil fog-chaff comparisons, is needed to see to what extent the chaff concentration profile is correctable at larger distances.

Ground clutter removal: As discussed in Chapter 4, extensive computer processing was used to remove spurious ground clutter signals from the data. The final method chosen (a threshold on signal strength, followed by a threshold on velocity, followed by the deletion of individual spurious points) resulted in a data set with no points biased high by ground clutter, but with occasional data points near the ground unavoidably removed with the clutter. This effect is only present in the lowest 100 m of data, and only when the plume passed over

regions of high clutter. The result of this effect is to occasionally bias measurements of s_z, x_{yz}, and $\bar{z}$ low by a few percent at a few downwind distances.

Blockage: Blockage of the radar beam by nearby terrain caused an underestimate of chaff concentration at the lowest elevation angles. A study of blockage done by using topographic maps of the experimental area, revealed that at 0.5°, the lowest elevation angle used in the experiment, 60% of the beam was blocked in the worst case (at the azimuth of the most severe blockage). Blockage causes data below z = 80m to be biased low by amounts ranging from 0% to 60%.

Log averaging: As discussed in Chapter 4, synthetic radar sweeps were interpolated between each two radar sweeps as a part of the interpolation process. For the CONDORS 82 data, direct averaging was done on the log reflectivity data (resulting in the geometric, rather than the arithmetic, mean). The effect of this is to bias the chaff concentrations slightly low in the synthetic sweeps. For CONDORS 83 the processing was corrected so that the absolute reflectivity data were averaged, resulting in the arithmetic mean. The bias should be negligible in nearly all cases, but possibly may be non-negligible (albeit slight) in regions of high vertical gradients of concentration in CONDORS 82.

Minimum detectable signal: For the processing used in CONDORS, the threshold on received power was -85.5 dBm (dB above 1 milliwatt). This translates into 0.37 and 0.58 chaff filaments per $(50m)^3$ at downwind distances of 2.5 km and 4.0 km, respectively. Thus, regions of very low chaff density are invisible to the radar. The effect of this can be seen in the x_{yz} values shown in the tables of Chapter 9 and in the figures of Appendix B. In these data, the

total integrated chaff concentration is seen to decrease with increasing range. This effect causes a slight underestimate of plume width in the horizontal and vertical, not exceeding a few percent, and tending to increase with range.

Transcription: The data incorporated in the downwind averages presented in the tables of Chapter 9 were transcribed by hand from computer printouts. After the data were transcribed from the printouts, the data were proofread twice. In an effort to assess the number of typographical errors generated in the transcription process, we injected known (by us) errors into the transcribed data before the final proof reading. The final proofreaders found 28 of the 29 injected errors, and found 12 of the unknown number of errors created during the transcription and not caught in the initial proof reading. Thus, there is a probability of about 1/3 that there is at least one transcription error somewhere in the tables of Chapter 9.

C.3. Gas Tracer Measurements[1]

The gas tracers deployed are species which are detectable by highly sensitive Electron Capture Gas Chromatography (ECGC). ARLFRD operates a laboratory of ECGC analyzers which are computerized and semi-automated. These were operated in Idaho Falls for tracer analyses during the CONDORS study. These gas chromatographs (GCs) have been used on several other studies in essentially the

---

[1]Excerpted from the Quality Assurance Summary Report prepared by NOAA/Air Resources Laboratory Field Research Division, Idaho Falls, Idaho, January 1986. QCER Report in full available from EPA through Project Officer, G. A. Briggs.

same modes of operation with the same types of gaseous tracers. Comprehensive, post-CONDORS audits were performed as part of the EPA Full Scale Plume Study (FSPS) by the Meteorological Standards Institute during August 1984. Their findings are descriptive of the GCs as configured and operated for CONDORS and provide additional, independent calibration assessments.

The tracer analysis laboratory consisted of eight GCs which were designed and built by ARLFRD. Three of these GCs were actually used during the CONDORS program. These GCs were based upon the fundamental ECGC design of Lovelock and incorporated adaptations of the backflushing techniques described by Dietz. These GCs contained 5 ml whole air sample loops. During GC analyses, both calibration standard and field sampled tracer air mixtures were inserted into the 5 ml loops from 2 liter sampling bags. The GC electrical output signals were input to an electronic integrator (Spectra Physics SP4000). The output values of chromatogram areas from the integrator were transmitted to a Perkin-Elmer 7/16 minicomputer. The computer stored the data from the SP4000 on disk media along with values of atmospheric pressure, GC internal temperature, sample ID# (from a barcode reader system), date and time of analyses, and GC analyzer used. Printed listings of the analyses were made to provide a copy of the information and to assist the laboratory manager in monitoring the analysis activities.

Concentrations of tracers in samples are directly related to the integrated tracer peak areas of the chromatograms. The electronic integrator (SP4000) has resolution and sensitivity from 10 to 100 times greater than the typical baseline noise levels of the GCs. The relationship to area is determined for each chromatograph using a set of reference mixtures which bound the range of con-

centrations of interest. Periodic calibrations were performed to allow a temporal description of the GC behaviors as well. Each GC is unique in its sentitivity and baseline noise level. Typical minimum detectable concentrations of SF_6 were 2.5 ppt (vol./vol.), where ppt denotes parts of tracer per trillion parts of air. Typical minimum detection concentrations of 13B1 were about 50 ppt.

Atmospheric pressure and the internal temperature of the GC were used to adjust for density differences of the sample gas in GC sample injection ports during each analysis. Temperatures and pressures were measured with thermocouples and an aneroid barometer to sufficient accuracy (to the nearest whole degree Kelvin and to the nearest 0.01 inch of mercury) to determine density corrections within an uncertainty of ±1% or smaller.

Calibration mixtures utilized were commercially provided by Scott-Marrin, Inc., Riverside, California. These mixtures were dual concentrations of SF_6 and 13B1 in ultra-pure air. The overall accuracy of these reference mixtures was addressed for the 1984 FSPS audit. In essence, the ARLFRD calibration mixtures used were judged to be the values claimed by the vendor, within his stated accuracies. These were ±20% for the most dilute mixture (4 ppt SF_6 and 58 ppt 13B1), ±10% for the next most dilute mixture (10 ppt SF_6 and 150 ppt 13B1), and ±5% for all more concentrated mixtures.

Calibrations of each operational GC were repeated several times each day using the mixtures from the Scott-Marrin cylinders. Calibrations were always made using initially clean tracer sampling bags filled with tracer mixtures from the reference cylinders. The auditor's assessments and ARLFRD calibrations

agree in their findings of reproducibility and accuracy of GC performances. The analyzed tracer concentrations are judged to be within ±10% of their true values for SF_6 values >50 ppt and for 13B1 values >1000 ppt. Below these concentration values, the uncertainty gradually increases to ±100% near the minimum detectability limits (2.5 ppt for SF_6 and 50 ppt for 13B1). For the two most dilute calibration gas mixtures (concentrations specified in the previous paragraph), the reproducibility of GC responses ranged from ±15% to ±50%. (In Sec. 5.5 it was noted that, during CONDORS, plume centerline concentrations were about 40 ppt for SF_6 and 70 ppt for 13B1. The accuracy of centerline GC determinations for CONDORS was roughly ±10% for SF_6 and ±50% to 100% for 13B1. We conclude that the 13B1 tracer plumes were too dilute to be reliably measured by these GC's.)

After conclusion of the gas chromatograph (GC) analyses of field-collected samples from CONDORS, it was observed that the concentrations of 13B1 in samples from all but the first field test were from two to three orders of magnitude larger than expected. The SF_6 concentrations from the last three tests were also too large by similar factors. During the following two years, diagnostic examinations and controlled tests were conducted to seek the reason for these very large values of tracer concentrations.

The tracer concentrations determined from the GC analyses for the above tests were systematically and consistently too large. Yet, the behaviors of the GCs used for the analyses were very stable. The calibrations throughout the entire CONDORS laboratory operation were highly consistent and reasonable when compared with the GC performance during the many previous months of operation. Therefore, the GCs were not likely to be the source of erroneously large concentrations.

If faulty GC analyses were not the reason for the problem, then what were the other possibilities? Those remaining possibilities reduce to either a contamination of the samples or an erroneous calculation of concentrations from the GC analysis output values. These two primary sources of error are possible from the following potential causes.

1. Contaminated sample bags sent to the field.
2. Spacing between arc samplers assumed to be too large.
3. Tracer source strength larger than believed.
4. Sample bags stored near leaking cylinders of tracers.
5. Bags contaminated by release personnel at time of collection.
6. Bags contaminated by release personnel at time of deployment.
7. Bag cross-contamination during storge and/or transportation.
8. GC sample loops contaminated.
9. GC electrical constants in error.
10. Conversion constants in error.
11. Calculational method in error.

Each potential source was reviewed and researched. Conclusions concerning each of these items are addressed in the following paragraphs.

Item 1 postulates that contaminated sample bags were sent to the field site. There are several reasons why this was ruled out. First, the CONDORS concentrations were larger than any determined for 13B1 from prior tests and so could not be the residual from some prior use. Each sample bag was filled with clean nitrogen gas and evacuated several times as part of a bag cleaning process prior to use in field sampling. Each step of the cleaning cycle results in

about a 100-to-1 dilution of any tracer containing air within the sample bag. Two or more cleaning cycles are run on newly constructed bags and four or more cycles are run on used bags. The dilution of pre-existing air in the bag by 4 to 8 or more orders of magnitude virtually eliminates this source of sample contamination. The tracer sampling bags were made from 4 mil thick Tedlar plastic film. Experience has shown that tracer adsorption and desorption by this bag material is not significant when the air is used for whole air sample analyses by the GCs. A bag was selected randomly from every 25 to 30 clean bags readied to be shipped to the field site. Each of these bags were filled with clean nitrogen gas and analyzed by a GC to check for residual contamination. If any detectable amount was found the entire group (a box of about 100 bags) was returned for additional cleaning and cleanliness checks. All sample bags sent to and used at the field site were cleaned and checked in this manner. This method of cleaning and checking for contamination has been used for several field studies both prior to and after CONDORS. There has never been a contamination problem in the bags.

Item 2 could not be the cause because a recheck of the surveyed spacings of the samplers on the sampling arc showed that the values were reasonable in magnitude. They could not be in error by factors of 100 to 1000.

Item 3 appeared unlikely because the tracer release source strengths were monitored by calibrated linear mass flow meters. The total release amounts were also verified by total net weight loss from the gas cylinders used during each test. The source strengths were accurate to within a few percent of the calculated values. They certainly could not be 100 to 1000 times larger than stated; there was not near that much tracer available for release at the field site.

Item 4 is believed to be the cause of the contaminated samples. It will be discussed in later paragraphs, after discussion of the rationale for elimination of the remaining items.

Items 5 and 6, contamination by relase personnel, were not the causes. The personnel who released the tracer materials did not directly handle the sample bags. Before they returned to the vicinity of the filled sample bags they returned to their motel rooms, showered and changed clothes. By the time they returned to the field site the third (sample servicing) technician had completed the bag collections. Individual, separate debriefings of the three field servicing personnel confirmed that the tracer release technicians did not handle and contaminate the sample bags.

Item 7, cross-contamination of bag tracer concentrations during storage and transportation, was not the cause. Controlled tests of storage of bags with large and small (null) concentrations have never revealed evidence of this effect. If this process were to have occurred, there would have had to been some source of extra large concentrations to allow it. There would have been at least several additional orders of magnitude of dilution of the source of tracer contaminate as it diffused from its point of origin through the storage environment surrounding the boxes of sample bags. There were no sample bags filled with such massive amounts of tracers.

Item 8 was ruled out because contamination of the GC sample loops did not occur. One of the reference gases utilized during calibration checks of the GCs was tracer-free nitrogen. These check analyses with nitrogen consistently showed a null response. If the sample loops were contaminated (for most test

analyses) there could not have been the null values routinely found for nitrogen calibration checks.

Item 9 was not the cause. Repeated calibrations showed consistent responses for each calibration mixture, day-in and day-out. There were no jumps or dramatic changes in GC responses; they would have had to occur if this were a factor.

Items 10 and 11 were also ruled out because the conversion constants used in the sample calculations were the same values used for the calibration calculations. They also were consistent with similar values used both prior to and following the CONDORS program. The computational methods were the same as used in several other tracer programs. Those methods have been shown to yield correct computations.

The overwhelming conclusion reached was that there was no plausible way for such high values of concentration to have occurred naturally in the atmosphere at the time of field sampling, given the rates of controlled tracer releases used during CONDORS. The contamination of bag samples must have occurred following their shipment to the CONDORS field site and prior to GC analyses. Every known pathway, except contamination due to close proximity to the cylinders of tracer, was eliminated. Most other contamination pathways could never provide the very high observed levels of contamination concentrations, even if they had existed.

The sample bags from the last three tests were returned for analyses to the ARLFRD GC laboratory as one shipment at the conclusion of the field measurement program. (Bags from earlier tests were shipped immediately after each test.) This last shipment included all of the supplies and equipment deployed to the

field site. In spite of very explicit instructions to the contrary, it included the cylinders of tracer gases. High levels of contamination of both SF_6 and 13B1 were found throughout these samples; high levels of SF_6 were not found prior to these last three tests. The three day proximity in the van of bags containing samples from Tests 7, 8, and 9 and cylinders of the tracer resulted in a total contamination of those samples. High levels of 13B1 contamination were found from the end of Test 1 through the remainder of the CONDORS tests. Contamination of 13B1 levels in the Tests 1-6 samples was related to storage of cylinders of 13B1 in the same area (on the CONDORS site) as the bags which were to be used, or had been used for sample collections. Bags from Test 1 escaped contamination having been shipped before the cylinders were moved in.

By a process of elimination, the probable cause of sample bag contamination was identified as direct contamination from a strong source, such as cylinders of the tracer gases. However, before accepting this pathway as the answer, some additional tests were conducted in Idaho Falls. Two main questions remained to be addressed. First, was it credible that the sample bags could be exposed to sufficiently high levels of tracer for a non-contaminated sample to develop levels of tracer contamination consistent with the GC analyses from the CONDORS program? Second, if this were so, where would the contaminate tracer reside on the sample bag and could this place of residence and means of entering into the analyzed sample be found?

Before addressing these two questions a few supplemental facts should be stated. It is unfortunate but true that all valves on pressurized gas cylinders leak. Normally, the rate of leakage is so small that it is of little consequence in most situations (e.g., the loss of mass may be a few thousandths of

one percent of the cylinder content per day, perhaps one gram of gas). However, in the case of highly sensitive tracer sampling and analyses, it is important. In the event that a valve is slightly degraded in its sealing capacity, the leak rate could be considerably more. Within a somewhat closed storge setting such as a 30 foot trailer it is quite possible for ambient tracer concentrations to be at levels of tens of ppm due to slow cylinder leakage. If only 0.1 to 0.01% of this level of contamination were combined with CONDORS sampled tracer, the observed levels of masking tracer contaminations could occur.

In order to test the possibility of cylinder leakage and the build-up of tracer concentrations within a confined area, actual cyclinders of tracer gas were placed in the same trailer used by ARLFRD to transport and store CONDORS materials and equipment. Prior to placement of the gas cylinder in the trailer, air samples collected in the van were free of tracer. Within four hours after the cylinder was left in the van, interior ambient levels of tracer were of the order of parts per million or greater. As a next step, clean nitrogen-filled sample bags were placed in the contaminated van interior and left there overnight. Analysis of those nitrogen-filled (clean) sample bags yielded analyzed samples which had contamination levels very comparable to the CONDORS values of contamination. Thus, it was shown that a typical pressurized tracer gas cylinder , within a somewhat sealed storage area, could provide the levels of ambient tracer concentrations necessary for sample bag contaminations. It was also shown that the samples could indeed become contaminated in such a setting during even a relatively short period.

The last remaining question centered on how the ambient tracer contamination became intermixed with the tracer sample contained within the sample bag. Past

experience had shown that samples contained within properly sealed Tedlar bags remained reasonably stable for fairly long periods of time (several weeks). On this basis a diffusive exchange with ambient air is unlikely. There should be no significant change in the internal bag concentration by this process. Certainly a one or two order of magnitude change within a day or so is most unlikely. The only other pathway for entry of contamination is the segment of surgical tubing and connector on the inlet stem of each bag.

The attached bag connections were indeed the pathway for contamination. At the inlet/outlet end of the tubing was a plastic friction fitting which facilitates the connecting of the bag to either the sampler or the GC analyzer. The contamination was determined to reside upon either the plastic fitting or upon the section of surgical tubing between the plastic fitting and the point at which a hose clamp sealed the bag by pinching the tubing closed. This was the only part of the sample bag apparatus which was exposed to the ambient air. The confirmation of this pathway was made by replacing the segments of contaminated tubing. When a clean section of tubing was placed upon a known contaminated sample bag, a non-contaminated GC analysis resulted. When the contaminated tube was placed upon a bag filled with tracer-free air, the resulting GC analysis was contaminated. Follow-up checks revealed that the contamination had a finite lifetime on the tubing segment. After four or more weeks, a large fraction of the adsorbed tracer desorbed back into the atmosphere. These diagnostics also revealed that the sample within the sealed bag was not really contaminated. The contamination entered the GC sample loop when air was drawn from the bag for analysis. The drawing of air across the tracer-contaminated inner surface of the connecting tube segment carried a mixture of both sample air and the residual contamination into the sample loop.

In summary, it was found that SF_6 tracer concentrations for the last three tests were contaminated beyond usefulness. Likewise, 13B1 tracer samples were contaminated after the first test. Contamination occurred in the field through an unauthorized storing and or transporting of tracer-containing cylinders with sample-bags. The contamination was found to have been adsorbed upon the connecting segment of tubing and/or plastic fitting, external to the sealed volume of tracer containing air within the sample bag.

*U.S. GOVERNMENT PRINTING OFFICE: 1986-0-676-002/40030